PHD

The use of novel bifunctional peptides in non-viral gene delivery

Agyeman, Alfred Owusu

Award date:
2002

Awarding institution:
University of Bath

The Use of Novel Bifunctional Peptides in Non-Viral Gene Delivery

submitted by Alfred Owusu Agyeman
for the degree of Doctor of Philosophy
of the University of Bath
2002

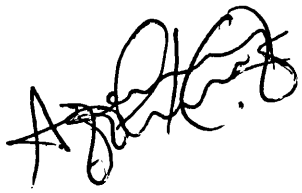

COPYRIGHT

ProQuest LLC
789 East Eisenhower Parkway
P.O. Box 1346
Ann Arbor, MI 48106-1346

Summary

The therapeutic applications of gene therapy have been realised for over a decade. One of the many approaches to transferring DNA into cells is the inclusion of a membrane active peptide (termed **fusogenic peptide**). In this project, fusogenic peptides based on the 23 amino terminus of the haemagglutinin sub-unit (HA-2) of the influenza virus were synthesized using solid-phase peptide synthesis method. Fusogenic peptides with 10 or 25 lysine residues attached to the carboxyl terminus (termed **"bifunctional peptides"**) were also synthesized. Complexes consisting of DNA, oligolysine and fusogenic peptides (termed **ternary complexes**) were formulated by sequential mixing of DNA and oligolysine followed by mixing with fusogenic peptide (in a process termed "**two-step complex formation**"). The *in vitro* transfection efficiency of ternary complexes were compared with that of complexes of bifunctional peptides with plasmid DNA (termed "**binary complexes**"). The latter were prepared by mixing solutions separately containing the two components (a process termed **"single-step complex formation"**). It was found that complexes formed with the novel bifunctional peptides (containing a 25-lysine chain) were 100- to 74000-fold more active than ternary complexes at transfection *in vitro* in six mammalian cell lines tested. The ability of both the fusogenic peptides and bifunctional peptides to disrupt cell membranes was demonstrated at pH 5 and pH 7 using an erythrocyte lysis assay. The bifunctional peptide with a 10-lysine chain attached did not show transfection activity even though it had membrane disruptive activity and could bind to DNA (though higher molar concentrations were required than the peptide containing a 25-lysine chain). The ability of the bifunctional peptide to effectively bind to DNA was demonstrated by comparison to polylysine and oligolysine, using an ethidium bromide exclusion assay. It was shown that the length of the lysine chain in the bifunctional peptide had to greater than 10 residues in order to achieve transfection activity. It was also shown that at the charge ratio optimum for *in vitro* transfection, bifunctional peptides protected DNA from degradation by serum proteases and thus enzymatic degradation was not responsible for the total loss of transfection activity observed in the presence of 10% (v/v) serum. Physical characterisation experiments to determine the particle size and zeta potential of binary complexes were performed in 5% (w/v) glucose solution. It was also discovered that a single amino acid deletion from the fusogenic component of the bifunctional

peptide resulted in over 100-fold reduction in transfection activity *in vitro*.

Preliminary *in vivo* testing of bifunctional peptides complexed with DNA was performed by injecting bifunctional peptide/DNA complex formulations in muscle and into dermal RIF-1 tumours implanted in host C3H mice. There was no transfection activity of bifunctional/DNA complexes in either muscle or tumour tissue at charge ratios which were optimum *in vitro* (+/- 3.2). However at a charge ratio of 0.8, there was a 2-fold increase in transfection activity in muscle compared to naked DNA, but this effect was not statistically significant.

Attempts were made to synthesis a fusogenic peptide with an oleoyl chain attached covalently via the side chain (ε-amino) of a lysine residue. This peptide proved difficult to purify by HPLC using the equipment available within the research group. Preliminary transfection studies showed that it could have a potential to increase the transfection efficiency of complexes made with the cationic lipid DOTAP.

This project is proof in principle that a single polypeptide consisting of a DNA-binding oligolysine component and a fusogenic component is a better and more robust gene delivery agent *in vitro* than systems that use self-assembly process via ionic interaction between positively charged oligo/polylysine and negatively charged fusogenic peptides (ternary complexes). The synthesis of a single, long bifunctional peptide by solid-phase synthesis was costly and the product was tedious to purify, but the end product had the advantage of guaranteed co-localisation of the functional components in the required orientation to make it a superior and consistent transfection agent *in vitro*.

Dedication

to my family

Acknowledgements

My sincere thanks go to my supervisors, Professor Colin Pouton and Dr. Stephen Moss, for their support throughout the course of this work. I thank Colin for creating an environment where new ideas could be tested.

I am grateful to the Royal Pharmaceutical Society of Great Britain for financial support. Financial and practical support from Pfizer Ltd are gratefully acknowledged. I especially wish to thank Dr. Mike Humphrey and Mrs. Jo Bennett from Pfizer for their interest in the work and I thank Dr. Klaus Rumpel for running Maldi-TOF samples at very short notice. I am also grateful to Professor D.J. Davies and Professor J. Westwick for providing the research facilities in Bath. My special thanks to Dr. Pauline Wood for her assistance with the *in vivo* work and to Dr. Steve Abbott for help with the flow cytometry work. I also thank Mr Mick Holton, Glaxo Ltd, Ware for assistance with particle size and zeta potential measurements. I am very grateful to "mon amie" Dr. Charareh Pourzand for her encouragement and for allowing me to perform countless luminometer assays in her lab at night. I thank Dr. Sukhi Bansal (King's College, London) and Dr. Richard Kinsman (School of Chemistry, University of Bath) for numerous advices with peptide synthesis.

To all the friends I made at Bath University, its been a pleasure knowing you.

Table of contents

Table of Figures

Tables

Abbreviations

AV	Adenovirus
AAV	Adeno-associated virus
bp	Base pairs
BSA	Bovine serum albumin
cDNA	complementary deoxyribonucleic acid
CF	cystic fibrosis
CFTR	cystic fibrosis transmembrane conductance regulator
CMV	Cytomegalovirus
DC-chol	3β[N-(N',N'-dimethylaminoethane)-carbamoyl]cholesterol
DDDW	double distilled deionised water
DIPEA	diisopropylethylamine
DMEM	Dulbecco's modified Eagle's medium
DMF	*N,N*, Dimethylformamide
DMSO	dimethylsulphoxide
DNA	deoxyribonucleic acid
DNase	deoxyribonuclease
DOGS	dioctadecyamidoglycyl spermine
DOPC	dioleoylphosphotidylcholine
DOPE	Dioleoylphosphotidylethanolamine
DOSPA	2,3-dioleyloxy-N-[2(sperminecarboxamido)ethyl]-N,N-dimethyl-1-ropanaminium trifluoroacatate
DOTAP	N-[-1-(2,3-Dioleoyloxy)propyl]-N,N,N-trimethylammonium methylsulphate
DOTMA	N-[1-[2,3-dioleyloxy)propyl]-N,N,N-trimethylammonium
EDTA	ethylene diamine tetraacetic acid
EGFP	enhanced green fluorescent protein
FCS	foetal calf serum
Fmoc	9-Fluorenylmethoxycarbonyl
g	gram(s)
GALA	amino acid sequence:WEAALAEALAEALAEHLAEALAEALEEALAA
GDV	gene delivery vector

HA	haemagglutinin
HA-2	haemagglutinin subunit 2
HATU	O-(7-azabenzotriazol-1-yl)1,1,3,3-tetramethyluronium hexafluorophosphate
HEPES	N-(2-hydroxyethyl)piperazine-N-2'-ethane sulphonic acid
HBS	HEPES Buffered Saline
HF	hydrofluoric acid
HOAt	1-hydroxy-7-azabenzotriazole
HPLC	high pressure/performance liquid chromatography
JTS1	amino acid sequence: GLFEALLELLESLWELLLEA
KALA	amino acid sequence: WEAKLAKALAKALAKHLAKALAKALKACEA
K8	amino acid sequence: $YKAK_8WK$
$lacZ^{-ve}$	β-galactosidase negative
$lacZ^{+ve}$	β-galactosidase positive
LB	Luria Bertani
LDL	low-density lipoprotein
μ	Micro
m	Milli
M	molar
MEM	Eagle's minimum essential medium
MPS	mononuclear phagocytic system
MTT	2-[4,5 Dimethylthiazol-2-yl]-2,5-diphenyltetrazolium bromide
MUG	4-methylumbelliferyl-β-D-galactoside
NEAA	non-essential amino acids solution
NaOH	sodium hydroxide
NLS	nuclear localisation signal
PBS	phosphate buffered saline
PCS	photon correlation spectroscopy
PEG-PS	polyethylene-glycol-polystyrene
PEI	polyethylenimine
pHPMA	poly-[N-(2-hydroxypropyl)methacrylamide]
pLL	poly-L-lysine

PVA	polyvinyl alcohol
PVP	polyvinyl pyrrolidone
RES	reticuloendothelial system
RLU	relative light unit
RMM	relative molecular mass
RNA	ribonucleic acid
RV	retrovirus
rpm	revolutions per minute
RSV	Rous sarcoma virus
SEM	standard error of the mean
tBoc	tert-butyloxycarbonyl
TAE	Tris-acetate EDTA
TE	Tris-EDTA
Tf	transferrin
TFA	trifluoroacetic acid
TfpL	transferrin-polylysine
Tris	Tris(hydroxymethyl)aminomethane
U	units
UV	ultraviolet
v/v	volume per volume
w/v	weight per volume
λ	wavelength
X-gal	5-bromo-4-chloro-3-indolyl-β-galactoside

1 INTRODUCTION

The objective in human gene therapy is to transfer plasmid deoxyribonucleic acid (DNA) encoding for deficient or defective proteins/peptides into human somatic cells *in vivo* in order to treat the resulting diseases from enzyme, transmembrane protein or hormone deficiencies. Due to their large and polar natures, gene expression vectors cannot overcome the lipid cell membrane barrier to enter cells in therapeutic quantities. Also, once internalised, the DNA has to escape from the endosome to avoid lysosomal degradation[1] and overcome the barrier of the nuclear membrane[2]. Gene therapy depends on efficient and safe devices for the delivery of nucleic acid into the target cells. A gene transfer particle has to serve at least two major delivery functions: (i) it has to deliver the gene within the patient from the site of administration to the surface of the target cell/tissue and (ii) it has to aid the uptake and successful trafficking of DNA to the nucleus of the cell. Combining the functions of a gene delivery vehicle (GDV) to meet the extracellular and intracellular requirements for successful gene delivery is a major challenge.

Gene delivery vehicles can be broadly divided into viral and non-viral gene reagents. The distinction between viral and non-viral gene therapy relates to the methods used for gene delivery. The viral gene therapy approach employs genetically engineered viral particles to deliver genes to the target cell, and the non-viral gene therapy approach employs gene delivery systems comprised of synthetic and semi synthetic gene formulations[2]. Viral gene delivery systems are effective and make use of the highly evolved mechanisms of viruses to transfer the therapeutic gene. The main drawback of viral systems is one of safety. Non-viral delivery vehicles are safe but suffer from low gene transfer efficiency *in vivo*. The solution to achieving safe and efficient gene delivery systems may be a compromise of the two methods: non-viral/synthetic "virus-like" particles.

There are a variety of non-viral gene delivery systems that are capable of transfecting cells *in vitro* [1,3,4,5,6]. However, little concordance has been observed between the effectiveness of transfection in immortal or primary cell lines *in vitro* and their effectiveness for gene delivery *in vivo*[7]. Since human gene therapy is aimed at treating

human diseases *in vivo*, it is important that candidates for GDVs and gene delivery protocols are selected and developed based their *in vivo* activity via a practical (potential clinical) route of administration as an initial step, before they are proposed as possible gene delivery vehicles for human gene therapy. Generally, GDVs are more efficient at *in vitro* gene transfer than *in vivo*.

The following sections will briefly describe some of the main viral and non-viral GDVs tested *in vitro* and/or *in vivo* to date and then concentrate on the *in vivo* barriers (intra- and extra- cellular) to the delivery plasmid DNA using non-viral gene delivery vehicles, and the attempts that researchers in the field are making to overcome the barriers to gene delivery.

1.1 VIRAL VECTORS

Viruses have evolved efficient strategies for transferring their genetic material from one host cell to the other. The principle of viral gene delivery is that genes encoding viral functions (which results in host cell death) may be replaced with genes encoding therapeutic functions within the infectious viral particles without eliminating the ability of the virus to infect the target cell efficiently and direct the expression of the gene product[2].

Viral vectors, such as recombinant adenovirus vectors have a number of advantages for gene transfer, including their high transfection efficiency and their wide range of cell targets *in vivo*[8]. However viral vectors have a number of disadvantages including the fact that they can generate several types of immune response reducing the effectiveness of subsequent administration of the vector. Research in cotton rats has shown that the immunological responses to administration of viral vectors can be reduced by treating them with immunosuppressive drugs prior to administration of recombinant adenoviral vector[9]. Also viral vectors often contain viral genes which can be transcribed, and there is a possibility of recombination with a wild-type virus, to produce a replication competent virus[2,7]. The advantages and disadvantages of three of the main viral approaches to gene therapy are discussed here.

1.1.1 RETROVIRAL VECTORS

Retroviruses (RV) are enveloped RNA viruses that can introduce genes permanently into somatic cells by integration its genetic material into chromosomal DNA of dividing cells[10]. Recombinant RV vectors can accommodate up to 6-7 kb of foreign sequences[11,12] and represent the most widely used vectors for human gene therapy, accounting for over 50% of current phase I trials. For the purposes of gene therapy, RV has been introduced into cells ex-vivo where cells have been stimulated with growth-promoting media or specific factors, before re-introduction into the host. Direct *in vivo* approaches including injection of retroviral vector producing cells into the brain[13] or intramuscular injection[14] have been described. Recombinant retroviruses are rapidly cleared from the systemic circulation by a complement mediated inactivation process[15], however, the use of alternative human packaging cell lines has partly resolved this problem[16]. A major disadvantage with RV is the possibility of inducing cancer by insertional mutagenesis; a consequence of random integration of the vector into the host cell chromosome[17]. Stable transformation of cells by RV vectors is often cited an advantage but the permanent integration of therapeutic genes by retroviral vectors removes the ability to modify or terminate the therapy in response to any adverse side effects or cure of the disease. Also, RNA viruses can recombine with other viral or cellular RNAs to produce new oncogenic viruses or replication-competent retroviruses of unknown characteristics[11,15].

1.1.2 ADENOVIRAL VECTORS

Adenoviruses are double-stranded DNA viruses capable of efficiently transducing dividing and non-dividing cells such as airway epithelial cells, endothelial cells, hepatocytes and cancer cells[18]. Due to its natural tropism for respiratory tissue, AV was first used to study the cystic fibrosis transmembrane conductance regulator (CFTR) gene transfer to patients with cystic fibrosis[19]. Adenoviruses do not integrate genes within the host cell chromosome hence transgene expression is only transient and there is the need for repeat administration if prolonged gene expression is necessary. The ability of adenoviruses to cause inflammation and stimulate other immunological response is a major disadvantage in their use for human gene therapy. Attenuated adenoviral vectors

express several viral proteins that can lead to immunogenic responses directed toward the adenoviral vectors and inflammation in the target tissues[20] thus making further administration of AV vectos inefficient or impossible[21]. In addition to the humoral response, a cellular immune response (cytotoxic T lymphocytes) against the transduced cells has been reported[20,22]. Some of the efforts that have been made to reduce inflammatory responses involve deletion of E1 and E4 genes[23], pre-treatment with anti-inflammatory drugs such as dexamethasone[9] or simultaneous administration with cyclophosphamide (an alkylating agent used in the treatment of cancers)[24]. Clinical data in cystic fibrosis patients treated with adenoviral vector containing the gene encoding for CFTR protein have been rather disappointing[25].

1.1.3 ADENO-ASSOCIATED VIRUS (AAV)

Adeno-associated viruses (AAV) are single-stranded DNA paroviruses, which are not associated with any known human diseases. This naturally defective virus, which requires co-infection with a helper virus (adeno, herpes or vaccinia virus) for replication, is capable of permanently inserting their genome into the chromosomes of the host cell[26]. The main advantage of the AAV for gene therapy is its ability to infect both dividing and non-dividing cells although chromosomal integration may not occur in quiescent cells[27]. As a DNA virus, AAV may be less susceptible to recombination than retroviruses[28]. A major drawback to the use of AAV in gene therapy is that only a small size of foreign DNA can be incorporated (3.5-4.0 kb). There are also difficulties in developing packaging cell lines that produce sufficient titres of virus without the presence of a helper virus[29]. Successful *in vivo* application of AAV vector mediated gene delivery include transduction CFTR gene in rabbit lung[30], the expression of δ-sarcoglycan gene in a hamster model of limb girdle muscular dystrophy[31]. Wang *et al.* have reported the efficient *in vitro* expression of CFTR using AAV vectors, which contain a downsized CFTR cDNA, thus allowing for the inclusion of an efficient promoter in the vector[32]. It remains to be seen how this "second generation" AVV vectors[32] will perform *in vivo*.

1.2 NON-VIRAL GENE DELIVERY SYSTEMS

Non-viral gene transfer formulations[2, 33,34,35,36] are attractive for the following reasons:
(a) The whole diversity of chemical reactions and physical interactions may be utilised for the synthesis and assembly of transfection material, in contrast to viral vectors which have to be assembled by cells in a biological environment, therefore being restricted to a proteinaceous composition. (b) They can be generated by assembly of few, defined components. (c) They can be very flexible regarding the size of DNA to be transported.
(d) Plasmid DNA and transfection reagents can be produced at large scale with rather low costs.
(e) Safety testing of synthetic material is less laborious than testing of recombinant material.

Non-viral gene delivery methods may be classified into two categories: a) naked DNA gene transfer systems and b) particulate gene delivery systems.

1.2.1 NAKED DNA GENE TRANSFER SYSTEMS

Intramuscular application of naked DNA results in efficient gene expression in rodent muscle[33]. In addition, conditions have been worked out for the local gene transfer of naked DNA to the skin[37], the liver [38,39], heart[40], the lung epithelium[41] and tumours[42,43]. Intramuscular injection of naked DNA has been used to introduce the dystrophin gene into muscles in animal models of Duchenne muscular dystrophy yielding long term expression of dystrophin in a limited number of muscle fibres and protection of those fibres against degeneration[44,45].

Transfection efficiency using injected naked DNA is species-dependent and very large amounts of DNA have to be applied. Nevertheless, there appears to be room for further improvement by optimising the formulation. Naked DNA have been formulated in polymers like polyvinyl pyrrolidone (PVP) and polyvinyl alcohol (PVA) [46] which are designed to be protective, interactive, non-condensing (PINC) for intramuscular gene delivery to the muscle resulting in higher and longer transgene expression[47].
Alternatives to injection by needle include administration by needle-free jet injection[48]

or biolistic delivery of DNA loaded gold microparticles[49] by the use of the gene gun or the pneumatic gun[50,51]. Improved local expression was obtained by electropermeation of the DNA-loaded area with some few microsecond electrical pulses[52]. The naked DNA technology has been successfully applied in murine models for genetic vaccinations[53,54].

1.2.2 PARTICULATE GENE DELIVERY AGENTS

Cationic lipids and cationic polymers have been used to condense DNA to form cationic lipid-DNA complexes (lipoplexes) and cationic polymer-DNA complexes (termed "polyplexes") respectively, or combination of both (lipopolyplexes) and to enhance DNA uptake by cells and have formed the bases of the development of non-viral gene delivery vehicles.

1.2.2.1 CATIONIC LIPIDS AND LIPOSOMES

Since the first description of successful *in vitro* transfection with cationic lipid transfection by Felgner *et al.* in 1987[55], there has been substantial progress their application of liposomes in their application for gene delivery[3,4,56]. Following some early structure-activity relationship studies of cationic lipids it was hoped that some 'magic' lipid could be discovered. While some new lipids are more efficient than the first generation cationic lipids in gene transfer, that goal will find a 'magic' lipid has been far from being realized[57]. A variety of cationic lipids (see Figure 1.1) currently available for liposome formulation consist of molecules with spacers of differing lengths and a variety of positively charged single or multiple amine head groups (reviewed by Gao and Huang[58]). The first generation of cationic lipids contained polar head groups with a single protonable amine (e.g. DOTMA, DOTAP). Other cationic lipids e.g. DOSPA and DOGS, incorporate multiple amine groups derived from spermine[59,60,61]. Other types of lipidic structure with good transfection activity include facial amphiphiles[62], peptido-lipids[63,64], pH sensitive liposomes[65], and cationic pH-sensitive liposomes[66]. Although various cationic lipids and lipid combinations exhibits quantitatively different gene delivery efficiencies in different cells, no clear patterns have emerged concerning the features of the lipid carriers that are necessary or optimal for gene delivery[2].

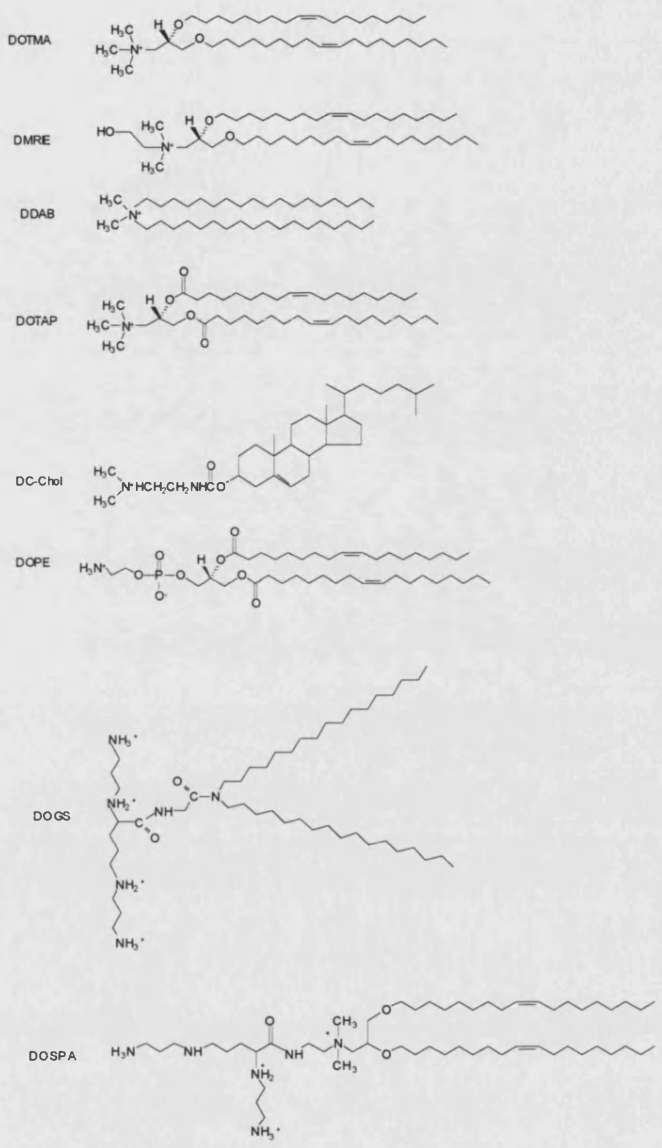

Figure 1.1 Structure of some commonly used cationic lipids.

Legend: DOTMA, 1,2-dioleyloxypropyl-3-trimethyl ammonium chloride;

DMRIE, 1,2-dimyristyloxypropyl dimethyl 2-hydroxyethylammonium;

DDAB, dimethyldioctadecylammonium;

DOTAP, N-[1-(2,3,-dioleoyloxy)propyl]-N,N,N-trimethylammonium;

DC-chol, 3β[N'-(N'-dimethylaminoethane)carbamoyl]cholesterol;

DOPE, dioleoylphosphatidylethanolamine; NSCC, 3-β (N^2-spermine)carbamoyl cholesterol;

DOGS, dioctadecyldimethylammonium chloride

DOSPA,2,3-dioleyloxy-N-[2(sperminecarboxamido)ethyl]-N,N-dimethyl-1-ropanaminium trifluoroacetate.

The efficiency of cationic liposomes *in vivo* is relatively low in comparison with viral vectors but they have the advantage of low toxicity and are unlikely to provoke inflammation or immune response on repeated administration[7]. The activity of liposomes and cationic lipids and modifications that have been made to improve lipidic transfection efficiency *in vivo* are discussed in sections 1.4.2.1 and 1.4.3.1. Some efforts that have been made by scientists to overcome cellular barriers are discussed in section 1.5.2.1.

1.2.2.2 CATIONIC POLYMERS

Cationic polymers self-assemble with DNA to form small composite particles that protect DNA against enzymatic degradation and are suitable for cellular uptake. When formulated with positive charge, these particles interact readily with cell surfaces and are internalized by endocytosis. Like cationic lipids, cationic polymers are generally non-immunogenic and can be easily applied to nucleic acid-based macromolecules of varying sizes. Cationic polymer-based delivery systems can be more stable than cationic lipids because their polyvalent interactions with DNA are not readily reversed. The main cationic polymers that have been used to condense DNA and transfect cells include linear polypeptide polymers like polylysine (PLL), polyarginine and polyornithine[67,68,69], histones[70] poly[(2-dimethylamino)ethyl methacrylate][71] and other chromosomal proteins[72] and branched polymers including polyamidoamine cascade polymer ("starburst dendrimer")[73,74] and polyethylenimine (PEI)[5].

Multivalent cations and polycations readily self-assemble with DNA and induce DNA compaction. In general, DNA is condensed to small toroidal or spherical structures with diameters as small as 30 nm. For cationic polymer-induced compaction, the structures of the resulting polyplexes have a greater dependency on the structure of the cationic polymer than on the structure of the DNA. DNA molecules of various lengths, sequences and forms (plasmid or linear) condense with cationic polymers in water to particles with similar dimensions.

Condensation efficiency is affected by polymer molecular weight and structure. High molecular weight polymers act similarly in DNA condensation. Tang *et al.* studied DNA

condensation by PLL (27 kDa), PEI (25 kDa), intact dendrimers and fractured dendrimers (sixth generation) and reported no differences in the size or zeta potential of the resulting polyplexes. All cationic polymers completely excluded ethidium bromide intercalation into DNA by charge ratios of +/- 1 (charge ratio is the positive charge of the polymer divided by the negative charge of the DNA) and condensed plasmid DNA to small toroids (40 to 60 nm in diameter)[75].

Cationic oligomers are also able to self-assemble with and condense DNA. Because condensation is thought to be driven by entropic forces arising from counter ion release, a minimum number of charge sites per polymer chain are necessary for achieving condensation. Gottschalk *et al.* and Plank *et al.* each found the minimum consensus polycation for DNA condensation to contain six to eight charges; however, these oligomers required high charge ratios for DNA condensation[76,77]. Additionally, the polymer structure influences DNA condensation efficiency. Incorporation of a single tryptophan residue into oligomers of polylysine greatly increased DNA binding[78]. Polymers with charge centres located close to the backbone are more efficient in DNA condensation and show increased stability to competitive displacement by anions[78]. Structure-function studies with cationic, cyclodextrin-based polymers revealed a significant DNA-binding dependence on charge centre distance from the sterically bulky cyclodextrin moieties but no differences in DNA condensation between polymers with charge centres separated by four to ten methylene units along the polymer backbone[79].

The use of polyplexes for gene delivery is hampered by inefficient mechanisms of endosomal escape and requires lysosomotropic agents such as chloroquine and ammonium chloride to enhance *in vitro* gene transfer[80]. Efforts to improve polyplexes gene delivery efficiency *in vivo* are discussed in detail the next section (section 1.3).

1.3 BARRIERS TO NON-VIRAL GENE DELIVERY FOR CATIONIC POLYMERS

PLL, PEI and dendrimers were not specifically developed for gene therapy applications. Recent developments in cationic vectors have included the preparation of new classes of polymers prepared specifically for gene delivery applications that reveal improvements in toxicity, solubility and biodegradability; however, the majority of research has

focused on modifying the more traditionally used polymers to increase their suitability for *in vivo* gene delivery. Major improvements in gene delivery have been made by modifying cationic polymers such as PLL and PEI with agents that enhance transfection efficiency, *in vivo* stability and tolerability. As a class of materials, cationic polymers generally utilise the same physicochemical interactions to bind and condense DNA, and the resulting polyplexes ultimately face the same barriers in *in vivo* delivery. Three major classes of barriers that need to be overcome in the development of non-viral, *in vivo* gene delivery systems are barriers to formulation and manufacturing, and extracellular and intracellular barriers.

1.3.1 FORMULATION BARRIERS

Cationic polymer-mediated delivery of gene-based drugs at a therapeutic dose requires high concentrations of polyplexes. Aggregation of these colloidal systems occurs with neutral particles, in concentrated solutions, or in the presence of salt. Formulation of polyplexes at near neutral zeta potential results in rapid aggregation of particles due to van der Waals interactions. For charge-mediated uptake, this problem is bypassed by formulating polyplexes with positive zeta potentials. However, positively-charged polyplexes also aggregate more readily as their concentration increases and they quickly precipitate out of solution above their critical flocculation concentration. For example, PLL-based polyplexes precipitate at 20 μg DNA/ml water[81], thereby severely limiting the injectable dosage of these particles. The concentration of polyplexes can increase with the hydrophilicity of the cationic polymers. Conjugation of hydrophilic polymers or proteins to the cationic polymers also increases polymer solubility. PEGylated (polyethylene glycol-conjugated) polylysine-based particles show no aggregation even at neutral zeta potentials[82,83]. The solubility of PEG-PLL particles depends on the degree of PEGylation[84] and molecular weight of PEG[85], with formulated concentrations as high as 2 mg DNA/ml in water[85]. Ogris *et al.* were able to concentrate PEGylated PEI to 400 μg/ml water without precipitation[86]. Dextran-modified PLL also increases the solubility of complexes to 40 μg of DNA/ml[87], as does conjugation of water-soluble proteins such as transferrin (increases the concentration of PLL-based polyplexes to 300 μg DNA/ml water[88]). Thus, injection of cationic polymer-based gene therapies at a pertinent dose generally requires concentrations of polyplexes above their critical flocculation

concentration. Efforts to raise polyplex concentration limits by increasing their hydrophilicities and by providing steric stabilization have resulted in formulations appropriate for *in vivo* use.

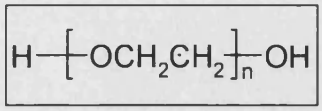

Figure 1.2 Structure of polyethylene glycol (PEG)

1.3.2 EXTRACELLULAR BARRIERS

Extracellular barriers to systemic delivery are hurdles to gene delivery that can be encountered from the point of injection to the surface of the cellular target.

1.4 BARRIERS TO GENE DELIVERY *IN VIVO*

There are a number of biological barriers to *in vivo* gene delivery depending on the route of administration and the on the location of the target cells. The location of the target tissues are as varied as there are diseases for which gene therapy are propounded to be useful in treating. Some relatively accessible target tissues that are candidates for direct injection include intratumoural, intrasynovium[82,89], intraoccular, intramuscular, subcutaneous, intrapericardial and intracranial administration. For less accessible target tissues, the intravenous route is the most practical route of delivery and presents most challenging and widest range obstacles to gene delivery.

1.4.1 BARRIERS TO INTRAMUSCULAR AND INTRATUMOURAL INJECTION

Naked DNA can be active *in vivo* after direct injection in muscle although 'naked' DNA plasmid has little or no activity in a typical cell culture transfection experiment [33,90,91]. Efficiency of transfection is low, usually with approximately 1% of cells being transfected after an intramuscular injection. It is conceivable that this level of activity could be the result of passive processes. It is not yet known how myocytes take up

plasmids *in vivo*, or how the DNA escapes lysosomal degradation. The unusual persistence of expression in muscle tissue has been attributed to the slow turnover of myofibre nuclei. In addition, access of DNA to the nucleus appears to be unusual in myocytes[92].

Staining of muscle or tumour tissues suggests that expression following direct injection of lipoplexes is often localized in regions that are close to the injection site. Formulations of plasmids with hydrophilic polymers appear to be more effective than particulate systems at promoting transfection in solid tissues[46], and the pattern of expression is more uniform and widespread, which supports the hypothesis that dispersion is a critical factor. As yet, it is not clear what the relative contributions of diffusion and convection are in the dispersion of DNA formulations within a solid tissue.

There are some similarities between expression of DNA in muscle and tumour tissue, although, in general, the levels of expression after intratumoural injection are much lower. Naked DNA appears to be as active as lipid formulations[93], presumably due to poor dispersion of particles within solid tumour tissue. Solid tumours lack effective lymphatic drainage, thus, gene delivery systems are likely to be forced towards the perimeter of the tumour tissue, where the material may become immobilized, unless extracellular fluid is able to drain into the surrounding tissue. High hydrostatic pressure within solid tumours presents a serious barrier to dispersion. In animal models, fluid may be forced away from the injection site after intratumoural administration. The use of micropump delivering 100 µl at a rate of 20 µl/min DNA formulation into solid tumours in mice has been successfully used to circumvent the problem of high hydrostatic pressure in tumours[43].

1.4.2 Barriers to lung administration

The lung as a target for gene delivery deserves a special mention because of the immense clinical interest for the treatment of cystic fibrosis. Cystic fibrosis (CF) is inherited as an autosomal recessive disorder, and is caused by mutations of a single gene coding for CFTR. CFTR is a cAMP-regulated chloride channel, which is required for

ion and water movement across the epithelial cell layers. Defective CFTR function leads to respiratory and intestinal disorders.

The lung is particularly attractive for gene delivery because it is easily accessible and avoids the need for any targeting component in a gene delivery product. The array of obstacles that oppose gene delivery particles reaching the cell surface and become internalised are reviewed by Pouton and Seymour[94]. Barriers to lung gene delivery include lack of endocytic capacity, lack of cell division, polarised epithilium with tough apical surfaces, which have tight junctions, and mucus, which acts as a physical and diffusional barrier. The dependence of successful gene delivery on mitotic activity can be modelled *in vitro*. Uduehi *et al.* showed that filter-cultured, differentiated Caco-2 cell could not be transfected, thus demonstrated the resistance of non-dividing cells to gene delivery by cationic lipoplexes[95]. Mortimer *et al.* have also shown the requirement of mitotic activity for lipid-mediated transfection of cells in culture[96]. The lungs also have alveolar macrophages, which would clear particulate material, which reaches the deeper respiratory airways.

1.4.2.1 CATIONIC LIPID/LIPOSOMES BASED GENE TRANSFER TO THE LUNG

Successful reporter gene expression to the lungs have been reported by several researchers using cationic lipoplexes to deliver reporter genes to the lung of various species including mice, rats, and sheep after intratracheal administration[97,98,99]. *In vivo* expression of therapeutic genes such as α_1 anti-trypsin[100] and CFTR[101,102,103,104,105] using cationic lipids in animal models have also been reported. These results suggested that DNA-cationic liposome complexes were efficient and relatively mild gene transfer agents for treatment in CF patients. Phase 1 human trials in CF patients using DC-chol/DOPE liposome-DNA complex applied by nasal drip to the nasal epithelium resulted in a partial restoration of chloride channel function (as measured by improvement in the membrane potential difference deficit in treated individuals)[106].

1.4.2.2 NAKED DNA DELIVERY TO THE LUNG

Suprisingly, naked DNA is seldom used as a standard for gene delivery vectors to be compared against in transfections to the lungs by direct instillation or aerosolisation. A

study by Zabner *et al.* found that a CFTR expressing pDNA partially corrected the electrophysiological abnormalities within the nasal epithelium of cystic fibrosis patients to the same extent as when administered alone or when complexed with a cationic lipid[107].

1.4.2.3 CATIONIC POLYMER-BASED GENE TRANSFER TO THE LUNG

Polylysine on its own is inefficient as a GDV for *in vivo* transfection but replication deficient adenoviruses coupled to transferrin polylysine has been shown to be efficient in transfection to the airways of cotton rats[108,109].

1.4.3 BARRIERS TO GENE DELIVERY VIA INTRAVENOUS ROUTE

The barriers to intravenous delivery of DNA complexes are quite formidable and are reviewed in detail by Pouton and Seymour[94]. The barriers include targeting to distal sites, opsonization and removal by mononuclear phagocytic system, degradation by serum enzymes, instability of particles when they come into contact with serum proteins, particle instability, difficulties with extravasation due to increased particle size and difficulty in crossing the extracellular matrix. In the absence of a hydrophilic surface, many particles interact with, and become coated by, specific plasma proteins (opsonins), which have evolved to participate in clearance of particles from the blood in a process known as opsonization. Opsonization prepares a particle for uptake by fixed macrophages of the mononuclear phagocytic system (MPS)[110]. The MPS is a collection of phagocytic cells that are present in tissues of the reticulo-endothelial system and are collectively responsible for clearance of particles from the circulation. Typically, 80-90% of hydrophobic and charged particles are opsonized and taken up by fixed macrophages of the liver and spleen, often within a few minutes of intravenous administration. Opsonization represents a major biological barrier to the delivery of DNA using condensed particles[94].

When the gene delivery particle all of the above-mentioned barriers, it also faces the obstacle of targeting the required tissue. Targeting of gene delivery to the cell surface is

best achieved by direct and local application, however this is not always possible. For example, in the use of gene therapy for cancer treatment, most work on targeted liposomes has been designed to deliver cytotoxic drugs to cancer cells. Miller and Vile have reviewed the incorporation of targeting functionality in liposomes[111]. Expression of a plasmid DNA in the target cells makes greater demands on the vector system when delivered via the intravenous route in that, it must not only target the appropriate cell type but also allow efficient delivery of undegraded DNA to the nucleus.

1.4.3.1 CATIONIC LIPID/LIPOSOME-BASED GENE TRANSFER VIA INTRAVENOUS ROUTE

In vivo use of conventional liposomes requires first avoiding the reticuloendothelial system (RES), and second, display of appropriate tropic and fusogenic molecules. Uptake by the RES can be considerably delayed, but not altogether avoided, by the use of "stealth" liposomes that display charged moieties such as the ganglioside GM1 and polyethylene glycol[112]. For most systemic purposes, the stealth formula is probably essential. Coupling of transferrin to liposomes followed by intravenous injection in a rabbit model resulted in significantly greater localisation to bone marrow erythroblasts[113], and incorporation of surfactant protein A into liposomes increased the uptake of the liposome cargo by alveolar type II cells[114].

Immunoglobulin complement coupled to liposomes ("immunoliposomes") has been shown to exhibit tropisms conferred by the displayed antibody. Coupling to liposomes of an antibody against glioma cells increased the efficiency of gene delivery to these cells *in vitro* by about 70-fold[115]. However, it is not sufficient merely to confer upon the vector a particular binding ability; the particle must bind to a ligand that also allows fusion of liposome and cell membranes. Such considerations of appropriate internalisation of vector cargo are especially important for gene delivery vectors, where the DNA must not only reach the appropriate cell type but also must reach the nucleus in an undegraded form[111].

Conjugating virions to liposomes or incorporating viral surface glycoproteins into liposomes might create a vector that has the efficient cell attachment and entry mechanisms of a virus but not the safety drawbacks; much work has been done in this

area with Sendai virus in particular[116]. Another system used liposomes that displayed only the fusogenic protein of Sendai virus (F-protein) and not the cell binding protein (haemagglutinin)[117]. However, although such approaches can make liposomes up to 10-fold more efficient than lipofection at gene delivery[116], in terms of targeting all it can do is confer upon the liposome the tropism of the virus, and there are very few native viral receptors that exhibit narrow and precise cell type specificity. Respiratory epithelium has been targeted by means of the surface proteins of respiratory syncytial virus (ReSV), which is responsible for infections of the lower respiratory tract. Liposome-type envelopes were constructed that displayed both the attachment and fusion proteins of ReSV, and these have been shown to enter all cells of a cultured respiratory epithelial cell line within 1 hour[118].

Cationic liposomes such as the commercially produced lipofectin can efficiently avoid the lysosomal pathway because the particular lipid composition allows direct fusion of liposome and cell membranes and have replaced conventional liposomes[111]. Several studies have shown that intravenous administration of cationic liposome-DNA or cationic liposome-polycation-DNA complexes gives systemic gene expression particularly to the lung[119,120,121,122,123,124]. Study of the dynamic changes in the characteristic of cationic lipidic vectors in serum have revealed that lipidic vectors undergo aggregation, then disintegration of vectors leading to degradation of DNA[125]. PEGylation of cationic lipids could offer a solution to the problem of serum protein recruitment[125], but its difficult to see how that could be achieved without compromising the ability of existing lipids to bind to DNA. A new class of cationic lipids with "stealth" properties could better meet intravenous delivery requirements.

1.4.3.2 NAKED DNA DELIVERY VIA INTRAVENOUS ROUTE

Naked pDNA is rapidly degraded in the presence of serum[125]. Intravenous injection of high doses (66 mg/kg) of pDNA in mice as a control in the study of cationic liposome-mediated intravenous gene delivery, showed that plasmid DNA only was capable of transgene expression in major organ tissues (heart, liver, spleen, kidney and uterus) but were between 57-fold (in the heart) and 1000-fold (in the spleen) lower than DNA-liposome complex[126].

1.4.3.3 CATIONIC POLYMER-BASED GENE TRANSFER VIA INTRAVENOUS ROUTE

For cationic polymer-based systems, the extracellular barriers to gene delivery that must be overcome can be summarised as follows: toxicity of the polyplex, interactions with serum proteins, extracellular matrices and non-specific cell surfaces, clearance by the innate immune system, aggregation due to physiological salt conditions and evasion of the adaptive immune response.

There has been a relatively few reported work on *in vivo* transfection using unmodified polylysine-based complexes since the early work by Wu and Wu[127] and this is a reflection of the difficulty with particle stability in serum and associated toxicity *in vivo*. In order to enhance uptake and specificity, Wu and Wu[128] generated polylysine-based, receptor-specific gene transfer system by incorporation of asialoorosomucoid-polylysine conjugates into DNA complexes to obtain expression of reporter genes in hepatocytes of normal animals. By attaching the DNA to a domain that can bind a cell surface receptor such as the asialoglycoprotein receptor, insulin, transferrin and CD3 receptors [128,129,130,131,132,133] efficiency of receptor-mediated endocytosis has been explored. Other published work included the use of low-density lipoprotein (LDL) receptor in LDL--deficient rats[134], albumin in analbuminemic rats and methylmalonyl CoA mutase in mice. Evidence of specific gene delivery to hepatocytes *in vivo* has been obtained with the use of hepatocyte-specific promoters and histological analysis[135]. The delivery of plasmids to hepatocytes *in vivo* has also been reported using polylysine covalently coupled to galactosyl residues as targeting ligands[136,137]. As with PEI, a reduction of surface charge by complexing with polyethylene glycol, should reduce toxicity and particle instability, but polylysine does not have the inherent pH buffering effect which is responsible for the efficiency of PEI.

The reduction of the surface positive charge of TfPEI-DNA complex by covalently linking polyethylene glycol (PEGylation) to TfPEI, has been shown to reduce interaction with blood components, increase particle stability against salt induced aggregation, extended the circulating duration of the resulting GDV, and cause less toxicity due to lung embolism following intravenous administration to mice[86,138]. This effort at solving the problem of aggregation of polycation-DNA particles in serum also

involved forming the transfection complexes at low DNA concentration (where the chance of formation of large aggregates was low) and then concentrating the PEGylated complexes up to the required DNA concentration[138]. The degree of PEGylation had to be balanced so as to provide adequate protection of the TfPEI-DNA complex without occluding the targeting ligand, and results in this work shows that this balance was achieved.

For effective *in vivo* gene delivery, polyplexes should have a number of properties: (i) it should remain non-toxic, small and discrete; (ii) it should bypass the immune system; and (iii) it should interact only with the cells of interest. Efforts to prepare polymer systems that endow polyplexes with these characteristics are discussed below.

1.4.3.3.1 Salt and serum stabilization

Injection of polyplexes systemically results in particle aggregation, thus limiting successful *in vivo* gene delivery. Although cationic polyplexes are stable in water, they aggregate in ionic solutions due to a decrease in the protective electrostatic double layer. Polyplexes aggregate rapidly in physiological salt concentration (~150 mM)[83]. Injection of PEI-based polyplexes into mice results in 50% lethality, with the likely cause being blockage of lung vasculature with aggregated polyplexes[86]. In addition to salt-induced aggregation, serum proteins readily adsorb onto positively charged particles, initiating rapid blood clearance by macrophage uptake (a first step in the removal of polyplexes by the innate immune system). PLL-based polyplexes are eliminated quickly with a half-life less than 5 minutes. Clearance from blood has been shown to correlate with the amount of plasma associated with the particles[139]. One approach to minimising salt-induced aggregation and nonspecific protein or cell surface adsorption is steric stabilization with hydrophilic polymers. Steric stabilization can be achieved by grafting a 'brush' layer of hydrophilic polymers to the surface of nanoparticles, thereby decreasing particle-particle and particle-protein interactions. Hydrophilic polymers used for polyplex modification include PEG, pHPMA (poly-N-(2-hydroxypropyl)methacrylamide], Figure 1.3), oligosaccharides[85,140] and soluble proteins. PEGylation and use of pHPMA have shown substantial promise in polyplex stabilization and will be discussed in more detail below.

1.4.3.3.1.1 Stabilization by PEGylation

Efforts to provide salt and serum stabilisation of polyplexes by PEGylation have yielded mixed results. The factors affecting the success of PEGylated polyplexes to resist salt and serum mediated aggregation include the degree of polymerisation (DP) of the cationic polymer, the PEG grafting density, the length of PEG and the method of PEGylation. The cationic polymer DP influences the efficiency of DNA binding and compaction, and the effects are magnified with low MW polymers. Conjugation of PEG to cationic polymers often reduces the charge density of the polymers by reacting away cationic amine groups while adding hydrophilic, bulky polymer fragments. Thus, PEGylation reduces the DNA-binding efficiency of cationic polymers and alters the thermodynamics of DNA condensation as manifested by changes in polyplex structure. PEGylation of PEI (MW 2000, 'PEI2K', DP ~ 45) resulted in polyplex structures with thick threads and donuts, which were incapable of DNA transfection. On the other hand, PEG-PEI25K condensed DNA to small dense granules without extended threads[141]. Similarly, PEGylation of PLL4K (DP = 19) altered the polyplex structure from toroids to rods. In addition, these structures were not stable against salt-induced aggregation, unlike PEG-PLL10K that offered salt stabilisation[83]. PEGylation of thermine derivatives (~ 4 charges per chain) also prevents DNA condensation[142]. Vinogradov *et al.*[143] and Kwok *et al.*[84] reported successful DNA condensation after PEGylation of short polycations (PEG-PEI2K + PEG-Polyspermine and AlkCWK18, respectively). The PEI2K-PEG complexes are stable at physiological salt conditions and the PEG-CWK18 complexes give high concentrations in water.

Steric stabilisation occurs by protection of particle surfaces with hydrophilic polymers. The thickness of the protective layer, i.e. the MW of PEG, therefore influences the degree of particle protection. Analysis of plasma protein adsorption to PEG-coated nanoparticles of sizes 160 to 270 nm as a function of PEG thickness revealed decreased protein adsorption with increased MW. PEG2K reduced protein adsorption by 43%, while PEG5K reduced protein adsorption by 73%. Further increases in PEG length offer only marginal increases in protein protection, indicating PEG5K to be a critical length for steric stabilisation of nanoparticles in this size range[144]. Indeed, PEGylation of PEI-based polyplexes with PEG3400 only slows salt-induced aggregation, while

PEG6K completely prevents aggregation in physiological salt conditions. PEG6K was also more effective than PEG3400 in preventing complement activation and serum binding[145].

The density of the PEG layer also influences the degree of stabilisation. PEGylated nanoparticle studies determined the threshold PEGylation density (by weight %) for maximum reduction of protein adsorption to nanoparticles to be 5%, with total adsorbed protein content decreasing as PEG density increased. The average distance between PEG strands at this density was calculated to be 1.4 nm[144]. It should be noted that while PEG significantly decreases protein adsorption, it cannot be completely eliminated due to the inability to completely coat particle surfaces. Nevertheless, protection from complement activation by PEGylation of PEI/DNA complexes depends on the amount of PEG associated with the particle surface[145]. Incorporation of PEG into polyplexes, in addition to providing salt and serum protection, can also reduce non-specific cellular uptake as a function of PEGylation density. PEG5K-PEI25K particles have reduced transfection potential that is dependent on PEG grafting density in the PEI: 10% modification of PEI amine groups renders the polyplexes completely inactive[141]. PEG550PLL25K polyplexes transfect optimally with 10% PEG grafting. Further increases in PEGylation reduce transfection, most likely by inhibiting uptake. Increasing the density of high MW PEG also affects the DNA-binding affinity of the cationic polymer, both by sterically interfering with DNA binding interactions and by reducing the number of cationic charges available for binding. High PEG:PLL ratios in PEG5K-PLL10K polymers result in decreased DNA binding and polyplexes with worm-like structures[83]. Therefore the following dichotomy exists: higher grafting densities and longer PEG chains are necessary to maximise salt and serum stabilisation; however, these conditions lead to particle destabilisation and low transfection efficiencies. An approach to circumvent this problem is to PEGylate the cationic polymers after polyplex formation in order to minimize disruption of DNA binding.

Two groups have demonstrated post-polyplex formation PEGylation. Ogris *et al.* modify transferrin-PEI (Tf-PEI) or PEI-based polyplexes by reacting activated PEG5K to primary amino groups in the PEI molecules[86]. This PEGylation method therefore modifies only surface-available amine groups and prevents polyplex instability due to

the PEG polymers trapped in the polyplex core. One-third of the primary amine moieties in PEI were modified without any change in polyplex size. In addition, the PEGylated particles were stable in ionic solutions up to 70 mM. PEGylation prevented plasma-mediated aggregation and significantly increased blood circulation (33% of the PEGylated particles remained in blood 30 minute after injection in mice versus 6% of unmodified particles). In addition, tumour-site gene expression was increased after systemic gene injection of PEGylated DNA/Tf-PEI complexes over unmodified complexes. Finsinger *et al.* also PEGylated preformed PEI and PLL polyplexes by the addition of anionic peptide-PEG conjugates[145]. The anionic peptide self-assembled to the polyplex surface by electrostatic interactions. The coated particles also retained their size and demonstrated steric stabilisation against physiological salt conditions and proteins such as BSA.

1.4.3.3.1.2 Stabilization with HPMA

Seymour and colleagues focused on particle stabilisation using the hydrophilic polymer, HPMA. Initial work concentrated on PLL grafting with HPMA. The copolymers formed were capable of binding to and condensing DNA and these copolymers slightly increased polyplex solubility[85]. In more recent years, Seymour *et al.* have also explored the modification of preformed complexes. Modification of preformed complexes involves HPMA grafting to PLL based particle surfaces in order to minimize disruptive interactions with the PLL/DNA core [146]. Complexes modified with monofunctional HPMA were stable in 150 mM salt solutions and relatively inert to serum protein binding. In spite of the encouraging *in vitro* results, the monofunctional HPMA-coated particles still suffered from low circulation lifetimes since they showed no improvement over unmodified complexes. A possible explanation for the lack of increased circulation time is the reversibility of polymer/DNA interactions, as was demonstrated by heparan sulphate displacement of the polymer from the DNA[146]. A major difference between the aforementioned modified polyplexes and Stealth liposomes that have long circulation times is the lateral stabilisation between lipids[147]. Polyplexes can be further stabilised by crosslinking polymer strands on particle surfaces, and efforts to crosslink preformed polyplexes are discussed below.

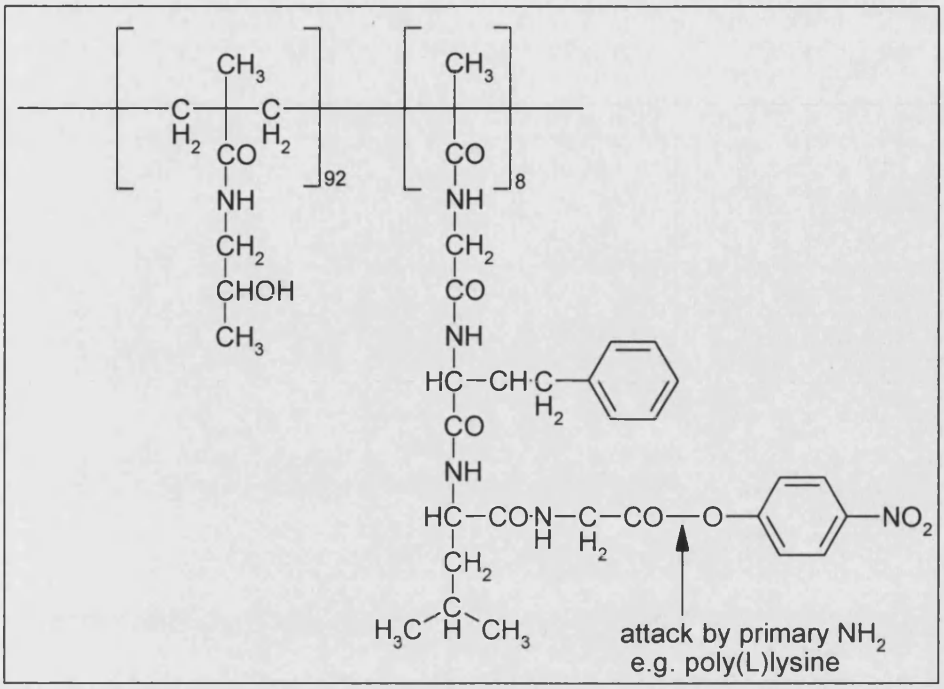

Figure 1.3 Structure of pHPMA polymer bearing pendant tetrapeptide (Gly-Phe-Leu-Gly) side chains terminating in reactive 4-nitrophenoxy groups.

1.4.3.3.1.3 Stabilization by crosslinking of polyplex surfaces

Seymour and coworkers further stabilised PLL-based polyplexes by including multiple reactive pendant groups on the HPMA that react with the primary amino groups of PLL and effectively crosslink PLL chains while coating the polyplex with HPMA polymers. The resulting complexes were negatively charged, discrete and spherical, and demonstrated serum stability and decreased non-specific cellular uptake[147]. Oligolysine-based polyplexes crosslinked by glutaraldehyde improved particle stability in that they exhibited enhanced resistance to serum endonucleases[148]. Transfection of these crosslinked, particles to cultured cells gave low, steady-state gene expression for 10 days. Crosslinked polyplexes can also demonstrate increased salt stabilization. Cationic polyplexes crosslinked with a short crosslinker were stable in salt solutions for at least 7 days; however, they were unable to provide gene delivery and were resistant to polymer displacement by dextran sulphate[149]. A proposed mechanism for stabilization by crosslinking is 'caging' of the DNA by preventing crossbridging of polymer chains between polyplex particles. While these crosslinking experiments demonstrate

important concepts for particle stabilization, future cross-linking methods need to be more labile to allow for DNA release after internalization.

1.4.3.3.2 Complement activation

Plank *et al.* reported that complement activation could limit the circulation half-life of polyplexes *in vivo*[150]. However, the complement-mediated haemolysis was obtained at elevated polymer concentrations with high molecular weight polymers. Additionally, the potential for complement activation by cationic polymers was found to strongly depend on polymer chain length; cationic oligomers were weak activators of the complement system[150,151]. Polymer complexation with DNA also greatly reduced the potential for complement activation. Dash *et al.* studied the mechanisms for polyplex clearance from the blood and found minimal contributions from complement at the concentrations tested[139]. Therefore, while complement activation should be monitored for stabilised, long circulating polyplexes, it may not be a major mechanism of polyplex clearance for stabilised particles at concentrations that are appropriate for gene delivery.

1.4.3.3.3 Toxicity

Toxicity, is a major drawback of polyplexes that has limited their progress in clinical trials. Although the molecular basis of toxicity is unclear, the polycationic nature of the polymers appears to be the main origin of toxicity. Thus, recent efforts to develop polymers with reduced toxicity have focused on low molecular weight polymers, biodegradable polymers and polymers with reduced cationic charge density.

Both polylysine and polyethylenimine complexes with DNA suffer from high toxicity in mammalian cells. The LD_{50} of high molecular weight forms of these polymers (25 kDa) in mice range from 5 to 30 mg/kg when complexed to DNA[152,153]. Low molecular weight (MW) preparations of PEI[154] and PLL[155] are significantly less toxic to cultured cells. In addition, low molecular weight chitosan demonstrates significant increase in tolerability *in vitro* over long-chain chitosan[156]. The lower molecular weight polymers are likely to have a higher packing efficiency on the DNA, resulting in less excess positive charges on the polyplex[157]. Biodegradable polymers such as poly(beta-amino

esters) also have reduced toxicity, possibly as a result of reduction to smaller units after internalization[158]. Polymer detoxification has also been achieved by reducing cationic charges. Glycolylation of amine groups in PEI reduces the number of free amines and introduces hydrophilic residues. Glycolylation of 70% amine groups resulted in a polymer with low cytotoxicity even at an N:P ratio of 30. PEGylation of polylysine by reacting with the primary amine groups also reduces the polymer amine content and yields polymers with significantly lower toxicities[85,159]. Polymers with high charge density, e.g. PEI and PLL, tend to have higher toxicities. Although the molecular mechanisms leading to cell death when cultured cells are exposed to polycations is not completely understood, it is clear that the spatial arrangement of charge along the polymer backbone has significant effects on the pathways leading to cell death. Thus, the polymer structure must be designed to effectively bind and condense DNA and to interact sufficiently strongly to protect the DNA from nucleases yet have arrangements of the charge sites that minimise toxicity.

1.5 Cellular Barriers

An effective gene delivery system will need to bind to an appropriate cell (targeting), be internalised (usually by endocytosis), escape the degradative pathway (endosomal escape) and ultimately allow delivery of the expression plasmid to the nucleus (nuclear uptake)[94]. Viruses have perfected these mechanisms and are often used as templates in designing of polymer based non-viral gene delivery systems. Some of the approaches taken to by researchers to surmount these obstacles are reviewed by Pouton and Seymour[94].

1.5.1 The barrier of the plasma membrane

The plasma membrane in non-dividing cells is a formidable barrier for macromolecules. Most macromolecules and particles have low solubility in lipid bilayers, thus limiting their uptake into cells by means of passive diffusion into cells[160]. Uptake of most marcromolecules or particles occur into cells by pinocytosis, adsorptive endocytosis, receptor mediated endocytosis or phagocytosis[161,162]. When the endocytosis inhibitor cytochalasin B was added to the medium during transfection *in vitro*, transfection was

inhibited[163]. In addition, electron microscopy images of gold-labelled plasmid have revealed an entry process typical of endocytosis[107]. Clathrin–mediated endocytosis is the major pathway for uptake of receptor-ligand complexes, including the transport mechanisms for transferrin and low-density lipoprotein (LDL)[160]. The formation of clathrin/AP2 adaptor-coated vesicles at the plasma membrane is preceded by the formation of a clathrin-coated pit, when there is concomitant mechanical invagination of a patch of membrane (associated with the formation of a clathrin polyhedral lattice) and sorting of selected membrane proteins into the pit. The invagination process continues under the control of a number of accessory/regulatory proteins until a mature vesicle is 'pinched off' the parent membrane. The vesicle coat, which consists mainly of mechanical clathrin scaffold and adaptors, is removed to allow the vesicle to fuse with its target membrane[164]. At least three other pathways of endocytosis have been described: i) macropinocytosis is induced in response to mitogenic factors and involves the formation of large, heterogeneous 'macropinosomes'. This mechanism may be responsible for the uptake of large lipoplexes or polyplexes by dividing cells in culture. ii) Non-coated vesicle formation can contribute to bulk pinocytosis and some receptor-mediated events. iii) Caveolae have been implicated in endocytosis and transcytosis involving uptake into endothelia from the vasculature[165]. Some receptor-mediated endocytosis takes place preferentially into caveolae including folate uptake and some 7-transmembrane domain cell surface receptors[166].

Ligand-mediated endocytosis are employed either to coffer rapid uptake or specific/selective uptake of gene delivery particles. The use of ligand-mediated endocytosis for the purpose of targeting liposome and cationic polymer vectors have already be reviewed in section 1.4.3.1 and section 1.4.3.3. Transferrin has been extensively used for ligand-mediated delivery of plasmid DNA into cells *in vitro*[86,167,168,169]. Cells of various phenotypes express transferrin receptors, so the use of transferrin does not offer opportunities for receptor mediated targeting but it does offer a means of rapid uptake. Peptide sequences that have affinity for integrins (heterodimeric membrane proteins found on all cells and important for attachment of cells to the extracellular matrix, cell-cell interactions and signal transduction), have been used to improve uptake of cationic lipid-based GDV into cells *in vitro* [170,171] and *in vivo*[172]. The low transfection activity of non-viral gene delivery systems *in vivo* is partly indicative of

the lack of rapid uptake mechanisms for these systems in the absence of mitotic activity[95,96,173]. Therefore the inclusion of ligands to increase the rate of uptake of particles is important to the success of non-viral gene therapy.

1.5.2 THE BARRIER OF ENDOSOMAL DEGRADATION

The default pathway particles taken up by endocytosis, in the absence of a mechanism of escape or a trafficking mechanism (which directs the particle to a specific intracellular organelle) will be fusion with lysosomes, resulting in degradation of biodegradable systems[160]. The implication is that a specific or generic means of escape is required, or much of the internalised DNA will be lost by degradation. Biological events like entry of viruses and toxins into cells, the action of antibacterial peptides, defense toxins, or the performance of complement, defensins, and perforins of the vertebrate immune system are examples demonstrating how efficiently nature can modulate membrane barriers. A series of natural membrane destabilizing agents has been characterised on the molecular level. In several cases the membrane-active principle was found to be located in defined, small amphipathic peptide domains[174,175,176,177,178]. Synthetic peptides derived from the N-terminus of influenza virus haemagglutinin[167,179,180,181] and the rhinovirus VP-1 protein[182], or artificial amphipathic peptides[167,183,184] have been used. Of the fusogenic/fusion peptides of viral origin known, the N-terminal sequence of influenza virus haemagglutinin HA-2 is the most studied or used for gene therapy[1,2,185,186,187,188]. The ability of influenza virus to escape from the endosome depends on a conformational change in the haemagglutinin (HA) at the low pH of the endosome (between 5 and 6) to expose a fusogenic peptide sequence[189], which in itself changes conformation to form a membrane disruptive amphiphilic α-helix[167]. Fusogenic peptides sequences based on the N-terminal sequence of the influenza virus haemagglutinin HA-2 have the ability of disrupt liposomes[179,181] and cause erythrocyte lyses[167]. The erythrocyte lysis activity (rather than the liposome disruptive activity) of fusogenic peptides was particularly shown to correlate with enhancement of gene expression when fusogenic peptides were complexed through ionic interactions to polylysine-transferrin/DNA complexes[167]. It is this ability of fusogenic peptide sequences to disrupt membranes at low pH that has been exploited to enhance gene expression mediated by polylysine/DNA/fusogenic peptide complexes.

The following discussion will look the main groups of non-viral gene delivery agents (cationic liposomes and cationic polymers) and how researchers are working to meet the cellular requirements for endosomal escape in order to improve gene delivery.

1.5.2.1 ENDOSOMAL ESCAPE OF CATIONIC LIPID-BASED VECTORS

Although lipidic systems are the most progressed non-viral systems in terms of reported work *in vivo* and clinical trials, their development has usually been empirically driven[57,190]. The need for further improvement in transfection efficiency *in vivo* is however leading to the gradual departure from synthesis of the 'magic' lipidic structure, and towards incorporating features of viruses to overcome cellular barriers.

Complexes of DNA and cationic lipids can bind to the cell surface by charge interactions[3,191,192]. Experimental data suggest that uptake proceeds via endocytosis[65,107, 193,194] and can be observed in membrane bound perinuclear vesicles[107]. The mechanism by which lipoplexes escape the membrane bound vesicles [107] is not well understood but the release of DNA from the endosome to the cytoplasm, release of DNA from the cationic lipid, and transfer to the nucleus[107,195] are considered to represent bottlenecks in lipid-based gene transfer. The cationic lipids may mix with the cellular anionic lipids[195,196] which may trigger destabilisation of the endosomal membrane. Gene expression can be enhanced by the inclusion of helper lipid DOPE to lipoplexes[197], DOPE presumably induces destabilisation of the endosomal membrane by membrane transition to the inverted hexagonal phase[198,199].

The activity of lipoplexes (in the presence or absence of another DNA-binding protein) has been enhanced by mixing with Sendai virus envelopes[200,201]. This approach and related systems utilizing neutral lipids and liposome-like reconstituted envelopes ("virosomes") based on Sendai virus (which triggers membrane fusion at the cell surface)[202,203] or influenza virus (which promotes delivery via fusion with the endosomal membrane after endocytosis)[204] have been found effective for gene delivery.

The amphipathic cationic peptide gramicidin S was included into a DOPE lipid/DNA composition; this has been found to strongly facilitate DNA delivery[205,206].

Incorporation of gramicidin S and DNA into asialofetuin-labeled liposomes was used for receptor-mediated gene transfer into primary hepatocytes[207]. Wagner *et al.* [208] and Kamata *et al.*[209] have investigated the influence of influenza-based peptides on cationic lipid-based transfection. When positively charged lipospermine/DNA complexes were used, only a slight but significant (3- to 30-fold) enhancement of the gene expression was obtained by association with the peptides[208]. Kamata *et al.* [209] showed that influenza-derived peptides could increase the level of gene expression of a lipofectin formulation by up to 5-fold, in related findings. Thus, escape from endocytic vesicles seems to be no major barrier for optimised, positively charged DNA/lipospermine or lipofectin complexes. However, for less positively charged lipospermine complexes gene transfer efficiency was found to be increased by a factor of 50 to 1000 by synthetic peptides INF6 (influenza virus derived sequence) and INF10 (artificial sequence)[208]. Simões *et al.* formed ternary complexes by ionic interactions of lipoplexes (DOTAP with or without DOPE) with GALA or HA-2 derived fusogenic peptides and showed that negatively charged ternary lipoplexes were efficient at transfection *in vitro*, and proposed the possibility of reduced interactions with negatively charged macromolecules *in vivo*. The real test will be how these systems perform *in vivo*[210].

Wilke and colleagues generated novel DNA complexes containing a palmitoyl modified DNA-binding peptide[173]. They demonstrated that association with an influenza peptide strongly enhances transfection activity. Gene transfer was found to be restricted to mitotic cells. The fact that mitotic activity (and subsequent disruption of the nuclear membrane) is required for transfection[211,212], suggests that nuclear entry of DNA from lipoplexes are takes advantage of the cellular disruptions that occur during mitosis. Although *in vitro* experimental results with these complexes are encouraging, *in vivo* results with these complexes have not yet been reported, and it remains to be seen if these complexes can meet the demands of the *in vivo* environment for successful gene delivery.

1.5.2.2 ENDOSOMAL ESCAPE OF CATIONIC POLYMER-BASED VECTORS

Although cationic polymer-based gene deliver vectors have progressed slowly towards *in vivo* transfection success and clinical trials, they probably hold more promise of

overcoming the extracellular and cellular obstacles to a successful gene delivery vector than do cationic lipid because of one main reason: cationic polymer-based GDVs have a large number of reactive sites available for the attachment of various ligands that may promote uptake of DNA/polymer complexes or provide a favourable intracellular trafficking pathway for the DNA/polymer complex. However, as it will be discussed later, the presence of these numerous unprotected reactive sites are a drawback if the aim is to produce a well defined, homogenous GDV.

Strategies for the delivery of DNA into target cells have been developed that are based on the construction of artificial viral-like particles incorporating only activities required for efficient DNA transport and expression but avoiding viral genomic information[2,35]. Complexes of DNA with ligand-polylysine conjugates for cellular uptake via receptor-mediated endocytosis fulfil some of the requirements of such reconstructed pseudo-viral vectors and have been developed extensively during the last years[213,214]. By covering plasmid DNA with polylysine molecules covalently attached to different ligand moieties, multimolecular toroid structures can be obtained which are small enough (80-100 nm) to be engulfed by endocytosis[167]. However, these particles lack the ability to actively escape from the endosome before reaching the lysosomal compartment, which strongly decreases transfection efficiency[169,215]. In several cell lines, the addition of chloroquine[216] or glycerol[217] considerably increases transfection efficiency, presumably by interfering with lysosomal degradation and enhancing the release of the DNA into the cytoplasm. Adenovirus particles have been incorporated to polymer-based vectors supply an endosome escape activity[218,219]. Addition of replication-defective adenovirus particles or rhinovirus particles either to the transfection medium[182,220] or directly linked to the PLL-DNA complex[1220,221,222] was found to strongly enhance gene delivery through the endosome destabilizing activity. Cotten *et al.* showed that it was possible to completely inactivate the viral genome, by treatment with methoxypsoralen plus irradiation and still retain endosmolytic activity carried by the viral capsid[223]. Although the adenovirus-enhanced trans(ferrin)fection system is highly efficient of *in vitro* and in *ex vivo* gene therapy, *in vivo* gene transfer efficiency however are relatively low, and further optimization is required[108,109].

Virus-free, synthetic systems have been generated containing specific cell binding ligands and synthetic membrane-destabilizing (fusogenic) peptides. Analogues of the 23 N-terminal amino acids of HA-2 ionically bound to polylysine-DNA complex (see Figure 1.4) has been shown to have endosome disruptive properties in a pH dependent manner and improve transfection efficiency[1]. The addition of fusogenic peptides of viral origin to the DNA-polylysine complex provides endosome escape activity in the absence of a viral genome, but is not able to fully reproduce the efficiency of the whole viral particle[1,167].

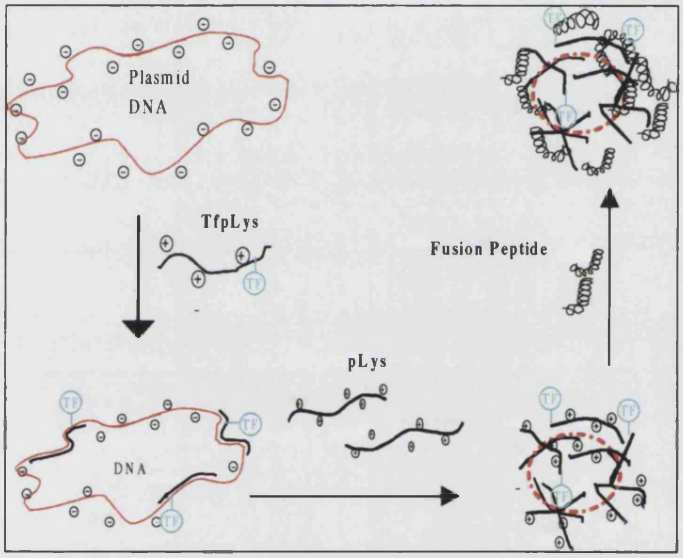

Figure 1.4 Schematic representation of the assembly of a quaternary gene transfer complex containing peptides ionically bound to polylysine. Abbreviations used are: TF/Tf, transferrin; TfpLys, transferrin-poly(L-lysine). Adapted from reference167.

Peptides have been incorporated into polylysine/DNA complexes by i) covalent linkage to polylysine[179,181] (ii) biotinylation and subsequent binding to polylysine-modified streptavidin[167] or (iii) noncovalent ionic interaction of the acidic, negatively charged peptides to positively charged DNA/polylysine complexes[167,183]. Often the DNA complexes also contained conjugates of polylysine with ligands for receptor-mediated endocytosis, but the effects of peptides were not dependent on the presence of a ligand. By the incorporation of the peptides, gene transfer was strongly (10 up to >1000-fold) enhanced in several cell lines. The enhancement of gene expression was strongly

dependent on the peptide sequence. Investigations with influenza HA-2-derived sequences[183] showed that the transfection levels largely correlate with the capacity of peptides to disrupt liposomes of natural lipid composition or erythrocytes in a pH-specific manner[167,183]. The hypothesis that the peptides enhance transfection activity by endosomal release is supported by the observation that the block of endosomal protonation by the specific inhibitor bafilomycin A reduces gene transfer activity[167]. There has as yet not been any reported *in vivo* work using polylysine/fusogenic peptide/DNA complexes.

The effect of membrane-active peptides on gene transfer with other polycation/DNA complexes has also been evaluated. Gottschalk and colleagues[76] replaced polylysine by the lysine-rich DNA-binding peptide K8 (sequence: YKA$(K)_8$WK). Transfections with DNA/K8 complexes resulted in modest expression levels; incorporation of an endosomolytic peptide, JTS-1, into these complexes enhanced gene expression by up to >1000-fold, similarly as previously seen with DNA/polylysine/peptide complexes. Wyman *et al.* have described another approach, which applies the cationic amphipathic peptide KALA (repeats of lysine-alanine-leucine-alanine) to serve for both DNA binding and membrane destabilization[224]. Efficient transfection of K562 and CV-1 cells was obtained with KALA/DNA complexes at a 10/1 (+/-) charge ratio. The efficiency was about 100-fold greater than found for polylysine/DNA complexes, but about 10-fold lower than with an optimized dendrimer developed by the same research lab (see below).

A positively-charged polyamidoamine cascade polymer ("dendrimer") has high transfection potential already in the absence of any membrane-active agent, as described in[73]. The polymer can be regarded as an endosomal buffering agent because of the low pKa of the terminal amines (6.9) and internal amines (3.9). This might prevent lysosomal degradation of the DNA and destabilize the endosomal/lysosomal vesicle. In agreement with this hypothesis, for optimum efficiency rather high dendrimer to DNA charge ratios (amine: phosphate, 6:1) have to be applied. At lower charge ratio (1:1, when amines are neutralized by the phosphates) the transfection activity is lost. When the pH-specific membrane destabilising peptide GALA[184] ('GALA', contains repeats of the motif Glutamic acid-alanine-leucine-alanine) is covalently attached to the

dendrimer, the transfection activity of the electroneutral complexes is recovered[73].

Similar findings were reported by using DNA complexes with the cationic polymer polyethylenimine PEI[15]. PEI is only partially protonated at physiological pH (only one of approximately 3-6 amino nitrogen molecules protonated). Upon acidification within the endosome/lysosome, PEI acts as proton sponge, with the protonation presumably triggering osmotic swelling and destabilisation of the endosomal/lysosomal vesicle. In order to improve transfection efficiency, cell-binding ligands have been incorporated by covalent linkage to PEI[225]. Incorporation of cell-binding ligands (transferrin or anti CD3 antibody) into DNA/PEI complexes resulted in an up to 100-fold increased transfection efficiency through the mechanism of receptor-mediated endocytosis. Notably, high-level gene expressions were found in the absence of chloroquine or DNA complex-linked adenovirus. Transferrin-PEI-mediated gene transfer can be significantly (up to 10-fold) augmented by the addition of an endosome-destabilizing influenza peptide[225]. Again, like with dendrimer but in contrast to the findings with polylysine or related peptides, the transfection is not strongly dependent on the presence of endosomolytic agents.

Wells and Fominaya have used genetic molecular biology techniques to engineer a modular multidomain DNA carrier protein (based on *Pseudomonas* exotoxin A) which has cell specific gene transfer ability but still needed polylysine to facilitate the condensation of the protein-DNA complex[226]. Whilst this approach may be more economical than chemical synthesis of large peptides/protein in large-scale manufacture, it is a very time consuming and tedious process which limits its use in research. It demonstrated however that a single multifunctional gene transfer agent could improve the transfection efficiency of DNA with a high degree of cell selectivity *in vitro*.

1.5.3 THE BARRIER OF LACK OF TRANSPORT WITHIN THE CYTOPLASM

Much research activity has focused on endosomal escape, the implication being that delivery to the cytoplasm would enable the particle to approach the nuclear envelope. However, the cytoplasm is a viscous fluid and diffusion of macromolecular particulate systems within this medium is slow[227, 228,229]. Escape early in the endosomal pathway may leave a condensed particle stranded some distance from the nuclear envelope.

Microinjection of plasmid into rat myotubes near the boundary of the nucleus resulted in a 56% rate of transfection, compared to 8% when injected 60 to 90 nm distal to the nucleus[92]. The transport of colloidal systems from one site to the other is a vital cellular process, but it is not a passive process. Vesicles, organelles and other colloidal structures are transported actively using molecular motors associated with the microtubule network or actin microfilaments[230.231,232,233,234]. Movement along microtubules is mediated by two classes of motor proteins in an orientated manner. Kinesins (+ kinesin-associated proteins) direct movement in an outward direction, usually linked to the secretory pathway while Dyneins (+ dynactin) move vesicles in the inward direction, normally associated with the endocytic pathway. The complex system of the secretory pathway at the molecular level is rapidly being unravelled. Viruses appear to have evolved mechanisms to use the dynein system, which directs vesicles from the endosome toward the perinuclear region. It is possible that binding domains for dynein could be present within viral capsids, allowing active transport of the virus in the cytoplasm.

The method of genetic mutation employed by biochemists to study the natural role of transport proteins, amongst others, has yet to be applied to the study of gene delivery vehicles. Gene therapy scientists have begun to explore the fate of transfection complexes once in the cytoplasm. Injection of naked DNA into Xenopus oocytes gave negligible expression but injection of either PEI or poly-L-lysine polyplexes into the cytoplasm of cells resulted in expression[235,236]. Researchers found that higher molecular weight poly-L-lysines/DNA complexes gave higher expression levels following injection into the cytoplasm. This observation suggests that polylysine probably protects DNA from nuclease degradation and that higher molecular weight poly-L-lysines provide better nuclease protection. An alternative explanation put forward by Wolfert and Seymour was that higher positive zeta potential of pLL/DNA complexes provided enhanced nuclear delivery by binding to nuclear-import protein[236]. Lipoplexes have also been injected into the cytoplasm. Zabner *et al.* and Pollard et al. found no expression following cytoplasmic injection of DOTAP or DMRIE/DOPE lipoplexes respectively[107,235]. Nuclear injection of lipoplexes also results in no expression unless the charge ratio is below neutrality[107]. The reason for expression following cytoplasmic injection of polyplexes but not lipoplexes may be because of the presence of cationic

residues on the surface of polyplexes which may act as nuclear localisation signals (NLSs) enhancing nuclear uptake (section 1.5.4) and/or due to the large size of the large size of lipoplexes.

For gene delivery vehicles to be effective in mediating gene delivery, following endocytosis, the must be utilising the cytoplasmic transport system to some extent. For example, Zabner *et al.* observed that lipoplexes, which remained within endosomal vesicles, appear to localise to the perinuclear region[107]. Also depolymerisation of microtubules and inhibition of microfilament formation by vinblastine and cytochalasin B respectively, prevented movement of DNA within endosomes and lysosomes towards the nucleus, resulting in reduced expression[237]. It seems likely that cytoplasmic transport is a limitation in non-viral gene delivery but these issues have yet to be adequately resolved.

1.5.4 THE BARRIER OF THE NUCLEAR MEMBRANE

The barrier of the nuclear membrane of non-dividing cells to macromolecules and particles that are not actively transported is formidable and has been demonstrated by the observation that a 1000-times more plasmid copies are required to achieve expression following injection into the cytoplasm compared with direct injection into the nucleus[235]. Pouton[238] has discussed the importance of the recognition of oligopeptide sequences termed nuclear localisation signals (NLS), which mediate the uptake of nucleoproteins, in a review of the requirements for active nuclear uptake of polynucleotides and supramolecular complexes. Sebestyén *et al.*[239] and Ciolina *et al.*[240] have both reported the enhancement of nuclear uptake of modified plasmid DNA, but not expression of reporter protein, following the linking of NLS sequences to DNA and incubating with digitonin-permeabilized cells. The preservation of the function of NLS sequences in a GDV after endocytosis and endosomal escape to provide a significant enhancement of transduction in non-dividing cells *in vitro* and particularly *in vivo* remains a challenging prospect.

The nuclear membrane prevents uptake of the majority of macromolecules greater than 70 kDa into the nucleus, unless they are able to interact with the nuclear transport

system[241,242,243]. Poor access of DNA plamids to the nucleus represents a major barrier to the success of non-viral gene therapy[107,173]. Dividing cells are easier to transfect as the DNA may enter the nucleus prior to the end of telophase and nuclear envelope reassembly. Wilke and colleagues found that over 40% of expressing HeLa or NIH3T3 cells occur as adjacent pairs with comparable expression, suggesting they are the products of a previous mitotic event[173]. Feldherr and Akin[244], found that the rate of nuclear uptake was also slower in non-dividing confluent NIH3T3 cells compared to dividing NIH3T3 cells. Since most of the target cells *in vivo* are in a non-dividing (quiescent) state the aim of non-viral delivery development must be the improvement of gene expression within *in vitro* models of quiescent cells.

Research on viral tropisms suggests that some viruses have evolved means of interaction with nuclear transport systems[245,246,247,248], and there is a good chance that active transport can be utilized for delivery of plasmids[238]. The nuclear transport system involves both stationary components and mobile factors acting in concert to move macromolecules through the nuclear pore complex (NPC). The nuclear membrane of mammalian cells usually has several thousand NPCs embedded in them. The NPC allows passive diffusion of molecules up to diameters of 9 nm, although even smaller nucleoproteins, such as histones, are actively transported through the NPCs. Nucluoproteins include motifs terms nuclear localization signals (NLSs), which interact with cytosolic receptors known collectively as importins, and initiate the active transport of nucleoproteins through the nuclear pore into the nucleus[238]. Nucleoprotein NLSs do not have a strict consensus sequence but are characterised by clusters of four or more cationic residues and are often flanked by the a-helix-breakers, proline or glycine[238]. It is clear that poor access of DNA plasmids to the nucleus represents a major barrier to the success of non-viral gene delivery. Researchers are studying the possibility of including NLSs sequences to gene delivery vehicles to improve uptake of plasmids into the nucleus and ultimately to improve transfection efficiency[239,240].

Another group of researchers are investigating the role of DNA base sequences indirectly promoting plasmid DNA uptake. Work by Dean has suggested that plasmid sequences can mediate nuclear localisation in non-dividing cells without the need for nuclear localisation peptides[249]. Nuclear import was found to be sequence specific: a

region of SV40 DNA contains binding sites for many transcription factors. Since these transcription factors contain NLSs to facilitate their nuclear targeting/uptake and bind DNA, they may interact with the cytoplasmic DNA and then shuttle it to the nucleus. Nuclear targeting sequences were shown to be able to mediate increased expression in liposome and polycation- transfected non-dividing cells in a cell-specific manner[250]. This result is significant, as the level of expression obtained in non-dividing cells has to date been low. The barrier of the nuclear membrane will have to be overcome in order to improve gene delivery to non-dividing cells.

1.6 AIMS AND OBJECTIVES

Commercially available polylysine used in polymer-based vectors are very heterogeneous, containing between 50-200 lysine residues, based on viscosity measurement and molecular sizing chromatography[76]. Such a high degree of heterogeneity is less than ideal in the development of a gene delivery product. Gottschalk *et al.* showed that shorter and chemically pure 13-mer peptide, K8, (with eight lysine residues in a central cluster) was better than commercially available polylysine in condensing DNA and was much less toxic[167].

The dependence on commercially available polylysine to condense DNA has meant that many attempts to construct a synthetic virus-like gene transfer agent utilise a multi-staged process of self-assembly by spontaneous electrostatic interactions of charged reagents[1,35,167,] as illustrated in Figure 1.4. Other attempts that have been made by some researchers to depart from the reliance on commercially available polylysine involved the use of a cyclic integrin-binding peptide with a DNA-binding l6-lysine tail (a bifunctional peptide) which has been reported to be effective *in vitro*[170,171] and *in vivo* (in combination with lipofectin)[172].

This project involved the design, synthesis, assembly, characterisation and biological evaluation of polypeptides that could be used to improve the delivery of plasmid DNA, using solid-phase synthetic peptide chemistry. The aim of this project was to construct a single polypeptide which has three components: (i) a biologically active peptide to promote the escape of the DNA-polymer complex from the endosome (fusogenic

peptide), (ii) an oligolysine section to provide a biodegradable DNA-binding region and (iii) a ligand to promote receptor-mediated uptake.

The approach taken was to biologically test the initial bifunctional construct using *in vitro* and *in vivo* transfection experiments before making modifications to it in order to overcome any *in vivo* barriers to gene delivery that would be encountered. The N-terminal sequence of influenza virus haemagglutinin HA-2 was used as a template to synthesize analogues of fusogenic peptides linked to an oligolysyl chain as a first step towards a synthetic virus-like gene transfer agent.

Chapter 2 describes the synthesis of membrane-active fusogenic peptides and DNA-binding oligolysyl peptides, and novel bifunctional peptides that combine the two capabilities: DNA-binding and endosomal escape. A schematic representation of how a bifunctional peptide might interact with plasmid DNA is shown in Figure 1.5.

Attempts were also made to synthesize and purify fusogenic peptides with oligo/polylysyl and oligo/polyhistidyl chains. The investigation of the effect of charge ratio on the ability of bifunctional peptides to promote gene transfer in mammalian cells *in vitro* and comparison with ternary complexes consisting of membrane-active fusogenic peptides and DNA-binding oligolysyl peptides are described in Chapter 3. Also the initial investigation into effect of a novel fusogenic peptide with an oleoyl attachment on the transfection efficiency of a cationic lipid is described in Chapter 3. Physical characterisation of bifunctional peptides (particle size and zeta potential measurements) and investigation of the effect of serum, serum albumin and chloroquine on the *in vitro* transfection efficiency of bifunctional peptides are also described in Chapter 3. Chapter 3 also describes the *in vivo* transfection activity of bifunctional peptides following intramuscular and intratumoural injection in mice.

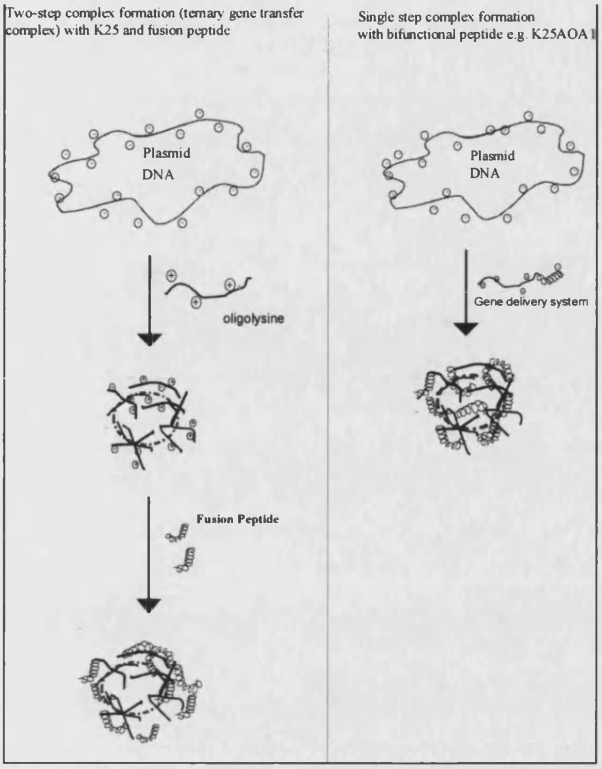

Figure 1.5 Schematic representation of two-step ternary complex formation (left) by ionic self- assembly obtained by sequential mixing of excess oligolysine with DNA followed by addition of fusogenic peptide. The right pane shows a single-step complex formation of a binary complex between a linear bifunctional peptide consisting of a DNA-binding moiety and a fusogenic peptide moiety. The positively charged component would interact and condense DNA whilst the negatively charge fusogenic component would be repelled by negatively charged DNA towards the surface of particle, freeing it to interact with membranes.

2 SYNTHESIS AND PURIFICATION OF PEPTIDES

2.1 INTRODUCTION

This chapter describes the synthesis and extent of purification of fusogenic peptides, oligo/polylysine peptides, oligo/polyhistidyl polylysine, and bifunctional peptides comprising oligolysine coupled to fusogenic peptide sequences with or without oligohistidyl sequences. The synthesis and purification attempt at an oleoyl analogue of a fusogenic peptide is also described.

2.1.1 OVERVIEW OF SOLID-PHASE PEPTIDE SYNTHESIS

Solid-phase peptide synthesis is the step-wise construction of a polypeptide chain attached to an insoluble polymeric support. Solid-phase peptide synthesis strategy retains the chemistry proved in solution while adding a covalent attachment step that links the peptide chain to an insoluble polymeric support. This strategy permits unreacted reagents to be removed by simple washing steps without loss of product. A schematic overview of this process is shown in Figure 2.1. An overview of the chemistry behind the method is described below.

Synthesis proceeds from the carboxyl terminus to the amino terminus of the polypeptide to minimize the risk of racemization. The carboxyl group of each incoming amino acid is activated by one of several strategies and couples with the group of the preceding amino acid. The N^{α}-amino group of the incoming amino acid is temporarily protected in order to prohibit peptide bond formation at this site. The "temporary" protecting group of the N^{α}-amino group of the newly attached amino acid is deprotected (removed) at the beginning of the next synthesis cycle. In addition, reactive side chains on the amino acids are protected with "permanent" protecting groups. Repeating the synthesis cycle extends the polypeptide chain. Excess reagents and high concentrations of reagents drive reactions as close to completion as possible. This generates the maximum possible yield and highest quality of the final product.

When the peptide has been fully assembled, the side chain protecting groups are removed and the peptide is released from the solid support, using conditions that inflict

minimal damage on labile residues. Following synthesis and cleavage, the product is analysed to verify the sequence and, if necessary, can be purified by gel chromatography or high performance liquid chromatography (HPLC).

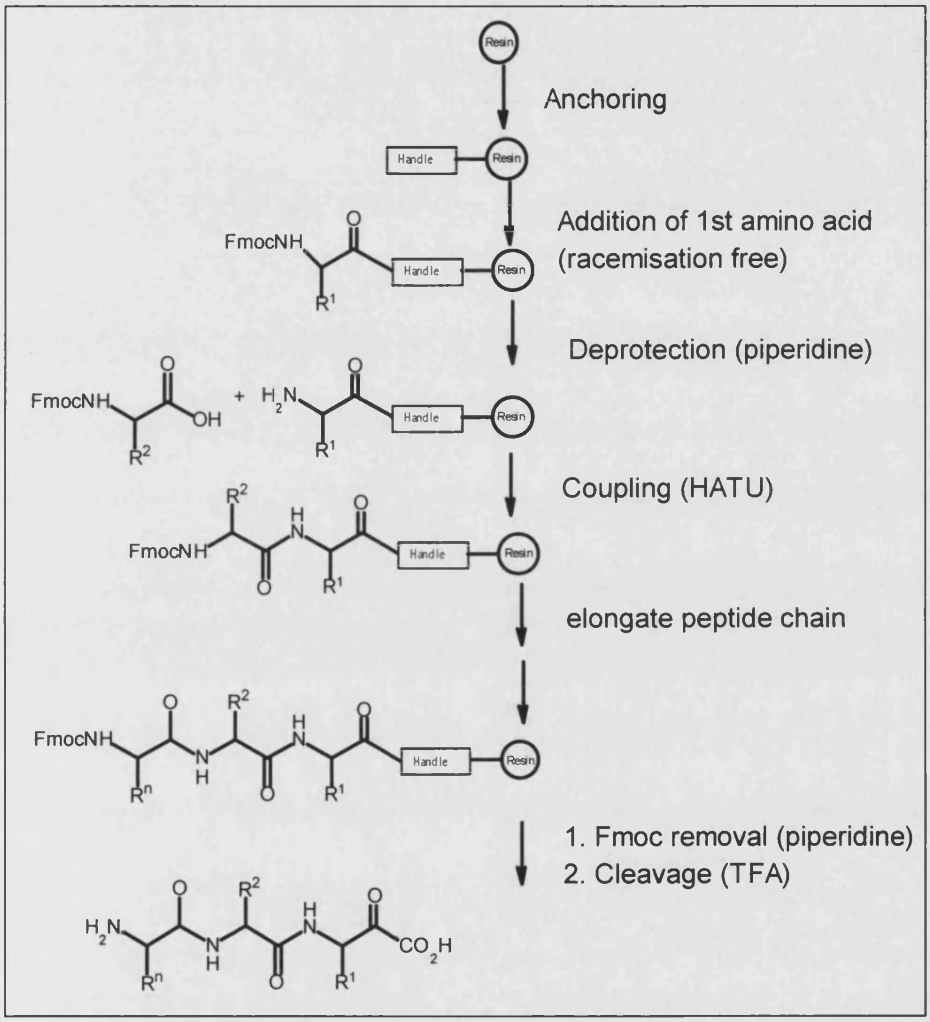

Figure 2.1 Schematic overview of solid-phase peptide synthesis.

2.1.2 TEMPORARY AND PERMANENT PROTECTING GROUPS

The identity of the N^{α}-amino blocking group determines both the synthetic chemistry employed and the nature of the side chain protecting groups. The two most commonly used N^{α}-amino protecting groups are Fmoc (9-Fluorenylmethoxycarbonyl, Figure 2.2) and tBoc (tert-butyloxycarbonyl).

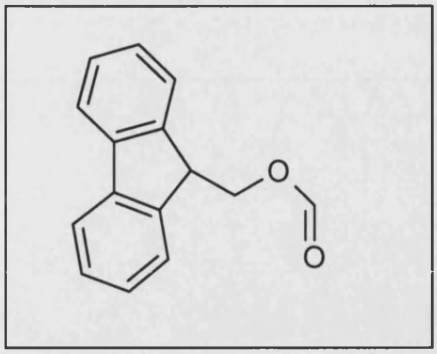

Figure 2.2 9-fluorenylmethoxycarbonyl (Fmoc).

In Fmoc chemistry, the N^{α}-amino groups are protected using the Fmoc (9-fluorenylmethoxycarbonyl) group, while side chain protection is generally provided by ester, ether and urethane derivatives of tert-butanol. The Fmoc protecting group is base-labile, and is usually removed with a base such as 20% (v/v) piperidine in *N,N*-dimethylformamide (DMF). The mechanism of deprotection of the N^{α}-amino Fmoc group is shown in Figure 2.3. Synthesis conditions used in Fmoc chemistry procedures are much milder than those employed in tBoc chemistry. In Fmoc chemistry, the peptide chain is not subjected to acid solution at each cycle and the final deprotection and cleavage step can be achieved using TFA rather than the much stronger HF acid conditions required for tBoc peptide chemistry.

At the end of the synthesis using Fmoc peptide chemistry, the side chain protecting groups are removed by a single treatment with trifluoroacetic acid (TFA), which also cleaves the bond anchoring the peptide to the resin support (see Figure 2.4 and Figure 2.5 for mechanisms). In tBoc chemistry, the tBoc protecting group is removed with a mild acid (usually dilute TFA), and hydrofluoric acid (HF) is used both to deprotect the amino acid side chains and to cleave the peptide from the resin support.

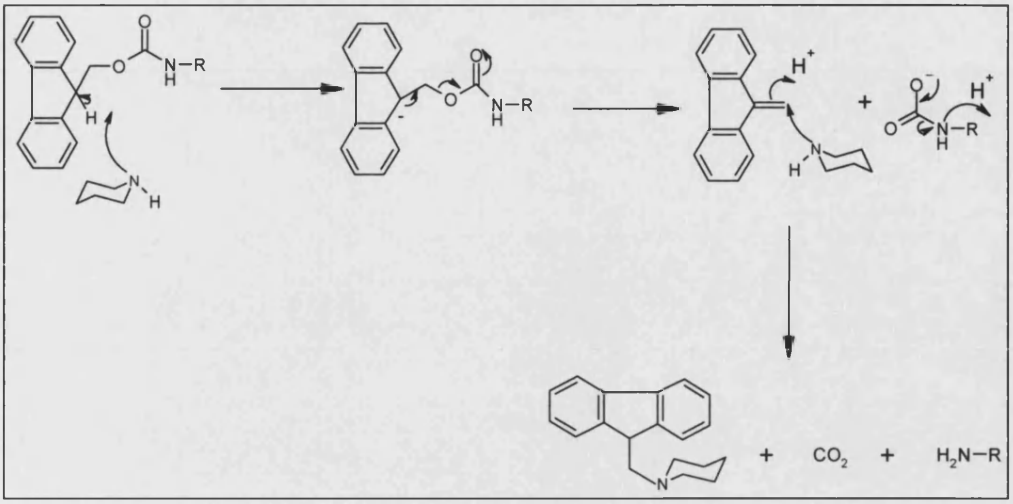

Figure 2.3 Mechanism of deprotection of temporary Fmoc group using 20% (v/v) piperidine in DMF.

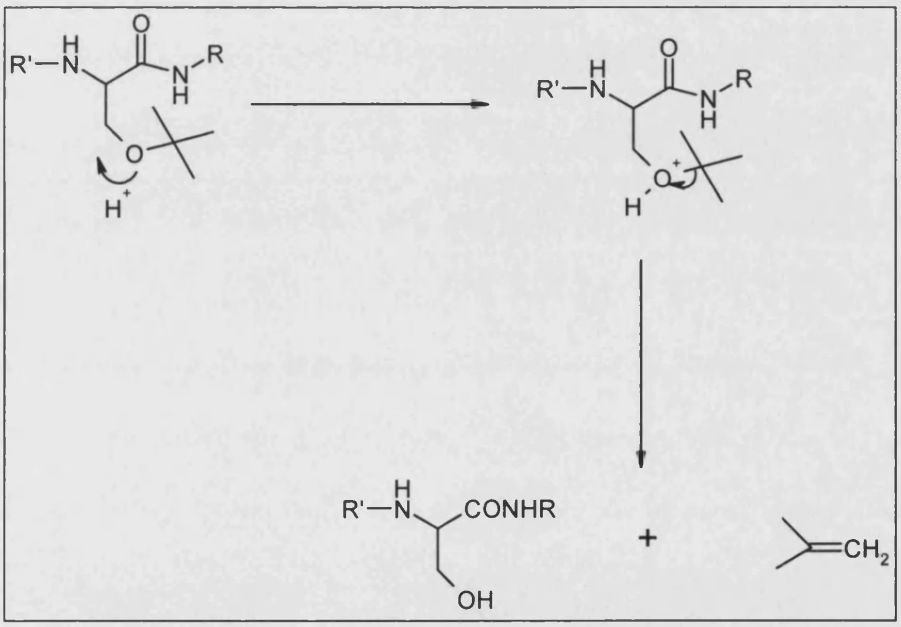

Figure 2.4 Mechanism of deprotection of permanent side chain protection groups using 90% (v/v) TFA and 10% (v/v) scavengers (thioanisole/ethanedithiol/anisole).

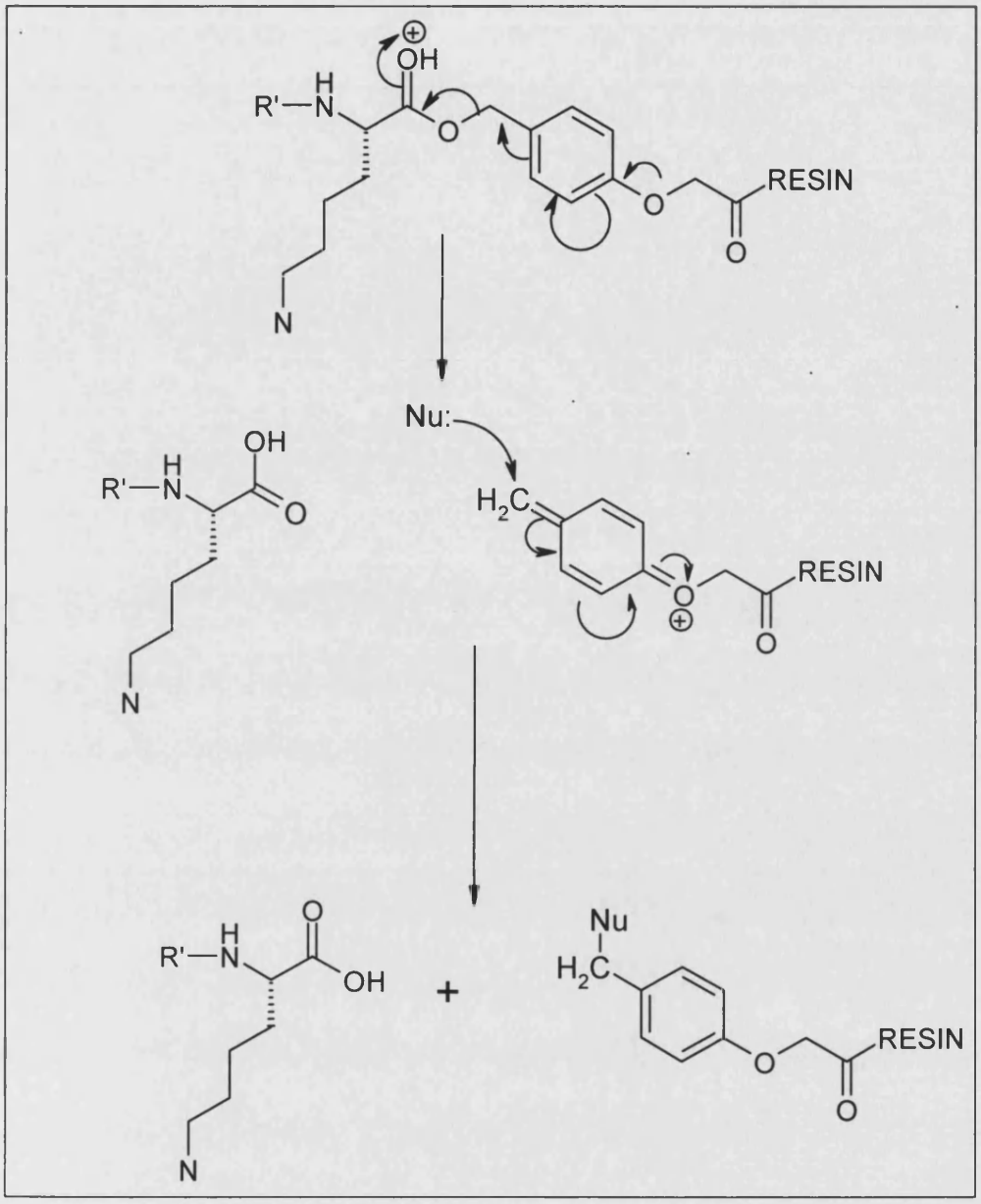

Figure 2.5 Mechanism of deprotection of peptide from resin using 90% (v/v) TFA and 10% (v/v) scavengers (thioanisole/ethanedithiol/anisole).

2.1.3 ATTACHMENT OF FIRST AMINO ACID TO SOLID SUPPORT: ANCHORING

Polyethylene glycol polystyrene (PEG-PS) is the current solid support of choice for Fmoc chemistry. The PEG incorporated on the resin closely matches the hydrophilic nature of the growing peptide backbone and side chains. This effects a higher level of solvation of the growing peptide and thus more efficient coupling and deprotecting reactions[251]. The PEG-PS resin is available prederivatised with a linker, hydroxymethylphenoxyacetic acid (HMPA) as peptide acid resin (PAC-PEG-PS, Figure 2.6) from PerSeptive Biosystems, Framingham, MA, USA. Attachment of the C-terminal amino acid to the PAC-PEG-PS support is by an esterification procedure where the activated amino acid is coupled in the presence of 0.1 equivalent of 4-dimethylaminopyridine. This method ensures coupling of the first amino acid to the support with minimal racemization.

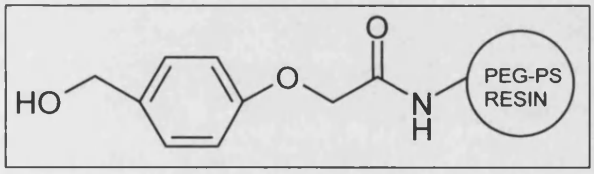

Figure 2.6 Peptide Acid PEG-PS resin.

2.1.4 COUPLING REACTIONS

The carboxyl group of the incoming amino acid must be activated to provide a better leaving group and activation generally utilises several methods two of which are described as follows: 1) Preactivated active esters/HOAt: These are pentafluorophenyl (OPfp) esters of the amino acids. Coupling reactions using preactivated active esters are catalysed by 1-hydroxy-7-azabenzotriazole (HOAt). The mechanism of the coupling reaction is shown in Figure 2.7. 2) In situ activation by HATU: The amino acid derivative is mixed with O-(7-azabenzotriazol-1-yl)1,1,3,3-tetramethyluronium hexafluorophosphate (HATU) together with diisopropylethylamine (DIPEA). HATU enhances reactivity, reduces racemization and is suited for hindered amino acids and difficult couplings[252]. The mechanism of coupling reaction of amino acid catalysed by HATU is shown in Figure 2.8.

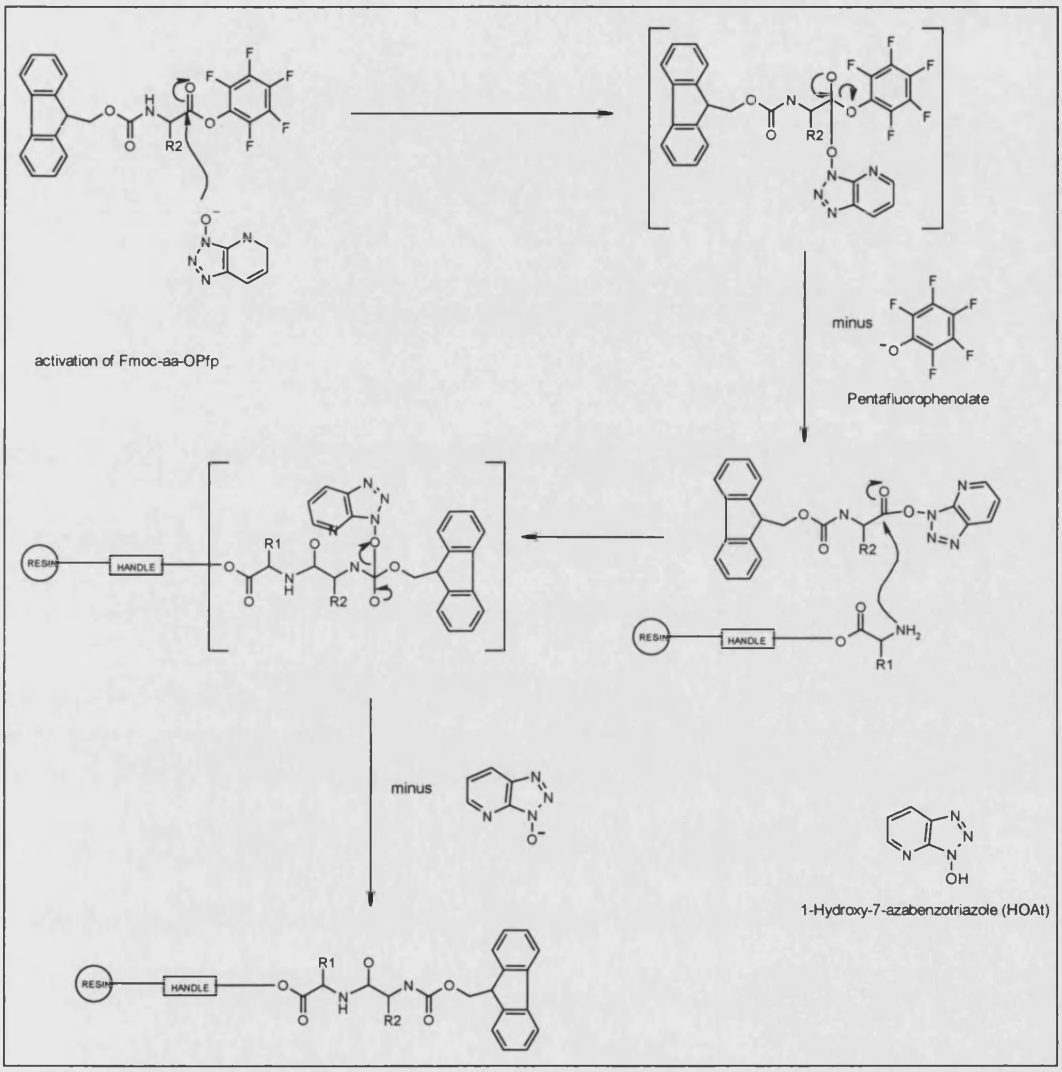

Figure 2.7 Mechanism of coupling reaction of Fmoc-protected L-amino acid preactivated ester mediated by HOAt.

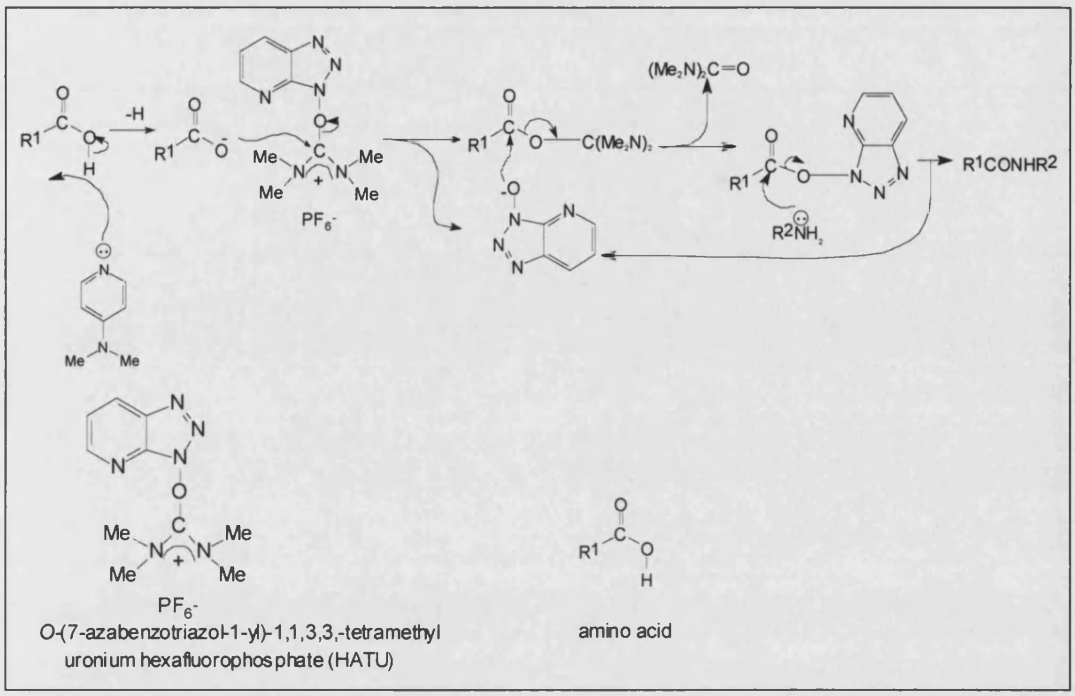

Figure 2.8 Mechanism of coupling reaction of amino acid catalysed by HATU.

2.1.5 POST SYNTHESIS WORK-UP

After completion of the automated synthesis, the PEG-PS support to which the peptide is attached is washed in succession with DMF, methanol and dichloromethane. After thorough drying under high vacuum, the solid support is transferred to a flask for the cleavage reaction. When the PAC-PEG-PS support is used to produce the peptide acid, cleavage is achieved using trifluoroacetic acid (TFA) plus appropriate scavengers. In Fmoc solid-phase peptide synthesis strategy, the protecting group and resin linkage design is such that the final release of the peptide chain from the support can be carried out without the use of strong acids or bases to provide the C-terminal residue either as the acid or carboxamide. Peptides synthesized by this approach are released at room temperature by TFA scavenger cocktails with concurrent side chain deprotection. The presence of scavengers with the cleavage reagent is required to suppress the damaging effect that the carbonium ions, produced during cleavage, can have on amino acid residues most at risk to damage (methionine, cysteine, tryptophan and possibly tyrosine). Cleavage of peptides containing methionine, cysteine and tryptophan require conditions using the mixture TFA/anisole/1,2-ethanedithiol (95:2.5:2.5; v/v/v) as scavenging reagents.

2.2 MATERIALS AND METHODS

2.2.1 PEPTIDE SYNTHESIS

Peptides were assembled on a Millipore 9050 plus PepSynthesizer™ (Millipore Corp. Bedford, MA, USA) using Fmoc solid-phase peptide synthesis method (the Atherton-Sheppard approach)[253]. All peptides should be assumed as L- isomers, unless specifically stated as D- isomers.

Polyethylene-glycol-polystyrene (PEG-PS) (Perseptive Biosystems, Framingham, MA, USA), pre-derivatised with a linker group and the first amino acid residue of the desired peptide sequence to be synthesized, was used as the solid support resin. For D-amino acid peptide analogues, the first amino acid (lysine) was coupled onto PAC-PEG-PS (Figure 2.6) in the presence of 0.1 equivalent of 4-dimethylaminopyridine. Amino acids protected at the primary amino end with Fmoc and activated as Opfp esters, (Perseptive Biosystems) were coupled for 30 minutes in situ using 0.3 M 1-hydroxybenzotriazole (HOAt) in N,N-Dimethylformamide (DMF, peptide synthesis grade; Rathburn Ltd, Scotland). Where unactivated Fmoc protected amino acids were used, HATU was used as the activating/coupling reagent. All coupling reactions were performed using reagents at a 4-fold excess of the required molar equivalent. The side chain protection groups for the amino acid used were as follows: Asp(*tert*-butyl ester), Glu(*tert*-butyl ester), Lys(*tert*-butyloxycarbonyl), Tyr(*tert*-butyl ether). Deprotection of primary amino group was achieved by washing the resin with 20% (v/v) piperidine in DMF for 5 minutes followed by the automated removal of piperidine traces by a DMF-wash cycle for 10 minutes prior to each coupling step. After the final coupling and deprotection step, the resin was washed in succession with DMF, dichloromethane (DCM) and diethyl ether and dried by passing nitrogen gas.

The removal of side chain protecting groups from relevant amino acids and the cleavage of the peptide from the resin and was achieved by treating 1 g of resin with 5 ml of Trifluoroacetic acid (TFA)/thioanisole/ethanedithiol/anisole (90:5:3:2) for 4 hours. The duration of cleavage from the resin was arrived at by performing small-scale cleavage reactions (trial deprotections) at time points 1.5, 2, 2.5, 3, 3.5, 4, 5 and 6 hours after

adding TFA/scavengers mixture and analysing the precipitated peptide (procedure described below) by HPLC (conditions described below). The resin was separated from the liquid mixture of peptide/TFA/scavengers by filtrating through a sintered glass funnel under vacuum. Removal of TFA from the reaction mixture was achieved by adding 5-fold volume petroleum spirit (40-60%) and gently decanting off the petroleum spirit layer. This process was repeated twice, leaving a yellow oily liquid residue containing a mixture of the cleaved peptide, residual TFA and scavengers. The peptide was precipitated by gentle addition of ether (3 x 20 ml) and decanted to remove the scavengers. The crude peptide was dissolved in distilled water (sometimes adding a drop of ammonia solution to aid dissolution of the fusion peptides sequences which have a net negative charge) and lyophilised.

2.2.2 SYNTHESIS OF OLEOYL-FUSOGENIC PEPTIDE

A fusogenic peptide sequence GLF EAIA GFI ENGW EGMI DGWYGK-**(allyloxycarbonyl)** was first synthesized by solid-phase method as described above. An allyloxycarbonyl group protected the side chain ε-amino of lysine in the sequence above, whereas all the other residues requiring side chain protection had tert-butyl protection as mentioned above. The resin with the completed peptide sequence and N-terminal temporary Fmoc capping was washed in succession with DMF, dichloromethane (DCM) and diethyl ether and dried under high vacuum for 1 hour. The following procedure to remove the allyloxycarbonyl group was carried out under oxygen-free argon conditions, using an Atmos™ bag (Sigma-Aldrich): tetrakistriphenylphosphine palladium (0) ($Pd(PPh_3)_4$, 1 gram), in a solution of chloroform (5 ml) containing 5% (v/v) acetic acid and 2.5% (v/v) *N*-methylmorpholine, was added to resin in an aluminium foil-covered round-bottomed glass flask under argon. The reaction mixture was stirred with a magnetic flea and stirrer for 2 hours. The resin was recovered by filtering off (sintered glass funnel) the reaction mixture and washing the resin with a solution of 0.5% (v/v) DIPEA and 0.5% (v/v) sodium diethyldithiocarbamate in DMF to remove trace metal ions. The resin tested positive to a ninhydrin test, confirming that the allyloxycarbonyl group had been successfully removed. After drying the resin under high vacuum for 1 hour, a five-fold excess of oleoyl chloride (Sigma-Aldrich) to the dried resin in a round-bottomed flask and stirred

under argon for 1 hour. The resin was then recovered from the reaction mixture by filtering off the excess oleoyl chloride followed by washing the resin in succession with DMF, DCM and diethyl ether. The resin was then dried under high vacuum for 1 hour. The resin tested negative to a ninhydrin test, confirming that the coupling of the oleoyl chain unto the side chain amino group of lysine was successful. The N-terminal Fmoc protection group was then removed by adding a 5 ml aliquot of 20% (v/v) piperidine in DMF for 5 minutes, followed by washing in succession with DMF, DCM and diethyl ether. The peptide was then cleaved from the resin, with the concomitant removal of the *tert*-butyl side chain protecting groups by treating 1 g of resin with 5 ml of Trifluoroacetic acid (TFA)/thioanisole/ethanedithiol/anisole (90:5:3:2) for 4 hours and precipitating the peptide as previously described above.

2.2.3 PEPTIDE PURIFICATION

The fusogenic peptides were purified using reverse phase high performance liquid chromatography (HPLC). Fusion peptides were dissolved in 5% (v/v) acetonitrile, 0.3% (v/v) aqueous ammonia solution and pumped (ConstMetric™ 400 pump, Thermo Separation Products or Waters™ 600 multisolvent delivery system under the control of the Waters™ 600E Systems controller, MilliQ™, USA) onto a 2.5 x 25 cm POROS™ column (POROS™ packing material obtained from PerSeptive Biosystems, Framingham, MA, USA, and column assembled in our laboratory). Fusion peptides were eluted with a variable linear gradient between 5% (v/v) acetonitrile, 0.3% (v/v) aqueous ammonia solution and 50% (v/v) acetonitrile and 0.3% (v/v) ammonia solution. POROS™ columns are polymer based and suitable for pH ranges between 1 and 14. Fusion peptides with oligolysyl chains (bifunctional peptides) were dissolved in 0.1% (v/v) aqueous TFA (HPLC grade, redistilled from glass), 5% (v/v) acetonitrile and pumped onto a 10 x 25 cm Vydac™ C18 column and eluted with a varied gradient (see results section for details) between 0.1% (v/v) aqueous TFA, 10% (v/v) acetonitrile and 0.1% (v/v) aqueous TFA, 65% (v/v) acetonitrile. The purity of the peptides was determined by analytical HPLC using either Waters™ 600 multisolvent delivery system or the ConstMetric™ 400 pump and the absorption of the elute measured by the Waters™ 490E Programmable multiwavelength UV detector or LDC Analytical SpectroMonitor™ 5000 photodiode array detector, respectively, at the wavelength of 217 and 277 nm.

2.2.4 ANALYTICAL METHODS

The identities of the synthesized peptides were determined by MALDI-TOF mass spectrometry or amino acid sequencing. Matrix-assisted laser desorption/ionization (MALDI) enables a soft ionisation to take place, with little or no fragmentation, and this coupled with time-of-flight mass spectrometry (TOF-MS), permits the accurate measurement of biomolecules like DNA, proteins and long peptides. The MALDI technique involves co-depositing a solution of a relatively volatile, UV-absorbing organic compound, known as the matrix, with the biopolymer on a metal sample plate. During evaporation of the solvent, the biomolecule is incorporated into the matrix crystalline lattice. The materials in the matrix crystal are then ionised by a short laser pulse. The laser energy is primarily absorbed by the matrix and transferred to the biomolecule, which ionises with little or no fragmentation. 1 μl of this solution was then deposited onto the MALDI plate and allowed to dry at ambient temperature. The samples were analysed by Klaus Rumpel at Pfizer Central Research (Sandwich, Kent) on an MALDI-TOF Voyager-DE STR BioSpectrometry workstation in positive ion, linear mode at an accelerating voltage of 20 kV. Alpha-cyano-4-hydroxycinnamic acid was used as the matrix for all samples except for target compounds $K_{25}H_{10}$AOA1 and $K_{25}H_{20}$AOA1, where sinapinic acid was used. The α-cyano-4-hydroxycinnamic acid matrix solution was made by preparing a saturated solution of the solid matrix in 50% (v/v) acetonitrile/0.3% (v/v) TFA in water. The sinapinic acid matrix solution was made by preparing a saturated solution of the solid matrix in 60% acetonitrile/ 0.3% (v/v) TFA in water. All samples were dissolved in 100 μl of 0.1% (v/v) TFA in water except for those compounds that were insoluble in this solvent, in which case they were dissolved in 100% TFA and then diluted 1:10 with water prior to spotting. An aliquot of 0.5 μl of each sample was spotted on the MALDI plate with 0.5 μl of matrix. K_{25}AOA1, K_{25}AOA1#1 (the whole peak of K_{25}AOA1, without peak-splicing, see section 2.3.2.1) and $K_{25}H_{20}$ were calibrated externally with a calibration spectrum of insulin in α-cyano-4-hydroxycinnamic acid matrix. Samples named $K_{25}H_{10}$AOA1 and $K_{25}H_{20}$AOA1 were calibrated for externally with a calibration spectrum of high mass protein standards: horse myoglobin, bovine insulin and thioredoxin in sinapinic acid matrix. All the other samples were calibrated externally with a calibration spectrum of low mass protein standards: des-Arg1-Bradykin, Angiotensin 1, Glu1-Fibrinopeptide B and

adrenocorticotropic hormone sequence residues 18-39 in α-cyano-4-hydroxycinnamic acid matrix.

Peptide sequencing was performed was by Dr. J.E. Fox (Alta Bioscience, The University of Birmingham) using the ABI 470A protein sequencer (Applied Biosystems) based on Edman's degradation reaction.

2.2.5 NOMENCLATURE OF PEPTIDES

The bifunctional peptides were named in the order in which the functional moieties were assembled on the peptide synthesizer, i.e. K_{25}AOA1 is HO_2C-K_{25}AOA1-NH_2.

The following peptides were synthesized (subscript denotes the number of consecutive lysyl or histidyl residues):

Name	Sequence
AOA1	H_2N-GLF EAIA GFI ENGW EGMI DGWYG-CO_2H
AOA2	H_2N-GLF EAIA GFI ENGW EGMI DGWYGF-CO_2H
INF7	H_2N-GLF EAIE GFI ENGW EGMI DGWYG-CO_2H
K_{10}AOA1	H_2N-GLFEAIA GFI ENGW EGMI DGWYG-K_{10}-CO_2H
K_{25}AOA1	H_2N-GLFEAIA GFI ENGW EGMI DGWYG-K_{25}-CO_2H
K_{25}INF7	H_2N-GLF EAIE GFI ENGW EGMI DGWYG-K_{25}-CO_2H
K_{10}INF7	H_2N-GLF EAIE GFI ENGW EGMI DGWYG-K_{10}-CO_2H
DK_{25}AOA1(N)	H_2N-GLF EAIA GFI E GW EGMI DGWYG-K_{25}-CO_2H
$K_{25}H_{10}$AOA1	H_2N-GLF EAIA GFI ENGW EGMI DGWYG-H_{10}-K_{25}-CO_2H
$K_{25}H_{20}$AOA1	H_2N-GLF EAIA GFI ENGW EGMI DGWYG-H_{20}-K_{25}-CO_2H

Table 2.1 Names and sequence of peptides synthesized in this project

Also, oligo/polylysyl sequences K_{10} and K_{25} were synthesized in order to compare binary and ternary complex formation systems (Chapter 3). In an attempt to investigate the effect of oligo/polyhistidine chain on the transfection activity of the bifunctional peptide K_{25}AOA1, oligo/polylysyl sequences with oligohistidyl chains $K_{25}H_{20}$ and

$K_{25}H_{10}$ were synthesized for use as control reagents in transfection experiments. The D-amino analogue of K_{25}AOA1 (named DK_{25}AOA1) was synthesized to investigate if resistance to protease degradation would make it active in transfection experiments in the presence of serum.

2.3 RESULTS

2.3.1 PEPTIDE SYNTHESIS

The quantities of the initial batches peptide that were synthesized and the yields obtained are summarised in the table below:

Name	Target quantity (number of moles)	Approximate yield of crude peptide (mg)
AOA1	0.03	69
AOA2	0.03	71
INF7	0.03	77
K_{25}AOA1	0.04	183
K_{25}INF7	0.03	137
K_{10}INF7	0.03	93
$K_{25}H_{20}$AOA1	0.025	154
$K_{25}H_{10}$AOA1	0.025	142
K_5	0.08	41
K_{10}	0.06	61
K_{15}	0.04	62
K_{25}	0.02	52
$K_{25}H_{10}$	0.05	183
$K_{25}H_{20}$	0.05	238

Table 2.2 Yield of crude peptides synthesized.

2.3.2 PEPTIDE PURIFICATION AND ANALYSIS

2.3.2.1 PURIFICATION AND ANALYSIS OF $LK_{25}AOA1$ AND $LK_{25}INF7$

Identical solvent gradients were used to purify LK_{25}AOA1, and LK_{25}INF7. The chromatogram for LK_{25}AOA1 shown in Figure 2.9 was obtained by running the solvent gradient shown in Table 2.3 on a Waters™ 600 HPLC system (Millipore, USA) at a flow rate of 20 ml/min through a Vydac™ C18 column using solvent A: 0.1% (v/v) aqueous TFA and solvent B: 95% (v/v) acetonitrile and 5% (v/v) of 0.1% (v/v) aqueous TFA. An investigative linear gradient between 95% (v/v) solvent A (0.1% (v/v) aqueous TFA) and 95% (v/v) solvent B (95% (v/v) acetonitrile and 5% (v/v) of 0.1% (v/v) aqueous TFA) over a period of 2 hours was run to determine at what percentage of solvent B the main peak was eluting, before using a shallower gradient around that percentage of solvent B to obtain better separation. The need to use such a long duration of gradient over a wide solvent hydrophilicity-hydrophobicity range was an indication of how difficult it was to separate the constituents of the crude compound by HPLC. As it can be seen from preparative and analytical chromatogram in Figure 2.9, the eluted peak rose from a high baseline of eluting related peptides, and it was impractical to separate the peptides within the high baseline by HPLC.

The main peak of LK_{25}AOA1 eluted at about 48% (v/v) of Solvent B. MALDI-TOF mass spectra of the pooled fractions of the peak splicing and the whole peak (see Figure 2.9) are shown in Figure 2.10A and B respectively. The main peak in the peak-sliced batch of LK_{25}AOA1 gave a peak at 5787. Other peaks of lower intensities were present at 5664 and 5736, the calculated mass. It was difficult to determine what species accounted for the extra mass of 61 in the largest peak. Partial deprotection seemed to be the only possible explanation for the difference between theoretical molecular mass and the mass determined by MALDI-TOF, however, a protecting group species with a mass of 61 could not be identified. The sequence of the first 23 N-terminus amino acid residues of this batch of LK_{25}AOA1 was also confirmed by amino acid sequencing (see sequencing report in Figure 2.11). A third batch of LK_{25}AOA1 (named K_{25}AOA1#3) was synthesized on contract by Dr. Graham Bloomberg (Department of Biochemistry, University of Bristol). The request had been made for this batch of peptide to be

supplied as a purified peptide with a minimum estimated purity of 90% of the target compound. However K_{25}AOA1#3 was supplied as the crude peptide cleaved from the resin due to reported insurmountable problems at attempts to purify K_{25}AOA1#3 by HPLC. Analysis of K_{25}AOA1#3 by HPLC (Figure 2.12) using the solvent gradient in Table 2.3 showed the absence of a single main peak to isolate by preparative HPLC. The mass spectrum of K_{25}AOA1#3 (Figure 2.13) suggested that the crude product to contain approximately 70% of the target peptide. Separately collecting the peptides from the various peaks in HPLC trace in Figure 2.12 and analysing them by protein sequencing and mass spectrometry could have resolved the discrepancy between the two methods of analysis, HPLC and mass spectrometry.

Time (minutes)	% (v/v) Solvent A (aqueous)	% (v/v) Solvent B (organic)
0	90	10
5	90	10
55	55	45
80	45	55
85	35	65
90	35	65
105	90	10
110	90	10

Table 2.3 Table of gradient of solvents used in HPLC purification and analysis of K_{25}AOA1: solvent A: 0.1% (v/v) aqueous TFA; solvent B: 0.1% (v/v) aqueous TFA, 95% (v/v) acetonitrile.

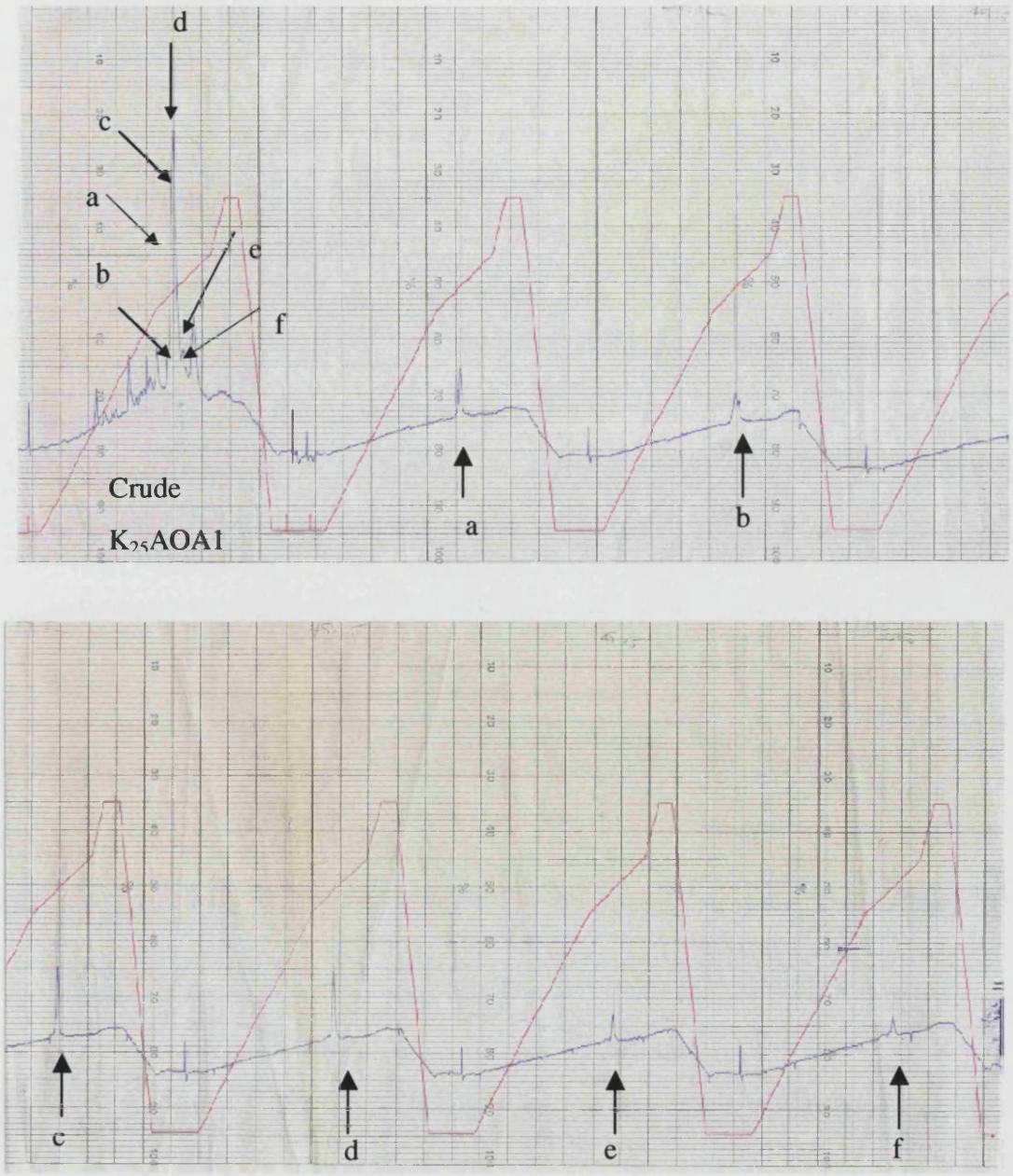

Figure 2.9 Representative preparative high-pressure liquid chromatogram of crude LK$_{25}$AOA1 showing analytical chromatogram of collected peak-splicing fractions a, b, c, d, e and f. The red line shows the charting (on the 2-channel LKB 2210 chart recorder) of the solvent B gradient between 10% (v/v) and 65% (v/v) at a rate of 20 ml/min over a period of 90 minutes (see Table 2.3 for details). The blue line is the absorbance of the elute measured at a wavelength of 277 nm using the Waters™ 490E multiwavelength UV detector.

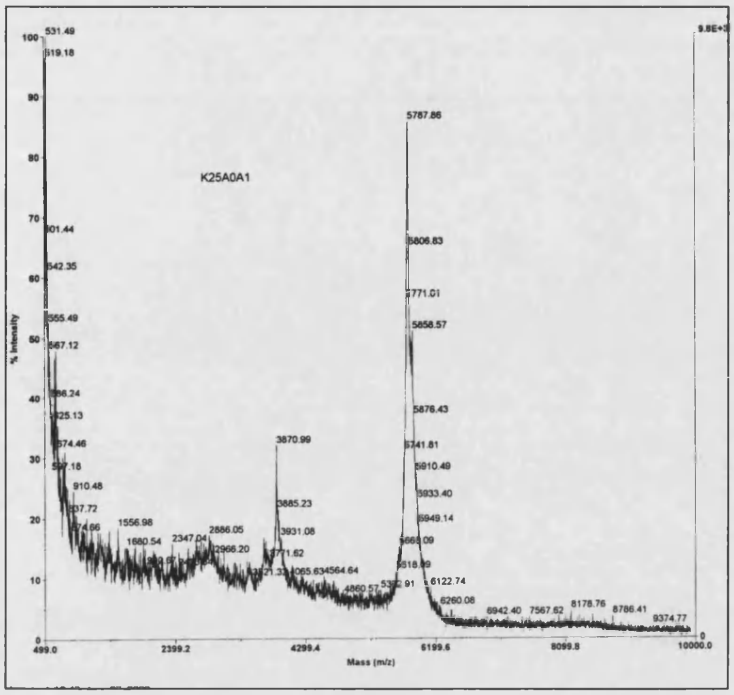

A

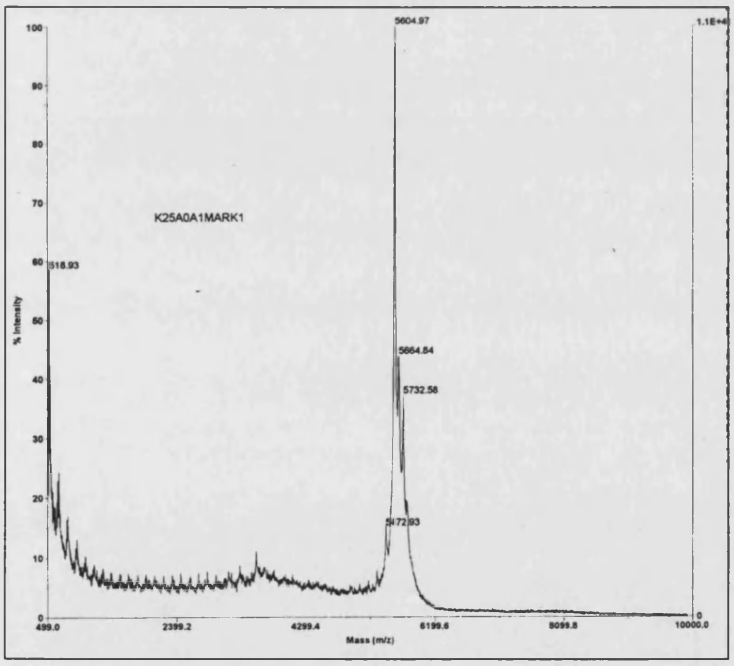

B

Figure 2.10 MALDI-TOF mass spectra of (A) $LK_{25}AOA1$, purified by collection of peak-splicing of main peak and pooling fractions around the apex of the peak as described in section 2.2.3 above and illustrated in HPLC chromatogram in Figure 2.9 (B) $LK_{25}AOA1$, purified by collecting the main peak fractions a-f as illustrated in HPLC chromatogram in Figure 2.9. Samples were analysed on PerSeptive Biosystems Voyager –DE STR. The calculated mass of $LK_{25}AOA1$ was 5736.

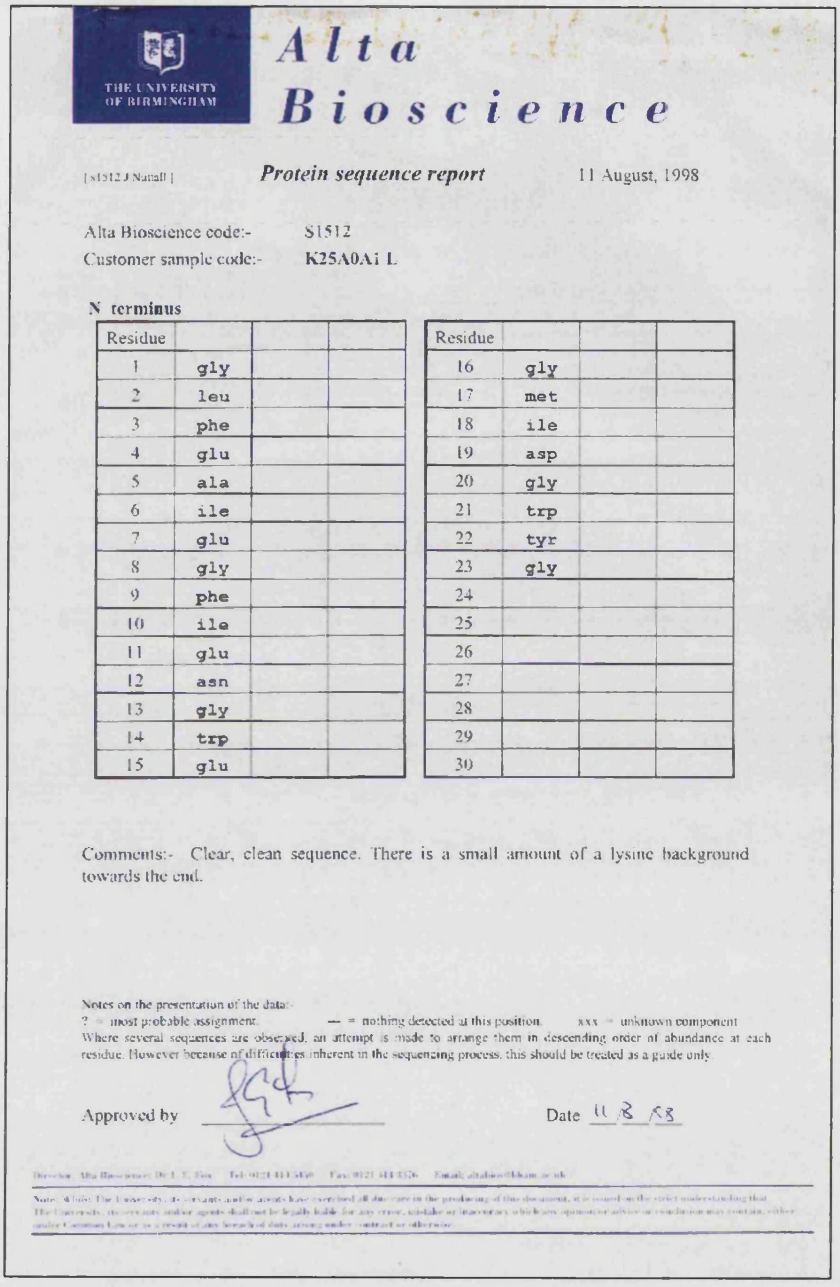

THE UNIVERSITY OF BIRMINGHAM

Alta Bioscience

[s1512] Natalf] *Protein sequence report* 11 August, 1998

Alta Bioscience code:- S1512
Customer sample code:- **K25A0A1 L**

N terminus

Residue				Residue			
1	gly			16	gly		
2	leu			17	met		
3	phe			18	ile		
4	glu			19	asp		
5	ala			20	gly		
6	ile			21	trp		
7	glu			22	tyr		
8	gly			23	gly		
9	phe			24			
10	ile			25			
11	glu			26			
12	asn			27			
13	gly			28			
14	trp			29			
15	glu			30			

Comments:- Clear, clean sequence. There is a small amount of a lysine background towards the end.

Notes on the presentation of the data:-
? = most probable assignment. — = nothing detected at this position. xxx = unknown component
Where several sequences are observed, an attempt is made to arrange them in descending order of abundance at each residue. However because of difficulties inherent in the sequencing process, this should be treated as a guide only.

Approved by _____ Date 11/8/98

Figure 2.11 Amino acid sequencing report of bifunctional peptide $LK_{25}AOA1\#2$. The automatic amino acid sequencing of the first 23 N-terminal amino acid residues (performed on ABI 470A protein sequencer) were requested and showed that a clean clear fusogenic sequence was obtained. The lysine background towards the end of the sequence was as a result of random cleavage inherent within the process of Edman degradation reaction used.

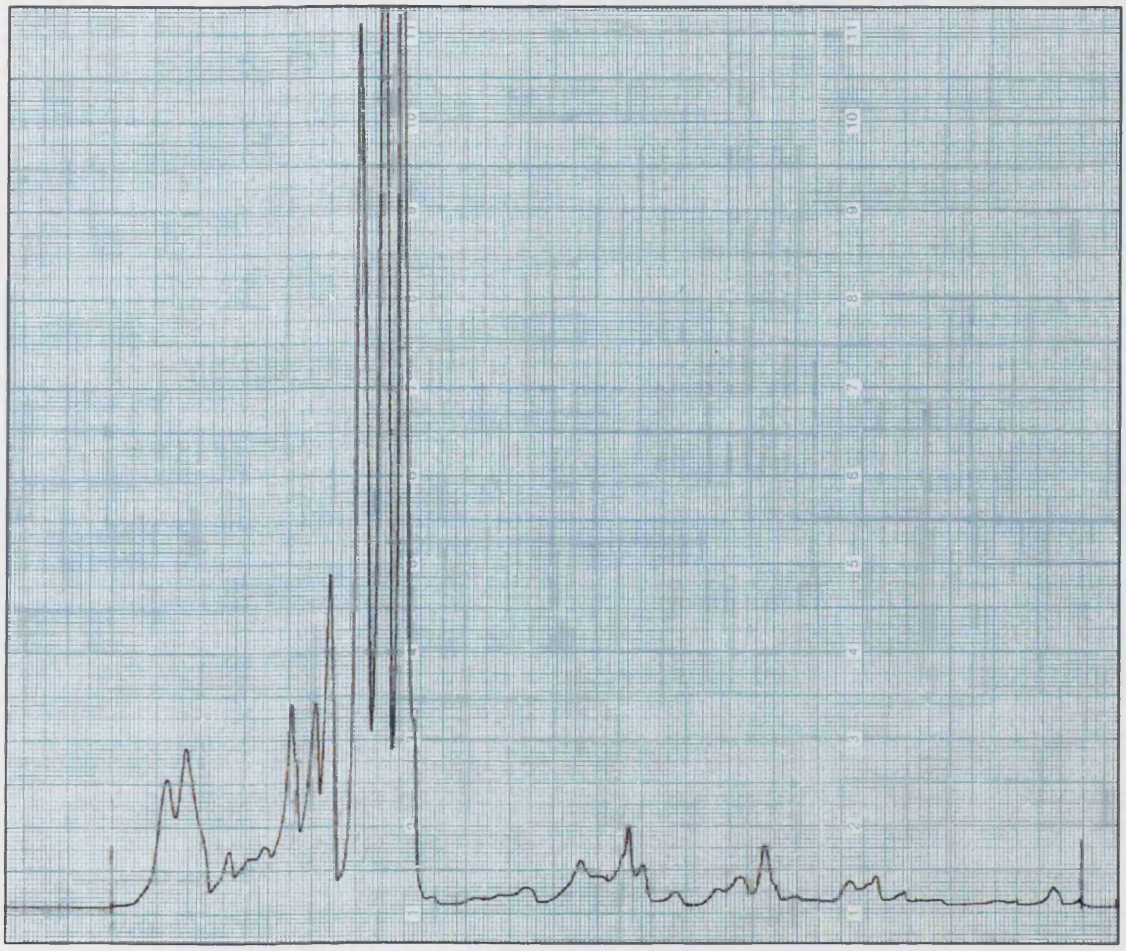

Figure 2.12 Analytical high-pressure liquid chromatogram of crude K_{25}AOA1#3 showing the absorbance of elute measured at a wavelength of 277 nm, using the Jasco™ programmable ternary pump and UV detector. The peptide was eluted by running a varied gradient between 90% (v/v) solvent A (0.1% (v/v) aqueous TFA) and 65% (v/v) solvent B (5% (v/v) aqueous TFA (0.1%), 95% (v/v) acetonitrile) as detailed in Table 2.3.

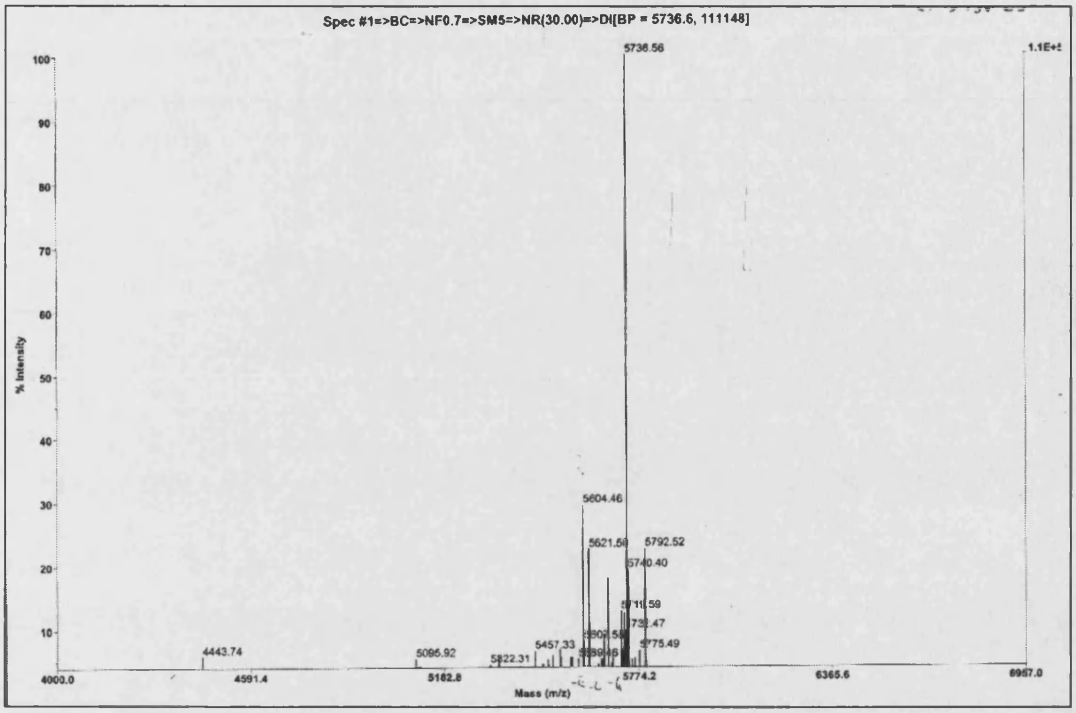

Figure 2.13 Mass spectrum of crude LK$_{25}$AOA1#3 performed on a VG Quattro™ triple quadruple instrument with electrospray ionisation. The calculated mass of LK$_{25}$AOA1 was 5736.

2.3.2.2 PURIFICATION AND ANALYSIS OF DK$_{25}$AOA1

The first batch of the D- amino bifunctional peptide DK$_{25}$AOA1 was purified using the gradient detailed in Table 2.3. A representative chromatogram of the preparative HPLC is shown in Figure 2.14. Biological testing in transfection experiments (chapter 3) showed that the D analogue was over 100-fold less active than LK$_{25}$AOA1#1. As this was not expected, amino acid sequencing was performed and this revealed that an amino acid had been omitted from the sequence. The reason for this omission is believed to be due to steric hindrance by the bulky triphenylmethyl side chain protection of asparagine which prevented the coupling of asparagine to the growing peptide chain. This first batch of DK$_{25}$AOA1 with a deleted asparagine (Asn) was named DK$_{25}$AOA1(N). When asparagine without a side chain protection was used as in the case of the previous L- amino peptide synthesis and subsequent DK$_{25}$AOA1 batches were synthesized, transfection activity was restored (Chapter 3). The second batch of DK$_{25}$AOA1, which had transfection activity comparable to LK$_{25}$AOA1#1 was named DK$_{25}$AOA1.

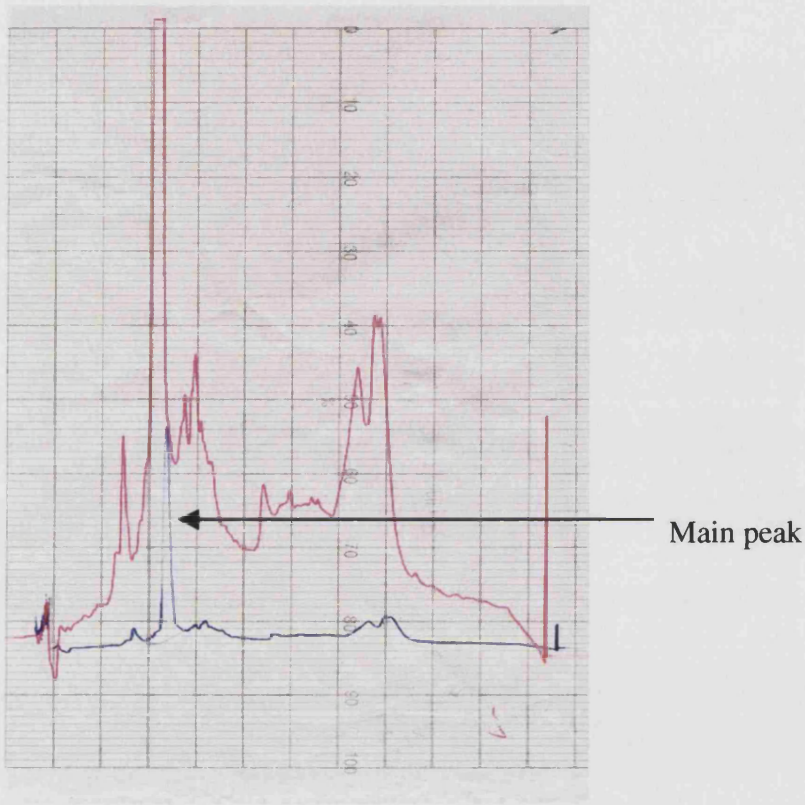

Figure 2.14 Representative preparative high-pressure liquid chromatogram of crude $^{D}K_{25}$AOA1 showing the absorbance of the elute measured at a wavelength of 214 and 277 nm, red and blue traces, respectively, using the Waters™ 490E multiwavelength UV detector. The peptide (40 mg in 20 ml solvent A) was pumped (Waters™ 600 multisolvent delivery system) at 20 ml/min unto a 10 x 25 cm Vydac™ C18 column and eluted by running a varied gradient between 90% (v/v) solvent A (0.1% (v/v) aqueous TFA) and 65% (v/v) solvent B (5% (v/v) aqueous TFA (0.1%), 95% (v/v) acetonitrile) as detailed in Table 2.3.

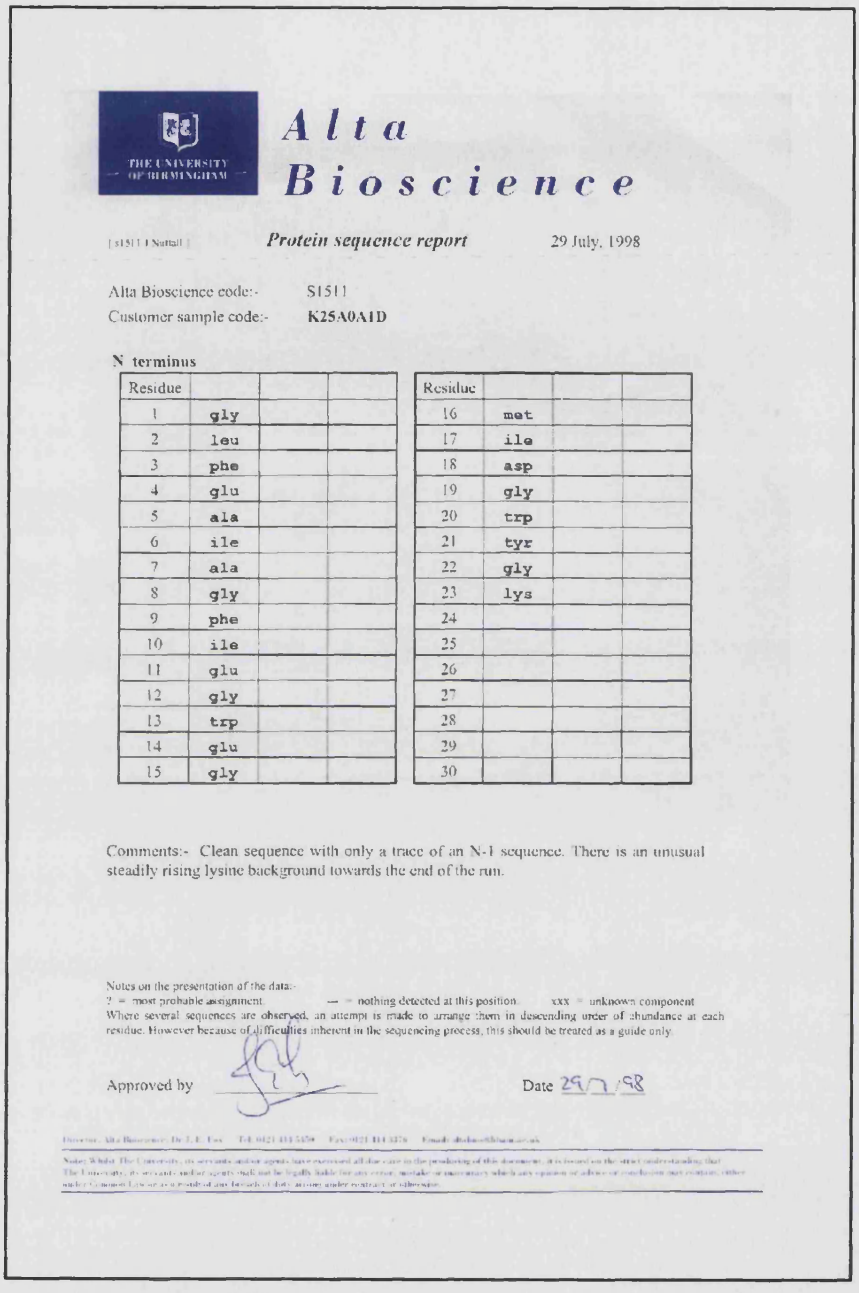

THE UNIVERSITY OF BIRMINGHAM

Alta Bioscience

[s1511 Naftali] *Protein sequence report* 29 July, 1998

Alta Bioscience code:- S1511
Customer sample code:- **K25A0A1D**

N terminus

Residue				Residue			
1	gly			16	met		
2	leu			17	ile		
3	phe			18	asp		
4	glu			19	gly		
5	ala			20	trp		
6	ile			21	tyr		
7	ala			22	gly		
8	gly			23	lys		
9	phe			24			
10	ile			25			
11	glu			26			
12	gly			27			
13	trp			28			
14	glu			29			
15	gly			30			

Comments:- Clean sequence with only a trace of an N-1 sequence. There is an unusual steadily rising lysine background towards the end of the run.

Notes on the presentation of the data:-
2 = most probable assignment. — = nothing detected at this position. xxx = unknown component
Where several sequences are observed, an attempt is made to arrange them in descending order of abundance at each residue. However because of difficulties inherent in the sequencing process, this should be treated as a guide only.

Approved by Date 29/7/98

Director, Alta Bioscience: Dr J. E. Fox Tel 0121 414 5459 Fax 0121 414 3278 Email jfox@bham.ac.uk

Figure 2.15 Amino acid sequencing report of bifunctional peptide $DK_{25}AOA1(N)$. The automatic amino acid sequencing of the first 23 N-terminal amino acid residues (performed on ABI 470A protein sequencer) were requested and showed that asparagine (Asn) was omitted from the sequence at position number 12. The lysine background towards the end of the sequence was as a result of random cleavage inherent within the process of Edman degradation reaction used.

2.3.2.3 PURIFICATION AND/OR ANALYSIS OF $LK_{10}INF7$

The bifunctional peptide $LK_{10}INF7$ was purified by pumping (Waters™ 600 multisolvent delivery system) the peptide (40 mg in 20 ml solvent A) at 20 ml/min unto a 10 x 25 cm Vydac™ C18 column and eluted by running a linear gradient between 95% (v/v) solvent A (0.1% (v/v) aqueous TFA) and 95% (v/v) solvent B (5% (v/v) aqueous TFA (0.1%), 95% (v/v) acetonitrile) in 120 minutes. The main peak was eluted between 53% (v/v) and 57% (v/v) of solvent B after 69 minutes and the pooled fractions that were lyophilised were analysed by automatic amino acid sequencing and MALDI-TOF mass spectrometry. The sequencing results showed that the main peak collected contained approximately 1% of an N-1 sequence and about 3% of another unrelated sequence (Figure 2.17). MALDI-TOF analysis spectra confirmed that the main peak had a molecular mass of 3873, which was the calculated mass. The spectra also show the presence of impurities, consisting of deletion peptide sequences, accounting for the high level of background peaks before and after the main peak.

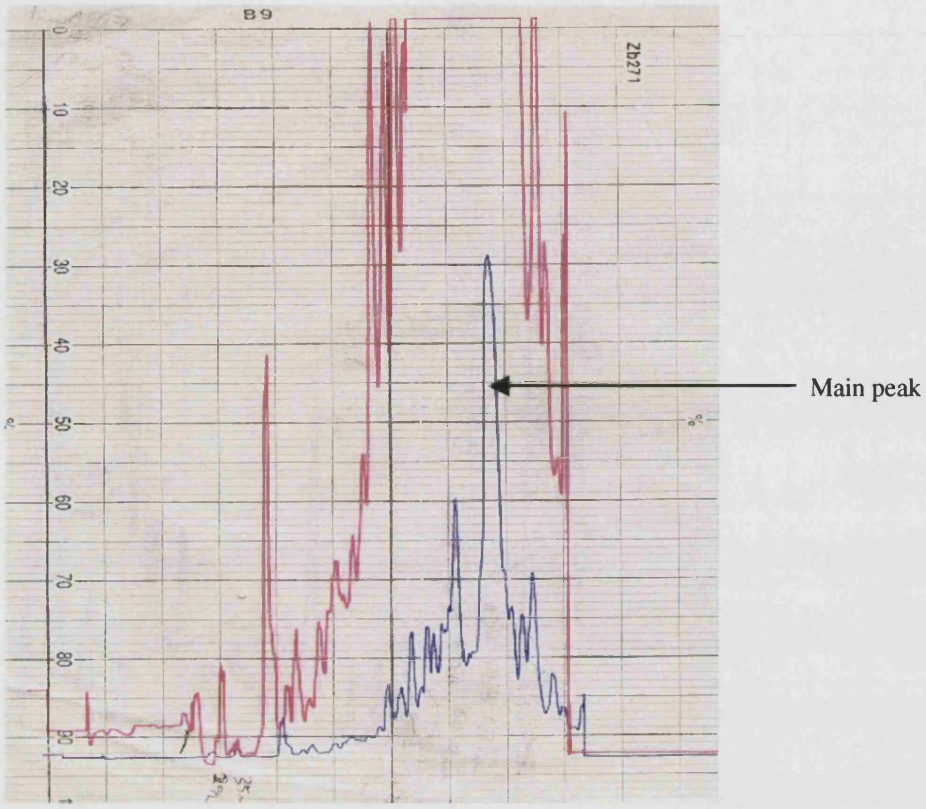

Figure 2.16 Representative preparative high-pressure liquid chromatogram of crude $LK_{10}INF7$ showing the absorbance of the elute measured at a wavelength of 214 and 277 nm, red and blue traces, respectively, using the Waters™ 490E multiwavelength UV detector. The peptide (40 mg in 20 ml solvent A) was pumped (Waters™ 600 multisolvent delivery system) at a rate of 20 ml/min unto a 10 x 25 cm Vydac™ C18 column and eluted by running a variable linear gradient between 95% (v/v) solvent A (0.1% (v/v) aqueous TFA) and 95% (v/v) solvent B (5% (v/v) aqueous TFA (0.1%), 95% (v/v) acetonitrile) in 120 minutes.

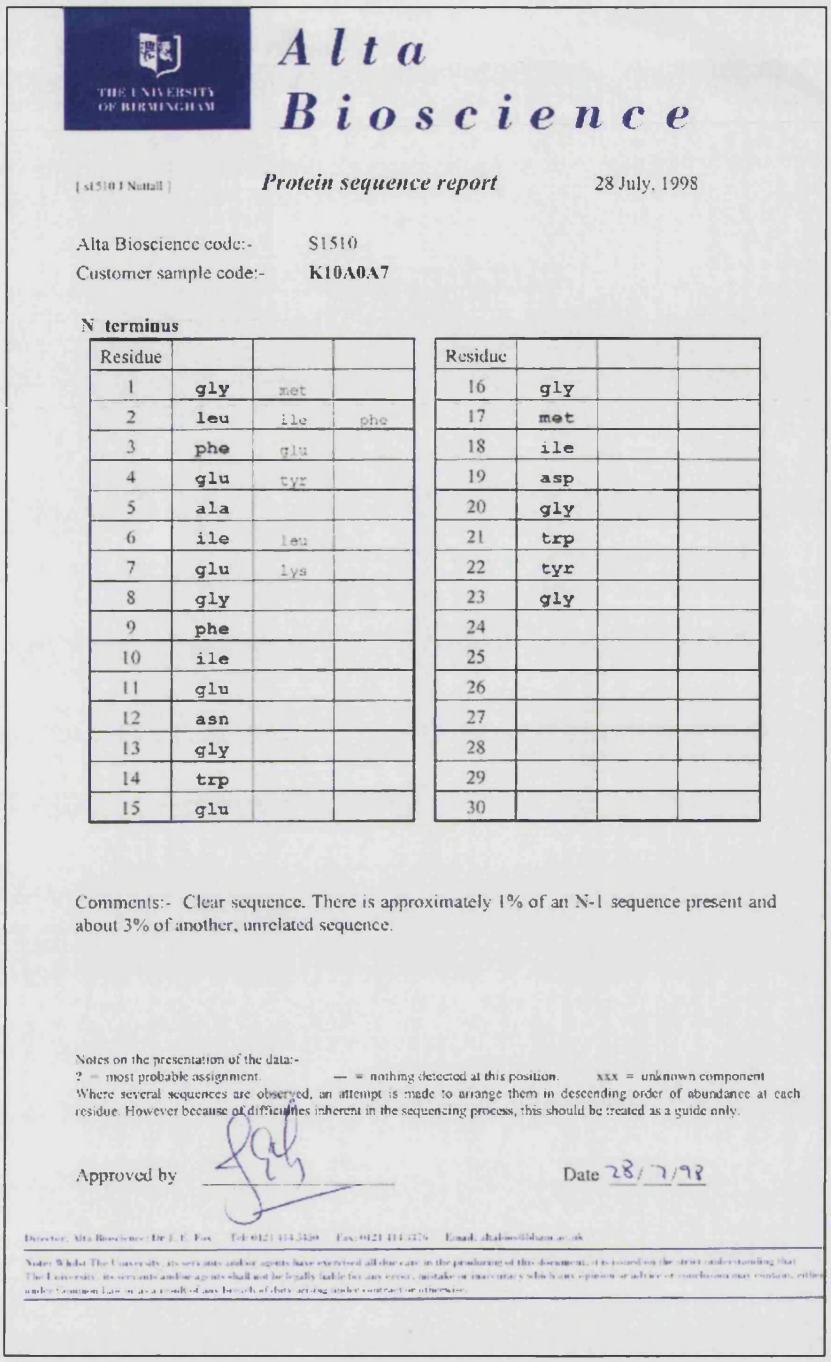

THE UNIVERSITY OF BIRMINGHAM

Alta Bioscience

[s1510 Natall]

Protein sequence report

28 July, 1998

Alta Bioscience code:- S1510

Customer sample code:- **K10A0A7**

N terminus

Residue				Residue			
1	gly	met		16	gly		
2	leu	ile	phe	17	met		
3	phe	glu		18	ile		
4	glu	tyr		19	asp		
5	ala			20	gly		
6	ile	leu		21	trp		
7	glu	lys		22	tyr		
8	gly			23	gly		
9	phe			24			
10	ile			25			
11	glu			26			
12	asn			27			
13	gly			28			
14	trp			29			
15	glu			30			

Comments:- Clear sequence. There is approximately 1% of an N-1 sequence present and about 3% of another, unrelated sequence.

Notes on the presentation of the data:-
? = most probable assignment. — = nothing detected at this position. xxx = unknown component
Where several sequences are observed, an attempt is made to arrange them in descending order of abundance at each residue. However because of difficulties inherent in the sequencing process, this should be treated as a guide only.

Approved by

Date 28/7/98

Director, Alta Bioscience: Dr J. E. Fox Tel: 0121 414 3539 Fax: 0121 414 3376 Email: jfox@bham.ac.uk

Note: Whilst The University, its servants and/or agents have exercised all due care in the producing of this document, it is issued on the strict understanding that The University, its servants and/or agents shall not be legally liable for any error, mistake or inaccuracy which is any opinion or advice or conclusion may contain, either under Common Law or as a result of any breach of duty arising under contract or otherwise.

Figure 2.17 Amino acid sequencing report of bifunctional peptide $LK_{10}INF7$. The automatic amino acid sequencing of the first 23 N-terminal amino acid residues (performed on ABI 470A protein sequencer) were requested and showed that a clean clear fusogenic sequence was obtained. The lysine background towards the end of the sequence was as a result of random cleavage inherent within the process of Edman degradation reaction used.

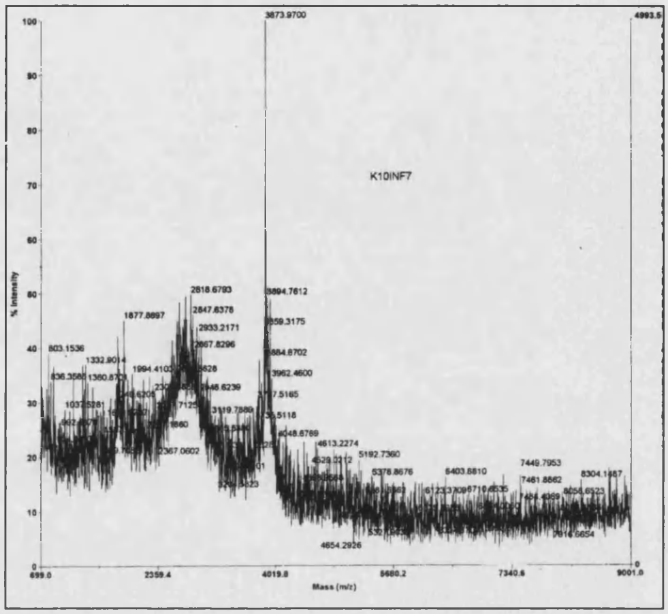

Figure 2.18 MALDI-TOF mass spectrum of $LK_{10}INF7$, purified by collecting the main peak in HPLC chromatogram in Figure 2.16. Samples were analysed on PerSeptive Biosystems Voyager–DE STR. The calculated mass of $K_{10}INF7$ was 3873.

A batch of $K_{10}AOA1$ was synthesized by Dr. Graham Bloomberg using Fmoc chemistry on a PerSynthesizer 9050 plus™ automatic peptide synthesiser and was supplied as the crude peptide cleaved from the resin. The mass spectra of $K_{10}AOA1$ suggested that the target compound was about 80% of the crude product (see Figure 2.19). Analysis of $K_{10}AOA1$ by HPLC (Figure 2.20) using the solvent gradient in Table 2.3 showed the absence of a single main peak to isolate by preparative HPLC. Ideally, the various peaks present in the HPLC trace could have been collected and further analysed to find which fraction contained the target peptide, but such considerations were not possible due to financial constraints.

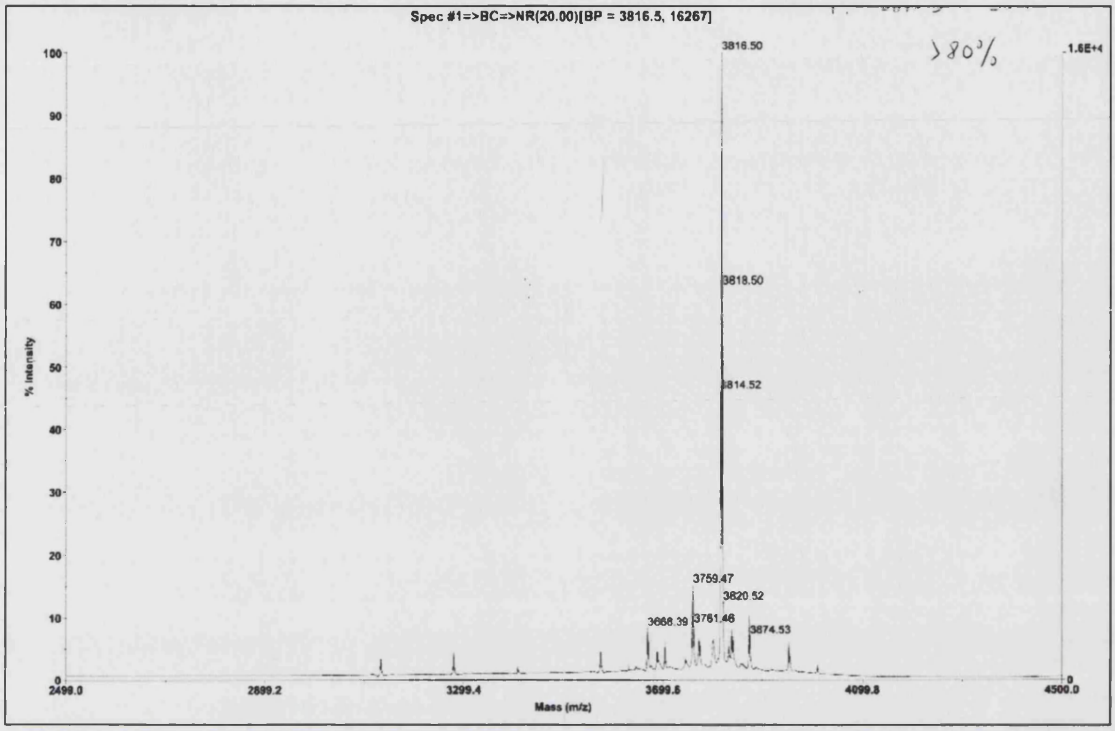

Figure 2.19 Mass spectrum of crude K_{10}AOA1 performed on a VG Quattro™ triple quadruple instrument with electrospray ionisation. The calculated mass of K_{10}AOA1 was 3815.

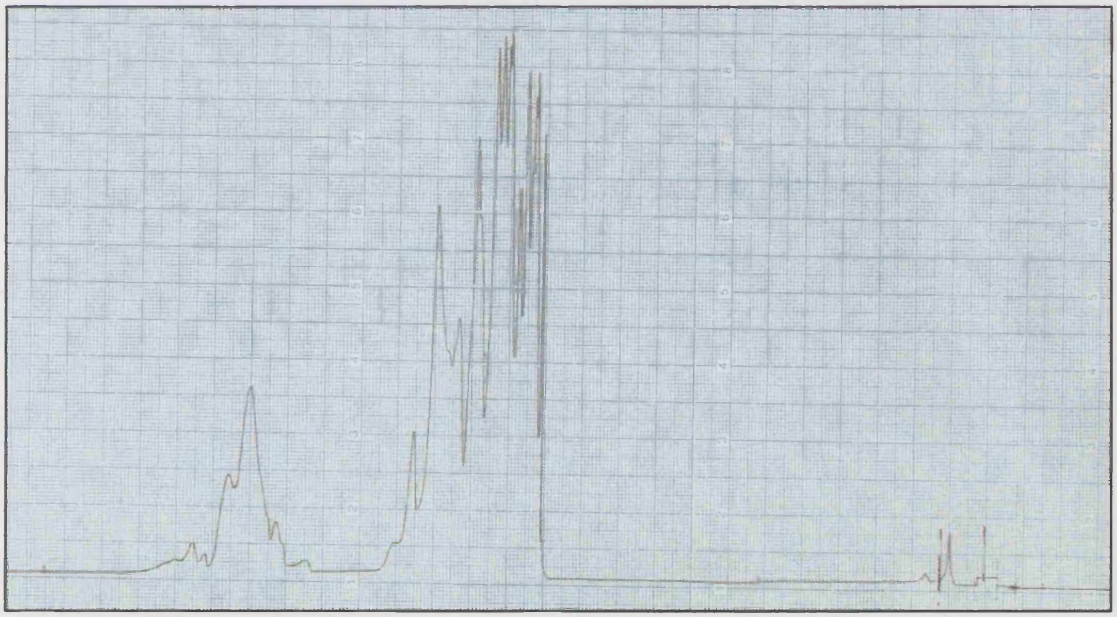

Figure 2.20 Analytical high-pressure liquid chromatogram of crude K_{10}AOA1 showing the absorbance of elute measured at a wavelength of 277 nm, using the Jasco™ programmable ternary pump and UV detector. The peptide was eluted by running a varied gradient between 90% (v/v) solvent A (0.1% (v/v) aqueous TFA) and 65% (v/v) solvent B (5% (v/v) aqueous TFA (0.1%), 95% (v/v) acetonitrile) as detailed in Table 2.3.

2.3.2.4 PURIFICATION AND ANALYSIS OF AOA1, oleoyl-AOA1 and INF7

In the absence of a low-pressure pumping and detection equipment required for use in ion-exchange separation method to purify the fusogenic peptides, the decision was taken to use reverse-phase HPLC separation method. The reverse-phase HPLC separation of fusogenic peptides was attempted by using a POROS™ 20 column (self-pack POROS™ 20 media was obtained from PerSeptive Biosystems (Framingham, MA, USA) and used to pack a 2.5x25 cm steel liquid chromatography column in the laboratory). The use of POROS™ column had the advantage of enabling HPLC to be performed at pH of 10 without risk of degradation of the solid phase, an occurrence associated with conventional C18 columns. Unfortunately, the fusogenic peptides degraded at high pH (sodium hydroxide or ammonia 0.3%), evidenced by the emergence of multiple peaks after purification (Figure 2.21). MALDI-TOF mass spectra of INF7 and oleoyl-AOA1 showed that the compounds were highly impure (Figure 2.22). Due to the fact that the purity of the first batches of AOA1 and INF7 synthesized were questionable according to mass spectra analysis, this batch of AOA1 is marked with asterisks (*) in this report to differentiate it from a later batch of crude AOA1 (synthesized by Dr. Graham Bloomberg) with an estimated purity of 90% (Figure 2.25). The expected molecular masses of INF7 and oleoyl-AOA1 were 2590 and 3000 respectively. In the absence of pure AOA1, another synthetic fusogenic sequence JTS1 was obtained from GeneMedicine, Texas, USA, to use as a comparison in transfection experiments involving bifunctional peptides. An analytical HPLC of JTS1, showed that it was pure and a single species (Figure 2.23) and MALDI-TOF mass spectra analysis showed that the main species present had a mass of 2340, a potassium adduct of JTS1, molecular mass 2301 (Figure 2.24).

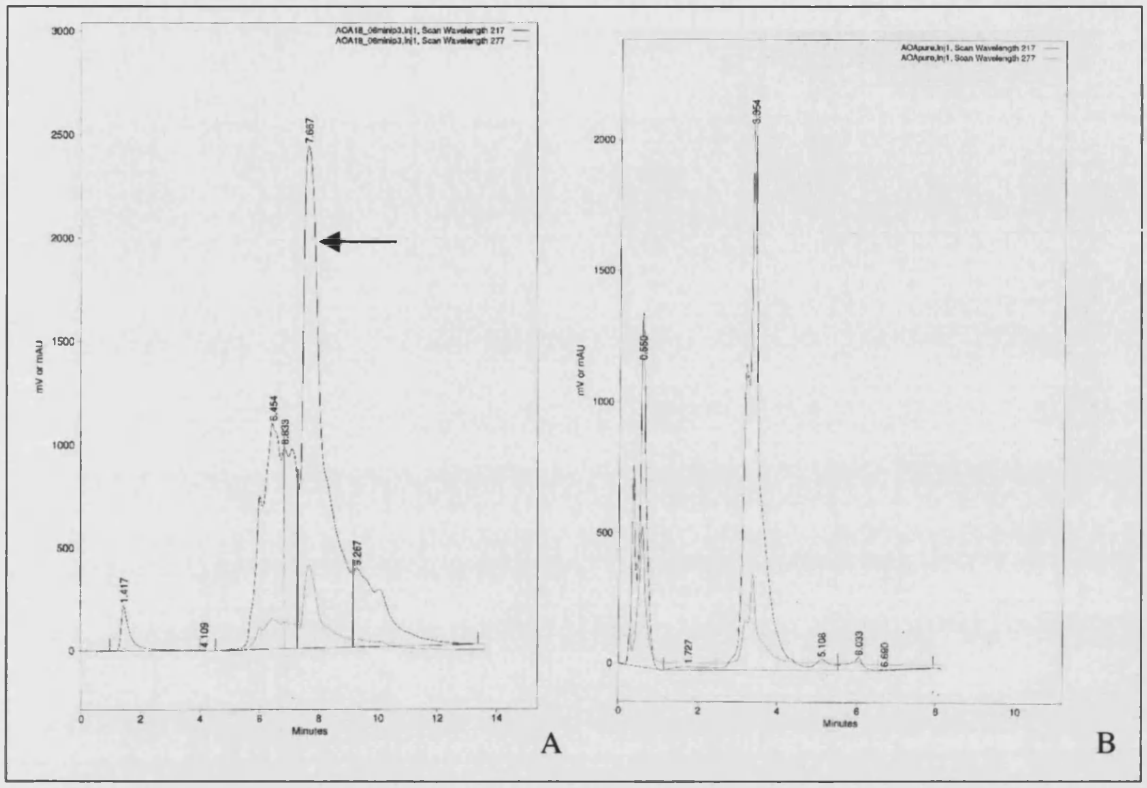

Figure 2.21 Analytical high-pressure liquid chromatogram of (A) crude and (B) purified AOA1*. Purified AOA1* was obtained by collecting the main peak, arrowed in (A). Chromatogram shows the absorbance of the elute measured at a wavelength of 217 and 277 nm, red and blue traces, respectively, using the LDC Analytical SpectroMonitor 5000 photodiode array detector. Peptides (0.5 mg) were dissolved in 0.3% (v/v) aqueous ammonia (in 0.5 ml) and pumped (ConstaMetric™ 4100 solvent delivery system) unto a POROS™ column and eluted between a variable linear gradient of solvent A: 0.3% (v/v) aqueous ammonia, pH 10, and solvent B: 0.3% (v/v) aqueous ammonia, 50% (v/v) acetonitrile, pH 10, for 15 minutes at a rate of 5 ml/min.

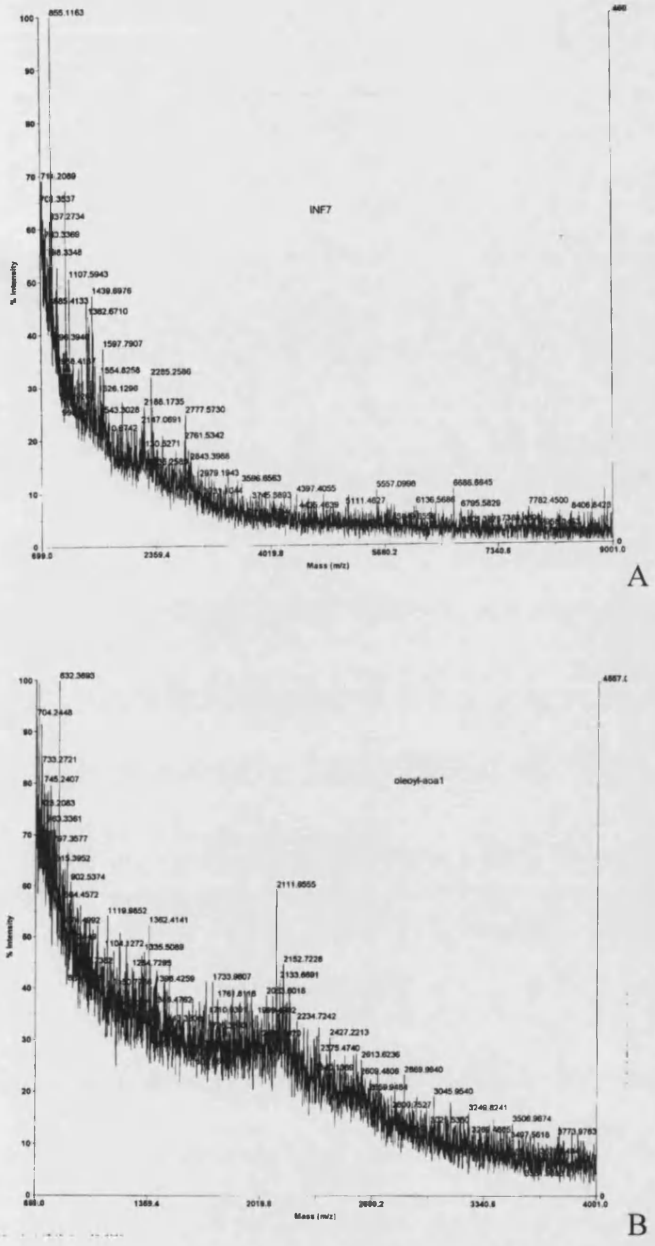

Figure 2.22 MALDI-TOF mass spectra of (A) INF7* and (B) oleoyl-AOA1, purified by collecting the main peak in HPLC chromatogram in Figure 2.21 Samples were analysed on PerSeptive Biosystems Voyager–DE STR. The calculated mass of INF7 and oleoyl-AOA1 are 2590 and 3000 respectively.

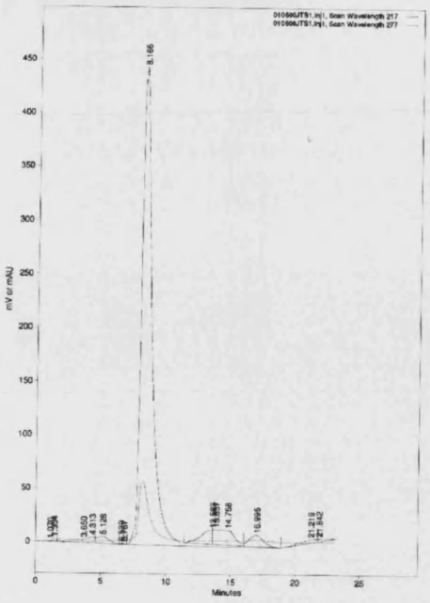

Figure 2.23 Analytical high-pressure liquid chromatogram of JTS1 (a gift from GeneMedicine, Texas, USA) showing the absorbance of the elute measured at a wavelength of 217 and 277 nm, red and blue traces, respectively, using the LDC Analytical SpectroMonitor 5000 photodiode array detector. Peptides (0.5 mg) were dissolved in 0.3% (v/v) aqueous ammonia (in 0.5 ml) and pumped (ConstaMetric™ 4100 solvent delivery system) unto a POROS™ column and eluted between a linear gradient of solvent A: 0.3% (v/v) aqueous ammonia, pH10, and solvent B: 0.3% (v/v) aqueous ammonia, 50% (v/v) acetonitrile, pH 10, for 15 minutes at a rate of 5 ml/min.

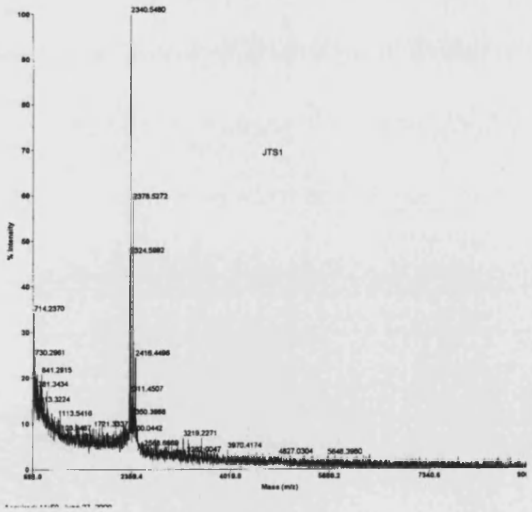

Figure 2.24 MALDI-TOF mass spectrum of JTS1 (a gift from GeneMedicine, Texas, USA), with analytical HPLC chromatogram shown in Figure 2.23. Samples were analysed on PerSeptive Biosystems Voyager–DE STR. The expected molecular mass of JTS1 is 2301.

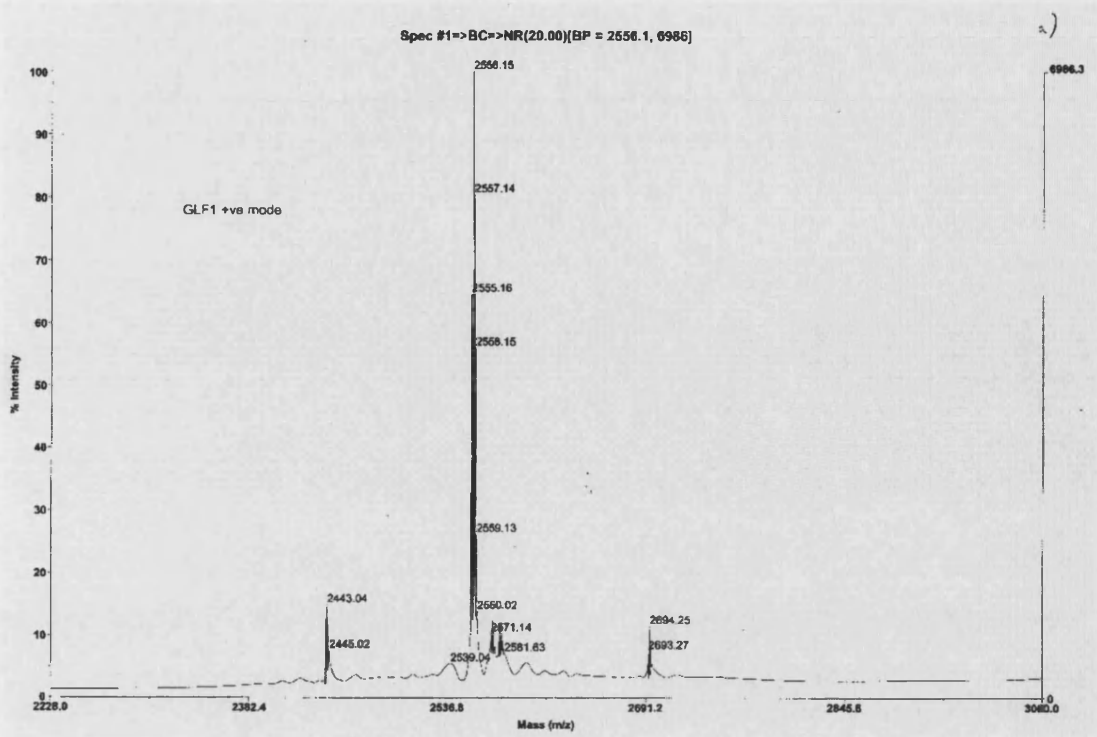

Figure 2.25 Mass spectrum of crude AOA1 performed on a VG Quattro™ triple quadruple instrument with electrospray ionisation.

2.3.2.5 PURIFICATION AND ANALYSIS OF K_{10}, K_{25}, $K_{25}H_{10}$ AND $K_{25}H_{20}$

The analytical HPLC of crude oligolysine peptides K_{10} and K_{25} were revealed that they were >90% pure by HPLC analysis but they purified by HPLC essentially to remove any traces of scavengers that may have been present. Peptides K_{10} and K_{25} had very high hydrophilicity at pH 2 (0.1% (v/v) TFA) and eluted with the solvent front, making any attempt at separation from the scavengers impossible. In order to increase the hydrophobicity of K_{10} and K_{25}, peptides were dissolved in 0.3% (v/v) aqueous ammonia and pumped unto a 2.5x25 cm POROS™ column and eluted between a variable linear gradient of solvent A: 0.3% (v/v) aqueous ammonia, pH 10, and solvent B: 0.3% (v/v) aqueous ammonia, 90% (v/v) acetonitrile, pH 10. The solvent gradient used is shown in Table 2.4. This allowed the removal of scavengers from crude K_{10} and K_{25}. MALDI-TOF mass spectrometry on K_{10} showed that the main peak had a mass of 1300 (expected molecular mass) and 1312 (100%), and these peaks had sodium and potassium adducts with masses of 1322 and 1338 respectively. MALDI-TOF mass

spectrum of K_{25} showed the calculated mass of 3223 and sodium adduct of mass 3245. The mass spectrum of K8, a gift from GeneMedicine, Texas, USA, showed the expected molecular mass peak of 1720 and potassium adduct with a mass of 1758. There is also an unexpected peak at 1734. Another batch of K_{10} and K_{25} synthesized by Dr. Graham Bloomberg, Department of Biochemistry, University of Bristol were not purified by HPLC, but each crude oligolysine had a high estimated purity of 95% of the target peptide present as evidenced by the mass spectra in Figure 2.28.

Time (minutes)	% (v/v) solvent A (aqueous)	% (v/v) solvent B (organic)
0	95	5
1	95	5
11	50	50
13	50	50
18	95	5
21	95	5

Table 2.4 Table of gradient of solvents used in HPLC purification and analysis: solvent A: 0.3% (v/v) aqueous ammonia; solvent B: 0.3% (v/v) aqueous ammonia, 90% (v/v) acetonitrile.

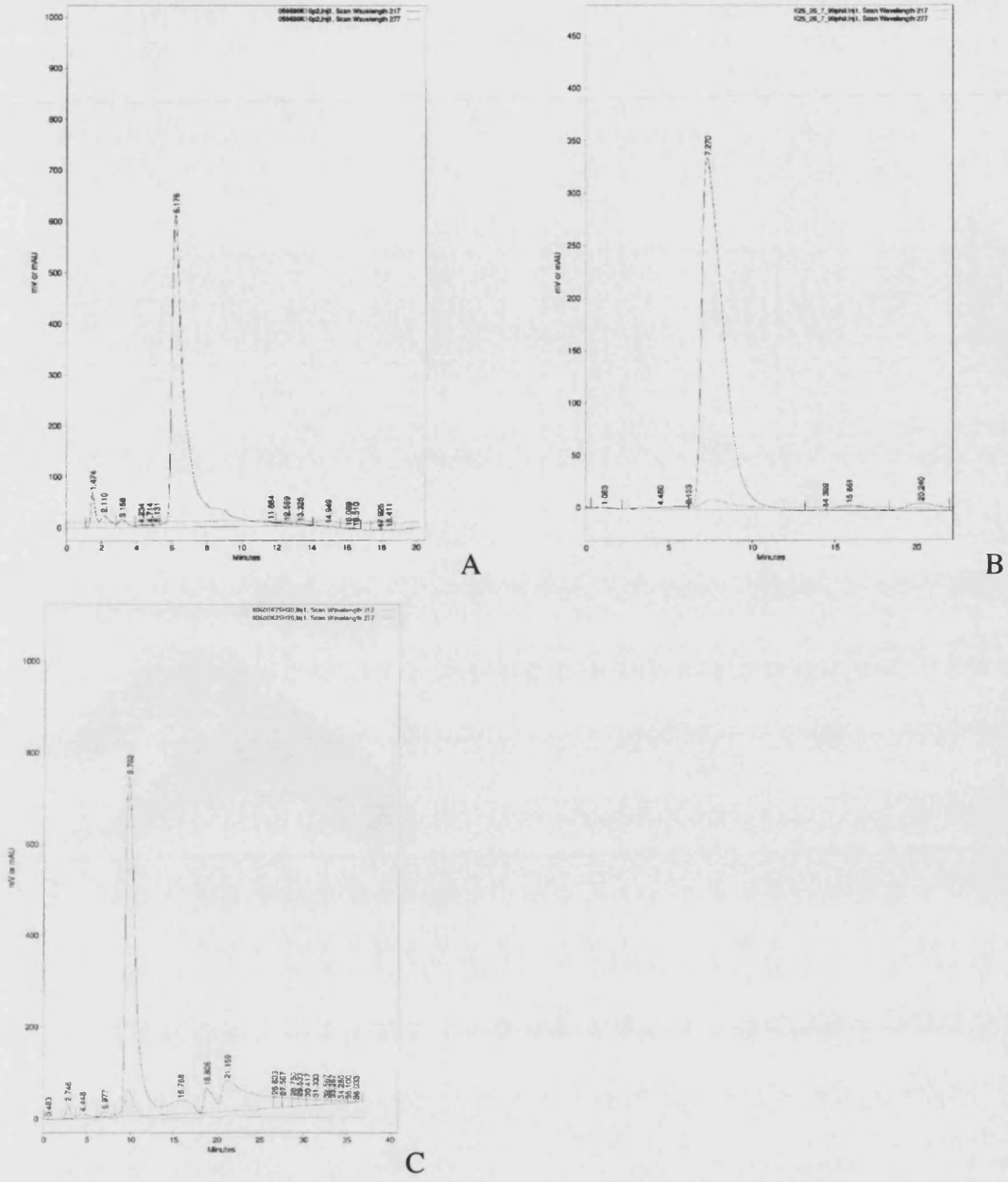

Figure 2.26 Representative preparative high-pressure liquid chromatogram of (A) crude K_{10}, (B) K_{25} and (C) $K_{25}H_{20}$ showing the absorbance of the elute measured at a wavelength of 217 and 277 nm, red and blue traces, respectively, using the LDC Analytical SpectroMonitor 5000 photodiode array detector. Peptides (5-10 mg) were dissolved in 0.3% (v/v) aqueous ammonia (in 2.5 ml) and pumped (ConstaMetric™ 4100 solvent delivery system) unto a POROS™ column and eluted between a variable linear gradient of solvent A: 0.3% (v/v) aqueous ammonia, pH 10, and solvent B: 0.3% (v/v) aqueous ammonia, 50% (v/v) acetonitrile, pH 10 at a rate of 10 ml/min.

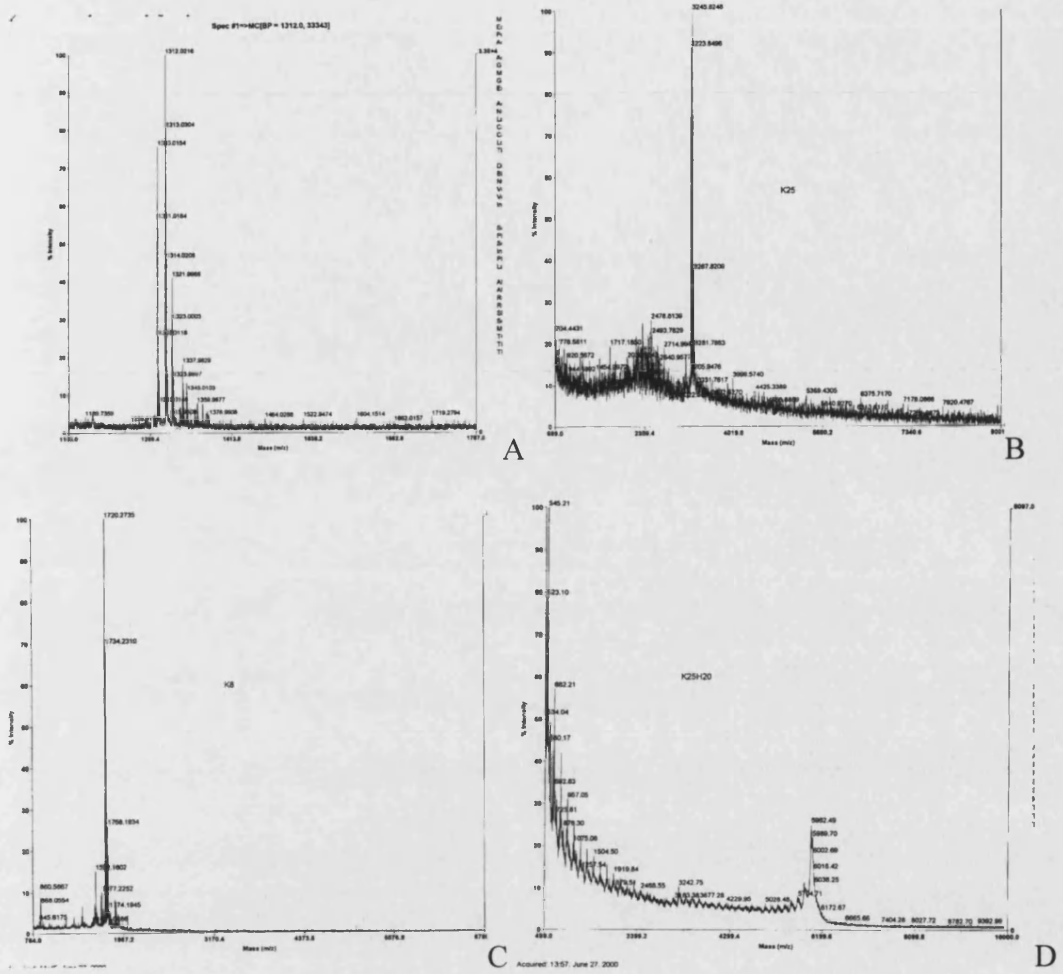

Figure 2.27 MALDI-TOF mass spectra of the oligolysine (A) $K_{10,}$ (B) K_{25} and (C) K8. K_{10}, K_{25} and (D) $K_{25}H_{20}$ purified by collecting the main peak in reverse phase HPLC, representative in Figure 2.26. K8 was a gift from GeneMedicine, Texas, USA. Samples were analysed on PerSeptive Biosystems Voyager–DE STR. The expected molecular mass of $K_{10,}$ K_{25} and K8, and $K_{25}H_{20}$ are 1300, 3221, 1720 and 5962 respectively.

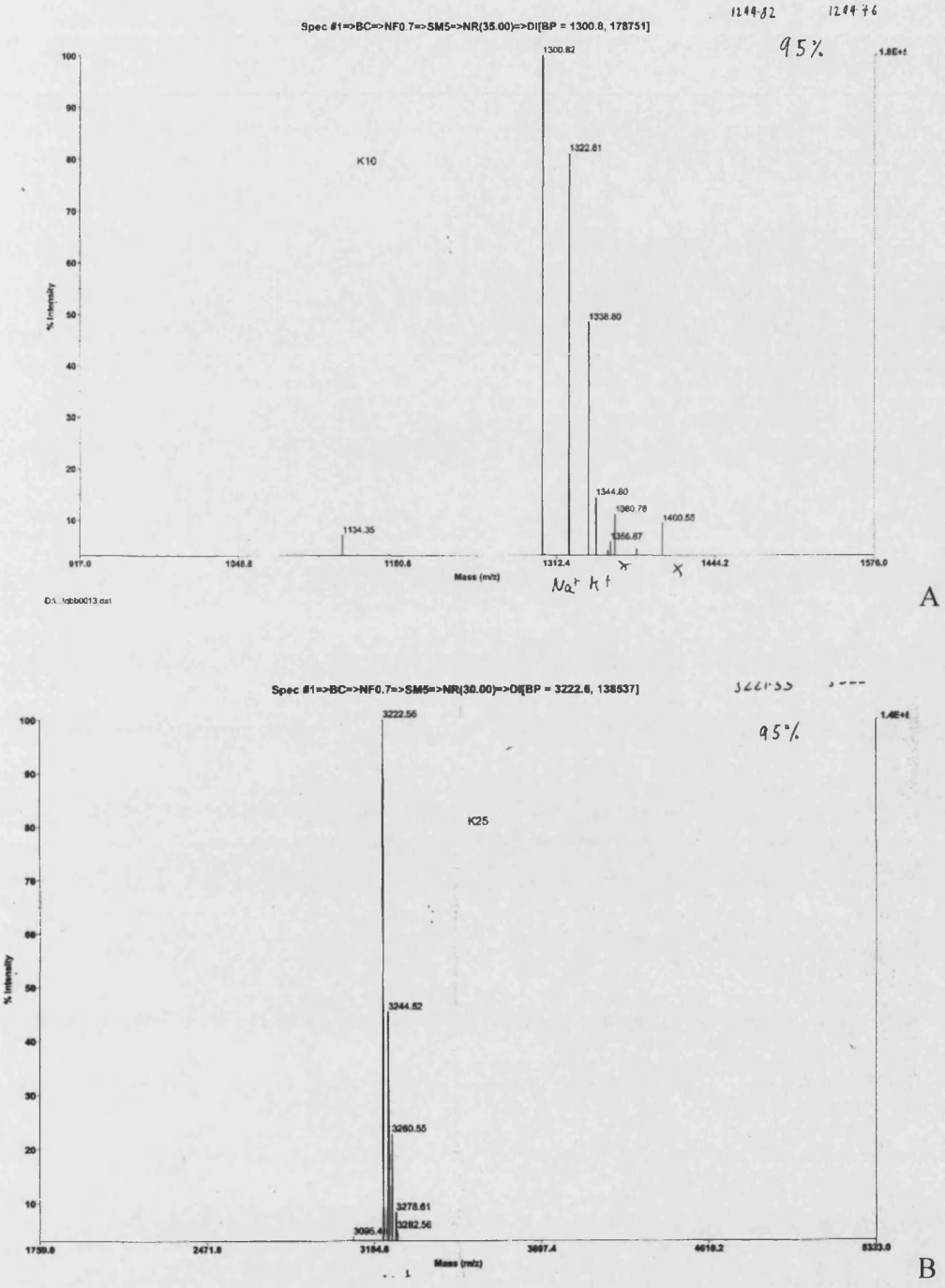

Figure 2.28 Mass spectra of crude K_{10} (A) and K_{25} (B) performed on a VG Quattro™ triple quadruple instrument with electrospray ionisation. The calculated masses of K_{10} and K_{25} were 1300 and 3221 respectively.

2.3.2.6 *PURIFICATION AND ANALYSIS OF $K_{25}H_{10}AOA1$ AND $K_{25}H_{20}AOA1$*

Initial attempts to purify crude peptides $K_{25}H_{10}AOA1$ and $K_{25}H_{20}AOA1$ by reverse phase HPLC using a variable linear gradient between 95% (v/v) solvent A (0.1% (v/v) aqueous TFA) and 95% (v/v) solvent B (5% (v/v) aqueous TFA (0.1%), 95% (v/v) acetonitrile) in 80 minutes showed that separation of the mixture could not be achieved (Figure 2.29A). Other organic solvents that were tried in place of acetonitrile, using similar gradients mentioned above included isopropyl alcohol and ethanol. When TFA was replaced with ammonia in the above-mentioned gradient, again separation could not be achieved. Since the histidyl side chain has a protonable nitrogen with a pKa of about 6.0, it was thought that a variation in pH of the solvent system could bring about a resolution of the mixture. A three-solvent acidic-to-basic variable linear gradient system from pH 2 (0.1% (v/v) aqueous TFA, solvent A) to pH 10 (0.1% (v/v) aqueous ammonia, solvent B) gradient was run in the presence of a 10% (v/v) acetonitrile (solvent C). Attempts at separation of the mixture using acidic-to-basic gradient (Table 2.5) was unsuccessful (Figure 2.29B), but when the gradient was reversed to a basic-to-acidic gradient (Table 2.6), signs separation began to appear (Figure 2.29C). Increasing the percentage of acetonitrile from 10% (v/v) to 15% (v/v) appeared to be sufficient to bring about the separation of $K_{25}H_{10}AOA1$ from impurities (Figure 2.29D), but not sufficient for $K_{25}H_{20}AOA1$. A further increase of the percentage of acetonitrile to 20% (v/v) appeared sufficient to bring about resolution of the components of $K_{25}H_{20}AOA1$. Two main peaks could be observed at approximately 11 minutes and 28 minutes, corresponding to 40% (v/v) and 0% (v/v) solvent B (0.1% (v/v) aqueous ammonia) during the purification of $K_{25}H_{10}AOA1$. The peak at 28 minutes was collected and lyophilised based on the assumption that the target peptide would have the sharpest and largest peak. The chromatogram of $K_{25}H_{20}AOA1$ was similar to those of $K_{25}H_{10}AOA1$, so only representative traces of the latter are shown (Figure 2.29).

According to the MALDI-TOF mass spectrometry results of target compounds $K_{25}H_{10}AOA1$ and $K_{25}H_{20}AOA1$ obtained at the end of the project (Figure 2.30A and B), respectively, attempts to purify these two compounds were unsuccessful. Due to lack of access to mass spectroscopy equipment, the scientifically compromised approach of assuming that the sharpest and largest peak during HPLC was the target peptide, proved

to be flawed in this instance. Ideally, once a solvent system had been developed to separate the components of the mixture, various fractions should have been identified by MALDI-TOF mass spectrometry to determine which fraction contained the desired peptide, before proceeding with the purification process for such long peptides.

Time (minutes)	% (v/v) Solvent A (pH2)	% (v/v) Solvent B (pH10)	% (v/v) Solvent C (acetonitrile)
0	90	0	10
2	90	0	10
21	0	90	10
31	0	90	10
51	90	0	10
60	90	0	10
70	90	0	10

Table 2.5 Acidic-to-basic HPLC gradient Table of gradient of solvents used in HPLC purification and analysis: solvent A: 0.1% (v/v) aqueous TFA; solvent B: 0.1% (v/v) aqueous ammonia, solvent C: acetonitrile.

Time (minutes)	% (v/v) Solvent A (pH2)	% (v/v) Solvent B (pH10)	% (v/v) Solvent C (acetonitrile)
0	0	85	15
1	0	85	15
21	85	0	15
31	85	0	15
51	0	85	15
60	0	85	15
70	0	85	15

Table 2.6 Basic-to-acidic HPLC gradient: Table of gradient of solvents used in HPLC purification and analysis: solvent A: 0.1% (v/v) aqueous TFA; solvent B: 0.1% (v/v) aqueous ammonia, solvent C: acetonitrile.

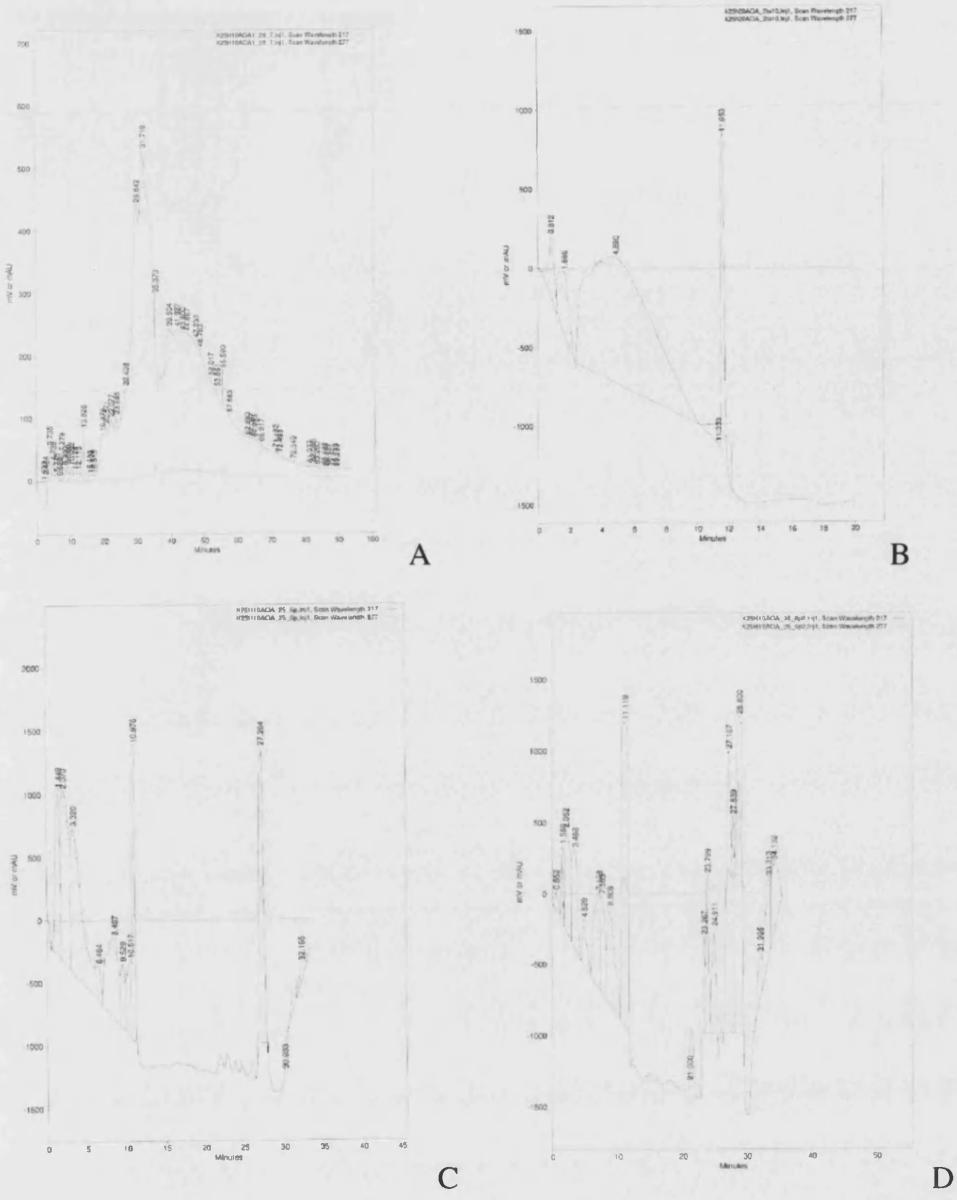

Figure 2.29 High-pressure liquid chromatogram of crude $K_{25}H_{10}AOA1$ showing the absorbance of the elute measured at a wavelength of 217 and 277 nm, red and blue traces, respectively, using the LDC Analytical SpectroMonitor 5000 photodiode array detector. Solvents systems were pumped (ConstaMetric™ 4100 solvent delivery system) solvents through a POROS™ column at various linear gradients summarised below: Trace (**A**) was obtained running a gradient between 95% (v/v) solvent A (0.1% (v/v) aqueous TFA) and 95% (v/v) solvent B (5% (v/v) aqueous TFA (0.1%), 95% (v/v) acetonitrile) in 90 minutes, and trace (**B**) was obtained by running a pH gradient three-solvent acidic-to-basic linear gradient system from pH 2 (0.1% (v/v) aqueous TFA, solvent A) to pH 10 (0.3% (v/v) aqueous ammonia, solvent B) gradient was run in the presence of 10% (v/v) acetonitrile (solvent C), see Table 2.5 for details. Chromatogram (**C**) and (**D**) was obtained by running a basic-to-acidic three solvent system in the presence of 10% (v/v) and 15% (v/v) acetonitrile (solvent C) respectively, see Table 2.6 for details of gradient.

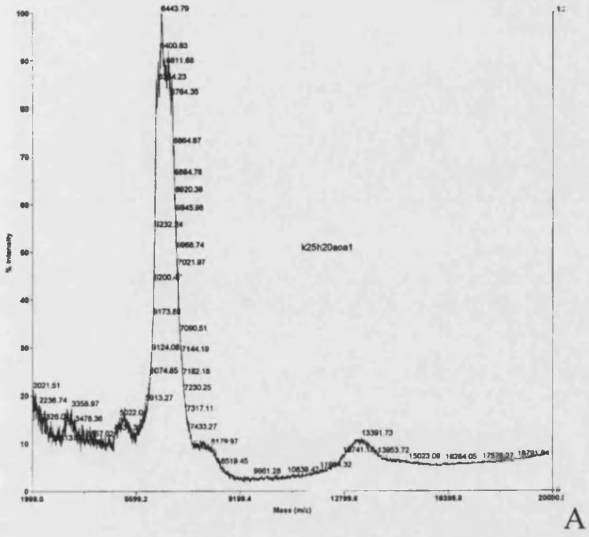

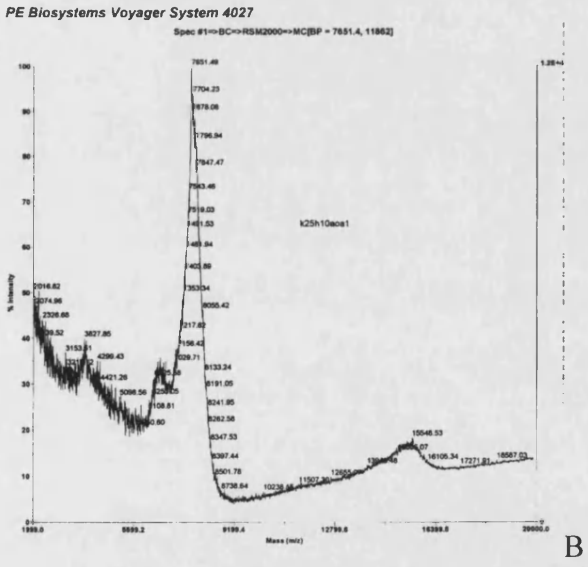

Figure 2.30 MALDI-TOF mass spectra of (A) $K_{25}H_{10}AOA1$ (B) $K_{25}H_{20}AOA1$ purified by collecting the main peak in reverse phase HPLC, representative in Figure 2.29. Samples were analysed on PerSeptive Biosystems Voyager–DE STR. The expected molecular masses of $K_{25}H_{10}AOA1$ and $K_{25}H_{20}AOA1$ were 7106 and 8477 respectively.

2.4 DISCUSSION

Solid-phase peptide synthesis can be employed routinely to create oligopeptides up to 20-25 residues in length. When larger peptides are synthesised the purity decreases because each subsequent coupling gives an incomplete yield, so that when synthesis of peptides greater than 50 residues is attempted, the yield of target peptide becomes vanishingly small. Such peptides are very heterogeneous and purification is challenging. Assuming a 99% yield per coupling reaction, a 48-mer peptide sequence would potentially have a 0.99^{47} or 63% yield of target peptide before cleavage reactions were performed. To ensure a high yield of target peptide, it is important that coupling and cleavage reactions are optimised. A ready access to a protein sequencer and MALDI-TOF mass spectrometry are essential during the time of small-scale synthesis of long peptides as a back-up to, or in place of an on-line UV monitoring detector during automated peptide synthesis, to confirm that reactions are proceeding satisfactorily, before large scale synthesis is undertaken. The synthesiser used for this project lacked any form of on-line monitoring, and there was no access to analytical equipment at the time of synthesis. Synthesis and purification of the peptides had to be performed by observation of the appearance of the materials on HPLC. An attempt was made to purify each material to a single peak, and a sample collected was analysed by outside collaborators in due course.

These were challenging and expensive syntheses. The high cost of materials used limited the number of batches that could be prepared, so in some cases biological experiments were performed on partially purified materials, in the knowledge that the bulk of the material was the target peptide. The actual cost of each batch of 0.2 mmol of 48-mer peptide was about £1500.00 before purification. The availability of an instrument for small-scale peptide synthesis and analysis, followed by amino acid sequencing would have been beneficial, ensuring that difficult couplings could be identified and compensated for, before larger scale synthesis was undertaken. Unfortunately this resource was not available, so that medium-sized batches had to be prepared for each peptide under investigation. Thus optimisation of the syntheses with small-scale batches was not possible during this project. In an attempt to get the largest number of peptides in the least number of syntheses, thereby cutting the unit cost, in

retrospect the batches of some compounds were too small leading to difficulties with HPLC purification. An early decision was taken to synthesize 6 peptide analogues in parallel, and tests for their *in vitro* efficacy in transfection before synthesizing larger batches. The initial peptides that were synthesised were K_{25}AOA1, K_{25}INF7, K_{10}INF7, AOA1, K_{25}, and K_{10}. The intention was that the synthesis of these peptides would allow the bifunctionality of K_{25}AOA1 and K_{10}INF7 to be evaluated against the published literature of three-component mixtures (i.e. DNA + condensing peptide + fusogenic peptide). The yield after the first isolation of the largest and sharpest peak was typically 40% but analytical HPLC revealed that the peptides were still impure. At this stage any attempt to further purify these small batches of fusogenic and bifunctional peptides would have resulted in insufficient peptide with which to perform biological experiments, so these peptides were used at 75-90% (?) purity (as determined by protein sequences) for the biologically active fusogenic moiety. The decision was then taken to synthesize a larger batch of the most active peptide, K_{25}AOA1 (as tested by ability to mediate gene delivery *in vitro*, Chapter 3), to enable a thorough purification, thus allowing sufficient biological experiments to be performed to determine that the observed activity was not due to a contaminant. At this later stage of this project, the PerSynthesizer 9050 plus™ became faulty: coupling reagents leaked considerably from the gasket of the on-line UV detectors of the PerSynthesizer 9050 plus™ during the coupling cycle. It was not possible to replace this gasket due to lack of funds, so the detectors were bypassed and subsequent synthesis had be performed without the benefit of on-line UV monitoring. It was possible to analyse the products retrospectively but the lack of access to a protein sequencer and MALDI-TOF mass spectrometer during the time of synthesis meant that it was not possible to confirm the identity of synthesized peptides until 2½ years into the programme of synthesis. Prior to this the only means of analysis available were (i) HPLC, to isolate the largest and sharpest peak and (ii) *in vitro* testing for transfection activity.

In many cases, for preliminary examination, peptides are used without preparative liquid chromatography, to establish biological activity. Larger batches can then be purified to give higher levels of purity. This was the strategy used in this study. Given that the materials were not 99% pure it is important to discuss what the expected nature of the contaminants were and what their effect would be on biological activity.

During purification of the large second batch of K_{25}AOA1 (K_{25}AOA1#2), 5 ml fractions of the main peak were collected from each run and samples from each fraction were analysed by analytical HPLC. The purest fractions were found to be those close to the tip of each main peak (i.e. fractions c and d in Figure 2.9). The pure fractions were considered to be those fractions from peak splicing which did not possess shoulders or multiple peak upon re-analysis by HPLC and these were pooled together and lyophilised, and called K_{25}AOA1#2. K_{25}AOA1#2 accounted for 6% of the crude peptide weight. The *in vitro* transfection activity of the pure peptide (K_{25}AOA1#2) was found to be 20% higher than the batch of K_{25}AOA1 in which the whole peak was used, named K_{25}AOA1#1. However, the high cost of these peptides meant that synthesis of larger batches of AOA1 and INF7 to enable thorough purification for purposes of comparison to K_{25}AOA1 was regarded as an unaffordable expenditure. Such considerations may prevent the widespread use of bifunctional peptides such as K_{25}AOA1, despite its excellent biological activity.

The analytical chromatogram of the bifunctional peptide K_{25}AOA1#2 indicated that the fractions pooled from the peak splicing had a sharp clean peak without shoulders. However this sharp peak emerged from a fairly high baseline representing the elution of related peptides that had absorbance at 277 nm. Considering that these bifunctional peptides were being purified using an exceptionally long duration of gradient over a wide solvent hydrophilicity-hydrophobicity range, the existence of the high baseline at 277 nm was an indication of the difficulty associated with the purification of peptides of this size and composition by HPLC. On the basis of the traditional (area under the peak) interpretation of the chromatogram of K_{25}AOA1#2, the estimated purity was perhaps less than 10% by HPLC. The mass spectra analysis of K_{25}AOA1#2 gave a result that was in agreement with the HPLC results suggesting the presence of a high percentage of contaminating related peptides present in the batch. Protein sequencing analysis of the first 23 N-terminal amino acid residues of K_{25}AOA1#2, however, did not detect the presence of any related peptide in this batch obtained by peak-splicing. The mass spectra of K_{25} (Figure 2.27B) which was synthesized in parallel with the K_{25} moiety of K_{25}AOA1#2 showed that there was a high degree of heterogeneity of oligolysine species of shorter lengths than the target 25 residues during that part of the synthesis. The inference from this evidence is that the fusogenic sequence with different lengths of

oligolysine chains had been produced during the synthesis that were close in numerical value had not been successfully resolved by HPLC. Similar inferences can be drawn from the analysis of $_DK_{25}$AOA1, K_{25}INF7 and K_{10}INF7. HPLC analysis of the batch of K_{25}AOA1#3 (which was synthesized by Dr. Graham Bloomberg and was not purified by HPLC (Figure 2.12)) showed that the three main peaks in the chromatogram emerged from and returned to a low baseline, suggesting that there was less heterogeneity in the lysine chain of this batch of K_{25}AOA1 and this was confirmed by the sharp peaks of the mass spectra of K_{25}AOA1#3. The mass spectra of the batch of K_{25} (Figure 2.28B), which was synthesized in parallel with the K_{25} moiety for K_{25}AOA1#3 showed a product with >95% of the of the target peptide, thus confirming the inference that the high absorbance baseline observed in the chromatogram of K_{25}AOA1#2 was due to the heterogeneity of the oligolysine moiety of K_{25}AOA1#2. The mass spectra of K_{25}AOA1#3 suggested that the crude product consisted of about 70% of the target compound, as determined by the ratio of the peak height of the target peptide as a proportion of the sum of all the major peaks in the spectra. The HPLC chromatogram of K_{25}AOA1#3 however suggested that the proportion of the target peptide could be less than 70%. Ideally, it would have been preferable to isolate each of the three main peaks identified in the analytical HPLC trace of K_{25}AOA1#3, analysed each peak by protein sequencing or mass spectrometry to identify the peak which contained the target peptide and then used that fraction in experiments. However such considerations were not possible as large quantities of K_{25}AOA1#3 were required for further erythrocyte lysis assays. The analytical chromatogram of K_{10}AOA1 showed the absence of a main peak and it suggested a very heterogeneous mixture of compounds, but the mass spectra showed that about 80% of the crude compound consisted of the target peptide in contradiction to inferences that could be made from the HPLC chromatogram. As analytical methods for such polypeptides, both HLPC and mass spectrometry have strengths as well as limitations. This disagreement between the levels of purity as determined by mass spectrometry and liquid chromatography of synthetic proteins of this composition was one which could only be resolved if there was substantial resources available to synthesize these peptides in large batches to enable peaks to be isolated by preparative liquid chromatography and the fractions analysed by protein sequencing and mass spectrometry.

Fusogenic peptides have an overall negative charge and thus can only be solubilised in solutions with high pH or solutions containing a high concentration of a solubilising agent e.g. guanidinium hydrochloride (GnHCl). At a high pH, (pH greater than 8), C18 packing material used as the stationary phase in reverse-phase chromatography disintegrates. Reported methods of purification of fusogenic peptides include ion-exchange[167] or solubilising the peptide in high concentration of GnHCl, pumping unto a C4 column and purifying by HPLC followed by desalting on a BioGel™ P-2 column[76]. Although there was an ion-exchange equipment within the department of Pharmacy and Pharmacology at the University of Bath, it was not available for use to purify the fusogenic peptides used in this project. The lack of ion exchange equipment (pump, column, detector) within the group to purify peptides with net negative charge meant finding alternative previously untested method to purify negatively charge peptides. The manufacturers of the POROS column had recommended the use of 0.3% ammonia (v/v) or sodium hydroxide (w/v) in the mobile phase, but this resulted in the degradation of the fusogenic peptides as evidenced by the appearance of new peaks after HPLC.

At a later stage of the project it was observed that the biological activity of bifunctional peptides were abrogated by the presence of 10% (v/v) serum so a decision was taken to synthesize a D-amino analogue of K_{25}AOA1 (DK_{25}AOA1) to investigate if resistance to enzymatic degradation[167] will result in restoration of transfection activity in serum. The outcome of this investigation is discussed in Chapter 3. The first batch of DK_{25}AOA1 peptide that was synthesized had an Asn residue totally omitted from the sequence (as seen in protein sequencing report in Figure 2.15), most likely due to steric hindrance of the side chain-protecting group (triphenylmethyl) used. The resulting peptide (named DK_{25}AOA1(N)) was over 100-fold less active in transfection experiments after complexation with DNA (see Chapter 3 section 3.3.13). A second batch of DK_{25}AOA1 synthesized used Asn with no side chain protection and the restoration of high transfection activity comparable to the L- amino acid analogue, suggests that the full sequence was present. Lack of funds did not permit a sequencing test to be performed on this second batch of DK_{25}AOA1.

Although the synthesis of these peptides would be challenging under any circumstances, the difficulties encountered during purification of the fusogenic peptides and K_{25}AOA1

with oligohistidyl chains ($K_{25}H_{10}AOA1$ and $K_{25}H_{20}AOA1$) were mainly due to lack of financial resources or lack of access to equipment. Nevertheless reasonable quantities of target peptides were obtained at purities, which enabled biological experiments to be conducted. It should be noted that in many instances biochemical activity is studied using crude peptides when the oligopeptide is above 30 residues in length.

Many of the peptides used in this study were of reasonable purity, but were not as pure as many analytical reagents used in scientific research. Typical purity for research materials of low molecular weight, which can be recrystallised several times without substantial loss of material, would be >95% and often >99%. This level of purity cannot be achieved with peptides of the size used in this study unless very large batches are available so that the peptides can be purified chromatographically and recovered from dilute solution.

3 PHYSICAL AND NON-PHYSICAL CHARACTERISATION, *IN VITRO* AND *IN VIVO* TESTING OF BIFUNCTIONAL PEPTIDES

3.1 PHYSICAL CHARACTERISATION AND *IN VITRO* TESTING OF BIFUNCTIONAL PEPTIDES

3.1.1 INTRODUCTION

Although little concordance has been observed between *in vitro* and *in vivo* transfection efficiency of GDVs, the high expense of animal experiments makes the use of *in vitro* transfection experiments for screening and optimisation of potential/novel GDVs a common practice by researchers in the development of novel GDVs. Because dividing cells in culture are generally easier to transfect than cells *in vivo*, it is usually safe to assume that if a putative GDV can not promote gene delivery *in vitro*, then it is unlikely to be effective *in vivo*. Different cell lines respond differently to different GDVs so it is common practice for researchers to report the transfection efficacy of novel GDVs in a panel of different cell lines *in vitro*. *In vitro* transfection experiments can be useful as a tool to estimate of the quantity of GDV that may be required to complex a nominal quantity of DNA for *in vivo* transfection efficacy (i.e. the polycation:polyanion charge ratio). *In vitro* experiments can also be used to investigate possible obstacles to gene transfer *in vivo* such as the effect of serum proteins or enzymes on transfection. Fully confluent/differentiated cells cultured on filters can be used to simulate the effect of the absence of cell division on transfection efficiency of a GDV. The major limitation to using dividing cells as a model is that the nuclear membrane becomes discontinuous during cell division, which allows DNA to be incorporated into the daughter nuclei. However, dividing cells remain the primary test for new non-viral GDVs, due to the simplicity of the methods.

The synthetic peptides described in Chapter 2 were tested for their ability to promote transfection *in vitro* using dividing cells. Particular attention was paid to comparing the activity of binary complexes formed between novel bifunctional peptides and DNA with ternary complexes formed by sequential mixing of poly/oligolysine with DNA followed by addition of fusogenic peptides. This latter approach has previously described by

Plank and colleagues[167] and Gottschalk and collegues[76]. In transfection studies, both the total level of gene expression in the culture as well as the proportion of cells transfected was determined. The effect of whole serum, serum albumin and chloroquine on the transfection efficiency of bifunctional peptides was also evaluated. Transfection studies using bifunctional peptides that both bind to DNA and provide membrane fusogens have not been previously reported. The work described here represents an attempt to produce a more reliable and reproducible endosome escape system than those that are currently available. As a positive control DNA complexes with the cationic lipid DOTAP or the cationic polymer polyethylenimine (PEI) were compared with peptide complexes. Preliminary i*n vivo* testing of the novel bifunctional peptides, which involved intramuscular and intratumoural injection of bifunctional peptide/DNA particles were performed in mice.

Physical and non-physical characterisation studies of the novel bifunctional peptide(s) that were carried out in this project included particle sizing and zeta potential measurements of peptide/DNA complexes, DNA affinity studies of peptides using ethidium bromide exclusion assays and erythrocyte lysis assays which are an established method measuring the membrane disruptive potency of a fusogenic peptides.

3.2 MATERIALS AND METHODS

3.2.1 CELL CULTURE MATERIALS

All biochemicals were of analytical grade and purchased from Sigma Chemicals, UK, except where indicated.

3.2.1.1 SOLUTIONS

3.2.1.1.1 Water

Freshly obtained Milli-Q water from a Milli-Q PF Plus system with ultrafiltration cartridge (Millipore UK Ltd.) was sterilised by autoclaving at 121°C for 15 minutes

before being used for the preparation of all culture media and solutions and was obtained.

3.2.1.1.2 Phosphate buffered saline

Phosphate buffered saline (PBS) tablets, without magnesium or calcium ions was obtained from Oxoid Ltd, UK. One tablet was dissolved in 100 ml of double-distilled, deionised water (DDDW) or Milli-Q water with a final pH of 7.3. Solutions were sterilised by autoclaving.

3.2.1.1.3 Sodium bicarbonate and sodium hydroxide

Solutions of 7.5% (w/v) sodium bicarbonate ($NaHCO_3$) and 1 M sodium hydroxide (NaOH) were prepared individually using Milli-Q water and sterilised by autoclaving.

3.2.1.1.4 Ethylene diamine tetraacetic acid (EDTA)

A 0.02% (w/v) solution of EDTA was prepared in PBS and sterilised by autoclaving.

3.2.1.1.5 Trypan blue

Trypan blue, used for assessing cell viability, was obtained from BDH Laboratory Reagents Ltd and was prepared as a 0.1% (w/v) solution in PBS.

3.2.1.2 CULTURE MEDIA AND ADDITIVES

All solutions used for the preparation of culture medium for mammalian cells were obtained from Gibco BRL, Paisley, UK, unless prepared as described above. Eagle's Minimum Essential Medium - Eagle's (MEM) with Earle's salts and Dulbecco's Modified Eagle's Medium (DMEM) were obtained as 10x concentrates. The media were supplied without sodium bicarbonate and L-glutamine but contained phenol red as an indicator. MEM non-essential amino acids solution (MEM-NEAA), L-glutamine

(200 mM), and penicillin (10000 IU/ml)/streptomycin (10000 μg/ml) were obtained as 100x concentrates. Foetal calf serum (FCS) from various suppliers was batch tested to determine which provided optimum growth of cells. Batches 30F3031S, 40Q1841F and O6Q7554F from Gibco were found to support growth of all cells and were thus used. Growth media were prepared aseptically according to the formulae shown below and stored at 4°C and used within three weeks of preparation. The quantities of the various media additives used for preparation of the culture media used in this project are summarised in Table 3.1.

Reagent	MEM with 10% [v/v] FCS (ml)	MEM with 20% [v/v] FCS (ml)	DMEM with 10% [v/v] FCS (ml)
MEM 10x	50	50	-
DMEM 10x	-	-	50
FCS	50	100	50
MEM-NEAA	5	5	-
L-Glutamine	5	5	5
Penicillin-Streptomycin	5	5	5
7.5% [w/v] $NaHCO_3$	15	15	25
Milli Q water	to 500	to 500	to 500
1 M NaOH	to pH 7.4	to pH 7.4	to pH 7.4

Table 3.1 Formulae for the preparation of cell culture media.

3.2.1.3 EQUIPMENT

3.2.1.3.1 Laboratory equipment

All aseptic techniques were carried out in a laminar flow cabinet (MDH Ltd) designed for vertical re-circulation of air. Cells were cultured in an LEEC PF2 anhydric incubator (Laboratory and Engineering Company).

Growing cell cultures were viewed daily under an inverted light microscope (WILD M4, Wild Heerbrugg Ltd). For determination of cell concentration in suspension, appropriately diluted samples were counted on a standard double grid haemocytometer (Neubauer 0.1 mm Dept, Weber, UK).

3.2.1.3.2 Disposable items

Sterile 175 cm^2 tissue culture flasks were obtained from Falcon, Becton and Dickinson and Co, UK. Six- and 96- well plates were obtained from Nunc, (Denmark). 24 mm diameter, 0.4 and 3 μm pore PTFE/collagen treated tissue culture inserts (Transwell-COL™) were obtained from Costar, UK. Cryopreservation ampoules used for storing frozen cells in liquid nitrogen were obtained from Nunc, (Denmark).

3.2.2 CELL CULTURE METHODS

3.2.2.1 CELL LINES

All cell lines were maintained at 37°C in a humidified atmosphere consisting of 95 % (v/v) air / 5% (v/v) CO_2. Cells were visually assessed on a daily basis for evidence of microbial contamination.

B16 cells, a murine melanoma cell line, were donated by L.R. Kelland, Institute of Cancer Research, Sutton. B16 cells were grown in Eagle's MEM medium containing 10% (v/v) FCS. For routine culture, cells were subcultured 1 in 10 twice weekly and the medium changed every 48 hours.

A549 cells, a human adenocarcinoma cell line derived from the alveolar region of the lungs (alveolar type II), were obtained from M. Watson, Department of Pharmacy and Pharmacology, University of Bath, UK. A549 cells were maintained in DMEM medium containing 10% (v/v) FCS. For routine culture, cells were subcultured 1 in 4 twice weekly and the medium changed every 48 hours.

COS-7 cells, a fibroblast-like cell line established by SV40 transformation of CV-1 African green monkey kidney cells, were obtained from the European Collection of Animal Cell Cultures (ECACC), UK. COS-7 cells were cultured in Eagle's MEM containing 10% (v/v) FCS. For routine culture, cells were subcultured 1 in 5 twice weekly.

HeLa cells, human carcinoma cells, were obtained from the European Collection of Animal Cell Cultures (ECACC), UK. HeLa cells were cultured in Eagle's MEM containing 10% (v/v) FCS. For routine culture, cells were subcultured 1 in 3 twice weekly.

Primary human fibroblasts from newborn human foreskin (FEK4) were obtained from Professor R.Tyrrell, Department of Pharmacy and Pharmacology, University of Bath, UK, were cultured in DMEM supplemented with 15% (v/v) foetal calf serum.

The human fibroblast cell line NIH3T3, and the human emboynal kidney line HEK293 were obtained from the European Collection of Animal Cell Cultures (ECACC). NIH3T3 cells were cultured in Eagle's MEM containing 10% (v/v) FCS. For routine culture, cells were subcultured 1 in 5 twice weekly.

Caco-2 cells (a human colonic adenocarcinoma cell line) were obtained from J. Bennett, Pfizer Central Research, Sandwich, UK. These cells were maintained in Eagle's MEM containing 20% (v/v) FCS (heat inactivated at 56°C for 30 minutes). In order to obtain differentiated monolayers, Caco-2 cells were cultured on semi-permeable membranes with a mean pore size of 0.4 μm which enabled feeding from both apical and basolateral surfaces. Cells were seeded at a density of 3 x 10^5 cells per 24 mm diameter collagen-coated tissue culture insert (Transwell-COL™, Costar). Cells were maintained on the filter for up to 30 days with a change of the culture medium every 48 hours.

All cells lines were grown as monolayer cultures and subcultured at 80-100% confluence. For subculture, 175 cm^2 flasks containing attached monolayers of FEK4 cells were rinsed three times with 10 ml aliquots of PBS and then incubated at 37°C with 2 ml of 0.02% (w/v) EDTA solution for approximately 5 minutes. Detached cells

were diluted to 10 ml with complete culture medium, counted on a haemocytometer and an appropriate aliquot of suspension transferred to a sterile 175 cm^2 flask containing 50 ml of fresh culture medium.

3.2.2.2 DETERMINATION OF CELL CONCENTRATION

Following detachment of cells from flasks, the cell suspension was briefly vortexed to break-up clumps of cells. To a 100 µl aliquot of cell suspension was added 200 µl of PBS and 200 µl of 0.1 % (w/v) Trypan blue solution. This sample was loaded on to a grid haemocytometer overlaid with a coverslip. Viable cells were detected by a bright 'halo' light around their cell membrane whereas dead cells were permeabilised by the dye and stained blue. The viable cell number in the four squares surrounding the central square were counted and this was repeated for the other side of the haemocytometer grid, using an inverted light microscope. The viable cell concentration in the original suspension was calculated using the following equation:

$$\text{Cells per ml} = \frac{\text{Total cell count in 8 chambers x dilution factor x } 10^4}{8}$$

Equation 3.1

3.2.2.3 CELL STORAGE AND RECOVERY

Cells were prepared for storage by detachment of a confluent monolayer according to the standard protocol (section 3.2.2.1) followed by centrifugation at 1000 rpm for 8 minutes. The supernatant was then discarded and the cells resuspended in filter sterilised (0.2 µm Acrodisc) solution of culture medium supplemented with 10% (v/v) dimethyl sulphoxide (spectrophotometric grade, Aldrich, UK) as a cryopreservative. Cell suspensions were then dispensed in 1.8 ml aliquots into Corning tubes and transferred to a Union Carbide BF6 biological freezer unit plug, which fitted into a Union Carbide LR-40 liquid nitrogen freezer. This permitted the cells to be cooled down to -70°C at a rate of approximately 1°C per minute. The cells were then

transferred to a Union Carbide LR-40 liquid nitrogen freezer where they were stored at approximately -148°C. For cell recovery, the contents of an ampoule were thawed rapidly by brief incubation in a 37°C water bath followed by dilution with 10 ml of fresh medium added dropwise. Cells were centrifuged for 8 minutes at 1000 rpm and the supernatant was discarded. The cells were then resuspended in 10 ml of fresh medium and then transferred into a 175 cm^2 flask containing 50 ml of medium and then incubated under standard culture conditions. Cells were cultured for at least two passages in order to establish them before any experiments were carried out.

3.2.3 MOLECULAR BIOLOGY METHODS

3.2.3.1 BACTERIAL STRAIN

Escherichia coli strain XL1-Blue (Stratagene, UK), which has resistance to tetracycline, was used for propagation of plasmids. Competent E.coli XL1-Blue cells were prepared as described in Appendix A and transformed with the appropriate plasmid using the heat shock technique (Appendix B1) as described by Sambrook *et al.*[254].

3.2.3.2 DEOXYRIBONUCLEIC ACID (DNA)

Two types of DNA plasmids, pRSV*lacZ* and pCMVluc, were used during the course of this project for transfection studies. pRSV*lacZ* contains the E.coli *lacZ* gene which encodes the β-galactosidase enzyme. pRSV*lacZ* was obtained from Dr. Ogilvie (Zeneca Pharmaceuticals, UK) and is a 7.8 Kb plasmid with the E.coli *lacZ* gene under the transcriptional control of the Rous sarcoma virus (RSV) long terminal repeat promoter/enhancer sequence. The RSV promoter is a moderate to high strength promoter causing moderate levels of transgene expression in mammalian cells. pCMVluc contains the firefly luciferase gene driven under the transcriptional control of the human cytomegalovirus (CMV) immediate early promoter/enhancer element. The CMV promoter is a strong viral promoter causing high levels of transgene expression in mammalian cells. pCMVluc was constructed by Dr. D. Milroy (formerly of Bath University), by ligating the luciferase gene into the backbone of pCMVβ (Clonetech),

after removal of the lacZ gene.

3.2.3.3 PLASMID PROPAGATION, ISOLATION AND PURIFICATION

A single colony of E.coli XL1-Blue containing the appropriate plasmid was isolated from an LB agar plate (Appendix C) supplemented with ampicillin and tetracycline (50 μg/ml and 12.5 μg/ml respectively - see Appendix D) and inoculated into 10 ml of LB broth containing the same antibiotics (primary culture). This primary culture was grown for 8 hours at 37°C on a shaking incubator at 300 rpm (New Brunswick Scientific, UK) and then a 5 ml aliquot was expanded in 500 ml of LB broth, also containing the appropriate antibiotics, and grown overnight. The plasmid was isolated by the alkaline lysis method[255] and the cell lysate purified by anion exchange chromatography using the Plasmid Maxi Kit (Qiagen Inc., USA) in accordance with the manufacturer's instructions. The isolated DNA was dissolved in TE buffer (Tris 10 mM, EDTA, 1 mM), pH 8 and stored at -20°C.

3.2.3.4 SAMPLE PURITY AND QUANTIFICATION

For quantification of plasmid DNA, a 10-20 μl aliquot of sample was diluted to 1 ml with distilled water and the absorbance of the solution measured at 260 nm (A_{260}) and 280 nm (A_{280}). The concentration of DNA in the original solution was calculated as follows:

Concentration of DNA (μg/ml) = Dilution factor x 50[1] x A_{260}

Equation 3.2

The purity of DNA was calculated as follows:

$$Ratio = \frac{A_{260}}{A_{280}}$$

Equation 3.3

Ratios between 1.8 and 2.0 were consistently obtained.

---

[1] Based on the assumption that a 50 μg/ml solution of double stranded DNA has an absorbance of 1 at 260 nm.[254]

3.2.3.5 SAMPLE IDENTIFICATION

A sample of purified DNA was linearised with a restriction endonuclease (usually Xba I or Sma I for pRSV*lacZ* (enzyme from New England Biolabs, UK) for one hour at 37°C and then loaded on to a 1% (w/v) agarose (Ultrapure grade, Gibco, UK) gel in 1x TAE (0.04 M Tris-acetate, 0.001M EDTA). Controls of undigested DNA and molecular weight markers (Appendix E) were run alongside digested plasmid to verify the presence of other contaminating nucleic acids (genomic DNA or RNA) and to confirm the size.

3.2.4 RETENTION OF PEPTIDE FUNCTIONALITY

The ability of the bifunctional peptides such as K_{25}AOA1 to bind to DNA and lyse erythrocytes simultaneously was investigated using gel mobility shift assay, ethidium bromide exclusion assay and erythrocyte lysis assay as described below.

3.2.4.1 GEL MOBILITY SHIFT ASSAY

Agarose gels were produced by dissolving electrophoresis grade agarose 1% (w/v), (Gibco BRL) in 1x TAE at 100°C. The solution was cooled to about 60°C, poured into the gel tray and allowed to set to room temperature. The gels were then mounted in an electrophoresis tank (Bio-Rad mini-sub DNA cell) and submersed in 1x TAE buffer.

Plasmid DNA, (3 µg pRSV*lacZ*) was diluted to 125 µl with HBS in a sterile micro-centrifuge tube. Various quantities of the peptides (K_{25}AOA1 and K_{25}) were separately diluted to 125 µl in sterile micro-centrifuge tubes and were subsequently pulse centrifuged (Jouan microfuge, France) to concentrate samples to the bottom of the tube. The GDV solution was then added to an equal volume of DNA solution by gentle mixing (pipetting up and down five times). Mixtures were incubated for 30 minutes under ambient conditions. After this time, 40 µl of solution were diluted to 50 µl with electrophoresis loading buffer. Six µl of this sample was loaded on to a 1% (w/v) agarose gel in 1x TAE and subjected to electrophoresis at 80 volts for one hour in 1x

TAE. The gels were stained with ethidium bromide in water at a concentration of 0.5 μg/ml for 10 minutes. The agarose gel was then viewed under a ultra-violet transilluminator and photographed using a Polaroid 55 film fitted into a Polaroid CU-5 camera.

3.2.4.2 Ethidium Bromide Exclusion Assay

Six μg of pRSV*lac*Z was diluted to 125 μl with HBS in a sterile micro-centrifuge tube. Various quantities of the GDV were separately diluted to 125 μl in sterile micro-centrifuge tubes. The samples of DNA and GDV were mixed by pipetting up and down five times, incubated for 30 minutes and then diluted to 3 ml with 20 mM sodium chloride solution. The fluorescence was monitored at $\lambda_{excitation}$ 260 nm and $\lambda_{emission}$ 600 nm immediately following the addition of 3 μl of a 0.5 mg/ml solution of ethidium bromide (final concentration of 0.5 μg/ml), on a RF-540 spectrofluorimeter (Shimadzu, UK) using 1 cm cells with slit settings of 5 nm for both the excitation and emission monochromators.

3.2.4.3 Erythrocyte Lysis Assay

Erythrocyte lysis capabilities of the peptides were tested using the method described by Plank *et al.*[167]. Freshly prepared human erythrocytes were washed with HEPES buffered saline (HBS: 20 mM HEPES, 150 mM sodium chloride, pH 7.4) and resuspended in a 2 x assay buffer of the appropriate pH (300 mM NaCl, 30 mM sodium citrate) at a concentration of approximately 5 x 10^7 cells/ml. An aliquot of 80 μl of the erythrocyte suspension was added to 80 μl of a serial dilution of the peptide in water (concentration of peptides ranged from 0.078125 to 5 μg/μl) in a 96-well microtitre plate and incubated for 1 h at 37°C with constant shaking. After removal of the unlysed erythrocytes by centrifugation (1000 x g, 5 min), 55 μl of the supernatant was transferred to a new microtitre plate and haemoglobin absorption determined at 490 nm (background correction at 750 nm). 100% lysis was determined by adding 1 μl of a 10% (v/v) Triton X-100 solution prior to centrifugation. The haemolytic units were calculated as the reciprocal value of the peptide concentration, where 50% leakage was observed (i.e. the

volume (μl) of erythrocyte solution which is 50% lysed, per μg of peptide). The experiment was performed in triplicates for each peptide concentration.

3.2.5 INVESTIGATION OF TOXICITY USING MTT ASSAY

B16 cells were plated in a 96-well plate at a density of approximately 4000 cells per well in 100 μl media. Peptides to be tested were made up at twice the required concentration in 100 μl of PBS and added to the wells. The first column had no cells, the sixth column had cells incubated with 100 μl PBS (no cytotoxic agent). Ten serial dilutions were prepared such that expected 50% cell kill was straddled evenly by maximum and minimum concentrations. The cells and agents were incubated at 37°C for 3 days. The medium was then removed and the plates washed twice with 200 μl PBS. A 10 mg/ml stock solution of MTT (2-(4,5-dimethylthiazol-2-yl)-2,5-diphenyltetrazolium bromide, from Sigma Chemicals Ltd, Louis MO USA) was made in PBS and diluted with serum free media (no FCS, no amino acids) to produce a 1 mg/ml solution. The cells were then incubated with 200 μl of 1 mg/ml MTT in serum free medium for 3 hours at 37°C. The medium was then removed by quick overturn of the 96-well plate. Two hundred microlitres DMSO was added to each well and the plate was placed on an orbit mixer moving at medium speed for 5 minutes to dissolve the formazan. Absorbance was read at 540 nm (background readings at 690 nm). A graph of absorbance versus log concentration of cytotoxic agent was plotted. The extracellular concentration of cytotoxic agent which kills 50% of cells compared to control (EC_{50}) was determined.

3.2.6 TRANSFECTION OF MAMMALIAN CELLS

For transfection of exponentially growing cultures, cells were seeded at a density such that at the time of transfection monolayers were 40-50% confluent. For the various cells types studied, seeding densities on 35 mm well plates (6-well plates) were as shown in Table 3.2. Following seeding, cells were grown for 16-20 hours under standard conditions in the appropriate culture medium prior to transfection. Transfections were carried out in the presence of Opti-MEM™, which is a serum-free medium specifically designed for transfection experiments.

Cell Line	Cell Number per 6-well Plate
B16	1×10^5
NIH3T3	4×10^5
HEK293	2×10^5
COS-7	2×10^5
A549	2×10^5
HeLa	1×10^5
Caco-2	3×10^5
CHO	1×10^5
FEK4	5×10^5

Table 3.2 Seeding densities on 6-well plates for the transfection of various mammalian cells lines.

3.2.7 PROTEIN ASSAY

The protein content in cell extracts was measured using the Bio-Rad protein assay kit. Samples were prepared according to the manufacturer's protocol (macro assay) and calibration curves were constructed using bovine serum albumin as a standard. Spectrophotometric measurements were made at 595 nm. A typical standard curve is shown in Appendix F.

3.2.8 PEPTIDE-DNA COMPLEX FORMATION

Three batches of $LK_{25}AOA1$ were used in this project. The first batch ($K_{25}AOA1\#1$) consisted of the whole main peak collected during HPLC and had an estimated purity of 70-80%. This batch of peptide was used for erythrocyte lysis assay, ethidium bromide assay and initial transfection experiments. The second batch ($K_{25}AOA1\#2$) consisted of peak splicing of the main peak (Figure 2.9) and has an estimated purity of 75-90% (based protein sequencing and analytical HPLC results). The yield of this batch after purification was 6% and was used only for transfection. A third batch of $K_{25}AOA1$

(K_{25}AOA1#3) was crude peptide, which did not undergo any HPLC purification process. K_{25}AOA1#3 has an estimated purity of 70% according to MALDI-TOF mass spectrometry (Figure 2.13) analysis. This batch was used for the second erythrocyte lysis assay in section 0, and experiments with Bafilomycin A_1 (section 3.3.7).

A solution containing 6.4 μg DNA was made up to 800 μl with HBS in a sterile microcentrifuge tube. For single-step complex formation, aliquots of appropriate quantities of peptide solutions taken from a 1 mg/ml stock solution were placed in separate microcentrifuge tubes and made up to 800 μl with HBS. The peptide and DNA solutions were mixed by pipetting up and down 5 times. This method was found to be the optimum mixing method for polycation/DNA complexes[256]. For two-step complex formation, 6.4 μg of DNA in 400 μl HBS was mixed with an appropriate quantity of K_{25} or K8 in 400 μl HBS and left for 30 minutes before mixing with appropriate quantity of fusion peptide in 800 μl HBS and incubating for a further 30 minutes.

An hour prior to transfection, monolayers of rapidly dividing cells were washed twice with warm transfection medium and then 1.5 ml of this medium was added to each well. Five hundred microlitres of complex containing 2 μg of DNA and variable quantities of gene transfer agent were added to each well. Transfection was carried out for 4 hours at 37°C after which time the transfection medium was replaced with fresh complete culture medium and cells were cultured for a further 44 hours for RSVlacZ plasmid or 20 hours for CMVluc plasmid before harvesting for analysis. For all transfection studies, each data point represents the mean ± standard error of the mean (SEM) of triplicate samples and each experiment was performed on at least two occasions to ensure reproducibility of results.

3.2.9 OLEOYL-FUSOGENIC PEPTIDE/DOTAP/DNA COMPLEX FORMATION

DOTAP/oleoyl-fusogenic liposomes were prepared by an adaptation of the reverse phase evaporation method previously described by Szoka and Papahadjopolous[257]. DOTAP powder was dissolved in chloroform to produce a 2 mM stock solution. An appropriate volume of solution was transferred to a clean amber sample vial. Oleoyl-AOA1 peptide solution was prepared by dissolving in 0.1% (v/v) aqueous ammonia. An

appropriate amount of ethanol (approximately 1:1 v/v) was added to both the chloroform layer and aqueous layer before mixing the two layers to form a clear homogenous solution containing various molar proportions of DOTAP/oleoyl-AOA1. The clear homogeneous mixtures containing DOTAP/oleoyl-AOA1 were evaporated by bubbling nitrogen gas, eventually leaving a thin film on the glass wall. Residual amounts of liquid were removed by placing vials under high vacuum (Edwards) overnight. The lipidic film was subsequently re-dispersed in sterile water. The aqueous dispersion was vortexed for 1 minute at full speed under ambient conditions to generate large multilamellar vesicles. Following preparation, the lipidic fusogenic peptides were stored at 4°C and used within 7 days.

3.2.10 ANALYTICAL METHODS

3.2.10.1 PREPARATION OF CELL EXTRACTS FOR ANALYSIS OF GENE EXPRESSION

Solutions used during analysis are listed below. Their composition is found in section 3.2.1.1 above.

Phosphate buffered saline (PBS)

0.02% (w/v) EDTA solution

0.1M sodium phosphate buffer (pH 7.3)

Lysis buffer (0.1% [w/v] Triton X-100 in 250 mM Tris buffer pH 8)

Washed cell monolayers were treated with 250 µl of lysis buffer per well and plates were frozen at - 70°C. After thawing at room temperature, the cell extracts were collected and transferred into sterile micro-centrifuge tubes and centrifuged for 10 minutes at 1000 rpm and the supernatant used for analysis.

3.2.10.2 ASSAY METHODS

3.2.10.2.1 4- methylumbelliferyl -β-D-galactoside (MUG) method

300 mM MUG in DMSO

Buffer Z	0.1 M sodium phosphate buffer (pH 7.3) 10 mM potassium chloride 1 mM Magnesium sulphate
STOP buffer	300 mM Glycine 15 mM EDTA adjusted to pH 11.2 with concentrated solution or pellets of sodium hydroxide

A 300 mM stock solution of MUG was prepared in DMSO (10 mg/ml) and stored at 4°C for up to one month. When required, this solution was diluted 1:100 to a 3 mM working solution in buffer Z (reducing the DMSO concentration to ≈ 1% [v/v]) and heated in a boiling water bath to aid solubilisation when necessary.

An appropriate volume of cell extract (maximum of 105 µl) was diluted to 120 µl with buffer Z in a 96-well plate to which 30 µl of 3 mM MUG solution was added. The contents in each well were mixed and the plate was incubated at 37°C for 60 minutes after which time the reaction was terminated by the addition of 75 µl of STOP buffer. Fluorescence was measured using a multiwell plate scanning spectrofluorimeter (Titretek Fluoroskan II) at $\lambda_{excitation}$ 350 nm and $\lambda_{emission}$ 460 nm. A typical calibration curve is shown in Appendix G1.

3.2.10.2.2 Luciferase assay

Luciferase levels within cells were quantified using the Promega luciferase assay system (Promega, UK) according to the manufacturer's instructions. As little as 0.001 pg of firefly luciferase can be measured using this kit. A standard curve of light units versus relative enzyme concentration was produced using purified firefly luciferase *(*Appendix G2 and G3*)*. The lysis protocol detailed above was followed, substituting the Promega lysis buffer (25 mM Tris-phosphate, pH 7.8; 2 mM DTT 2 mM 1,2-diaminocyclohexane-N,N,N',N'-tetraacetic acid; 10% (v/v) glycerol; 1% (v/v) Triton X-100 and BSA I mg/ml) for the phosphate buffer. Supplementation with 1 mg/ml BSA

ensured that luciferase was not lost from solution by adsorption onto container walls. After centrifugation of the cell lysate, 20 µl of room temperature cell extract (supernatant) was mixed with 100 µl of luciferase assay reagent (luciferase assay substrate plus 10 ml of assay buffer) at room temperature. The disposable test tube containing the reaction was then immediately placed into the luminometer (TD-20/20). The instrument settings were as follows: sensitivity 25.1, delay 2 seconds and the integration 10 seconds.

3.2.10.2.3 Cytochemical staining for β-galactosidase activity

Solutions used:

Phosphate buffered saline (pH 7.3)

Fixative solution
1% (v/v) glutaraldehyde
1 mM magnesium chloride
0.1M sodium phosphate pH 7.3

X-gal solution
0.2% (w/v) 5-bromo-4-chloro-3-indolyl-β-galactoside (X-gal) in dimethylformamide
1 mM magnesium chloride
150 mM sodium chloride
3.3 mM potassium ferrocyanide, $K_4Fe(CN)_6$
3.3 mM potassium ferricyanide, $K_3Fe(CN)_6$
0.1M sodium phosphate

Forty-four hours post transfection, cell monolayers were rinsed twice with 2 ml of PBS and then permeabilised by overlaying with 2 ml of the fixative solution followed by incubation at 4°C for 5 minutes. The fixative solution was aspirated, the cells rinsed once with PBS and then overlaid with 1 ml of X-gal solution, followed by incubation overnight at 37°C. Cells were then washed twice with PBS and viewed under an inverted light microscope. Cells expressing the β-galactosidase enzyme were stained blue against a background of unstained cells. Where appropriate, photographs were taken using a Nikon F-301 camera with Fujichrome 200 or 400 DX film.

3.2.10.2.4 Fluorescence Cytometry

Cells were transfected as usual in 6-well plates with DNA/peptide complexes with plasmid DNA encoding for the enhanced green fluorescent protein (EGFP) complexed with either $DK_{25}AOA1$, $LK_{25}AOA1\#2$, K8+JTS1, PEI, or PL219 in the presence or absence of chloroquine at a concentration of 100 μM at their respective optimum charge ratios for the respective cell lines. Twenty-four hours after initiation of transfection, the culture medium was aspirated and the cells were washed twice with 2 ml aliquots of PBS. Transfected cells were detached by incubating cells with 250 μl of 0.02% (w/v) EDTA solution per well at 37°C for 2 minutes. In order to remove EDTA from the cells, the cell suspension was transferred into a 1.5 ml microcentrifuge tube and centrifuged at 13000 rpm for 1 minute. The supernatant was removed and the cells were resuspended in 1 ml Opti-MEM® supplemented with 10% (v/v) foetal calf serum (FCS), centrifuged at 13000 rpm for 1 minute and the supernatant removed. This last process was repeated once. Cells were then resuspended in 1 ml Opti-MEM® supplemented with 10% (v/v) FCS and placed on ice, ready for fluorescence cytometry analysis. Samples were analysed on a Becton Dickinson fluorescence cytometry Vantage with optics optimised for detecting EGFP.

3.2.11 CALCULATIONS

3.2.11.1 TRANSFECTION ACTIVITY

$$\beta\text{ - gal/luc activity per well} = \frac{250\,(\mu l) \times \beta\text{ - gal/luc activity per sample}}{\text{Sample volume}\,(\mu l)}$$

Equation 3.4

$$\text{Protein content per well} = \frac{250\,(\mu l) \times \text{protein content per sample}}{\text{Sample volume}\,(\mu i)}$$

Equation 3.5

$$\text{Specific } \beta\text{ - gal/luc per activity} = \frac{\text{Total } \beta\text{ - gal/luc activity per well } (\mu\text{U or mU})}{\text{Total protein per well (mg)}}$$

Equation 3.6

3.2.11.2 CHARGE RATIOS

$$\text{No. of mols of positive charges} = \frac{\text{Mass of GDV x No. of positively charged groups}}{\text{Molecular weight of GDV}}$$

Equation 3.7

$$\text{No. of mols of negative charges} = \frac{\text{Mass of DNA}}{330}\ ^{2}$$

Equation 3.8

$$+/-\text{ charge ratio} = \frac{\text{No. of mols of positive charges}}{\text{No. of mols of negative charges}}$$

Equation 3.9

Calculation of charge ratios

$$+/-\text{ charge ratio} = \frac{\text{Molarity of positive charges}}{\text{Molarity of negative charges}}$$

Equation 3.10

$$\text{Molarity of negative charges} = \text{molarity of nucleotides} = \frac{\text{mass of DNA}}{\text{RMM}_{\text{DNA}}}$$

Equation 3.11

RMM (relative molecular mass) = 330, based on an average molecular weight of a nucleotide monomer. There is one negative charge per DNA.

---

[2] Based on the assumption that the average molecular weight of a nucleotide is 330[4]

$$\text{Molarity of negative charge in 2 } \mu g \text{ of DNA} = \frac{2 \times 10^{-6} \times 1 \text{ (-ve charge)}}{330}$$

Equation 3.12

Molarity of positive charges = molarity of positive charges supplied by the cationic molecule. There is one positive charge per lysine residue. For peptide molecules with both positive and negative charges e.g. $K_{25}AOA1$, the net charge between positive and negative residues was used as the overall charge to calculate the quantity required to complex with DNA to provide the desired charge ratio for the complex. $K_{25}AOA1$ has 25 positive charges from lysine and 4 negative charges from glutamic acid and aspartic acid. Hence the net positive charge is 21.

$$\text{Molarity of positive charges} = \frac{\text{mass x net positive charge}}{RMM_{K_{25}AOA1}} = \frac{\text{mass x 21}}{5736}$$

Equation 3.13

For compounds with histidyl chains ($K_{25}H_{10}AOA1$and $K_{25}H_{20}AOA1$), the histidine side chain (pKa =6.0) was estimated to be uncharged at pH 7.0 and hence not included in the calculation of positive charges.

3.2.12 *IN VIVO* TRANSFECTION METHODS

Dr. Pauline Wood, the Home Office licence holder, assisted in animal studies and her considerable input into this study is gratefully acknowledged. Female C3H mice were obtained from Charles River at 6-7 weeks of age and then allowed to acclimatise for a further week prior to experiments. Murine fibrosarcoma RIF-I cells[258] were cultured in RPMI 1640 medium supplemented with 15% (v/v) foetal calf serum, penicillin and streptomycin, and were not passaged more than 7 times prior to trypsinisation for implantation. The mice were lightly anaesthetised using intraperitoneal Hypnorm (a mix of fentanyl citrate 0.315 mg/ml and fluanisone 10 mg/ml, 0.05 ml per mouse) about 2 hours before implantation. An injection of 0.05 ml PBS containing $2x10^5$ RIF-1 cells was made intradermally mid way along the back of the mouse after shaving off the fur

with clippers. Tumours were ready for gene delivery experiments 7-10 days post-implantation. The mice were weighed and the dimensions of the tumour recorded, one day before muscle injection with DNA/peptide complexes. The mice were then randomly assigned to the different treatment cages.

On day zero, a 20 µl suspension/solution containing DNA complexed with or without K_{25}AOA1 was made into the right hind leg muscle of each mouse. To facilitate intramuscular injection the mice were anaesthetised using a combination of Hypnovel (midazolam 5 mg/ml) and Hypnorm (1 ml of Hypnovel + 1 ml of Hypnorm + 2 ml sterile water, inject 0.1 ml intraperiotoneally) and the right hind thigh shaved with an electric shaver. On day five, the mice were each injected with a 20 µl suspension/solution containing DNA complexed with or without K_{25}AOA1 into each tumour. Muscle and tumour injections were made using a graduated 0.3 ml sterile B-D syringe (Becton and Dickinson and Co, UK) fitted with 8 mm, 30 gauge needle. Following each injection, the needle was left in place for a short period to prevent formulation being expelled by the back pressure in the tissue. The mice were killed by cervical dislocation on day seven. Tumours and right hind leg muscle tissues were excised and placed in 2 ml cryotubes (NUNC, Denmark) and snap frozen in liquid nitrogen and stored in a Union Carbide BF6 biological freezer unit plug which fitted into a Union Carbide LR-40 liquid nitrogen freezer until ready to be analysed.

3.2.13 Analysis of *in vivo* gene expression

Excised tissues were weighed then homogenised for 30 seconds in a screw cap sterile tube containing 5-fold v/w of lysis buffer/weight of tissue (0.1 M potassium phosphate buffer pH 7.8, 0.2% (v/v) Triton X-100) using an ultraturax homogeniser. The tissue suspension was then spun at 12000 g for 15min at 4°C to remove the cellular debris. Luciferase was quantified using the Promega luciferase assay system (Promega, UK) as described in chapter 3 (section 3.2.10.2.2). The protein content of this supernatant was analysed using the Bio-Rad Protein assay kit (section 3.2.7). Expression was normalised with respect to total muscle or tumour protein.

3.3 RESULTS AND DISCUSSIONS

3.3.1 RESULTS AND DISCUSSION: INVESTIGATION OF RETENTION OF BIFUNCTIONALITY

In ternary complexes consisting of plasmid DNA, cationic polymers and fusogenic peptide sequences, the presence and individual activity of the constituent reagents are recognised as important for the mediation of gene delivery[76,167]. Novel peptides consisting oligolysine chains of 10 and 25 residues linked covalently to fusogenic sequence were synthesized in this project. The following sections describe studies performed to determine if the two moieties of the novel peptide retained their functions after being synthesized as a single linear peptide and discuss the effect of low pH on the activity of the fusogenic sequence within the bifunctional peptide.

3.3.1.1 RETENTION OF DNA-BINDING ACTIVITY

The purpose of this study was to ascertain if the presence of the fusogenic component of the bifunctional peptide inhibited the ability of the peptide to bind and condense DNA, a prerequisite for any *in vitro* transfection activity[94]. The bifunctional peptide K_{25}AOA1 (batch #1) was compared with K_{25} using gel retardation assay and ethidium bromide exclusion assay, to investigate the effect of the presence of the fusogenic moiety and study the ability of bifunctional peptides to bind and condense DNA.

3.3.1.1.1 Gel mobility assay

To compare the complexation of K_{25}AOA1 and K_{25} with DNA, various quantities of either peptides were mixed with 3 μg of pCMVluc in HBS, as described in section 3.2.4.1. Following incubation, the migration of complexes on a 1% (w/v) agarose gel in 1x TAE buffer was examined after staining with ethidium bromide. DNA neutralisation was assumed to have occurred at the lowest charge ratio (+/-) where the DNA was completely immobilised within the well origin. Figure 3.1 shows the results of the effect of charge ratio of K_{25}AOA1/DNA or K25/DNA complexes on the pattern of migration of these complexes on 1% (w/v) agarose gel when a potential difference of 80 volts was applied for 1 hour. In lane 1, which had plasmid DNA only, there was a small degree of

smearing but a predominant proportion of the DNA formed a single band pertaining to supercoiled DNA (refer to Figure 3.27, which shows a supercoiled DNA band and a nick-circular DNA band appearing under different incubation conditions). When DNA was complexed with K_{25}AOA1 at a charge ratio of 0.96, (lane 2) there was a considerable amount of smearing, indicating that DNA had been partly neutralised and was moving at varying speeds through the gel depending on the extent of neutralisation. It was observed that some amount of DNA barely migrated out of the well, indicated by the dark band below the well (towards the positive end of the gel); this band represented the proportion of plasmid DNA which was fully neutralised. The dark band of DNA observed furthest from the well (in line with the DNA band in lane 1) represented the proportion of DNA that was not complexed with K_{25}AOA1. A similar observation was made for K25/DNA complexes formed at a charge ratio of 0.5. At charge ratios above neutral, that is 1.9, 3.8, 7.6 and 15.2 in lanes 3, 4, 5 and 6 respectively, no DNA/peptide migration was observed, indicating that the fully neutralised complexes were immobilized within the wells; the excess proportion of peptide not complexed with DNA would have drifted into the electrophoresis buffer towards the cathode. Lanes 8, 9 and 10 containing K25/DNA complexes at charge ratios of 1.0, 2.0 and 4.0 also showed that fully neutralised DNA complexes did not migrate much further beyond the boundary of the wells (Figure 3.1). This result provided evidence that the presence of the fusogenic moiety in K_{25}AOA1 did not inhibit the DNA binding function of the K_{25} component at the charged ratios used for transfection.

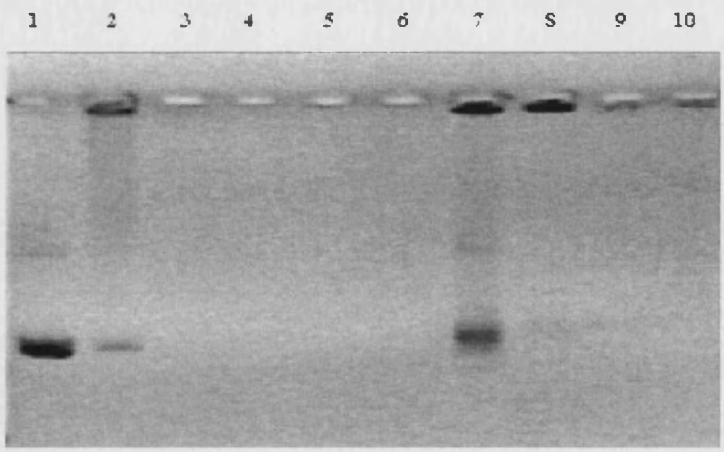

Figure 3.1 Agarose gel displaying the retardation of DNA/peptide complexes with increasing amounts of either K_{25}AOA1#2 (lanes 2-6) or K_{25} (lanes 7-10), free DNA is in lane 1. K_{25}AOA1/DNA complexes were formed at charge ratios of 0.96, 1.9, 3.8, 7.6, and 15.2 (lanes 2 to 6 respectively) by adding increasing amounts of K_{25}AOA1#2 to 3 µg DNA in 125 µl HBS. K_{25}/DNA complexes were formed at charge ratios of 0.5, 1.0, 2.0 and 4.0 (lanes 7 to 10). The complexes were prepared in HBS as detailed in section 3.2.8, and incubated for 30 minutes before loading onto a 1% (w/v) agarose gel and running at 80 Volts for one hour.

3.3.1.1.2 Ethidium Bromide exclusion Assay

The ability of the oligolysyl peptides and bifunctional peptides to interact and form complexes with plasmid DNA was also studied using the ethidium bromide (EtBr) exclusion assay. The binding of compounds to DNA prevents ethidium bromide from intercalating with DNA resulting in a quenching of florescence. The complexation of DNA was measured as a decrease in fluorescence intensity of ethidium bromide and the results expressed as a percentage of control (naked DNA) fluorescence, normalised to 100%. The quantity of each peptide used to complex DNA was expressed in terms of calculated charge ratios of peptide/DNA complexes to simplify comparisons. The results showed that increasing the amounts of oligolysine or bifunctional peptides complexing with a fixed quantity of DNA resulted in a decrease in fluorescence of DNA/EtBr complexes (Figure 3.2). The results also showed that the binding affinity of oligolysine K_{10} and K_{25} to DNA to the exclusion of ethidium bromide compared favourably with high molecular mass polylysine$_{214}$. Linking of fusion peptide sequences did not prevent binding if the oligolysine moiety was long enough. The quenching of EtBr florescence to minimal level occurred with pLL_{214} at a charge ratio of about 2.5

compared to the charge ratio of 3 to 4 for the bifunctional peptides K_{25}INF7 and K_{25}AOA1#1. Also, peptides K_{10} and K_{25}AOA1#1 or K_{25}INF7 bound to DNA more effectively than K_{10}INF7. Although K_{10} was efficient at condensing DNA, when the HA-2 analogue, INF7, was coupled covalently to K_{10} (to form K_{10}INF7) it was necessary to add a large charge excess to achieve condensation. This explains the undetectable transfection activity using the β-gal reporter plasmid, which is reported later in this chapter.

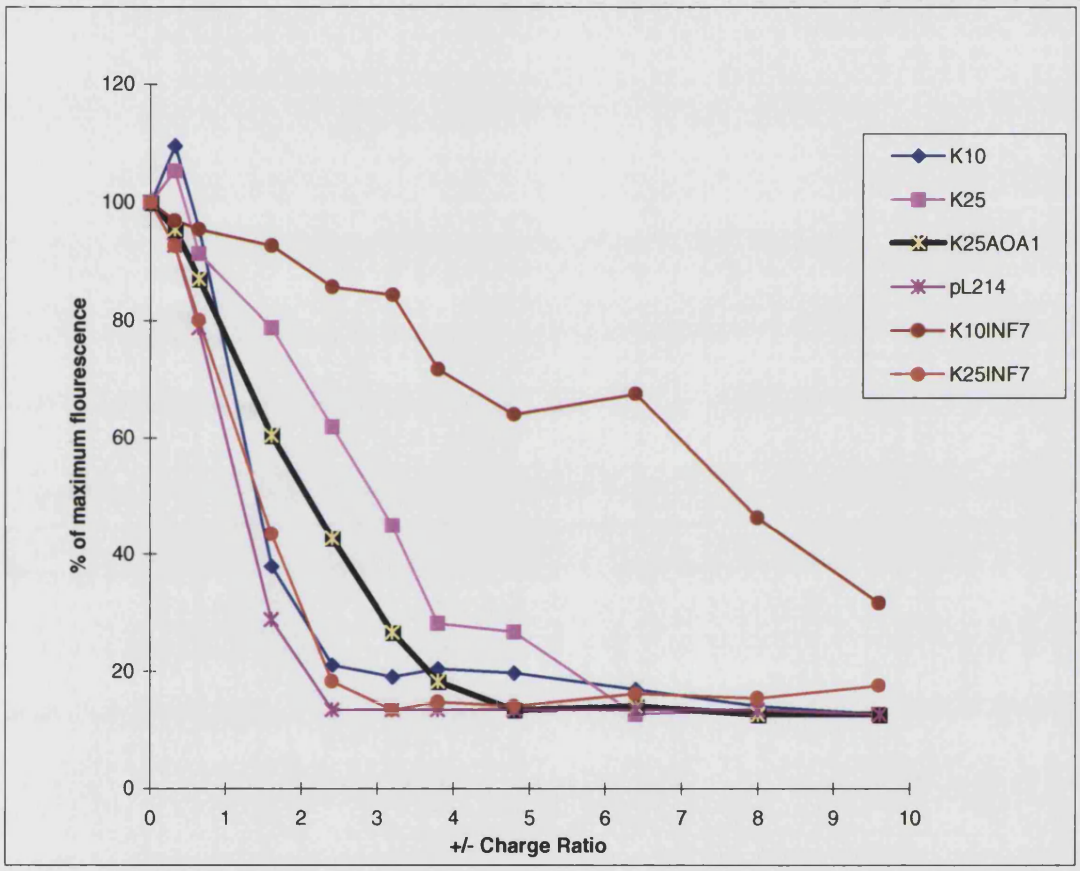

Figure 3.2 Ethidium bromide exclusion by various peptides at various charge ratios. Six μg of pRSV*lac*Z was diluted to 125 μl with HBS in a sterile micro-centrifuge tube. Variable quantities of the GDV were separately diluted to 125 μl HBS in sterile micro-centrifuge tubes to give the charge ratios indicated in the graph. Samples were mixed, incubated for 15-30 minutes and then diluted to 3 ml with 20 mM sodium chloride solution. The fluorescence was monitored at $\lambda_{excitation}$ 260 nm and $\lambda_{emission}$ 600 nm immediately following the addition of 3 μl of a 0.5 mg/ml solution of ethidium bromide (final concentration of 0.5 μg/ml), on a RF-540 spectrofluorimeter (Shimadzu, UK) using 1 cm cells with slit settings of 5 nm for both the excitation and emission monochromators.

The ability of K_{25}AOA1#1 to bind to DNA was demonstrated by ethidium bromide exclusion assay and gel retardation assay. The results demonstrated that the presence of fusogenic peptides did not inhibit the DNA binding activity once the number of lysine residues exceeded a certain threshold. The data suggested that the bifunctional peptides with 10 lysine residues had a lower binding affinity for DNA than bifunctional peptides with 25 residues of lysine. Given that K_{10} was able to bind to DNA (and exclude ethidium bromide) to practically the same degree as K_{25}AOA1 and K_{25}INF7, the inability of K_{10}INF7 to effectively bind to DNA can be explained by the fact that the relatively larger fusogenic moiety with negative charges interferes sterically and ionically with the binding of the positive lysine residues in K_{10}INF7. The inability of K_{10}INF7 to effectively condense DNA explains its lack of transfection activity (Figure 3.12). It will be of interest to determine the minimum length of the lysine chain required within a bifunctional peptide to restore DNA-binding activity to the level of K_{10} or K_{25}, because as it was shown in Chapter 2, the greater the number of residues in the peptide sequence, the more heterogeneous and expensive the product.

3.3.1.2 RETENTION OF FUSOGENIC ACTIVITY

The ability of synthetic fusogenic peptides to disrupt membranes is central to its capacity to improve *in vitro* transfection of cells[167]. Two established methods for ascertaining the fusogenic properties of peptide sequences are liposome leakage assay and erythrocyte lysis assay. The haemolytic activity of a fusogenic peptide as determined by the erythrocyte lysis assay had been shown by Plank and colleagues to have a better correlation with transfection activity than the liposome leakage activity of peptide sequences[167]. Peptide sequences that had liposome leakage activity but did not possess haemolytic activity were found not to augment transfection in a quaternary gene transfer system[167]. It was considered necessary to investigate if fusogenic activity was retained after the inclusion of oligolysine residues to the carboxyl terminal of the fusogenic peptide sequences. In view of the fact that these biophysical analytical studies required a considerable quantity of peptide material (20-60 mg) and there was a limited quantity of peptide material available, the erythrocyte lysis assay was chosen as the only method to show the fusogenic property of the bifunctional peptide. Erythrocyte lysis assay was performed at pH 5 and 7 to determine if the membrane-disruptive ability of

fusogenic peptides and bifunctional used in this project were pH- dependent. Peptides with a high degree of selective lytic activity at pH 5 compared to pH 7 have been shown to be better transfecting agents[167]. The data from this first erythrocyte lysis study, represented in Figure 3.3, showed that AOA1*, INF7* and their oligolysyl derivatives K_{25}AOA1#1 and K_{25}INF7, all had the ability to disrupt membranes of erythrocytes. Both fusogenic peptides AOA1* and INF7* and their K_{25} derivatives had 1.5-3-fold greater lytic activity at pH 5 than at pH7 as determined by comparing the concentration at which 50% of erythrocytes are lysed. Peptides K_{25}, $K_{25}H_{20}$ and the target sequence of $K_{25}H_{20}$AOA1 (data not shown) did not have any erythrocyte lytic activity.

In a repeat of the erythrocyte lysis study to confirm the previous data, the concentration of the peptides were calculated and compared in terms of molarity (M) to compensate for the large differences in relative molecular weights between AOA1 and the bifunctional peptides K_{10}AOA1 and K_{25}AOA1. The data from this second erythrocyte lysis study is represented collectively in Figure 3.4 and for individual peptides AOA1, K_{10}AOA1 and K_{25}AOA1#3 in Figure 3.5, Figure 3.6 and Figure 3.7 respectively. A detailed comparison of the haemolytic potencies of AOA1, K_{10}AOA1 and K_{25}AOA1#3 is described later and represented in Table 3.3.

The data showed that K_{10} and K_{25} did not have any haemolytic activity greater than water, the negative control. The visual appearance of the erythrocyte suspension in the assay buffer of pH 5 (but not pH 7) darkened with time (after about 1 hour), even in the absence of any test compound. Subsequently, the absorbance readings (at a wavelength of 490 nm) of the supernatant of the negative control, as well as the haemolytically inactive K_{10} and K_{25} were higher at pH 5 (ranging between 0.116 and 0.152) than at pH 7 (ranging between 0.051 and 0.062).

It was visually observed that on addition of erythrocyte suspension at pH 5 to a high concentration ($6.25x10^{-4}$ to $5x10^{-2}$ M) of peptide with fusogenic activity, the suspension turned into a clear red solution almost instantly, whereas, at pH 7, there was a delay from about 1 minute at the highest concentration to about 5-10 minutes at peptide concentration of $1.56x10^{-4}$ M. This observation suggests that the fusogenic sequence AOA1 is kinetically more haemolytic at pH 5 that at pH 7 and that at low

concentrations, the difference in speed of membrane disruption could be important in its activity as an adjunct in gene delivery. Allowing for the differences in background readings at pH 5 and 7, haemolytic activity of peptides AOA1, K_{10}AOA1 and K_{25}AOA1 was higher at pH 5 than at pH 7.

For comparison, adding 1 µl of a 10% (v/v) solution of triton X-100, which effects 100% lysis[167], gave average absorbance readings of 0.864±0.053 at pH 5 and 0.760±0.041 at pH 7. Based on this premise, both AOA1 and K_{10}AOA1 caused 100% lysis of erythrocytes from a peptide concentration of $1.56x10^{-4}$ M and above, at pH 5, but K_{25}AOA1 required a higher concentration, between $3.125x10^{-4}$ and $6.25x10^{-4}$ M (between 2- and 4-fold higher concentration) to cause 100% lysis at pH 5. At pH 7, AOA1 required $1.25x10^{-3}$ M (an 8-fold higher concentration compared to pH 5) to cause 100% lysis, whilst K_{10}AOA1 required $6x10^{-4}$ M (a 4-fold increase in concentration compared to pH 5) and K_{25}AOA1 required 2.5-5.0$x10^{-3}$ M (a 4 to16-fold increase in concentration compared to pH 5) to cause 100% lysis. It therefore appears that the attachment of the oligolysyl chain reduces the haemolytic activity of the fusogenic peptide AOA1 at a lysyl chain length of 25 residues but not 10 residues.

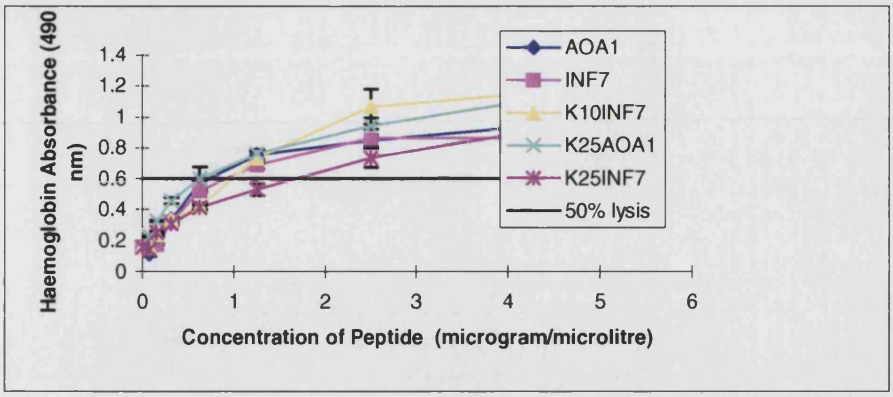

A

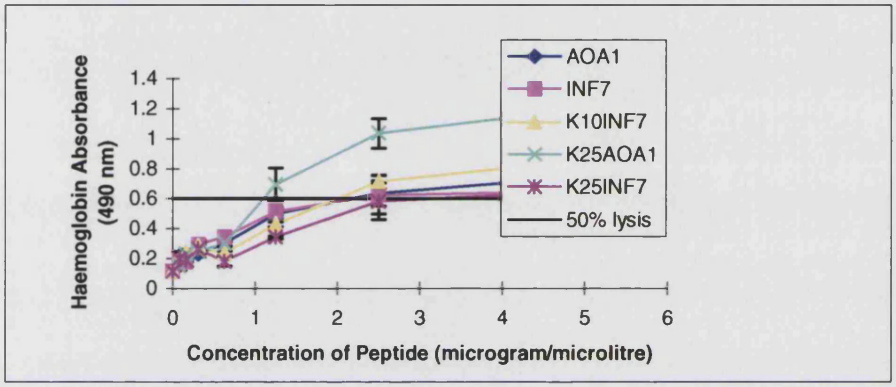

B

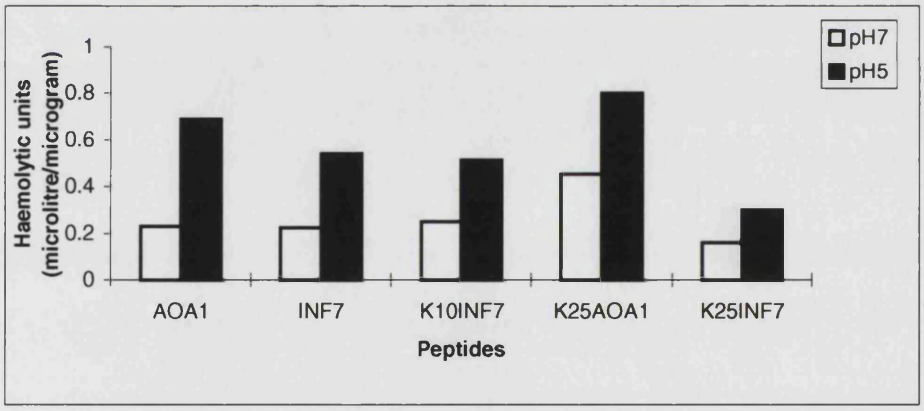

C

Figure 3.3 Haemolytic activity of synthetic fusogenic peptides at pH 5 and pH 7. Assay at pH 5 (A) and pH 7 (B) were performed as described in methods section 3.2.4.3. (C): The haemolytic units were calculated as the reciprocal value of the peptide concentration, where 50% leakage was observed (i.e. the volume (µl) of erythrocyte solution, which is 50%, lysed, per µg of peptide).

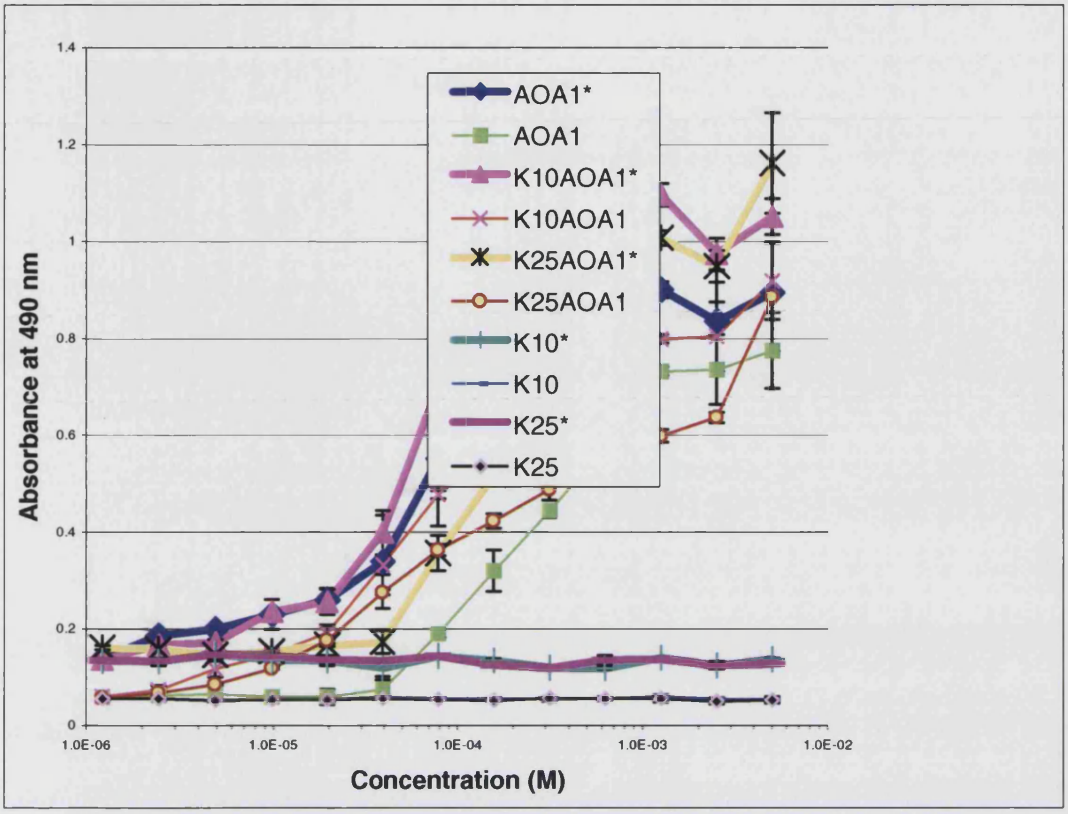

Figure 3.4 Haemolytic activity of synthetic fusogenic peptides at pH 5 and pH 7. Assays performed at pH 5 are represented as thick lines in the graph and marked with asterisks (*) in the legend.

It was observed that AOA1 was only partially soluble in water. A suspension of AOA1 in deionised water at a concentration of $5x10^{-2}$ M was visualised as a white, cloudy but uniform dispersion. The white haze of the suspension of AOA1 was present till the 9th serial dilution. From purification attempts of AOA1 (Chapter 2), it was known that AOA1 was not soluble at low pH, therefore it was suspected that the addition of erythrocyte suspension at pH 5 would further reduce the solubility of AOA1. Indeed, when erythrocyte suspensions were centrifuged after incubation, suspensions containing AOA1 had precipitates present from the highest concentration to the 5th serial dilution; the precipitates were visually greater in volume at pH 5 than at pH 7, thus supporting the notion that AOA1 solubility was further reduced after the addition of erythrocyte suspension at pH 5. This observation is important because it suggests that the haemolytic potency of AOA1 at pH 5 is reduced by its low solubility at pH 5. In other words, the attachment of lysine 10 residues to form K_{10}AOA1, increases the solubility of the compound and offsets any reduction in fusogenic effect as a result of the attachment of fusogenically inactive K_{10}. Increasing the lysine chain length to 25

residues (to form K_{25}AOA1), however, began to cause some reduction in the fusogenic activity, compared to that of AOA1.

Plank and colleagues[167] used the concept of haemolytic units to compare haemolytic activity of various peptides at pH 5 and 7. This method provided a snap shot comparison of haemolytic potency for peptides and was useful for demonstrating the specificity or selectivity of the haemolytic activity of peptides at different pHs. This method of analysis (haemolytic values) was used in the first erythrocyte lysis assay, results of which are shown in Figure 3.3, but the information it provided was limited because the peptides being compared were not specific or even selective at pH 5 but merely had a higher haemolytic activity at pH 5 compared to pH 7. A modified concept of haemolytic units has been applied below, for each peptide with a fusogenic component, at multiple concentration points where the graph of absorbance versus concentration exists in the same absorbance range, to produce a more comprehensive picture of the effect of pH on the activity of AOA1, K_{10}AOA1 and K_{25}AOA1, based on the data represented in Figure 3.4. The data in Table 3.3 shows that the ratio of peptide concentration at pH 5 to pH 7, required to cause the same degree of haemolysis varies considerably with respect to the concentration of peptide incubated with erythrocyte suspension. The influence of low pH on the haemolytic potency of AOA1, K_{10}AOA1 and K_{25}AOA1#3 was highest at the top range of the concentrations of peptides tested. From a peptide concentration of 1.25×10^{-3} M and above, AOA1, K_{10}AOA1 and K_{25}AOA1#3 were about 10-fold more potent at causing haemolysis at pH 5 compared to pH 7. At a peptide concentration of about 3.125×10^{-4} M, the influence of pH on the haemolytic potency of the peptides AOA1 and K_{10}AOA1 had been reduced to 4.5-fold, and about 2-fold for K_{25}AOA1. The haemolytic activity of AOA1 exhibited the highest preference for pH 5 (against pH 7), as the haemolytic potency ratio at pH 5 compared to pH 7 did not decrease below 4-fold throughout the test range.

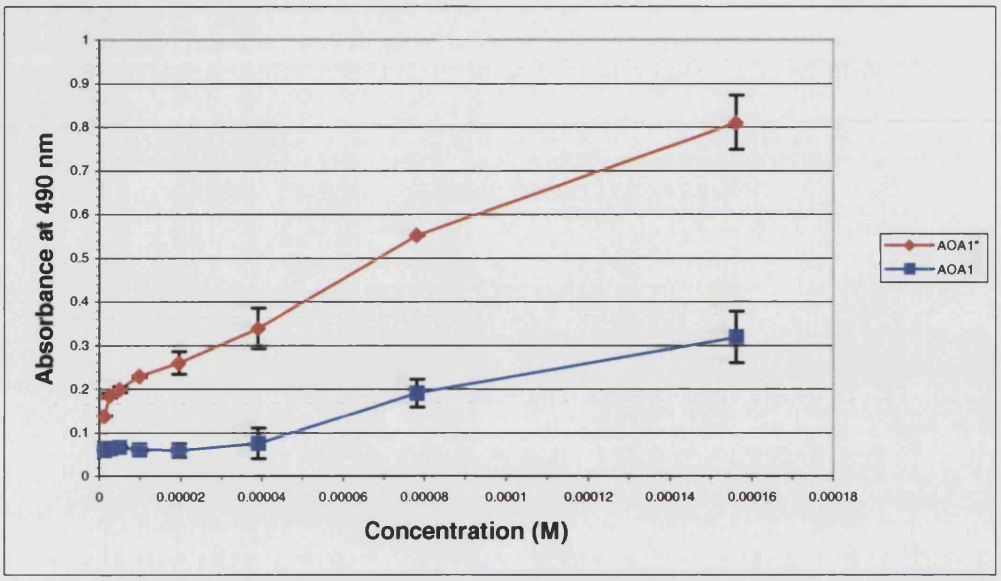

A

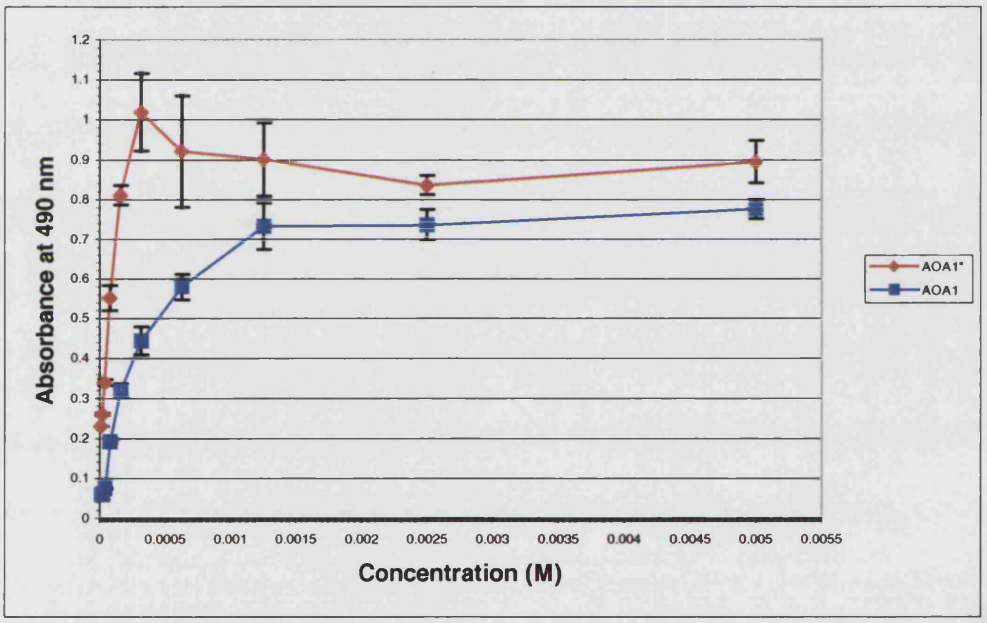

B

Figure 3.5 Haemolytic activity of AOA1 at pH 5 (red line and marked with asterisk (*) in legend) and pH 7 (blue line) at low peptide concentrations (A) and across the whole concentration range of 1.22 μM and 5.0 mM (B).

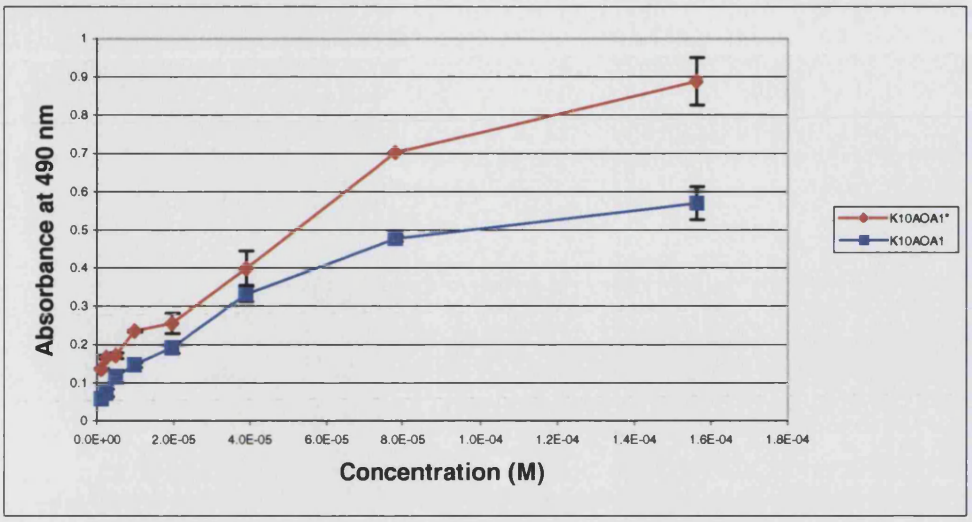

A

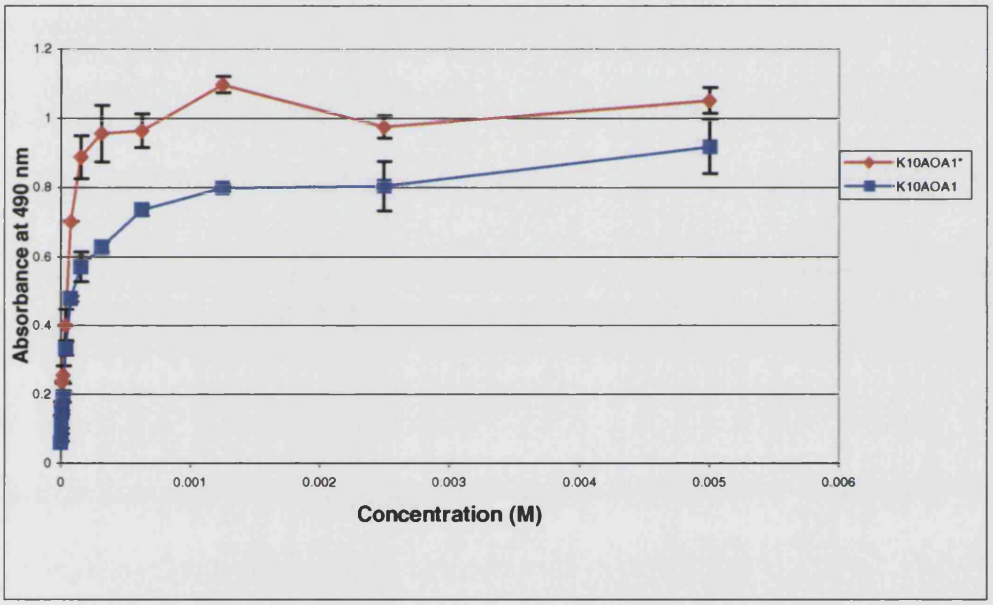

B

Figure 3.6 Haemolytic activity of K_{10}AOA1 at pH 5 (red line and marked with asterisk (*) in legend) and pH 7 (blue line) at low peptide concentrations (A) and across the whole concentration range of 1.22 μM and 5.0 mM (B).

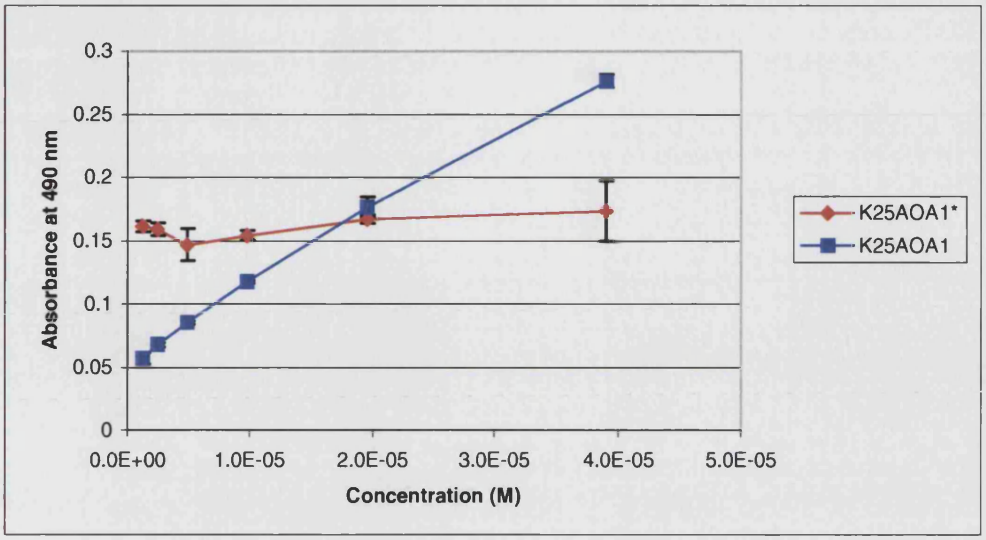

A

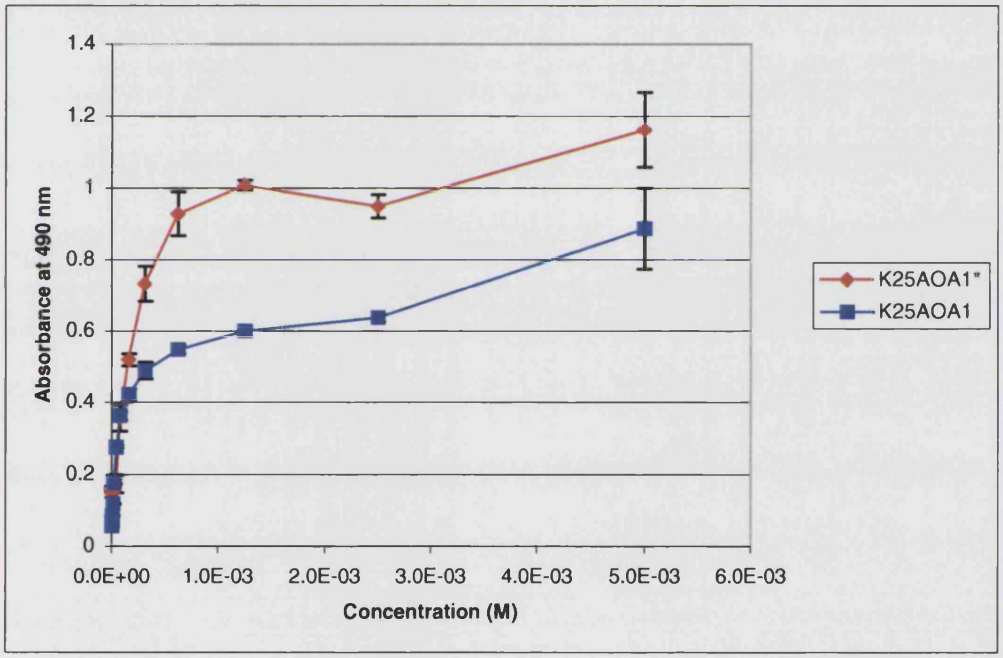

B

Figure 3.7 Haemolytic activity of K_{25}AOA1 at pH 5 (red line and marked with asterisk (*) in legend) and pH 7 (blue line) at low peptide concentrations (A) and across the whole concentration range of 1.22 μM and 5.0 mM (B).

Peptide	Average Absorbance reading	Concentration of peptide at pH 5 (M)	Concentration of peptide at pH 7 (M)	Ratio of concentration of peptide at pH 7 to pH 5 which caused the same average extent of haemolysis
AOA1	0.737	1.250E-04	1.250E-03	10.000
	0.579	9.000E-05	6.250E-04	6.944
	0.444	6.000E-05	3.125E-04	5.208
	0.339	3.906E-05	1.800E-04	4.608
	0.32	3.500E-05	1.563E-04	4.464
	0.23	9.766E-06	1.000E-04	10.240
K_{10}AOA1	0.799	1.200E-04	1.250E-03	10.417
	0.735	9.000E-05	6.250E-04	6.944
	0.627	7.000E-05	3.125E-04	4.464
	0.478	5.000E-05	7.813E-05	1.563
	0.332	3.050E-05	3.906E-05	1.281
	0.193	6.750E-06	1.953E-05	2.894
K_{25}AOA1	0.887	5.500E-04	5.000E-03	9.091
	0.637	2.500E-04	2.500E-03	10.000
	0.599	2.200E-04	1.250E-03	5.682
	0.489	1.400E-04	3.125E-04	2.232
	0.363	7.813E-05	7.813E-05	1.000
	0.276	6.000E-05	3.906E-05	0.651

Table 3.3 Showing a comparison of the concentration of peptides AOA1, K_{10}AOA1 and K_{25}AOA1#3 at pH 5 and pH 7, which was required to cause the same extent of haemolysis.

The influence of lower pH (pH 5 versus pH 7) on the haemolytic potency of K_{10}AOA1 was lowered to 1.3-fold, as the concentration of peptide being tested was decreased. To complete the trend, the haemolytic potency of K_{25}AOA1 started with a high preference for pH 5 against pH 7, but at a peptide concentration of $7.813x10^{-5}$ M, K_{25}AOA1 was equipotent at pH 5 and pH 7. A further reduction of concentration showed K_{25}AOA1 being more haemolytic (about 1.5-fold) at pH 7 than pH 5. These results suggest that the attachment of the lysyl chain to form bifunctional peptides reduces the fusogenic potency and pH-selectivity at lower peptide concentrations. This result is not unexpected because the attachment of a sequence with no fusogenic activity reduces the chance of close interaction (steric hindrance) of the fusogenic sequence to interact with the lipid bilayer and disrupt the bilayer of erythrocytes.

Destabilization of the target membrane bilayer is a prelude to membrane fusion [188]. The ordered architecture of the viral surface and the organised conformational changes by which influenza HA mediates membrane fusion, culminating in the formation of a fusion pore[188], is lacked in a synthetic complex consisting of DNA/polylysine/fusogenic peptide. Although fusogenic peptide sequences used in transfection experiments by Plank and colleagues were based in N-terminal sequences of the influenza HA-2, the only commonality between influenza HA-mediated fusion and fusogenic peptide mediated fusion, is the ability of either to destabilize the target lipid bilayer, a feature shared with amphipatic molecules such as detergents and cationic lipids. HA is a trimer of three identical subunits, each of which contains a fusion peptide, a conserved sequence containing many hydrophobic amino acids. The fusion peptides are tightly tucked into the subunit interface by a network of hydrogen bonds[188]. In response to low pH, the tertiary structure of HA is altered, exposing the fusion peptides and other sequences buried in the stem[259,260,261]. The exposed fusion peptides render the HA ectodomain hydrophobic and foster its immediate attachment to the target membrane[262] before significant lipid mixing occurs[188]. Additional conformational changes as well as rotational and lateral motions of HA trimers in the plane of the viral membrane[263] results in the aggregation of several HA trimers and formation of a fusion pore within the interior of the aggregate[188].

The observation by Cotten and colleagues that inactivated adenovirus particles (psoralen and irradiation) could still mediate endosmolytic activity and improve *in vitro* transfection[223], led to the study of the use of fusogenic sequences in influenza HA-2 as adjuncts for gene transfer[181]. The legacy of the method of forming ternary and quaternary complex originate from early studies in this field using modified polylysine as a means of condensing DNA and attaching inactivated viruses and receptor ligands to them[1]. Studies by Plank and colleagues had showed a high correlation between pH-specific (as opposed to pH-sensitive) erythrocyte lysis activity and gene transfer efficiency using ternary complexes[167] that included fusogenic peptide sequences.

The bifunctional peptides K_{25}AOA1 and K_{25}INF7 retained pH-sensitive lytic activity (Figure 3.3) in the erythrocyte lysis assay. However, the erythrocyte lytic activity of the bifunctional peptides was not highly selective at pH 5. At lower molar concentrations of K_{25}AOA1, the data from the second erythrocyte lysis assay showed that there was no measurable difference between haemolytic activity at pH 5 compared to pH 7. The significance of this observation is discussed later in section 3.3.9 when the lack of effect of the endosomal proton pump inhibitor on the transfection efficiency of K_{25}AOA1 is discussed. The erythrocyte lysis activity of the bifunctional peptides in these experiments were over 100-fold lower than the levels for INF6, as reported by Plank and colleagues[167]. Plank and colleagues also reported that INF6 had a high erythrocyte lysis activity but was not pH specific (about 2-fold higher at pH 5 compared to pH 7). Plank and colleagues also observed that fusogenic peptides that had a high haemolytic potential but did not display the strong specificity for low pH showed only a moderate augmentation of gene expression[167]. Therefore, on the basis of the findings by Plank and colleagues, bifunctional peptides K_{25}AOA1 and K_{25}INF7, which had a comparatively low haemolytic activity and weak pH specificity, would not be expected to augment gene expression. However, as it will be seen in section 3.3.3, *in vitro* transfection was very strongly improved using these bifunctional peptides. The peptide K_{25}, which did not have any erythrocyte lysis activity, did not show augmentation of gene expression, demonstrating that both DNA binding and fusogenic activity are required for *in vitro* transfection activity of bifunctional peptides.

These data on retention of functionality in conjunction with *in vitro* transfection studies data presented later in this thesis, suggest that, for augmentation of gene expression, the advantage of ensuring co-localisation of DNA/polylysine/fusogenic peptide in a peptide/DNA complex, outweigh the advantage of high haemolytic potency and pH specificity of the fusogenic peptide used. It is apparent that the structural integrity of viruses, which are being emulated in the construction of these virus-like particles, is crucial to success of viruses in transferring genetic material to host cells for expression. It is likely that the ionic interactions that are being relied upon to form the speculative ternary or quaternary complexes produce delivery systems that are less efficient and unreliable.

3.3.2 ZETA POTENTIAL AND PARTICLE SIZE MEASUREMENTS

3.3.2.1 INTRODUCTION

The surface charge of colloidal particles in solution has a considerable effect on flocculation of primary particles to form larger aggregates, and consequently on the apparent size of the secondary aggregates. Flocculation may explain why some peptide/DNA formulations are ineffective at *in vitro* transfection experiments. Therefore characterisation of zeta potential and size are important formulation parameters, and are useful to interpret the results of biological experiments.

3.3.2.2 PARTICLE SIZING BY PHOTON CORRELATION SPECTROSCOPY

Photon correlation spectroscopy (PCS) is a technique used for measuring the dynamic changes in light scattering associated with macromolecular and colloidal systems. Particles in solution undergo the random movement of Brownian motion, which occurs due to collisions with the smaller molecules of the continuous phase. The suspended particles are constantly in a state of motion, and hence undergo diffusion. Diffusion is governed by the average distance of travel before collision with another molecule, which causes a diversion from the original path of motion. When a solution of

macromolecules is illuminated, the light is scattered by the particles in Brownian motion, and the intensity of this light yields information regarding the molecular weight.

PCS analyses the constantly changing patterns of laser light scattered or diffracted by particles in solution, exhibiting Brownian motion. The rate of change of the scattered light during diffusion is monitored. The scattered light displays a spectrum of frequencies due to the Doppler effect. Fluctuations in the intensity arise because the centres of light scattering are constantly moving, producing different extents of interference. An autocorrelation function allows the intensity fluctuations to be characterised. The intensities are measured at short time intervals (5-10 μs) over a longer time period of several minutes, and recorded digitally. PCS allows estimation of the translational diffusion coefficient (D). D is related to the equivalent hydrodynamic radius of the particle by the Stokes-Einstein equation:

$$D = \frac{k_B T}{6\pi\eta r_h}$$

Equation 3.14

where k_B is the Boltzman constant, T is the absolute temperature (Kelvin), η is the viscosity of the solvent and r_h is the hydrodynamic radius.

CONTIN analysis was used to fit the experimental intensity decay curve with a curve calculated assuming a distribution of decay rates. This method extracts a smoothed or regularised size distribution by matrix techniques. Larger particles produce a greater intensity of scattered light, and this may interfere with the intensity from smaller species. In extreme cases, the intensity of light scattered from small particles may be masked by the interference and intensity from only a tiny percentage of large particles within the population.

Solutions, which contain more than one species, require correction for the intensity interference problems. The correlation function contains the same number of terms as species in the sample, but each term is weighted by the intensity of light scattered from each species. The output from CONTIN analysis includes information about weight and number distribution within the sample.

3.3.2.3 *ZETA POTENTIAL MEASUREMENT*

The surface charge, more specifically the surface charge density, plays an active role in colloidal stability. A colloid may be simply defined as a particle or molecule with a least one dimension less than, approximately, 1 μm and all dimensions greater than, approximately, 1 nm. The surface area per gram of material for colloidal-sized particles is orders of magnitude larger than it is for particles approximately 10 μm. Therefore, surface effects, which are normally negligible, become dominant in the description of colloidal behaviour. Condensed DNA/peptide complexes form colloids, and therefore the measurement of surface charge is important in explaining observed behaviour of these complexes.

Without going into detail, the zeta potential is a good approximation of the surface charge density. Zeta potential for DNA/peptide complexes was measured using the ZetaPlus Zeta Potential Analyser, (Brookhaven Instruments Corporation, New York, USA). In the ZetaPlus, charged particles in a dilute suspension move between two oppositely charge electrodes. Zeta potential can be calculated from the measurement of average drift velocity of charged colloidal particles as they move towards the electrode of opposite charge. Due to the motion of the charged particles, a frequency shift, called the Doppler Shift, occurs in a focused laser beam light (wavelength λ=670 nm) scattered by the particles. The velocity is deduced from the shift in the laser beam frequency.

3.3.2.4 *RESULTS OF ZETA POTENTIAL AND PARTICLE SIZE MEASUREMENTS*

The effective diameter in nm of DNA/DK_{25}AOA1 complexes at charge ratios of 0.4, 0.8, 1.6 and 3.2 shown in Figure 3.8 represents the complexes formed using 102.2 μg DNA (in 800 μl of 5% (w/v) glucose) complexed with 34.4 μg, 68.8 μg, 137.6 μg and 275.2 μg of DK_{25}AOA1 (in 5% (w/v) glucose) respectively. These quantities of DNA and peptide were used at 16-fold higher concentration than that used during *in vitro* transfection. The reason high concentrations were used is that lower concentrations did not generate enough scattered laser light with the available laser. One would need a

very powerful (perhaps 2W argon laser) to allow lower concentrations of DNA to be examined. The results show that the effective diameter was fairly constant between 120 and 140 nm for particles except at charge ratio of 1.6 when aggregation occurred to give particles with effective diameter 4-6 μm. Attempts to increase the charge ratio using 102.2 μg DNA beyond 3.2 resulted in precipitation of the sample. Previous work had established that precipitation can occur at concentrations of DNA above 40 μg/ml.

Complexes formed in HBS using the same amount of DNA (102.2 μg) complexed to varying amounts of $DK_{25}AOA1$ resulted in precipitation. A 25.6 μg DNA/68.8 μg $DK_{25}AOA1$ complex (representing a charge ratio of 3.2) produced particles with effective diameter of over 3 μm and a negative zeta potential of 58.78 (+/-8.6). This zeta potential reading is most likely an artefact caused by the presence of neutralizing ions. A 6.4 μg DNA/17.2 μg $DK_{25}AOA1$ complex in HBS resulted in particles with effective diameter ranging between 890 nm and 1070 nm zeta potential of the main population being –0.24 and two smaller populations with zeta potential of –8 mV and –16 mV.

For the purpose of comparison, 51.2 μg DNA was complexed with 92.16 μg PEI in 5% (w/v) glucose representing a nitrogen/phosphate ratio of 6 (approximate +/- charge ratio of 3) resulted in particle sizes between 136 and 156 nm and a mixed population of particles with zeta potential ranging from –2 to 13 mV. An attempt was made to reduce the chances of aggregation of particles by further decreasing the concentration complexes formed in HBS, but this was not possible as it resulted in poor sample quality (low count rates) for the instrument. A similar result was observed when K_{25} was used to complex DNA.

A tertiary complex sample consisting of 6.4 μg DNA (in 400 μl HBS)/ 9 μg K8 (in 400 μl HBS) /16 μg JTS1 (in 800 μl HBS) gave a poor sample quality, with the instrument returning a value of 714 nm as a possible effective diameter and also, a very heterogeneous zeta potential result ranging from –47 to 217 mV due to the presence ions in HBS.

3.3.2.5 *DISCUSSION: ZETA POTENTIAL AND PARTICLE SIZE MEASUREMENTS*

Particle stability in ionic solutions is essential for the success of gene delivery *in vivo*. Injection of polyplexes systemically results in particle aggregation, thus limiting successful *in vivo* gene delivery. Although cationic polyplexes are stable in water, they aggregate in ionic solutions due to a decrease in the protective electrostatic double layer. Polyplexes aggregate rapidly in physiological salt concentration (~150 mM)[83]. The advantage that single-step complex formation with bifunctional peptides has over two-step complex formation become important when particle stability and formulation difficulties associated with two-step complexes is considered. Complexes with K_{25}AOA1 can be formed at higher concentrations and are more stable from aggregation than K_{25}/DNA complexes. Particle size measurements and zeta potential measurements showed that even in glucose, K_{25}/DNA complexes were highly unstable and aggregated immediately at lower charge ratios. When K_{25}AOA1 complexes with DNA were formed in HBS, aggregation occurred but to a less extent than two-step complexes. It is not clear why the bifunctional peptide/DNA complexes are more stable in HBS than K_{25}/DNA complexes. The presence of uncharged residues in the fusogenic moiety possibly reduces the zeta potential of K_{25}AOA1/DNA particles. Another possible explanation is that the fusogenic moiety provides a steric stabilisation similar to the effect of PEGylation of polylysine/DNA complexes[86].

Both the zeta potential and sizing experiments required large masses of DNA and peptides, which could not be recovered. It would have been useful to extend these studies to optimise the formulation of particles but this was prohibited by their cost. The cost of formulation studies will have considerable impact on the commercial development of non-viral gene delivery systems. These studies will require a substantial commitment.

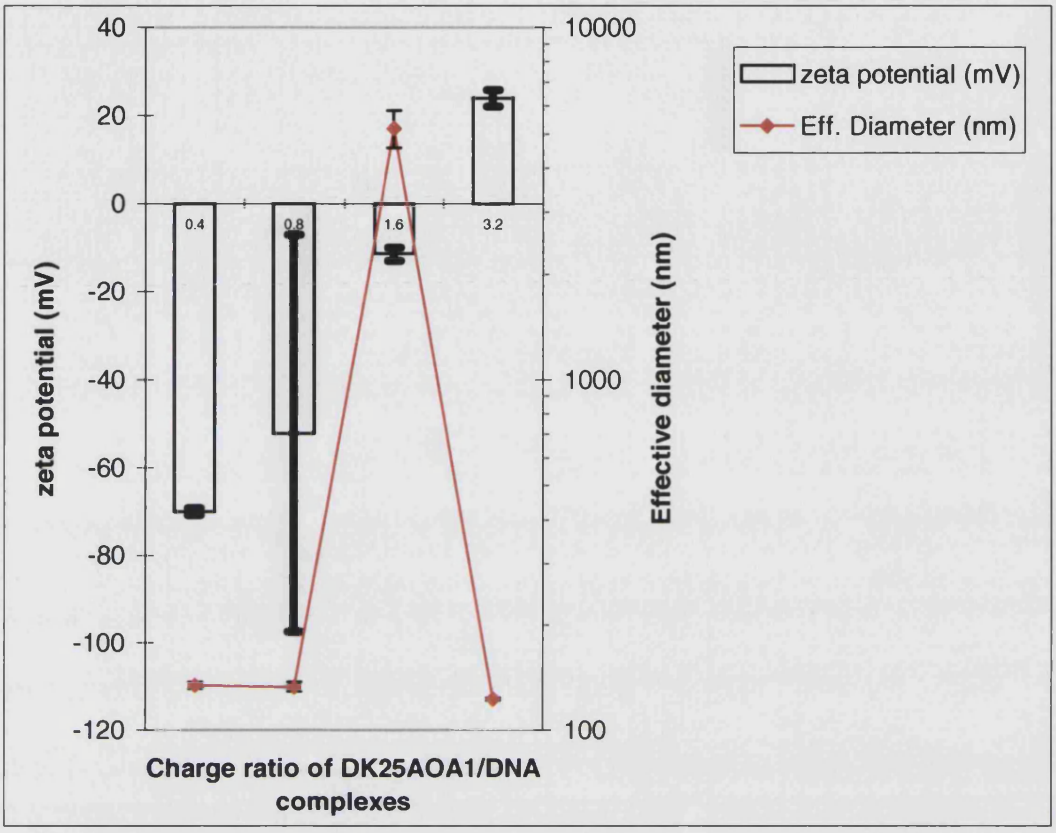

Figure 3.8 Determination of particle size and zeta potential of K_{25}AOA1/DNA complexes. The effective diameter in nm of DNA/DK_{25}AOA1 complexes at charge ratios of 0.4, 0.8, 1.6 and 3.2 shown in above represents the complexes formed using 102.2 µg DNA (in 800 µl of 5% (w/v) glucose) complexed with 34.4 µg, 68.8 µg, 137.6 µg and 275.2 µg of DK_{25}AOA1 (in 5% (w/v) glucose) respectively. These quantities of DNA and peptide represent a 16-fold increase in concentration compared to what is used during *in* vitro transfection. Zeta potential for DNA/peptide complexes was measured using the ZetaPlus Zeta Potential Analyser, (Brookhaven Instruments Corporation, New York, USA).

3.3.3 *IN VITRO* TRANSFECTION RESULTS

The transfection results presented in this thesis represent typical data from a single experiment. Experiments were carried out on at least two separate occasions to establish reproducibility of the data. Typically gene expression was variable from one batch of cultured cells to another, between replicate experiments. The data obtained from replicate wells was reproducible, and the relative effects of formulation parameters were reproducible.

3.3.3.1 *INVESTIGATION OF THE EFFECT OF CHARGE RATIO ON TRANSFECTION EFFICIENCY*

To determine the effect of charge ratio on transfection of dividing cells *in vitro*, increasing masses of each peptide were complexed with 2 μg of either pRSV*lacZ* or pCMV luciferase plasmid DNA and used to transfect B16, A549 or NIH3T3 cells (Figure 3.9 and Figure 3.10). Figure 3.9 shows the results of the effect of charge ratios

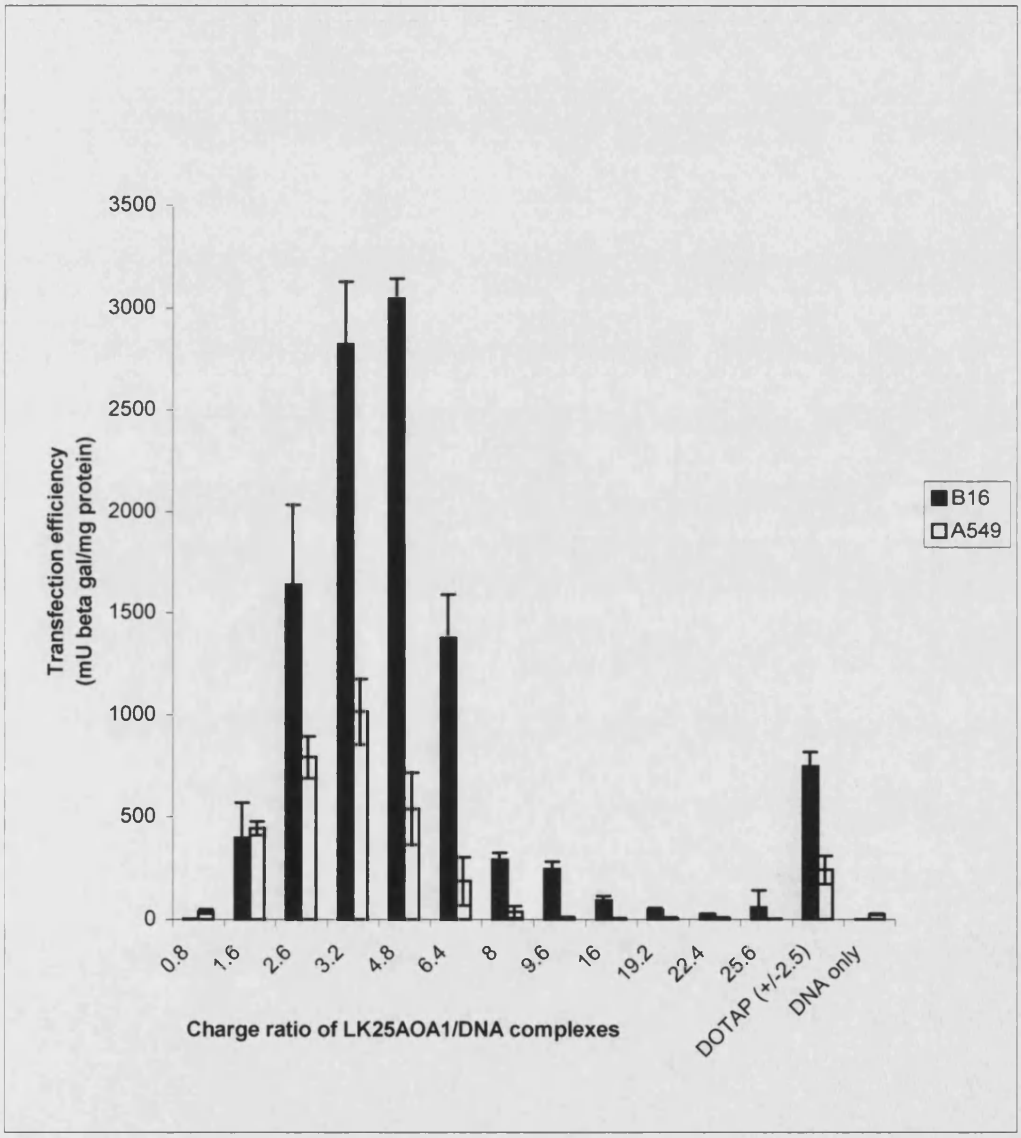

Figure 3.9 Effect of charge ratios on transfection efficiency in B16 melanoma and A549 cells. Complexes formed between pRSV*lacZ* (2 μg) and increasing quantities of $LK_{25}AOA1\#1$ were incubated with B16 melanoma and A549 cells for 37°C for 4 hours and cells harvested 48 hours post initiation of transfection for analysis. DOTAP at a charge ratio of +/- 2.5 was used as positive control. Data represent the mean of triplicate samples ± SEM, and is representative of two separate experiments.

	Calculation of β-gal expression				Calculation of protein content				Transfection efficiency	
CR of K25AOA1	Measured light units	Sample Vol For β-gal(μl)	β-gal/sample (μg)	β-gal/plate (μg)	Abs ODS 595nm	sample vol for prt.(μl)	Prt/sample (μg)	Prt/plate (μg)	Trans. Efficiency Units/μg Prt	Trans. efficiency (mU/mgPrt)
0.8	809	20	1.33E-05	0.0002	0.636	2	1.172	146.54	1.14E-06	1.14
0.8	1376	20	2.47E-05	0.0003	0.66	2	1.276	159.50	1.93E-06	1.93
0.8	1424	20	2.56E-05	0.0003	0.618	2	1.095	136.83	2.34E-06	2.34
1.6	2338	0.2	4.39E-05	0.0549	0.673	2	1.332	166.52	3.30E-04	329.72
1.6	2184	0.2	4.08E-05	0.0511	0.714	2	1.509	188.66	2.71E-04	270.62
1.6	3540	0.2	6.80E-05	0.0850	0.631	2	1.151	143.84	5.91E-04	590.61
2.6	4000	0.1	7.72E-05	0.1929	0.621	2	1.108	138.44	1.39E-03	1393.41
2.6	3500	0.1	6.72E-05	0.1679	0.584	2	0.948	118.47	1.42E-03	1417.37
2.6	5431	0.1	1.06E-04	0.2645	0.593	2	0.987	123.33	2.14E-03	2144.40
3.2	6798	0.1	1.33E-04	0.3328	0.608	2	1.051	131.43	2.53E-03	2532.32
3.2	9216	0.1	1.81E-04	0.4537	0.632	2	1.155	144.38	3.14E-03	3142.38
3.2	6848	0.1	1.34E-04	0.3353	0.587	2	0.961	120.09	2.79E-03	2792.25
4.8	7151	0.1	1.40E-04	0.3505	0.586	2	0.956	119.55	2.93E-03	2931.59
4.8	6707	0.1	1.31E-04	0.3283	0.56	2	0.844	105.51	3.11E-03	3111.26
4.8	8094	0.1	1.59E-04	0.3976	0.603	2	1.030	128.73	3.09E-03	3088.82
6.4	7557	0.4	1.48E-04	0.0927	0.576	4	0.913	57.07	1.62E-03	1624.05
6.4	7211	0.4	1.41E-04	0.0884	0.625	4	1.125	70.30	1.26E-03	1256.93
6.4	7158	0.4	1.40E-04	0.0877	0.626	4	1.129	70.57	1.24E-03	1242.74
8	1523	0.4	2.76E-05	0.0173	0.57	4	0.887	55.45	3.11E-04	311.35
8	1788	0.4	3.29E-05	0.0206	0.613	4	1.073	67.06	3.07E-04	306.84
8	1365	0.4	2.45E-05	0.0153	0.591	4	0.978	61.12	2.50E-04	250.15
9.6	1444	0.4	2.60E-05	0.0163	0.58	4	0.930	58.15	2.80E-04	279.91
9.6	1278	0.4	2.27E-05	0.0142	0.621	4	1.108	69.22	2.05E-04	205.18
9.6	1315	0.4	2.35E-05	0.0147	0.586	4	0.956	59.77	2.45E-04	245.35
16	4879	20	9.47E-05	0.0012	0.488	8	0.533	16.66	7.11E-05	71.10
16	6198	20	1.21E-04	0.0015	0.496	8	0.568	17.74	8.54E-05	85.36
16	6083	20	1.19E-04	0.0015	0.459	8	0.408	12.74	1.17E-04	116.56
19.2	4814	40	9.34E-05	0.0006	0.439	8	0.321	10.04	5.82E-05	58.15
19.2	3689	40	7.09E-05	0.0004	0.449	8	0.365	11.39	3.89E-05	38.92
19.2	3674	40	7.06E-05	0.0004	0.446	8	0.352	10.99	4.02E-05	40.18
22.4	5553	80	1.08E-04	0.0003	0.476	8	0.481	15.04	2.25E-05	22.49
22.4	3847	80	7.41E-05	0.0002	0.428	8	0.274	8.56	2.71E-05	27.06
22.4	5375	80	1.05E-04	0.0003	0.453	8	0.382	11.93	2.74E-05	27.41
25.6	3891	80	7.50E-05	0.0002	0.376	8	0.049	1.54	1.52E-04	152.27
25.6	1160	80	2.04E-05	0.0001	0.455	8	0.390	12.20	5.21E-06	5.21
25.6	2995	80	5.71E-05	0.0002	0.448	8	0.360	11.26	1.58E-05	15.84
DNA only	593	20	9.02E-06	0.0001	0.641	2	1.194	149.24	7.56E-07	0.76
DNA only	533	20	7.82E-06	0.0001	0.675	2	1.341	167.60	5.84E-07	0.58
DNA only	559	20	8.34E-06	0.0001	0.671	2	1.324	165.44	6.30E-07	0.63
DOTAP	3961	0.2	7.64E-05	0.0955	0.585	2	0.952	119.01	8.02E-04	802.31
DOTAP	3515	0.2	6.75E-05	0.0843	0.599	2	1.013	126.57	6.66E-04	666.30
DOTAP	4502	0.2	8.72E-05	0.1090	0.628	2	1.138	142.22	7.66E-04	766.43

Table 3.4 Investigation of effect of charge ratio on transfection efficiency in B16 cells (represented graphically in Figure 3.9. "Prt/plate" stands for protein quantity per 6-well plate.

of K_{25}AOA1#1/DNA complexes ranging from 0.8 to 25.6 after transfecting in B16 and A549 cells. Table 3.4 shows typical data describing the effect of charge ratio on cell protein content as well as the quantity of the reporter protein MUG expressed following *in vitro* transfection in B16 cells. These results show that below neutrality (at a charge ratio of 0.8) the transfection efficiency was only 2.7-fold above transfection with uncondensed 'naked' DNA (negative control) i.e. background activity. At a charge ratio of 1.6 (above neutrality), there was a 220-fold increase in transfection activity in B16 cells, compared with complexes formed at a charge ratio of 0.8. A further increase in charge ratio of peptide/DNA complexes from 1.6 to 2.6 resulted in a 4-fold increase in transfection efficiency. There were further improvements in transfection efficiency in B16 cells as the charge ratio of the peptide/DNA complexes was increased, to peak transfection efficiency at a charge ratio of about 4.8. Increasing the charge ratio of the peptide/DNA complexes beyond a charge ratio of 4.8 resulted in a decrease in transfection efficiency. Between the charge ratio of 4.8 and 6.4, there was over 2-fold decrease in transfection efficiency of B16 cells and nearly a 5-fold decrease in transfection efficiency between complexes at a charge ratio of 6.4 and 8. Figure 3.9 and Table 3.4 show that in B16 cells, the decline in transfection efficiency continued steadily with increasing charge ratio of complexes above 4.8. Table 3.4 shows that the cell protein content (see column labelled "prt/plate" in Table 3.4) also declined as charge ratio increased above 4.8. This observation is corroborated by MTT assay results (see section 3.3.13 and Figure 3.25) in which the toxicity of various GDVs were studied. These two separate experiments confirm that increasing toxicity due to increasing excess of peptides in solution was responsible for the decrease in transfection efficiency at higher charge ratios above the optimum.

In A549 cells, a similar trend of increasing charge ratio of complexes resulting in an increase in transfection efficiency up to a peak activity at a charge ratio of 4.8, followed by a decline in transfection efficiency (described for B16 cells above) was observed (Figure 3.9).

In a separate transfection experiment in NIH3T3 cells, the effect of charge ratio of LK_{25}AOA1#1/DNA was compared to that of DK_{25}AOA1 (estimated purity of >90%)/DNA complexes. A comparison between the transfection efficiency of the D-

and L- isomers of the bifunctional peptide K_{25}AOA1 revealed that DK_{25}AOA1 was about 10-20% less active than LK_{25}AOA1 at charge ratios between 2.7 and 5.4 (Figure 3.10). Plank and colleagues reported that transfection activity between ternary complexes formed with D- or L- isomers of fusogenic peptides were not significantly different[167]. The results obtained in this study were consistent with the observation that activity was independent of the isomeric form of the peptide.

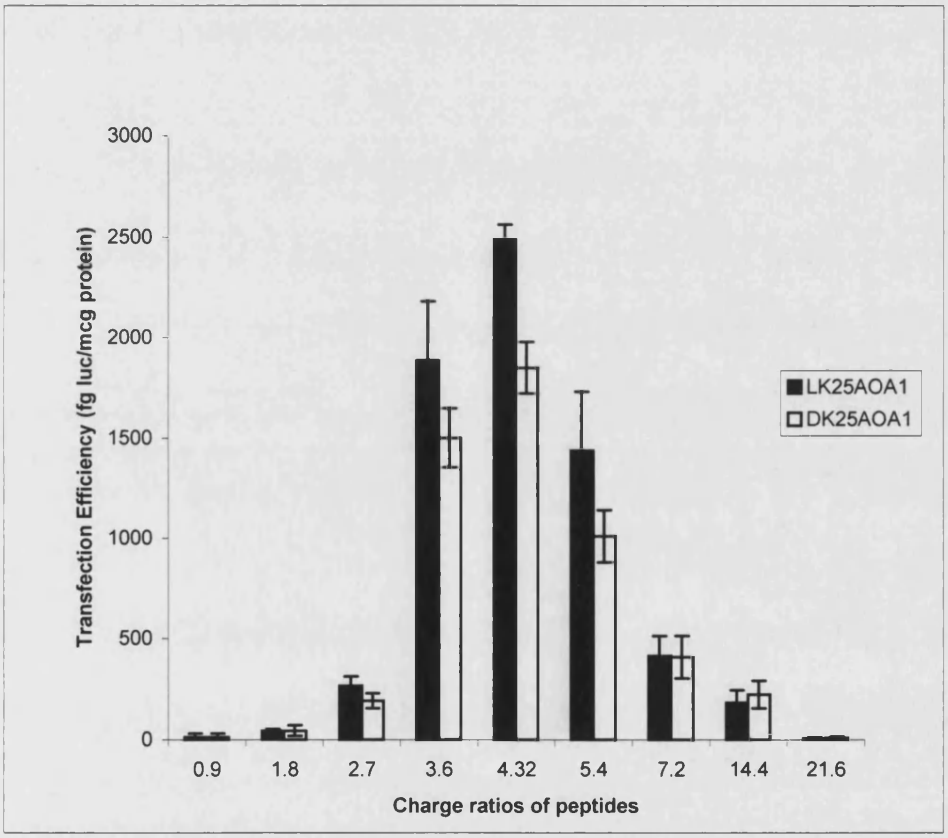

Figure 3.10 Effect of charge ratios on transfection efficiency in NIH3T3 cells. Complexes formed between pCMVluc (6.4 μg in 800 μl HBS) and increasing quantities of DK_{25}AOA1 and LK_{25}AOA1 (in 800 μl HBS) were incubated for 30 minutes before adding a 500 μl aliquot (containing 2 μg per 6-well plate) to cells. NIH3T3 cells were incubated with complexes at 37°C for 4 hours and harvested 24 hours post initiation of transfection for analysis. Data represent the mean of triplicate samples ± SEM, and is representative of two separate experiments.

The difference in activity observed in this experiment may have been due to the different levels of purity in the compounds used, though such small differences could also have been due to problems with the accuracy of weighing small masses of peptide for stock solutions. A comparison between transfection efficiency of the two batches of $LK_{25}AOA1$confirmed this to be the case (Figure 3.11) The highly pure batch of $LK_{25}AOA1$ ($K_{25}AOA1\#2$), (purified using peak splicing of main peak) was about 20% more active than the batch where the whole main peak had been collected, suggesting that the main peak consisted of approximately 85% target peptide.

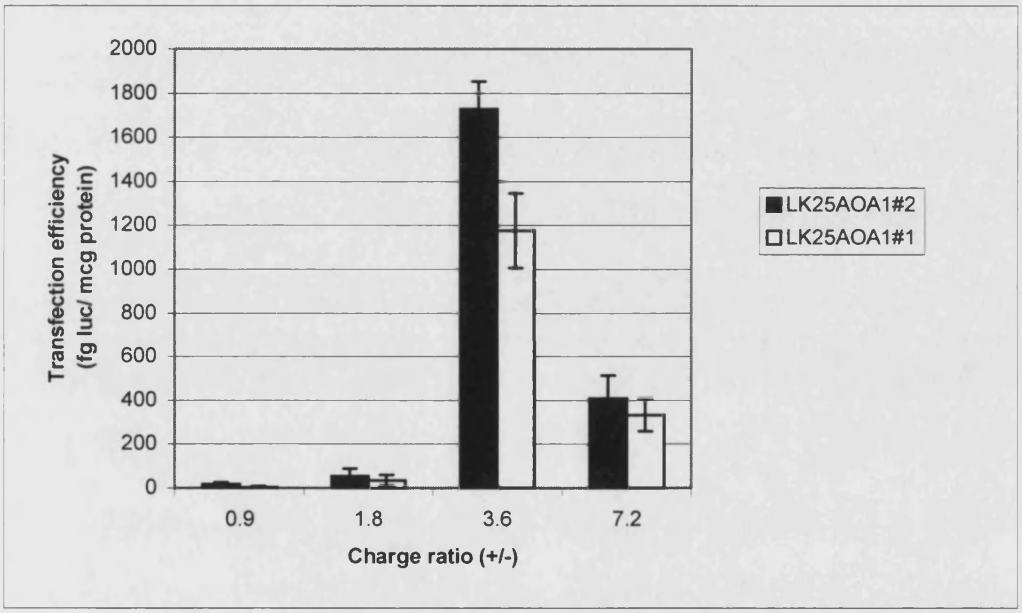

Figure 3.11 Comparison of transfection activity between two batches of $LK_{25}AOA1$ with different levels of purity: $LK_{25}AOA1\#1$ is estimated to be 70-80% pure, and $LK_{25}AOA1\#2$ is estimated to be 75-90% pure.

A comparison of the transfection activities of $LK_{25}AOA1\#1$, $LK_{25}INF7$ and $LK_{10}INF7$ (estimated purity of 90%) complexed with DNA were studied in B16 cells at charge ratios of 0.8, 1.6, 3.2, 4.8, and 6.4. The results of this experiment shown in Figure 3.12 showed that the transfection efficiency of $LK_{25}AOA1$ was between 2- and 6-fold greater than $LK_{25}INF7$ (Figure 3.12). The purity of $LK_{25}INF7$ used in this experiment was similar to that of $LK_{25}AOA1\#1$ and therefore the difference in transfection efficiency between the two peptides is due to the effect of replacing the glutamic acid residue at

position 7 from the N-terminus, with alanine (see Table 2.1 for sequence). The bifunctional peptide $LK_{10}INF7$, with a shorter lysyl chain did not show any ability to transfect cells when complexed with DNA (Figure 3.12). The lack of ability of $LK_{10}INF7$ to promote detectable gene expression in B16 cells when complexed with DNA can be explained by the fact that $LK_{10}INF7$ does not bind effectively to DNA, as evidenced by the results of ethidium bromide exclusion assay described in section 3.3.1.1.2 above.

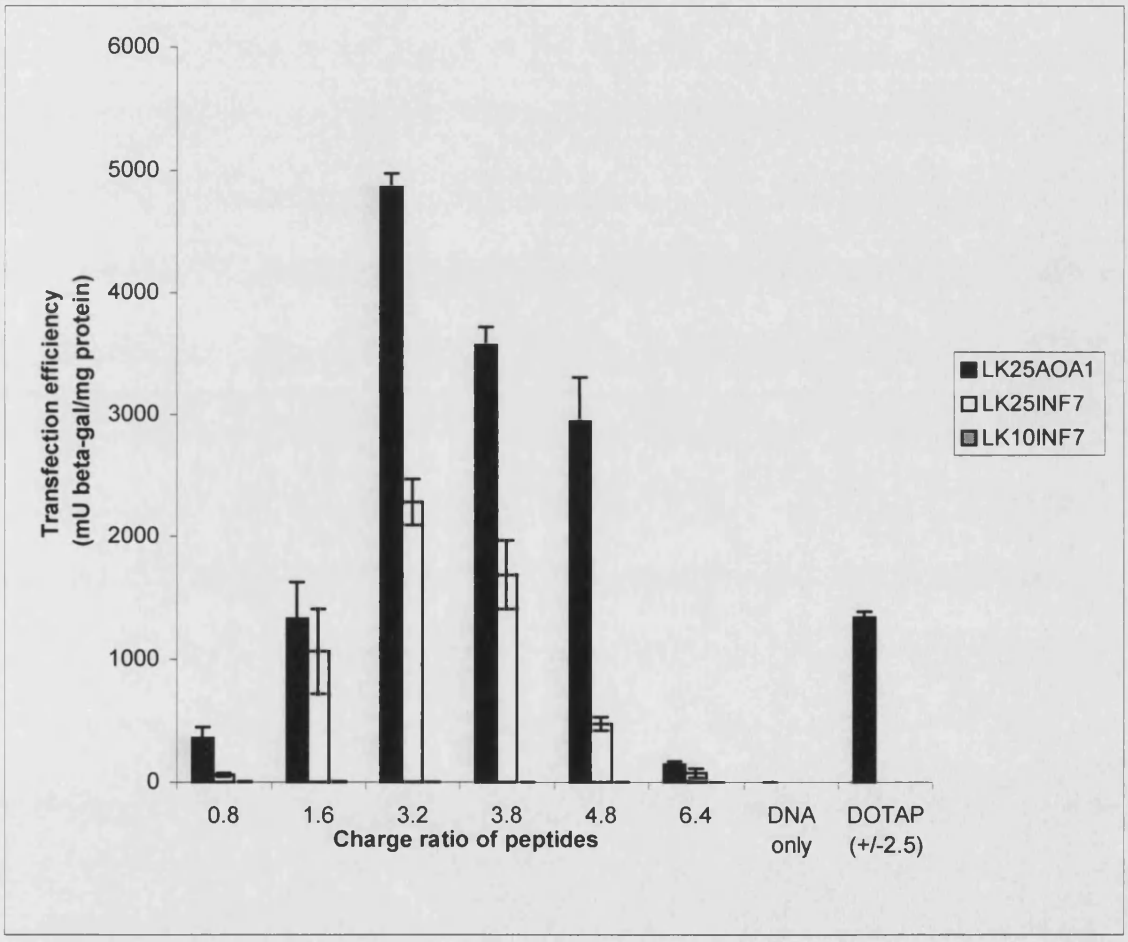

Figure 3.12 Comparison of transfection efficiency of various complexes in B16 cells. Complexes formed between (6.4 μg in 800 μl HBS) and various quantities of $LK_{25}AOA1\#1$, $LK_{25}INF7$, $LK_{10}INF7$ and DOTAP were incubated for 30 minutes before adding a 500 μl aliquot (containing 2 μg per 6-well plate) to cells. Cells were incubated with complexes at 37°C for 4 hours and harvested 24 hours post initiation of transfection for analysis. Data represent the mean of triplicate samples ± SEM, and is representative of two separate experiments.

3.3.3.2 *IN VITRO TRANSFECTION OF A PRIMARY CELL LINE*

The ability of $LK_{25}AOA1$/DNA complexes to transfect primary cells *in vitro* was investigated using primary skin fibroblast, FEK4 cells, obtained from the foreskin of newly born males. These cells had been shown to be refractory to transfection by traditional methods including calcium precipitation and lipofection (personal communication, Dr. Charareh Pourzand, Pharmacy Department, University of Bath). Cells were seeded at a density of 5 x 10^5 cells per well. To determine the optimum amount of complex needed for transfection, increasing amounts of pCMV luciferase DNA was complexed with $K_{25}AOA1$ at a charge ratio of 3.2 and incubated with cells as described in methods section 3.2.8. Increasing quantities of $K_{25}AOA1$/DNA complexes resulted in near linear increase in the levels of luciferase expression (Figure 3.13).

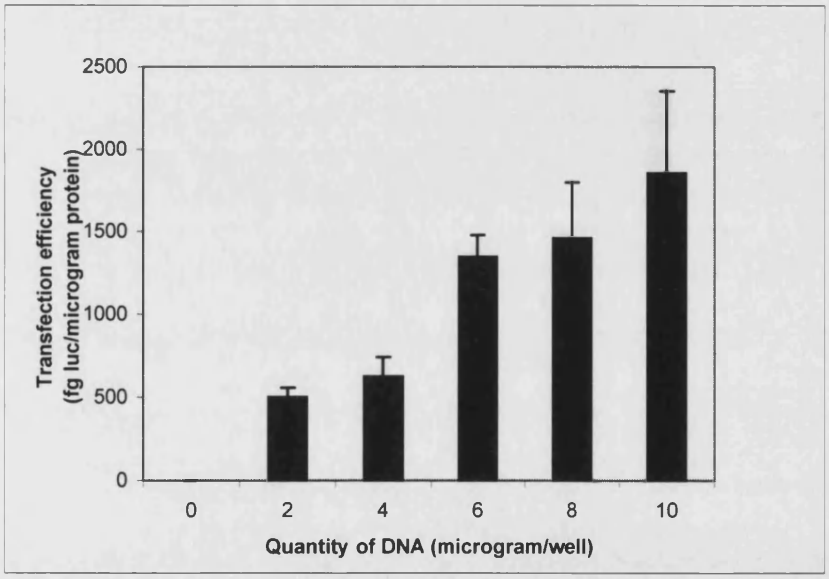

Figure 3.13 Complexes formed between increasing quantities of pCMVluc complexed with $LK_{25}AOA1$#2 at a charge ratio of 3.2 were incubated for 30 minutes before adding a 500 µl aliquot (containing 2, 4, 6, 8 or 10 µg per 6-well plate) to cells covered with 1.5 ml of serum free OPTI-MEM™. FEK4 cells were incubated with complexes at 37°C for 4 hours and harvested 24 hours post initiation of transfection for analysis. Data represent the mean of triplicate samples ± SEM, and is representative of two separate experiments.

Comparing levels of gene expression in FEK4 cells to immortal cell lines, this level of expression using 2 μg DNA at a charge ratio of 3.2 for example, was about 2-fold less than in A549 cells, 3-fold less than in NIH3T3 cells and over 5-fold less than in B16 cells (Figure 3.9, Figure 3.10 and Figure 3.13).

3.3.4 Discussion: Effect of charge ratio on transfection efficiency

The net charge of the complex formed with DNA significantly affects the transfection efficiency of a gene delivery vector[264]. The charge ratio is defined here as the molar ratio of positive charges provided by the gene delivery vector relative to negative charges from the DNA. An increase in the quantity of GDV (LK_{25}AOA1 and DK_{25}AOA1 and K_{25}INF7) (and hence charge ratio) led to an increase in transfection activity until a maximum was reached. Further increases beyond this optimum resulted in a reduced transfection efficiency as a result of toxic effects mediated by free gene delivery vector. MTT assay results (section 3.3.13) demonstrated that there was increased cell death in the presence of excess GDV, accounting for the decrease in transfection efficiency at high charge ratios.

A direct comparison of K_{25}AOA1#2 and K_{25}INF7 in B16 cells showed that they both had similar optimum charge ratios around 3.2 and that K_{25}AOA1 was between 2- and 6-fold better than K_{25}INF7 (Figure 3.12). In another experiment K_{25}AOA1#2 was compared to K_{25}INF7 as part of an experiments comparing binary and ternary complexes systems (Figure 3.17) and K_{25}AOA1#2 was found to be about 1.6-, 1.4-, 1.5- and 4.8-fold better than K_{25}INF7 in B16, NIH3T3, COS-7 and A549 cells, respectively. A comparison of the haemolytic activity between K_{25}AOA1 and K_{25}INF7 showed that that point mutation in the sequence of the bifunctional peptide was responsible for a greater haemolytic activity of K_{25}AOA1 at both pH 5 and pH 7 (Figure 3.3). A possible explanation for this difference in activity is that following the replacement of the glutamic acid residue at position 7 with a neutral residue, alanine, the negatively charged residues become more concentrated in a narrower region (less spread) resulting in greater polarity in the alpha helical structure of LK_{25}AOA1 compared to K_{25}INF7 (see Figure 3.14). This hypothesis is indirectly supported by work reported by Gottschalk and others who found that JTS1 was approximately 1000-fold more active than INF7 at

transfection when they were separately included in the ternary system with DNA and K8[76]. A comparison of sequence of amino acids in JTS1 compared to INF7, shows that the only functional change to the structure is the replacement of a charged residue (glutamic acid) with an uncharged leucine residue at position 7 (Figure 3.14).

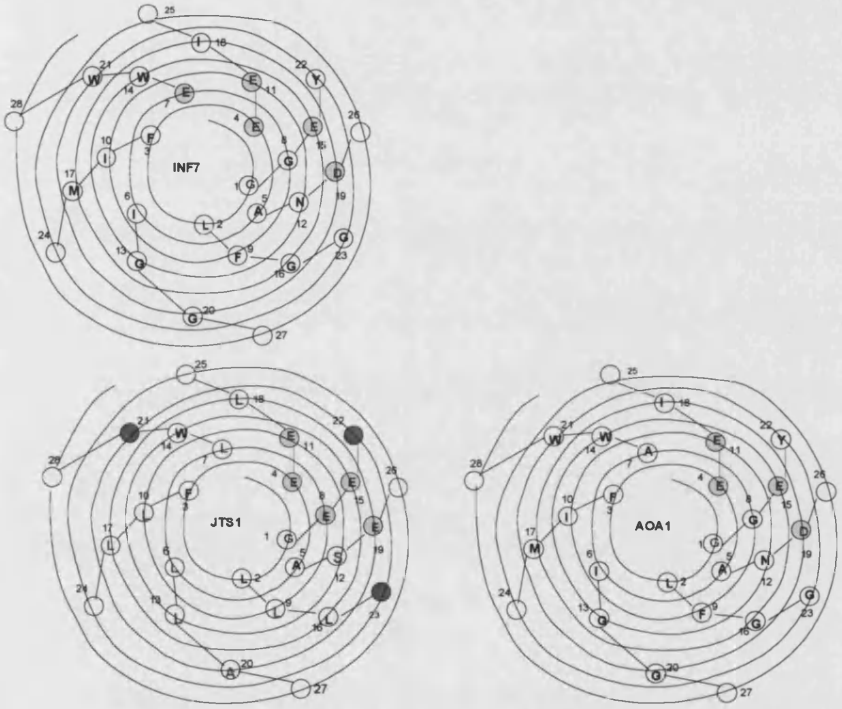

Figure 3.14 Schematic representation of alpha helical structure of fusion peptides AOA1, INF7 and JTS1

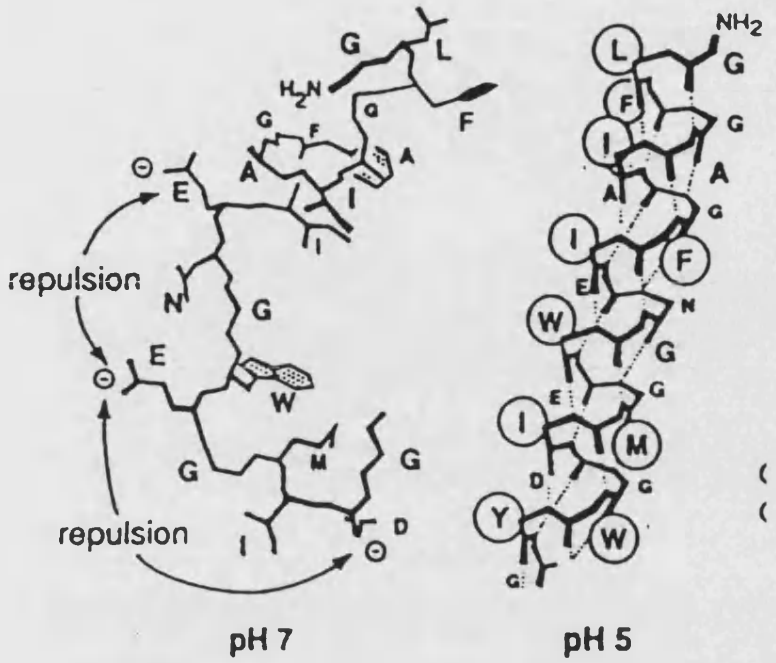

Figure 3.15 Amino-terminal fusogenic peptide of influenza haemagglutinin subunit HA-2 showing conformation at neutral pH, according to data from x-ray analysis[265] and α-helical conformation at low pH, consistent with references 266 and 267. Taken from reference 167.

Oligolysine/DNA complexes, K_{25}/DNA, or fusogenic peptide/DNA complexes, AOA1/DNA, were not effective at transfection (data not shown). This is in contrast to a report by Gottschalk *et al.* who found that K8/DNA complexes showed some transfection activity[76]. However, the ternary complex system K8/DNA/JTS1 was only marginally effective in this study. In our laboratory, polylysine$_{214}$ was only effective in the presence of chloroquine at a charge ratio of 1.5[268]. This optimum charge ratio for polylysine/DNA in the presence of chloroquine is lower than that of bifunctional peptide/DNA complexes and reflects the fact that long chain cationic polymers have a higher DNA condensation capacity than shorter chain polylysine. Endocytosed DNA/pLL complexes do not have a means of endosomal escape and require the concomitant use of lysomotropic agents or pH sensitive fusogenic peptides such as that derived from the influenza haemagglutinin HA-2 subunit[167].

3.3.5 COMPARISON BETWEEN *IN VITRO* TRANSFECTION ACTIVITY OF BINARY AND TERNARY COMPLEXES

Previous efforts to deliver DNA into dividing cells *in vitro* using polylysine or similar polycations have focused on ternary or quaternary complexes[167,179] due to the dependence on commercially available polycations. Reports by Gottschalk *et al.*[76] and Hart *et al.* [170] were among the first published work to synthesize oligocations or bifunctional peptides respectively for use as adjuncts in gene delivery. Work by Gottschalk and colleagues[76] was based on the ternary complex models using fusion peptides first described by Wagner *et al.*[179]. Studies done by Hart *et al.*[170] used oligolysyl chain as a means of anchoring an integrin targeting moiety to a lipid based gene delivery system, again a ternary system. The bifunctional peptide described in this work, which is a fusogenic peptide with an oligolysine chain is a novel non-lipid-based binary complex capable of transfecting dividing cells. This novel peptide-based system has two important advantages: 1) the relative ease of addition of different functional moieties, compared to lipid-based systems, during the initial synthesis without the risk of destroying the functions of other moieties and 2) the location/presence of each attached functional moiety is assured by design through the covalent peptide bond (as opposed to electrostatic interactions in a ternary or quaternary complex system). The transfection efficiency of the following novel bifunctional peptides LK$_{25}$AOA1, DK$_{25}$AOA1, LK$_{10}$AOA1 and LK$_{25}$INF7 were compared to the cationic lipid system DOTAP/DNA and the ternary complex system K8/DNA/JTS1. The cationic lipid DOTAP/DNA charge ratio complex used in this work was previously optimised in our laboratory by Dr. Aima Uduehi[256] and the charge ratio for the ternary system was as reported by Gottschalk *et al.*[76].

A direct comparison between binary complexes (bifunctional peptides/DNA) and ternary complexes (K$_{25}$/DNA/AOA1* or K8/DNA/JTS1) for *in vitro* transfection activity was investigated in six cell lines namely B16, HEK293, HeLa, A549, NIH3T3, and COS-7 cells. All complexes between bifunctional peptides and DNA (pRSV*lacZ* or pCMVluc DNA) were formed in HBS at charge ratios indicated in brackets of the x-axis label in Figure 3.16 and Figure 3.18. The bifunctional peptides studied were LK$_{25}$AOA1#2, LK$_{10}$AOA1, LK$_{25}$INF7, DK$_{25}$AOA1 and DK$_{25}$AOA1(N) (DK$_{25}$AOA1 without asparagine residue).

Figure 3.16A and B (linear and log scale representation of the same results) shows the results of a comparison of transfection ability between binary complexes formed with bifunctional peptides $LK_{25}AOA1\#2$, $LK_{25}INF7$, $DK_{25}AOA1$, $DK_{25}AOA1(N)$ (with omitted asparagine residue) or DOTAP and ternary complexes formed with K8/JTS1 in HeLa cells. This experiment was also used to determine the optimum charge ratio for $LK_{25}AOA1$/DNA complexes in HeLa cells. The results in Figure 3.16 show that, for $LK_{25}AOA1$/DNA complexes, at the optimum charge ratio of 3.2 (same optimum charge ratio as in B16 cells), the binary complex was over 43-fold or 127-fold better than the ternary complex of K8/DNA/JTS1, at a JTS1 concentration of 7 nM or 38 nM respectively. The bifunctional peptide $LK_{25}AOA1$ complexed with DNA at the optimum charge ratio of 3.2 was only marginally (1.7-fold) better than the binary complex of DOTAP/DNA in HeLa cells. The other bifunctional peptides $LK_{25}INF7$ and $DK_{25}AOA1$ were 14-fold and 37-fold better than the ternary complex of K8/DNA/JTS1 compared with 7 nM concentration of JTS1. The bifunctional peptide $DK_{25}AOA1(N)$ (with omitted asparagine residue) had similar transfection efficiency to that of the ternary complexes; the reason for the low transfection activity of $DK_{25}AOA1(N)$ is discussed in section 3.3.13.

In a separate experiment, the transfection efficiency of bifunctional peptides $LK_{25}AOA1\#2$, $DK_{25}AOA1$ (N), $LK_{25}INF7$ and $LK_{10}AOA1$ formulated as binary complexes with DNA at a charge ratio of 3.2 was compared to the lipid based binary complex of DOTAP/DNA and peptide based ternary complex of K8/DNA/JTS1 or K25/AOA1*/DNA in four cell lines, namely B16, NIH3T3, COS-7 and A549 cells and the results are showed in Figure 3.17. As expected, there were variations in the responsiveness of different cell lines to transfection by the same gene delivery agent in transfection experiment performed on the same day and under the same experimental conditions; but the differences in transfection efficiencies between various gene delivery agents can be clearly noticed in the results showed in Figure 3.17. The binary complex of bifunctional peptide $LK_{25}AOA1\#2$/DNA was over 12000-fold, 5700-fold, over 74000-fold and over 8000-fold better than the ternary complex of K8/DNA/JTS1 in B16, NIH3T3, COS-7 and A549 cells respectively. Similar orders of magnitude differences in transfection efficiencies were previously observed in B16 cells when $LK_{25}AOA1\#1$ was compared to the ternary complex system of K25/AOA1*/DNA prior

to obtaining pure K8 and JTS1 from Gottschalk *et al.*[76], but because the purity of the fusogenic peptide AOA1* was not known at this stage, the superiority of the binary complex involving the bifunctional peptide over the ternary complex system was uncertain. It now seems likely that AOA1 performed with similar efficient to JTS1. An explanation for the relative lack of transfection activity for the ternary complex systems reported in this work may be found from results of experiments to study the particle size (hence complex stability) in HBS of K_{25}/DNA complexes in HBS described in section 3.3.2. The large complexes formed are symptomatic of the sensitivity of the product, which may vary according to local differences in the nature of the mixing protocol.

The fold differences between transfection efficiencies of the bifunctional peptide LK_{25}AOA1 and DOTAP were relatively marginal: 1.6-, 1.2- and 2.3-fold in B16, NIH3T3 and A549 cells respectively and in COS-7 cells DOTAP was slightly better (1.1-fold) than the bifunctional peptide LK_{25}AOA1.

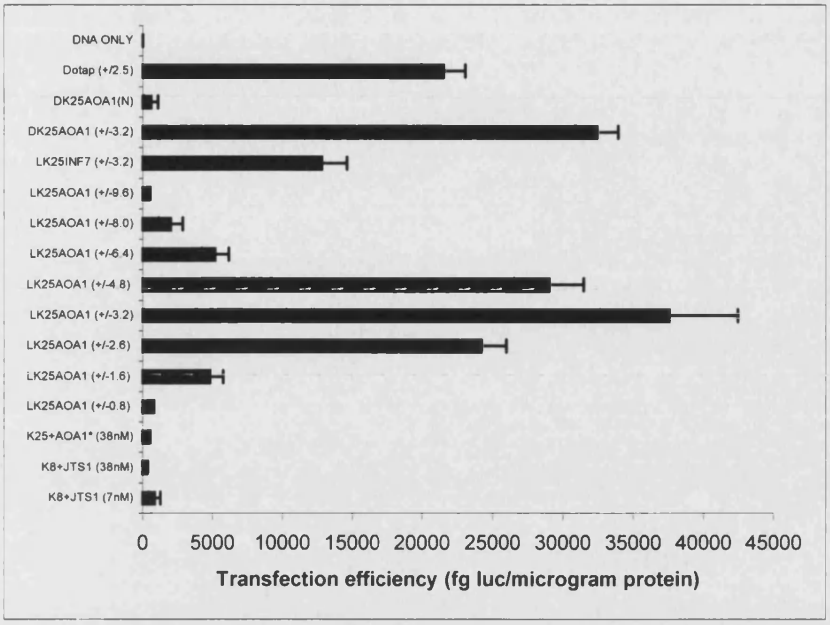

A

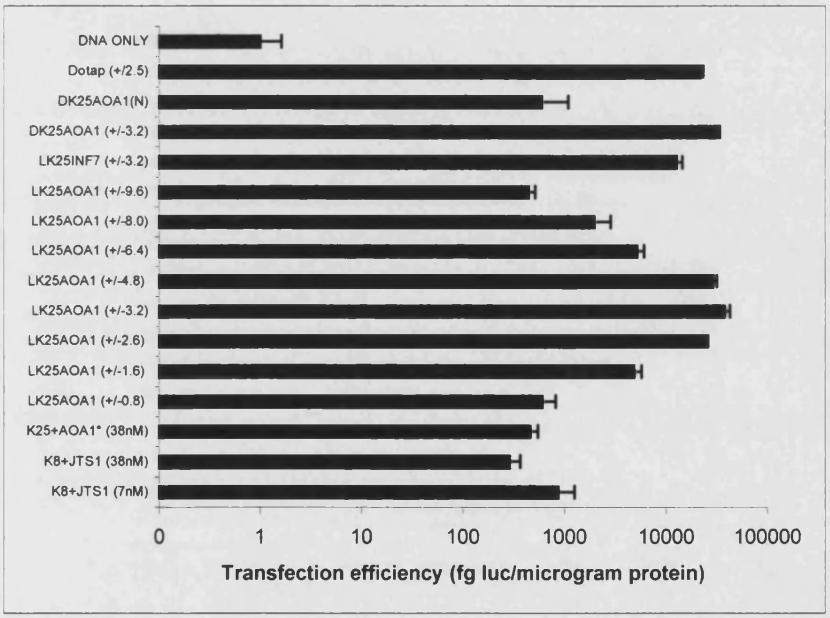

B

Figure 3.16 A and B: Linear and logarithmic scale representation of the comparison of transfection efficiency of various complexes in HeLa cells. For K8-DNA/JTS1 complexes, K8 (9 μg in 400 μl HBS) and pCMVluc (6.4 μg in 400 μl HBS) were mixed and incubated for 30 minutes followed by mixing with either 7 nM or 38 nM JTS1 or AOA1* (in 800 μl HBS) and a further incubation for 30 minutes before adding a 500 μl aliquot (containing 2 μg per 6-well plate) to cells. Bifunctional peptide/DNA complexes formed between pCMVluc (6.4 μg in 800 μl) and various quantities of $LK_{25}AOA1\#2$ (batch #2, estimated purity 95%), $LK_{25}INF7$ (estimated purity 80%), $DK_{25}AOA1$ (estimated purity: 95%) and DOTAP were incubated for 30 minutes before adding to cells. Cells were incubated with GDV for 4 hours 37°C for 4 hours harvested 24 hours post initiation of transfection for analysis. Data represent the mean of triplicate samples ± SEM, and is representative of two separate experiments.

Another distinctive result in this experiment was the total lack of transfection activity by bifunctional peptide with a shorter lysyl chain $LK_{10}AOA1$ in all four cell lines. The reason for this observation was that $LK_{10}AOA1$ did not effectively bind to DNA as inferred from ethidium bromide exclusion assay results in section 3.3.1.1.2. A fuller explanation has been provided in the discussion of the ethidium bromide exclusion assay and gel retardation assay results in section 3.3.1.

Figure 3.18 shows the results of the comparison between binary and ternary complexes for transfection efficiency in B16 and HEK293 cells performed in the early stages of this project when pRSVlacZ β-gal was used as the reporter gene. The results showed that the binary system of $K_{25}AOA1$#1/DNA was between 1.4 x 10^3 and 2.6 x 10^3-fold better at mediating transfection in B16 cells than the ternary system of K25/DNA/AOA1* at identical charge ratios. In HEK293 cells, $K_{25}AOA1$#1/DNA system was between 87-fold and 630-fold better than K_{25}/DNA/AOA1* ternary system. While using the β-galactosidase reporter gene assay method, the low transfection activity of the ternary complex systems were being concealed by the high background readings of the negative controls, represented by "no DNA" and "DNA only" columns: thus the real fold difference in transfection efficiency between the binary and ternary complex systems could not be accurately determined, and hence there was the need to change to the use of firefly luciferase reporter gene assay method.

Comparison of luminometer readings, a common practice with many researchers, indicated that the difference in between the two types of complexes was actually greater (>10^6-fold, per μg protein). The apparent discrepancy stems from the fact that it is not possible to obtain one standard curve of luciferase activity, which spans more than 5 orders of magnitude. The lack of linearity over 7-8 orders of magnitude of luciferase activity meant it was inaccurate to directly compare light unit readings from the lower end of the scale to the top part of the scale (Appendix G). Comparison of binary complexes with K8/DNA/JTS1 ternary complexes (using reported concentrations of 7 and 38 nM of JTS1)[76] again revealed the same level of superiority of bifunctional peptide/DNA complexes over the K8/DNA/JTS1 system (Figure 3.16). The purity of K8, JTS1 and $K_{25}AOA1$ were confirmed by MALDI-TOF mass spectrometry and therefore the results obtained by comparing the two systems using K8, JTS1 and $K_{25}AOA1$ were reliable.

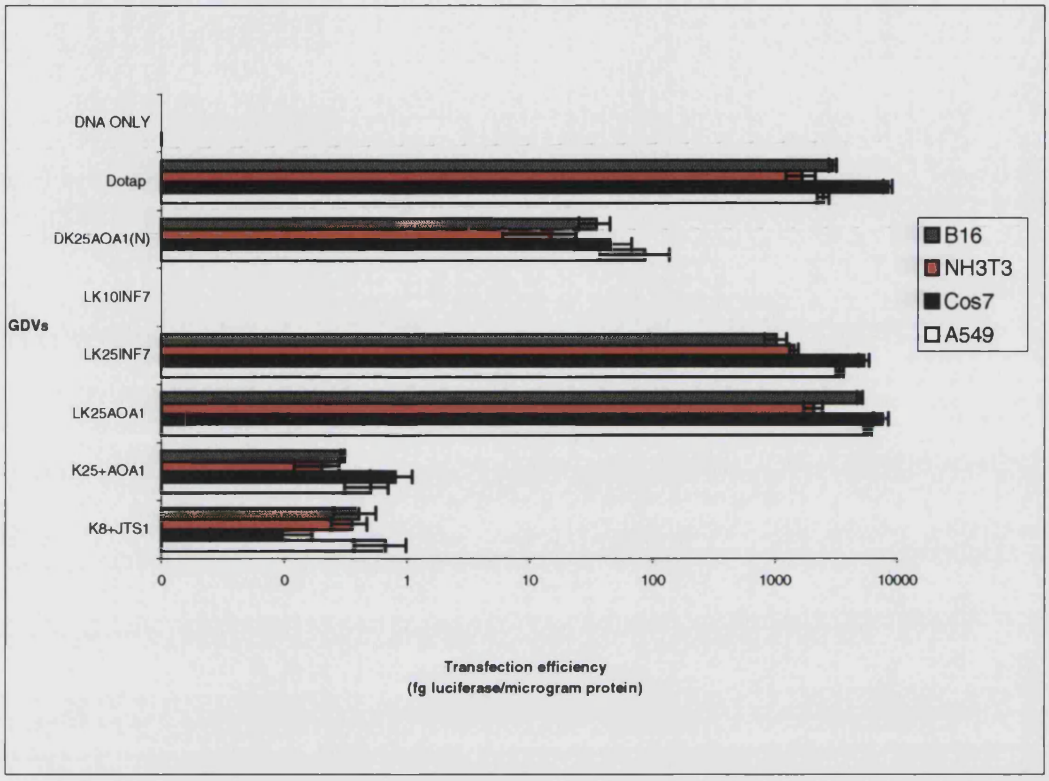

Figure 3.17 Comparison of transfection efficiency of various complexes in A549, COS-7, NIH3T3 and B16 cells. For K8 or K_{25}-DNA/JTS1 complexes, K8 or K_{25} (9 μg in 400 μl HBS) and pCMV luciferase (6.4 μg in 400 μl HBS) were mixed and incubated for 30 minutes followed by mixing with JTS1 at 38 nM (in 800 μl HBS) and a further incubation for 30 minutes before adding to cells. Complexes formed between pCMV luciferase (6.4 μg in 800 μl HBS) and previously determined optimised quantities of LK_{25}AOA1, LK_{25}INF7, DK_{25}AOA1(N) and DOTAP (in 800 μl HBS) were incubated for 30 minutes before adding a 500 μl aliquot (containing 2 μg per 6-well plate) to cells. Cells were incubated with complexes at 37°C for 4 hours and harvested 24 hours post initiation of transfection for analysis. Data represent the mean of triplicate samples ± SEM, and is representative of two separate experiments.

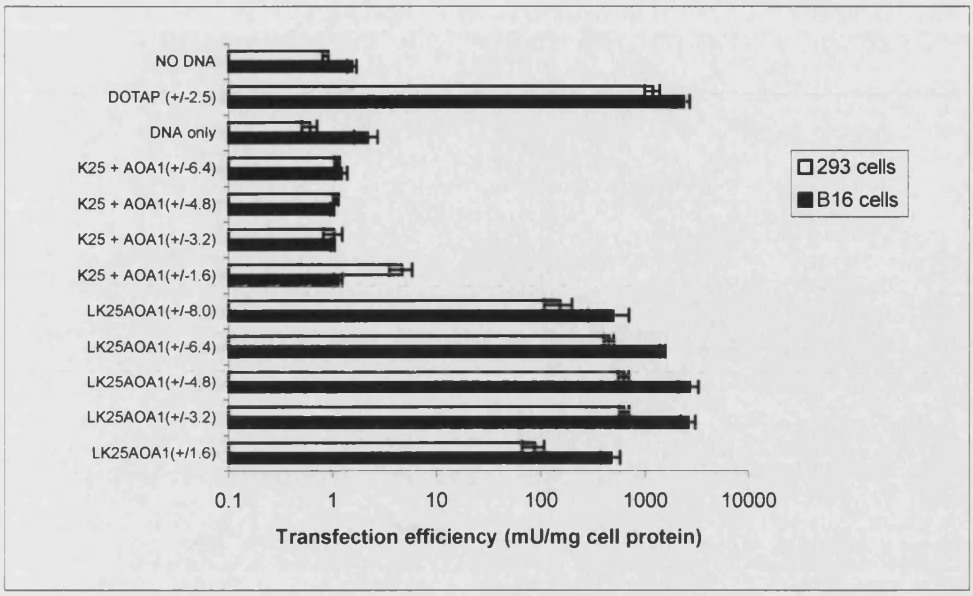

Figure 3.18 Comparison of transfection efficiency of various complexes in B16 and HEK293 cells. For K_{25}-DNA/AOA1 complexes, K_{25} (9 μg in 400 μl HBS) and pRSV*lac*Z (6.4 μg in 400 μl HBS) were mixed and incubated for 30 minutes followed by mixing with 800 μl HBS containing various quantities of AOA1 (to produce the charge ratios stated in brackets) and further incubation for 30 minutes before adding a 500 μl aliquot (containing 2 μg per 6-well plate) to cells. Complexes formed between pRSV*lac*Z (6.4 μg in 800 μl HBS) and various quantities of peptides (in 800 μl HBS) were incubated for 30 minutes before adding a 500 μl aliquot (containing 2 μg per 6-well plate) to cells. Cells were incubated with complexes for 4 hours at 37°C and harvested 48 hours post initiation of transfection for analysis. Charge ratios of DNA/peptide complexes are shown in brackets. Data represent the mean of triplicate samples ± SEM, and is representative of two separate experiments.

To help answer the question of why the ternary complex of K_{25}/DNA/AOA1* system did not work and extrapolate the results to account for the lack of transfection activity of K8/DNA/JTS1 systems, particle size and zeta potential measurements (see section 3.3.2) were performed in 5% (w/v) glucose (solution used by Gottschalk *et al.*[76]) and in HBS (buffer system used by Wagner and colleagues [167,179], the pioneering researchers in the use of fusogenic peptides in ternary/quaternary gene delivery systems).

3.3.6 DISCUSSION: COMPARISON BETWEEN *IN VITRO* TRANSFECTION ACTIVITY OF BINARY AND TERNARY COMPLEXES

Plank and colleagues[167] synthesized and studied the gene transfer enhancement ability of several sequences of peptides based on the 23 amino-terminal sequence of influenza virus X-31 in a self-assembled quaternary complexes dependent on ionic interactions. Of the sequences tested, INF7 and dimeric influenza peptides INF5, INF3DI and INF4DI were found to promote the highest gene expression (more than 5000-fold higher than in the absence of peptide) when formulated as quaternary complex using DNA/polylysine/ transferrin-polylysine/fusogenic peptide. The mechanism by which these peptide sequences were improving transfection was determined to be through endosomal escape of complexes: this inference was drawn from the observation that when cells in culture internalised FITC-dextran in endosomes through fluid-phase endocytosis, the presence of an endosomolytic peptide in the culture medium resulted in absence of bright vesicles, and the fluorescence spread over the cell: indicating the release of FITC-dextran into the cytoplasm. The presence of bafilomycin A_1, an inhibitor of vacuolar ATPase[269] that specifically blocks the endosomal proton pump, also blocked the peptide-mediated release of FITC-dextran from vesicles and gene expression. It had been observed that the peptide-mediated endosome disruption and gene expression were dependent on the concentration of the fusogenic peptide, but the question of whether ionically bound (to DNA/polylysine) or unbound fusogenic peptide was mediating gene expression was neither asked nor answered by the authors. The idea of self-assembly of a quaternary particle: that a DNA/transferrin-polylysine/polylysine particle with an overall positive charge could be formed, to which negatively charged fusogenic peptide could be ionically bound to the surface, was not demonstrated by Plank and colleagues[167]. It was very possible that it was unbound fusogenic peptide

present in the medium that was responsible for mediating gene transfer. If unbound fusogenic peptide was responsible for enhancing gene delivery, then could ensuring that the fusogenic peptide was associated with the DNA/polylysine particle to be released from the endosome further enhance gene expression? The hypothesised model for self-assembly of particle suggests that the negative residues of the fusogenic peptide interact ionically with the excess positive charges on the exterior of a DNA/polylysine particle. Since these complexes are formulated at pH 7, the acid residues (pKa 4 to 5) in the fusogenic peptide would be ionised, and the lysyl ε-amino groups (pKa 9) will also be partially protonated and therefore the binding of the fusogenic peptide to the surface of a "positively charged" DNA/polylysine particle can be assumed, but this can not be guaranteed in the presence of other ions present in solution, for example HBS. In a mixture containing DNA, polylysine and fusogenic peptide, the possible species present (depending on the relative quantities of each component added) are: DNA/polylysine, unbound polylysine, unbound fusogenic peptide, polylysine/fusogenic peptide, and perhaps the ternary complex, DNA/polylysine/fusogenic peptide. Contrary to the impression given by diagrams presented by proponents of self-assembled ternary or quaternary complexes, the fusogenic peptide should not exist as a sided alpha helix molecule at pH 7, because at pH 7, the glutamic and aspartic acid residues will be charged and oppose the formation of an alpha-helical structure (Figure 3.15). If on the other hand, bound fusogenic peptide was responsible for enhanced gene expression, was the ionic interaction between the fusogenic peptide and polylysine not hindering the fusogenic peptide from forming the alpha helix conformation (at the lower endosomal pH of 5.5) necessary for endosomal escape? The notion at the beginning of this project was that the peptide-mediated gene expression could be improved if the entire 3-D structure of the fusogenic peptide, complexed to DNA via oligolysine/polylysine was available to interact with the endosomal membrane. In order to achieve this aim, it was necessary to synthesize a peptide with both DNA binding and fusogenic moieties, a bifunctional peptide.

In this project, in all 6 cell lines tested, results showed that the binary complexes of DNA/bifunctional peptide D- or LK_{25}AOA1 were 43- to 74000-fold more effective than the ternary complex of DNA/K_{25} / AOA1* or K8/DNA/JTS1 (Figure 3.16, Figure 3.17, Figure 3.18 and Figure 3.21). One possible reason why the ternary complexes were

almost ineffective is that the complexes were formulated in HBS rather than 250 mM sucrose[76] which may have resulted in flocculation of particles producing aggregates which were not capable of transfecting cells. Attempts to formulate and measure zeta potential and particle size of ternary complexes (K8/DNA) in HBS at peptide concentrations used during transfection resulted in a poor sample quality, which made the accurate determination of zeta potential impossible. In contrast, when formulated in HBS, the sample quality of $DK_{25}AOA1$/DNA complexes was sufficiently good for particle size and zeta potential measurements to be made at usual concentrations used for transfection, although not at higher concentrations. Thus, K_{25}/DNA complexes had a much lower solubility and stability in the presence of ions and could account for the low transfection efficiency of the overall ternary complex.

The challenge of instability of complexes to salts *in vitro* and *in vivo* must be overcome by designing more robust GDVs. The decision to formulate K8/DNA/JTS1 complexes in HBS was taken in order to maintain formulation consistency with extensive optimisation experiments performed with $K_{25}AOA1$/DNA complexes formulated in HBS. This buffer was also used in work published by Plank and colleagues[167] and was prior to the publication of work by Gottschalk and colleagues with K8/DNA/JTS1 complexes[76]. The fact that DNA/K8/JTS1 complexes were reported to be highly effective by one group of researchers but not in our laboratory highlights the lack of robustness of this type of gene delivery formulation. The bifunctional peptide $K_{25}AOA1$ is an example of how a single multifunctional peptide can be constructed to overcome solubility problems and ensure that the required functional components of a successful gene delivery agent are present in the desired location within the complex. The advantage of a single multifunctional peptide is evident: the co-localisation of the required moieties in the desired relative positions to DNA can be achieved without the risk of compromising the functionality of the constituent moieties.

3.3.7 Effect of diluting bifunctional peptide with oligolysine

In a study to elucidate the importance of the DNA-binding moiety of $K_{25}AOA1$, a transfection experiment was performed in which the relative quantity of the fusogenic moiety present in a complex was diluted out. To achieve this dilution, optimum and

sub-optimum quantities (75%, 50% and 25% of optimum weight) of K_{25}AOA1 were complexed with DNA and their transfection efficiency compared with a parallel experiment in which the molar proportion of the DNA-binding moiety (K_{25}-) had been pre-incubated with DNA by addition of K_{25} 30 minutes before adding K_{25}AOA1. The data from this experiment represented in Figure 3.19, showed that in complexes where only 50% and 25% of K_{25}AOA1 was present in the complexes (i.e. 50% and 75% reduction in K_{25}AOA1), there was approximately 3700-fold and 21600-fold reduction in transfection efficiency. However, when a quantity of K_{25} equivalent to 50% and 75% of the mass of K_{25} in K_{25}AOA1 (i.e. replacing the 50% and 75% of K_{25} removed, which is equal to 4.5 μg and 6.9 μg respectively) was incubated with DNA 30 minutes prior to the addition of 50% and 25%, respectively, of the optimal quantity of K_{25}AOA1, the fold reduction in transfection efficiency (for complexes containing 50% and 25% of optimum weight of K_{25}AOA1) were 4-fold and 10-fold respectively. The result of this study also showed that the pre-incubation of DNA with K_{25} before adding the optimum or near optimum amount of K_{25}AOA1 was inhibitory, possibly because the amount of K_{25}AOA1 directly bound to DNA was reduced.

These results highlight two important issues: Firstly the plasmid DNA must be sufficiently condensed by the bifunctional peptide for transfection to take place. Effective DNA condensation by pre-incubating with K_{25} without fusogenic moiety restored some transfection activity. Secondly, synthesizing both components as a single peptide guarantees a high concentration and co-localisation of the fusogenic moiety on the surface of the DNA/peptide particle; both of these factors appear to be important for high gene expression mediated by fusogenic peptides in dividing cells.

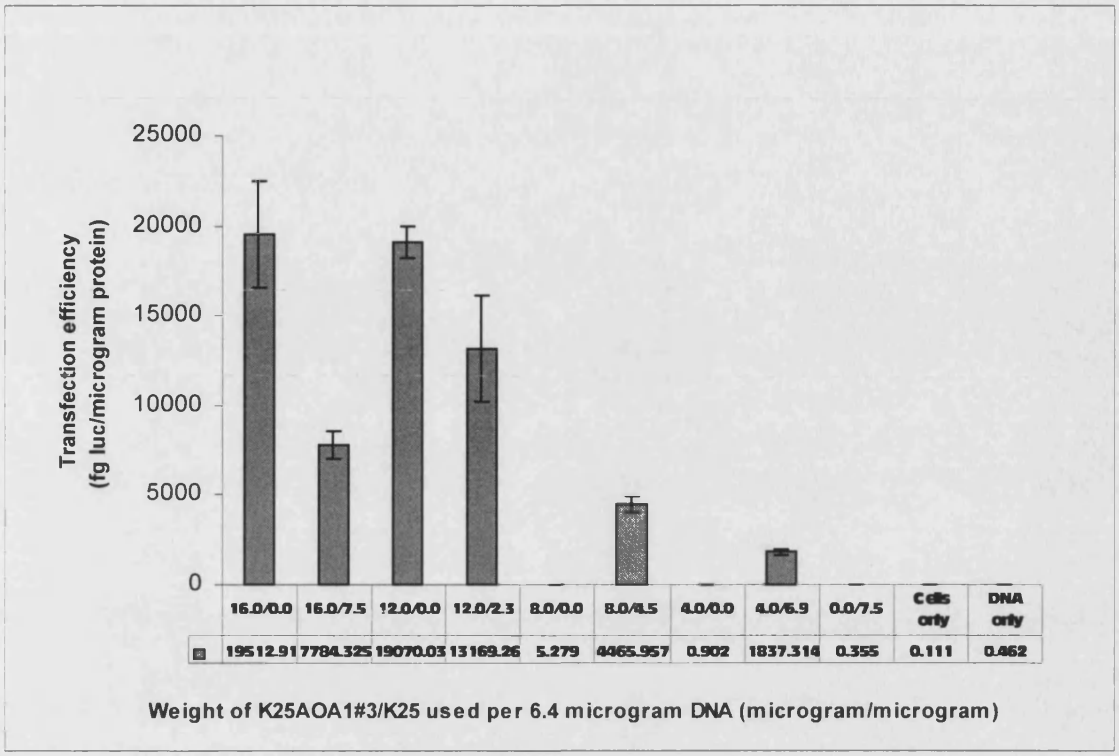

Figure 3.19 Transfection experiment showing the effect of diluting K_{25}AOA1#3 with K_{25} in HeLa cells. Quantities of K_{25}AOA1 and K_{25} added to DNA are shown in the first row of the data table and transfection efficiency is shown in the second row of the data table. Different quantities of K_{25} (in 400 µl HBS) were mixed with pCMVluc (6.4 µg in 400 µl HBS) and incubated for 30 minutes followed by mixing with different stated quantities of K_{25}AOA1 (in 800 µl HBS) and a further incubation for 30 minutes before adding a 500 µl aliquot (containing 2 µg per 6-well plate) to cells. Cells were incubated with GDV for 4 hours 37°C for 4 hours harvested 24 hours post initiation of transfection for analysis. Data represent the mean of triplicate samples ± SEM, and is representative of two separate experiments.

3.3.8 STUDY OF THE MECHANISM OF ACTION OF BIFUNCTIONAL PEPTIDES USING ENDOSOMAL PROTON PUMP INHIBITOR

Transfections of HeLa cells were performed in the presence or absence of bafilomycin A_1. Transfection experiments in the presence of bafilomycin A_1 were performed as described in section 3.2.2 with the exception that the transfection medium contained 200 nM bafilomycin A_1 (achieved by adding 10 µl of 40 mM stock solution of Bafilomycin A_1 in dimethyl sulfoxide (DMSO) to 6-well plates containing cells covered with 1.5 ml of Opti-MEM™ and 0.5 ml transfection complexes in HBS). Binary and ternary complexes were formed at a charge ratio of +/-3.2, and PEI/DNA complexes were formed at a mass ratio of 3.6 µg PEI per 2 µg DNA per well as done throughout this project.

The results (Figure 3.20) showed that with K_{25}AOA1#3/DNA complexes, luciferase readings were 1.9-fold less in the presence of bafilomycin A_1 and cell lysate protein content was also reduced by nearly 1.5-fold in samples containing bafilomycin A_1; therefore the net effect of bafilomycin A_1 was a 1.3-fold reduction in the transfection efficiency of K_{25}AOA1#3/DNA complexes. The toxicity of bafilomycin A_1 in DMSO was visually observed under the microscope as a higher number of detached cells from wells containing bafilomycin A_1 at 4-hours and 24-hours post transfection. The transfection efficiency of PEI decreased by 190-fold in the presence of bafilomycin A_1. The toxicity of PEI/DNA complexes to cells was evidenced by the observation that the cell lysate protein content of wells containing "PEI only" were low and similar to those which contained both PEI and bafilomycin A_1. The transfection efficiency of ternary complexes composed of K_{10} or K_{25}/DNA/AOA1 and the binary complex of K_{10}AOA1/DNA were similar to that of the negative control of "DNA only" and the effect of the presence of bafilomycin A_1 was insignificant due to the very low transfection activities of these complexes.

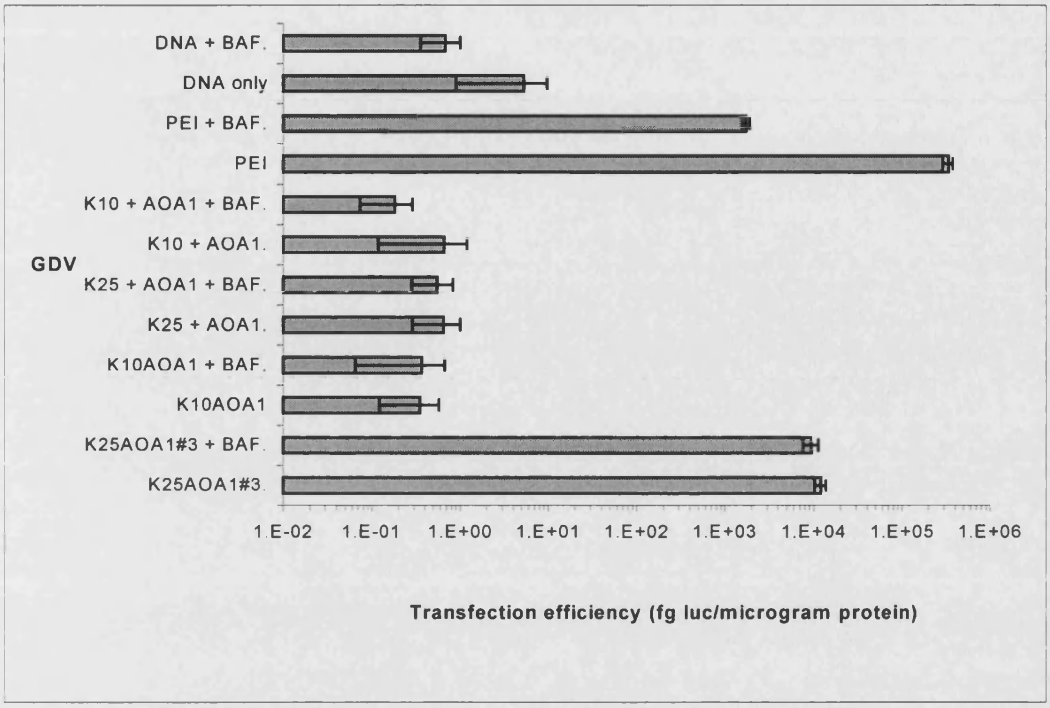

Figure 3.20 Transfection of HeLa cells in the presence or absence of 200 nM bafilomycin A_1. Complexes formed between pCMVluc and peptides LK_{25}AOA1#3, K10AOA1 (binary complexes) K_{25} + AOA1 and K_{10} + AOA1 (ternary complexes) were all at a charge ratio of 3.2. Cells were incubated with complexes for 4 hours at 37°C and harvested 24 hours post initiation of transfection for analysis. Data represent the mean of triplicate samples ± SEM, and is representative of two separate experiments.

3.3.9 Discussion: Study of the mechanism of action of bifunctional peptides using endosomal proton pump inhibitor

Fusogenic peptide sequences related to the N-terminal HA-2 sequence of the influenza virus which possess a low pH-selective haemolytic activity had been shown by a number of researchers to enhance gene transfer when added to DNA and oligolysine or polylysine complexes[76,167,236]. Plank *et al.* found a strong correlation of gene transfer efficiency of quaternary complexes that included fusogenic peptides with the capacity of the fusogenic peptides to lyse erythrocytes in an acidic environment. Crucially, Plank and colleagues observed that peptides that possessed a high haemolytic potential but did not display the strong specificity for low pH showed only moderate to insignificant augmentation of gene expression in quaternary DNA/TfpLys/pLys/fusogenic peptide complexes. Plank and colleagues also found that inhibition of endosomal acidification

by blocking the endosomal proton pump with bafilomycin A_1 considerably reduced peptide-mediated gene expression in quaternary DNA/TfpLys/pLys/fusogenic peptide complexes. The above observations, in conjunction with the observation that bafilomycin A_1 blocked fusogenic peptide-mediated release of FITC-dextran from endosomes formed the basis for the explanation of the mechanism of action of fusogenic peptides in quaternary complexes.

The above-mentioned observations by researchers have supported the theory that the fusogenic peptide sequences used in ternary or quaternary complexes undergo a conformational change at the low pH in the endosome to an alpha-helical structure in order to exert its endosomal escape properties; this mechanism is similar to the conformational change that occurs during influenza HA-mediated membrane fusion[188]. Based on this theory, other fusogenic peptide sequences with low pH-dependent haemolytic activity have been synthesised and tested for their ability to augment gene delivery by Plank *et al.* and Gottschalk *et al.* [167,76]. Plank and colleagues had not provided an explanation as to why synthetic peptides that possessed high haemolytic activity but lacked the low pH-selectivity, caused insignificant augmentation of gene expression. Perhaps, if and attempt had been made to address the question of why peptide sequences which do not need a low pH to be endosomolytically active, did not significantly improve gene delivery, this might have raised questions about the validity of the concept of step-wise complex formation of quaternary complexes involving fusogenic peptides. The question that needed to be answered was: if a peptide sequence had membrane disruptive activity at pH 7 and was endocytosed as part of a quaternary gene delivery complex, why did it not cause enhancement of gene delivery through endosomal escape in much the same way as a peptide which needed a low pH to be endosomolytically active? In other words, why should a non pH-selective membrane active peptide appear to lose its membrane-disruptive ability at a low pH? There seems to be no obvious reason for such an observation by Plank *et al.* In this project, ternary complexes consisting of K10 or K_{25}/DNA/AOA1 had very low transfection efficiency to the extent that the presence of bafilomycin A_1 did not cause a distinguishable difference.

The observation in this research project was that, the non pH-selective haemolytically active peptide K_{25}AOA1, was able enhance gene delivery. From erythrocyte lysis assay

results, K_{25}AOA1 had a higher haemolytic potency at pH 5 compared to pH 7, but this difference in potency varied depending on the concentration (see Table 3.3). At low peptide concentrations (below 7.8 x 10^{-5} M), the differences in the haemolytic potency of K_{25}AOA1 at pH 5 and pH 7 were not measurably different. Given that the trend pointed to a diminishing of pH-dependent haemolytic potency at lower concentrations, it is reasonable to assume that, at peptide concentrations used in transfection experiments (4.65 x 10^{-7} M or 5.3 μg in 2 ml), the difference in measurable haemolytic potency will be negligible at pH 5 compared to pH 7. Therefore the observation that the presence of the vacuolar proton pump inhibitor bafilomycin A_1 caused only a marginal reduction (1.3-fold reduction) in transfection efficiency of K_{25}AOA1 is consistent with conclusions which can be drawn from erythrocyte lysis assay results. The slight reduction in transfection efficiency of K_{25}AOA1 in the presence bafilomycin A_1 (in DMSO) may be due to other effects exerted by DMSO or bafilomycin A_1, which were sufficient to disrupt the cellular functions but not enough to result in cell detachment or cell death. The difference may also be attributed to the possibility that, at pH 5, there was a subtle increased effect on the lytic potency or lytic rate of K_{25}AOA1 that could not be detected by erythrocyte lysis assay method.

Plank and colleagues had observed a 6.5-fold reduction in measured light units in the presence of bafilomycin A_1 for the dimeric peptide INF5 that had a low pH (pH 5) specific haemolytic potency but it appeared that this reported result did not take the toxicity of bafilomycin A_1 into account[167]. It is therefore reasonable to speculate that had the protein lysate measurements been taken into account, this fold difference (between the presence and absence of bafilomycin A_1) would have been even less. For a peptide that depends entirely on activation at the low pH within the endosome to enhance gene delivery, a less than 6.5-fold reduction in the presence of bafilomycin A_1 raises more questions about the proposed mechanism of action of pH-dependent fusogenic peptides in quaternary complexes, than the experiment was meant to answer. A possible partial explanation for the relatively low effect of bafilomycin A_1 on the transfection activity of quaternary complexes that included INF5 could be that, the bafilomycin A_1 concentration (200 nM) was not high enough to reduce the transfection activity of INF5, and thus prove beyond doubt the dependence of INF5 on acidic environment for activation. However, in this project, the presence of 200 nM

bafilomycin A_1 resulted in a 190-fold reduction in transfection efficiency of PEI. The explanation for this significant reduction in the transfection efficiency of PEI is that, PEI needed a low pH to be protonated. The "proton sponge" effect of PEI at low pH contributed largely to its ability to act as an endosomolytic agent. The observation that the transfection activity of PEI was not completely abrogated in the presence of bafilomycin A_1 can be explained by the fact that PEI had a sufficiently high residual buffering capacity at pH 7 (the buffering capacity of PEI at around pH 7 could be observed during the preparation of PEI stock solution for transfection, which involved neutralizing PEI with hydrochloric acid) to exert an endosomolytic effect through osmolytic pressure. This result confirmed that the concentration of bafilomycin A_1 (200 nM) used in this study and in the study by Plank *et al.* was sufficient to block endosomal proton pump and significantly affect the transfection efficiency of gene delivery agents that were dependent on acidification of the endosomal compartment for activation.

The erythrocyte lysis results in section 3.2.4.3 and the transfection experiment in the presence of endosomal proton pump inhibition reported in this section provide a clear and consistent experimental evidence for the mechanism of action of binary complexes composed of K_{25}AOA1 and DNA. The mechanism of action is as follows: the bifunctional peptide K_{25}AOA1 binds to DNA by ionic bond of the K_{25} moiety with DNA and forms particles that have DNA and K_{25} in the core of the particle and the fusogenic moiety on the surface of the particle. However because these complexes are formed at high positive charge ratios (+/-3.2), there are likely to be extra concentric layers of K_{25}AOA1 on the surface of core K_{25}AOA1/DNA particles[270], as well as excess K_{25}AOA1 present in solution. During *in vitro* transfection studies, K_{25}AOA1/DNA particles become concentrated on the surface of cells by gravitational precipitation and would be taken up by cation-mediated endocytosis into endosomes. Due to the fact that the bifunctional peptides do not need the low pH environment of the endosome to be membrane disruptive, the disruption of the cell surface prior to uptake through cation-mediated endocytosis is also possible. Within the endosome, the concentration of the peptide/DNA complex would be high enough to cause endosomal lysis, independent of the acidification process. Endosomal acidification can be significantly reduced by the presence of bafilomycin A_1 but because the fusogenic activity of K_{25}AOA1 does not depend on low pH, the presence of bafilomycin A_1 in the transfection medium did not

significantly reduce the transfection activity of K_{25}AOA1. In the erythrocyte lysis assay results in section 3.2.4.3, it was stated that lytic activity of AOA1, K_{10}AOA1 and K_{25}AOA1#3 were visibly faster at pH 5 compared to pH 7, but this could not be investigated due to the limitation of the equipment and the compounds used in this study. It is therefore possible that the acidification process within the endosome may speed up the endosomolytic activity mediated by the fusogenic moiety of the bifunctional peptide resulting in the faster release of K_{25}AOA1/DNA complexes into the cytoplasm. Regardless of the functioning of the proton pumps however, K_{25}AOA1 is able to mediate the escape of the peptide/DNA complex from the endosome and hence escape lysosomal degradation. The mechanism by which the bifunctional peptide/DNA complex is transported towards the nucleus is not know but it is not likely to be dissimilar to the mechanism by which most particles with excess positive charge are transported through the cell. As mentioned in section 3.3.13, the process of mitosis of the cells in culture is vital to the gene transfer activity of bifunctional peptides and other polyplexes, not least because the barrier of the nuclear membrane is considerably reduced during mitosis.

3.3.10 Effect of chloroquine on transfection efficiency and proportion of transfected cells mediated by binary and ternary complexes

The possible effect of chloroquine on the transfection efficiency and proportion of transfected cells was studied by assaying the quantity of expressed reporter protein or determining the percentage of positively expressing cells by means of florescence cytometry.

3.3.10.1 Effect of chloroquine on transfection efficiency

Addition of chloroquine at a concentration of 100 μM to the transfection medium resulted in a 3- to 20-fold increase in transfection efficiency for DK_{25}AOA1/DNA complexes in COS-7, CHO, A549 and B16 cells and 1.2- to 15-fold increase in transfection efficiency for LK_{25}AOA1/DNA complexes in COS-7, CHO and A549 cells (Figure 3.21). The increases in transfection efficiency were greater in CHO cells than in other cell lines. The increases in transfection efficiency of bifunctional peptides due to

chloroquine in A549 and CHO cells were 1.5- to 2-fold higher than with increases in percentage of cells positively expressing the reporter gene (Figure 3.21 and Figure 3.23). This infers that chloroquine increased not only the number of cells expressing the reporter gene but also the amount of gene expression per cell. Disappointingly, K8/DNA/JTS1 complexes showed very little transfection activity, even in the presence of chloroquine.

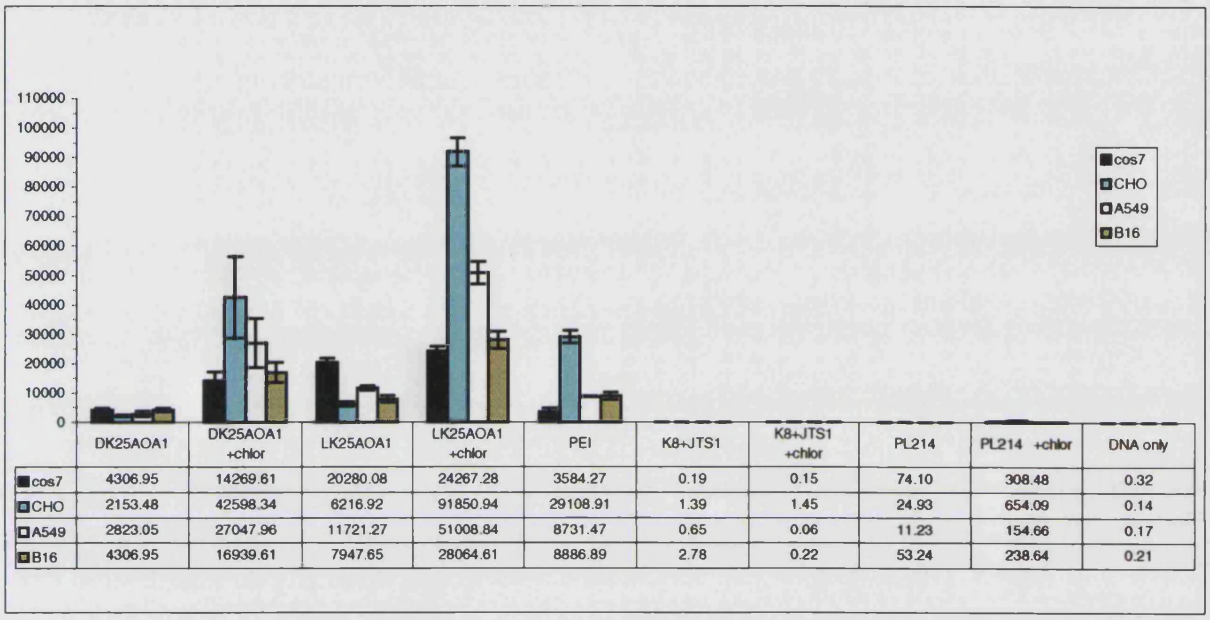

	DK25AOA1	DK25AOA1 +chlor	LK25AOA1	LK25AOA1 +chlor	PEI	K8+JTS1	K8+JTS1 +chlor	PL214	PL214 +chlor	DNA only
cos7	4306.95	14269.61	20280.08	24267.28	3584.27	0.19	0.15	74.10	308.48	0.32
CHO	2153.48	42598.34	6216.92	91850.94	29108.91	1.39	1.45	24.93	654.09	0.14
A549	2823.05	27047.96	11721.27	51008.84	8731.47	0.65	0.06	11.23	154.66	0.17
B16	4306.95	16939.61	7947.65	28064.61	8886.89	2.78	0.22	53.24	238.64	0.21

Figure 3.21 Effect of chloroquine on transfection efficiency of binary and ternary complexes in COS-7, CHO, B16 and A549 cells. For K8/DNA/JTS1 complexes, K8 (9 μg in 400 μl HBS) and pCMV luciferase (6.4 μg in 400 μl HBS) were mixed and incubated for 30 minutes followed by mixing with JTS1 at 38 nM (in 800 μl HBS) and a further incubation for 30 minutes before adding to cells. Complexes formed between pCMV luciferase (6.4 μg in 800 μl HBS) and previously optimised quantities of $LK_{25}AOA1$, $DK_{25}AOA1$, PLL219 and PEI (in 800 μl HBS) were incubated for 30 minutes before adding a 500 μl aliquot (containing 2 μg per 6-well plate) to cells in the presence or absence of 100 μM chloroquine. Cells were incubated with complexes at 37°C for 4 hours and harvested 24 hours post initiation of transfection for analysis. Data represent the mean of triplicate samples ± SEM, and is representative of two separate experiments.

3.3.10.2 Effect of chloroquine on proportion of transfected cells determined using Fluorescence Cytometry

Fluorescence cytometry is a process, which counts cells in accordance with their fluorescent properties. HeLa, HEK293, CHO and A549 cells were transfected with plasmid DNA encoding for the enhanced green fluorescent (EGFP) protein complexed with either D&LK_{25}AOA1, K8+JTS1, PEI, or PL219 in the presence or absence of chloroquine at a concentration of 100 μM at their respective optimum charge ratios for the respective cell lines. Transfected cells were harvested after 24 hours for analysis.

There was a wide variation in the percentage of cells expressing EGFP as determined by using fluorescence cytometry depending on the cell line and the results are shown in Figure 3.23. In all four cell lines used in this experiment, addition of chloroquine to the transfection media before adding LK_{25}AOA1/DNA complexes resulted in an increase in the percentage of cells expressing EGFP. The consistent trend that could be observed regarding the effect chloroquine on LK_{25}AOA1-mediated gene expression was that the higher the percentage of positive expressing cells, the lower the enhancement due to addition of chloroquine: for example in HeLa cells in which 28% of cells were counted positive for LK_{25}AOA1-mediated gene expression, the increase as a result of adding chloroquine to the media was marginal (1.1-fold), whereas in CHO cells there was nearly a 10-fold increase in the percentage of cells counted positive for gene expression. In A549 cells, addition of chloroquine resulted in a 2-fold increase in percentage of positively expressing cells from 5.5% to 11.3%. Using DK_{25}AOA1, chloroquine generally resulted in an increase in the percentage of positively expressing cells except in HeLa cells in which there was a decrease. Similar to LK_{25}AOA1-mediated transfection in CHO cells, the percentage of positively expressing CHO cells increase by 11-fold from approximately 2% to 25% following the addition of chloroquine.

11.4.3.3869596160167167

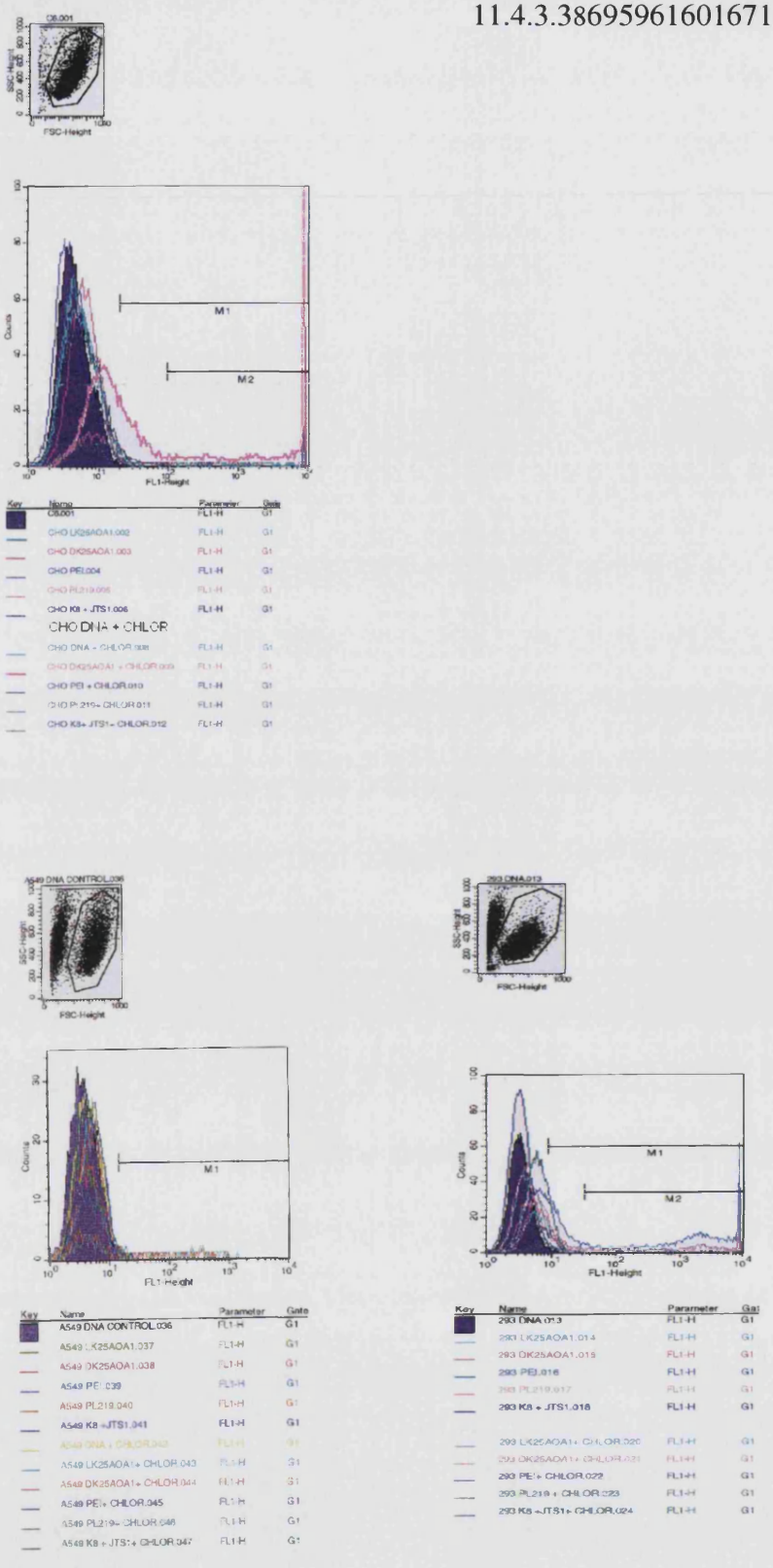

Figure 3.22 Florescence cytometry analysis of HeLa, A549, HEK293 and CHO after transfection with D- and LK_{25}AOA1, K8+JTS1, PEI, PL219 complexed with plasmid DNA encoding for EGFP protein, in the presence or absence of chloroquine at a concentration of 100 μM, as described in methods section 3.2.10.2.4. (FL1-Height on the x-axis represents the fluorescence intensity at 530 nm and Events on the y-axis represents the number of cells counted).

The effect of chloroquine in PEI-mediated transfection was mixed: addition of chloroquine to the media resulted in a decrease in the percentage of HeLa and HEK293 cells positively expressing EGFP but an increase in the percentage of CHO and A549 cells expressing EGFP. In HeLa cells for example, there was over 5-fold decrease in the percentage of positively expressing cells from 75.4% to 14.4% and approximately 10-fold decrease in HEK293 cells (from 34.7% to 3.6%) following the addition of chloroquine to the transfection medium.CHO cells were totally resistant to PEI-mediated transfection but addition of chloroquine to the media resulted in about 3.5% of cells positively expressing EGFP, in contrast to the trend observed in HeLa and HEK293 cells for the effect of chloroquine in PEI-mediated transfection. In A549 cells, there was a 1.4-fold increase in the percentage of PEI-mediated cells expressing EGFP as a result of adding chloroquine.

Polylysine (PL_{219})/DNA complexes mediated low gene expression in HeLa, HEK293 and A549 cells resulting in 3.6%, 0.6% and 0.9% of cells positively expressing EGFP respectively, but as with PEI, CHO cells were resistant to transfection. Addition of chloroquine resulted in a 2-fold increase in the percentage of HeLa cells but a 2-fold decrease in the percentage of HEK293 and A549 cells expressing EGFP mediated by PL_{219}. Almost consistently, K8/DNA/JTS1 complexes failed to promote the expression of EGFP, in some cases making it inferior to just $polylysine_{214}$ as a gene delivery vehicle.

Two consistent trends can be observed from these results: (i) single-step complexes with bifunctional peptides were more effective than the two-step K8/JTS1 system, (ii) the presence of chloroquine increased the proportion of cells positively expressing the reporter protein transfected with $DK_{25}AOA1$, $LK_{25}AOA1$ and polylysine but the effect on PEI-mediated transfection was mixed. As it was observed earlier, these modest increases in the percentage of expressing cells due to the presence of chloroquine did not always correspond with the larger increases in transfection efficiency as determined by measuring the quantity of reporter protein produced (section 3.3.10.1).

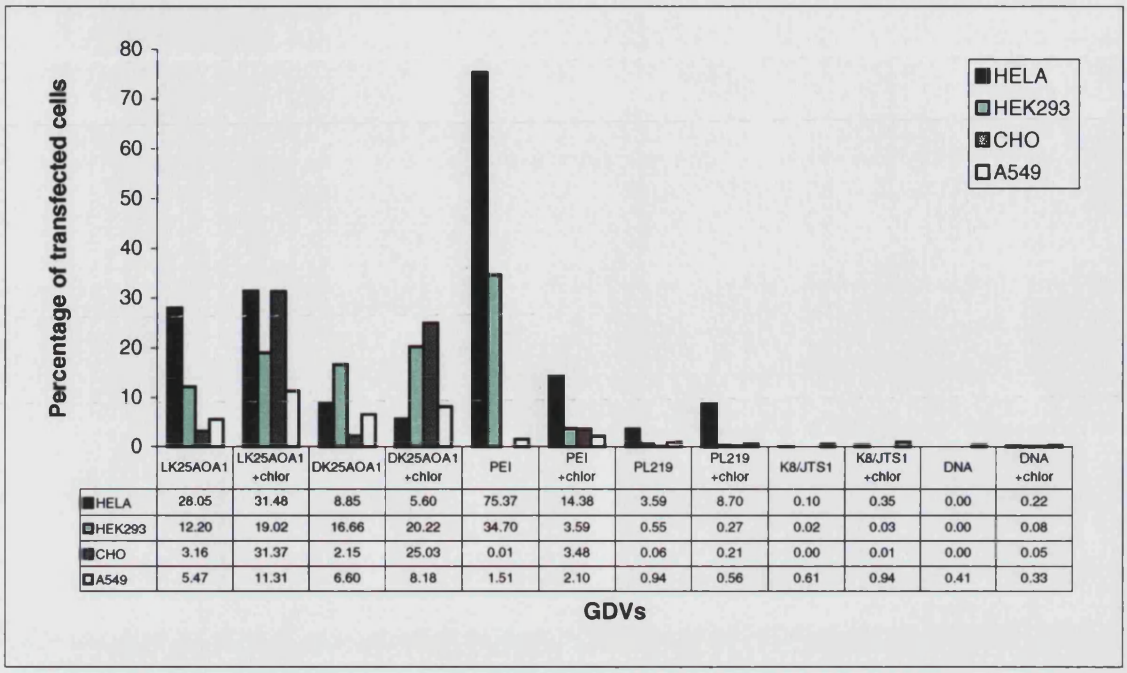

	LK25AOA1	LK25AOA1 +chlor	DK25AOA1	DK25AOA1 +chlor	PEI	PEI +chlor	PL219	PL219 +chlor	K8/JTS1	K8/JTS1 +chlor	DNA	DNA +chlor
HELA	28.05	31.48	8.85	5.60	75.37	14.38	3.59	8.70	0.10	0.35	0.00	0.22
HEK293	12.20	19.02	16.66	20.22	34.70	3.59	0.55	0.27	0.02	0.03	0.00	0.08
CHO	3.16	31.37	2.15	25.03	0.01	3.48	0.06	0.21	0.00	0.01	0.00	0.05
A549	5.47	11.31	6.60	8.18	1.51	2.10	0.94	0.56	0.61	0.94	0.41	0.33

Figure 3.23 Percentage of various cells (HeLa, A549, HEK293 and CHO) expressing enhanced green fluorescent protein (EGFP) as determined by fluorescence cytometry after transfection with D- and LK_{25}AOA1, K8+JTS1, PEI, PL219 complexed with plasmid DNA encoding for EGFP protein, in the presence or absence of chloroquine at a concentration of 100 μM, as described in methods section 3.2.10.2.4

3.3.11 Discussion: Effect of chloroquine on transfecfection efficiency of binary and ternary complexes

The effect of chloroquine on the transfection efficiency of D&LK_{25}AOA1 varied according to cell line, but generally, in the presence of chloroquine, there was an increase in transfection efficiency of between 3- and 20-fold. For endosomolytic effects, the lysomotropic agent chloroquine was used at a concentration of 100 μM. The mechanism of action of chloroquine is not well defined although it is generally assumed that its accumulation within acidic compartments of the cell, notably the endosome and lysosome prevents acidification and hence activation of hydrolase enzymes contained therein[271]. However, a simple buffering effect, resulting in the inhibition of transfer to the lysosomes cannot provide a complete explanation since there is no innate mechanism for transfer to the cytoplasm[236]. Hence endosomal bursting (a consequence of raised endosomal osmotic pressure) is an alternative mechanism that has been

postulated[226]. Wolfert and Seymour reported synergistic transfection activity between INF7-SGSC (INF7-serine-glycine-serine-cysteine) and chloroquine and postulated that a post-endosomal disruption of polylysine/DNA complex by INF7-SCSC could account for the observed synergy[226]. Under this hypothesis, it is suggested that INF7-SGSC may facilitate transcription by negative charge-mediated destabilisation of the pLL/DNA complexes. Despite similar synergism being observed between chloroquine and bifunctional peptide, the hypothesized mechanism of destabilisation for a ternary complex, post endosomal release, can not be possible with a binary complex of DNA/bifunctional peptide where the oligolysine moiety is covalently attached to the fusogenic moiety. The more plausible explanation is that the two agents (K_{25}AOA1 and chloroquine) mediate lytic activities on different subpopulations of intracellular vesicles or both agents have an additive lytic activity within the same endosome.

Wagner and colleagues also observed the synergistic effect of chloroquine on HA-2 sequences during transfection and suggested three mechanisms by which this effect may have occurred, namely: protection of conjugates from lysosomal degradation, osmotic destabilization of endocytic vesicles by internal accumulation of chloroquine, and/or by the observation that the influenza peptide conjugates display some residual leakage activity at neutral pH[179]. In this project, it was observed that the membrane disruptive activity of the bifunctional peptide K_{25}AOA1 occurred at neutral pH (see section 3.3.1.2), therefore the action of chloroquine to raise the pH of endosomes would not interfere with the fusogenic effect of K_{25}AOA1. The synergism between chloroquine and K_{25}AOA1 can thus be explained by a combination of all three mechanisms postulated by Wagner *et al.* [179].

In the presence of chloroquine, gene expression mediated by bifunctional peptide per cell was increased. The increase in the proportion of cells expressing the enhanced green fluorescence protein, as determined by fluorescence cytometry, is possibly due increased expression within a subpopulation of cells that hitherto had too low an expression to be sorted as positively expressing cells that now had high enough expression in the presence of chloroquine.

In terms of harnessing the effects of chloroquine in a putative gene delivery vector *in vivo*, it will be worth studying the effect of including an amino acid derivative of chloroquine into a multifunctional GDV although the resulting molecule will not be freely diffusible. An amino acid derivative with side chain containing nitrogen atoms of pKa values (10.2 and 8.1) [272] similar to that of chloroquine could confer acid buffering capabilities to the multifunctional molecule. PEI is an example of a reagent whose endosomolytic properties depend on osmolytic lytic effect due to acid buffering of the endosomal vesicle (see section 3.3.7). However, PEI is quiet toxic to cells at concentrations used to promote gene transfer (see section 3.3.7). The main advantage of synthesizing relatively smaller peptidic molecules for use as adjuncts for gene delivery is that of reduced toxicity. Gottschalk *et al.*[76] showed that K8 was at least 10^4 times less toxic than polylysine in HepG2 cells. Although polymers are inexpensive and some degree of control can be achieved in the attachment of ligands to polymers, it is still a relatively rudimentary process in terms of understanding the structural features of the end product[34]. The difficulty with modulating a polymeric reagent such as PEI with ligands to improve gene delivery (for example inclusion of targeting capability or nuclear localisation signal) is that efforts are hampered by the lack of control in the positioning of functional moieties due to the presence of multiple reactive sites on PEI. PEI was found to be 1.5 to 4-fold better than K_{25}AOA1 in B16 and CHO cells but K_{25}AOA1 was about 1.3-fold better than PEI in A549 cells and over 5-fold better than PEI in COS-7 cells. These results demonstrate that there is a high degree of cell-specific variations in transfection experiments *in vitro* and it is important for a putative gene delivery agent to be more amenable to specific and subtle changes for the purpose of improving them as gene transfer agents *in vivo*.

3.3.12 Determination of proportion of transfected cells using cytochemical staining for β-galactosidase activity

In order to visualize the proportion of cells expressing the reporter protein after transfection with the bifunctional peptide LK_{25}AOA1 or lipid DOTAP, the method of cytochemical staining for β-galactosidase activity was used. Cytochemical staining of cells with the substrate 5-bromo-4-chloro-3-indoly-β-D-galactoside (X-gal) is one of two methods available for evaluating β-galactosidase expression in single cells. Cells

expressing β-galactosidase hydrolyse this substrate to galactose and soluble indolyl compounds, which in turn are oxidised (by ferricyanide and ferrocyanide ions) to insoluble indigo coloured species[273]. Hence, the development of a deep blue colour following incubation with X-gal enables identification of β-galactosidase expressing cells. When cells were stained with X-gal, it was noted that there were more *lacZ*$^{+ve}$ cells on transfection with K_{25}AOA1 compared with DOTAP i.e. the number of and the intensity of blue staining in cells transfected with K_{25}AOA1 was higher than observed with DOTAP (Figure 3.24). Estimation of the proportion of cells stained blue is very subjective, but it is safe to conclude that more than 50% *lacZ*$^{+ve}$ cells were present after transfection with K_{25}AOA1, whereas the figure for DOTAP is less than 40%. The use of rapidly dividing cells for many gene delivery studies has been met with criticism since the many target organs for *in vivo* gene therapy comprise non-dividing/terminally differentiated cells. The lack of suitable *in vitro* cell culture models is now well recognised and requires the rapid development of intermediate *in vitro* systems with functional and morphological characteristics similar to the *in vivo* targets. Although it is impossible to emulate identically the conditions *in vivo*, studies with differentiated cell cultures should serve as a short-term compromise, making it possible for better correlation's to be made between *in vitro* and *in vivo* transfection data.

When cultured on membranes (PTFE or nitrocellulose), Caco-2 grow to confluence and undergo differentiation, ultimately exhibiting morphological characteristics (tight junctions, microvilli), brush border enzymes (various glycosidases, alkaline phosphatase, aminopeptidase N) and drug metabolising enzymes found in gastric enterocytes[274, 275, 276, 277, 278]. Differentiated Caco-2 cells thus represent a good *in vitro* model of the small intestinal mucosa and has been used extensively for elucidating the mechanism of drug transport and predicting the intestinal absorption of drugs[279, 280, 281]. As a result of these properties, differentiated Caco-2 cells were used as a model for evaluating LK_{25}AOA1 plasmid DNA delivery to the gut epithelium and to other epithelial monolayers. The human origin of this cell line makes it ideal for evaluating the feasibility of gene therapy to the colon for conditions such as cancer and irritable bowel disease. Cytochemical staining of 14- day old differentiated Caco-2 cells (cultured on semi-permeable membranes with a mean pore size of 0.4 μm on filter, see section 3.2.2.1) X-gal staining results showed that less than 0.5% of cells were

transfected using a $LK_{25}AOA1$/DNA complex at a charge ratio of 3.2 (data not shown).

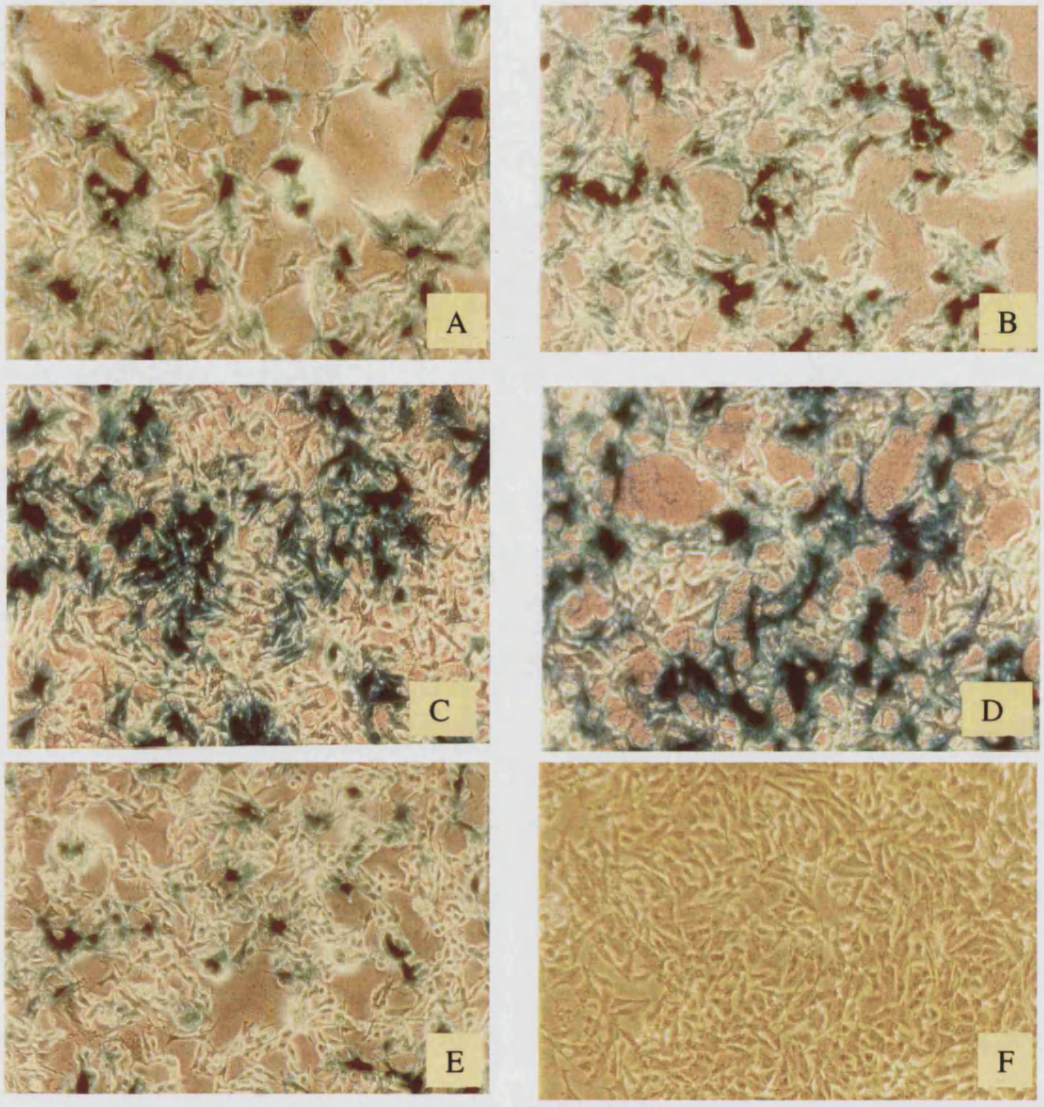

Figure 3.24 Cytochemical staining of B16 cells with X-gal. Cells transfected with complexes formed between pRSV*lac*Z (2 μg in 800 μl HBS) and various quantities of $LK_{25}AOA1$ at a charge ratio of 2.6 (A), 3.2 (B) and (C) same as (B) except the wells were overlayed with 3 ml of culture medium instead of the normal 2 ml, post transfection for 44 hours) or 4.8 (D) DOTAP (E) (in 800 μl HBS) or naked DNA (F) were incubated for 30 minutes before adding to cells. Cells were incubated with GDVs for 4 hours at 37°C. Cells were then washed and stained 48 hours post transfection as described in section 3.2.10.2.3. Cells positive for β-galactosidase activity stain blue with X-gal treatment. Cells were photographed at magnification x300. The fields shown are representative of the expression levels detected over the plates, with three wells transfected per formulation.

3.3.13 INVESTIGATION OF TOXICITY USING MTT ASSAY

The comparative toxicities of the uncomplexed peptides (D- & $LK_{25}AOA1$), polylysine, PEI (in the presence or absence of chloroquine) and DOTAP were determined using the MTT assay over concentration ranges relative amounts required for optimum transfection *in vitro* (Table 3.5).

Gene delivery agent	Concentration range
D&$LK_{25}AOA1$	1.3 - 334 μg/ml
PL_{214}	1.2 - 149.2 μg/ml
PEI	1.05 - 230.4 μg/ml
DOTAP	1.56 – 400 μg/ml

Table 3.5 Concentration range for GDVs used in MTT assay in toxicity studies.

There were wide variations in absorbance readings (10-30%) making interpretation of toxicity results less certain at GDV concentrations below 10 μg/ml, however it clear that DOTAP was the least toxic of the five GDVs tested (Figure 3.25). Between GDV concentrations of 10 and 100 μg/ml, the order of toxicity from the most to the least toxic was Pl_{214}, PEI, $DK_{25}AOA1$, $LK_{25}AOA1$ and DOTAP. The presence of chloroquine at a concentration of 100 mM with pLL_{214} was highly toxic to the cells. The significance of these results relate to complexes between DNA and GDVs formed at positive charge ratios. All the GDVs tested for toxicity have positive charge ratio for optimum transfection activity *in vitro*. At positive charge ratios, it is inevitable there will be free GDV present in the formulation and these toxicity results reflect the effect of free GDV on cell survival during transfection.

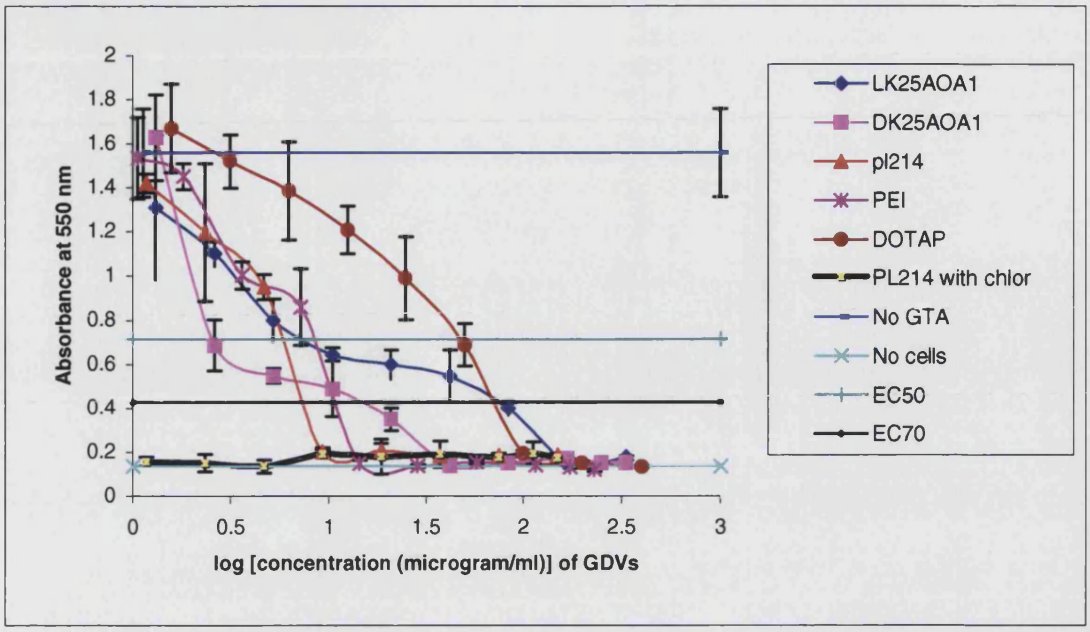

Figure 3.25 Comparison of toxicity of free $LK_{25}AOA1$, $DK_{25}AOA1$, PEI, polylysine $_{214}$, and DOTAP on B16 melanoma cells was determined by MTT assay as described in section 3.2.4 B16 cells were plated in a 96-well plate at a density of approximately 4000 cells per well in 100 µl media. Peptides to be tested were made up at twice the required concentration in 100µl of PBS and added to the wells. Ten serial dilutions were prepared such that expected 50% cell kill was straddled evenly by maximum and minimum concentrations. The cells and agents were incubated at 37°C for 3 days. The media was then removed and washed twice with 200 µl PBS. The cells were then incubated with 200 µl of 1 mg/ml MTT in serum free media for 3 hours at 37°C. The media was then removed and 200 µl DMSO added to each well to dissolve the formazan. Absorbance was read at 540 nm (background readings at 690 nm). A graph of absorbance versus log concentration of cytotoxic agent was plotted. The extracellular concentration of cytotoxic agent which, kills 50% of cells compared to control (EC_{50}) was determined. Data represent the mean of four samples ± SEM, and is representative of two separate experiments.

3.3.14 Discussion: Investigation of proportion of transfected cells

The cytochemical staining of B16 cells suggested that over 80% of cells were transfected by $K_{25}AOA1$ at a charge ratio of 4.2. However the cytochemical staining of cells also revealed that there was a high degree of toxicity resulting in cells being detached from the plates (compared to transfection with DNA only). The total proportion of blue cells is not known because the proportion of blue cells that detached could not be estimated and this situation probably resulted in misleadingly high percentage transfected cells. Data from studies performed to investigate the toxicity of

the various GDV using the MTT assay (section 3.3.13) confirmed that the formulations were toxic to cells. The aim had been to corroborate the cytochemical staining method of determining the proportion of transfected B16 cells with the use of fluorescence cytometry method, but this was not possible within the time available on the cytometer. However data from both cytometry and cytochemical staining methods independently confirm the ability of the novel bifunctional peptide K_{25}AOA1 to augment gene delivery in dividing cells *in vitro*.

Differentiated and non-dividing Caco-2 cells were very resistant to transfection with less than 1% of cells staining blue as *lacZ*$^{+ve}$ because of the lack of mitotic and perhaps endocytotic activity (data not shown). The requirement for mitotic activity for transfection has been reported by Wilke *et al.*[173]. During cell division, the nuclear membrane becomes discontinuous allowing entry of plasmid DNA into the nucleus. The lack of mitotic activity in differentiated Caco-2 cells and the consequent resistance to transfection led Uduehi and colleagues to conclude, rightly, that differentiated Caco-2 are a better *in vitro* model for *in vivo* transfection than dividing cells[95]. Therefore a greater use of differentiated Caco-2 should be made in future work to optimise these new bifunctional peptides as a more economical but realistic model for *in vivo* activity. The ability of bifunctional peptides to lyse cells suggest that they may have the ability to disrupt cell membranes and this ability may be exploited to enhance its entry into non-dividing cells by formulating complexes at sub-toxic charge ratios.

In conclusion, K_{25}AOA1 readily transfected dividing cells but not non-dividing cells, therefore the use of non-dividing cells will be a better *in vitro* transfection model for *in vivo* activity when testing novel multifunctional peptides.

3.3.15 Effect of foetal calf serum or serum albumin on transfection

Addition of 10% (v/v) foetal calf serum to the transfection medium resulted almost total loss of transfection using LK_{25}AOA1 or DK_{25}AOA1 complexes (Figure 3.26) but did not abrogate the activity of DOTAP (data not shown). The presence of 10% (w/v) bovine serum albumin (BSA) resulted in a 3-4-fold decrease in transfection efficiency (Figure 3.26).

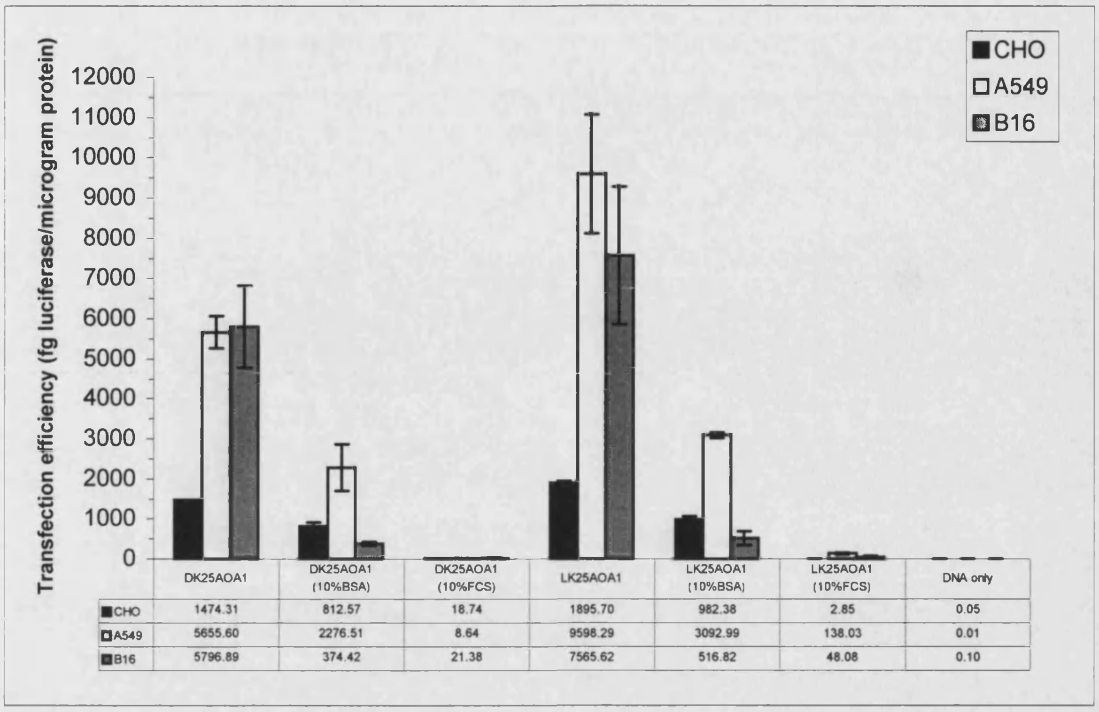

	DK25AOA1	DK25AOA1 (10%BSA)	DK25AOA1 (10%FCS)	LK25AOA1	LK25AOA1 (10%BSA)	LK25AOA1 (10%FCS)	DNA only
CHO	1474.31	812.57	18.74	1895.70	982.38	2.85	0.05
A549	5655.60	2276.51	8.64	9598.29	3092.99	138.03	0.01
B16	5796.89	374.42	21.38	7565.62	516.82	48.08	0.10

Figure 3.26 Investigating the effect of FCS or BSA on transfection efficiency *in vitro*. Complexes formed between pCMV luciferase (6.4 μg in 800 μl HBS) and previously optimised quantities of $^{L}K_{25}$AOA1#2 and $^{D}K_{25}$AOA1 (in 800 μl HBS) were incubated for 30 minutes before adding a 500 μl aliquot (containing 2 μg per 6-well plate) to cells in the presence or absence of 10% (v/v) foetal calf serum (FCS) or 10% (v/v) bovine serum albumin (BSA). Cells were incubated with complexes at 37°C for 4 hours and harvested 24 hours post initiation of transfection for analysis. Data represent the mean of triplicate samples ± SEM, and is representative of two separate experiments.

To investigate the reason for the loss of transfection activity in the presence of serum, K_{25}AOA1/DNA complexes were incubated in Opti-MEM supplemented with 10% (v/v) FCS at 37°C for 4 hours and then run on a horizontal electrophoresis gel. K_{25}AOA1/DNA complexes were formed at charge ratios below neutrality (+/- 0.5), at neutrality (+/- 1.0) and at the optimum charge ratio for usual *in vitro* transfection experiments (+/- 3.2). This was compared to K_{25}/DNA complexes at the same charge ratios because both K_{25}AOA1 and K_{25} had previously been shown to condense DNA in ethidium bromide exclusion assay (section 3.2.4.2) and retard electrophoretic migration of DNA (section 3.2.4.1). The various negative controls for this experiment were: absence of FCS, or absence of DNA or absence of peptide and are detailed in the table in Figure 3.27 below. The first of two general observations from the results of this experiment is that the presence of FCS resulted in the disappearance of the supercoiled

DNA band and the appearance of the nick-circular DNA band. Secondly, smearing of DNA bands occurred mainly when DNA was complexed with K_{25} or K_{25}AOA1 at a charge ratio below neutrality (+/- 0.5) (lanes 1 and 4, when no FCS was present, and lanes 9 and 10, when FCS was present). The result showed that for both K_{25}AOA1 and K_{25}, at a charge ratio below neutral (+/- 0.5), in the presence of FCS, lanes 9 and 12 respectively, there was some smearing of DNA bands, the disappearance of the supercoiled band and the appearance of the nick-circular band. At neutral charge ratio, there was complete retardation of DNA and no smearing for K_{25}/DNA (lane10) but some smearing and migration of DNA for K_{25}AOA1/DNA complexes (lane 12). At the charge ratio of +/- 3.2 (the optimum *in vitro* transfection for K_{25}AOA1/DNA complexes), for both K_{25} and K_{25}AOA1 complexes with DNA, there was complete retardation (lanes 3 and 6 for K_{25}AOA1 and K_{25}, respectively, when no FCS was present; and lanes 11 and 14, for K_{25}AOA1 and K_{25} respectively, when FCS was present). Comparison between naked DNA in the presence and absence of 10% (v/v) FCS (lanes 7 and 15 respectively) showed that the presence of FCS with DNA results in the disappearance of the band corresponding to supercoiled DNA and the appearance of the linear/nick-circular DNA band, however, there was not significant smearing. Thus, smearing of bands observed in this experiment was not due to fragmentation of DNA but rather due to partially complexed DNA moving at different speeds through the gel.

The lack of evidence of DNA degradation in the presence of FCS when K_{25}AOA1/DNA complexes were formed at a charge ratio of +/- 3.2, combined with the observation that the presence of BSA reduced transfection efficiency *in vitro*, suggests that binding of serum protein to complexes, and not enzymatic degradation, is responsible for the loss of transfection ability of K_{25}AOA1/DNA complexes in the presence of FCS.

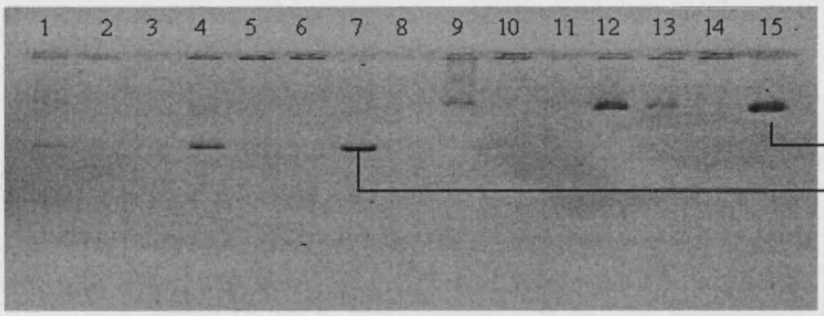

Lanes	1	2	3	4	5	6	7	8	9	10	11	12	13	14	15
K_{25}AOA1	0.5	1.0	3.2	-	-	-	-	-	0.5	1.0	3.2	-	-	-	-
K_{25}	-	-	-	0.5	1.0	3.2	-	-	-	-	-	0.5	1.0	3.2	-
DNA	+	+	+	+	+	+	+	-	+	+	+	+	+	+	+
FCS	-	-	-	-	-	-	-	+	+	+	+	+	+	+	+

Figure 3.27 Investigation of the effect of serum on peptide/DNA complexes. Agarose gel displaying the retardation of DNA/peptide complexes with increasing amounts of either LK_{25}AOA1 or K_{25}. LK_{25}AOA1/DNA and LK_{25}/DNA complexes were formed at charge ratios of 0.5, 1.0 and 3.2 as indicated in the table above, by adding increasing amounts of LK_{25}AOA1 in 125 µl HBS to 3 µg DNA in 125 µl HBS. The complexes were incubated for 30 minutes as detailed in section 3.2.8, and incubated in 1.0 ml Opti-MEM in the presence (+) or absence (-) of 10% (v/v) serum (FCS) for 4 hours at 37°C before loading onto a 1% (w/v) agarose gel and running at 80 Volts for one hour and prepared for viewing and photographing as detailed in 3.2.4.1.

3.3.16 Discussion: Effect of foetal calf serum or serum albumin on transfection efficiency of binary complexes

The presence of 10% (v/v) heat-inactivated foetal calf serum (Gibco Inc., UK) in MEM medium (see Table 3.1) during the 4-hour incubation period of K_{25}AOA1/DNA complex with *in vitro* cells was found to virtually abrogate transfection activity of bifunctional peptides *in vitro*. The process of heat-inactivation involves heating the serum at 56°C for 30 minutes and this process only destroys heat sensitive complements proteins C1q, C1r, C2, C8, C9, as well as factors B and H (Gibco Inc., UK), which can kill foreign cells by binding to and lysing their cell membranes[282]. This process of heat-inactivation still leaves enzymes such as proteases, nucleases and growth factors, present in serum largely unaffected. Therefore if GDVs were unable to protect DNA from degradation from serum nucleases, then that would partly explain the lack of transfection activity mediated by bifunctional peptides in the presence of serum. The use of the transfection medium Opti-MEM™ from Gibco Inc., UK, on the other hand, was able to support transfection activity mediated by bifunctional peptide/DNA complexes. Opti-MEM™ is a serum-free medium specifically designed for the *in vitro*

transfection of mammalian cells; it is an enriched medium lacking in serum proteins like serum albumin, globulin and fibrinogen, which can interact with DNA/GDV complexes but contains the essential growth factors necessary to maintain cell viability (telephone communication with technical support, Gibco Inc., UK).

In order to investigate whether enzymatic degradation of the DNA condensed by the bifunctional peptide was responsible for the loss of the ability of K_{25}AOA1 to mediate transfection *in vitro*, a gel mobility assay was performed in the presence or absence of FCS. The enzymatic degradation of K_{25}AOA1 (by serum proteases) would result in its loss of ability to protect DNA from degradation (by serum nucleases). At a charge ratio of 0.5, smearing of K_{25}/DNA or K_{25}AOA1/DNA complexes was seen to occur, as partially neutralised DNA, with a mixture of various net charges, travelled at varying speeds through the agarose gel under constant voltage (Figure 3.27). The results showed that when DNA was complexed with K_{25} or K_{25}AOA1 at a charge ratio of neutrality (1.0) and above, smearing did not occur, thus confirming that the DNA was fully complexed. At a charge ratio of +/-3.2 (optimum charge ratio for transfection experiments *in vitro*), K_{25}AOA1/DNA or K_{25}/DNA complexes remained in the well during electrophoresis and there was an absence of a nick-circular DNA band, providing evidence that the DNA in the peptide/DNA complex had been fully complexed and protected from the degradative nature of serum nucleases. Therefore degradation was not the course of loss of activity during transfection. Transfection with K_{25}AOA1/DNA complexes in the presence of 10% (w/v) BSA, which does not possess enzymatic activity, resulted in 3-4-fold decrease in transfection activity. This observation goes some way into supporting the view that binding of negatively charged serum macromolecules and not enzymatic degradation, was responsible for the loss of activity in the presence of serum. The use of enzyme degradation-resistant DK_{25}AOA1 did not prevent the loss of transfection activity in the presence of serum, again confirming that enzyme degradation of the bifunctional peptide and subsequently DNA was not the cause of loss of transfection activity.

The barrier of binding anionic macromolecules must be overcome if GDVs based on K_{25}AOA1 bifunctional peptide structure is to be active *in vivo*, particularly following systemic administration. Serum has been reported to have effects on the transfection

efficiency of many gene delivery vectors. Serum proteins readily adsorb onto positively charged particles, initiating rapid blood clearance by macrophage uptake (a first step in the removal of polyplexes by the innate immune system). PLL-based polyplexes are eliminated quickly with a half-life less than 5 minutes. Clearance from blood has been shown to correlate with the amount of plasma associated with the particles[139]. The effects of serum appear to be dependent on the cell type as well as the GDV under study. Felgner *et al.* observed that the transfection of mouse cells with lipofectin was reduced by 95% in the presence of 10% (v/v) serum whilst in COS-7 cells transfection was unchanged[55]. Legendre and Szoka reported an 80% reduction in transfection efficiency in CV-1 cells in the presence of 10% (v/v) serum with Lipofectin but in HepG2 cells, serum had no effect[283]. The transfection efficiency of DOTAP in B16 cells was unaffected by the presence of serum (data not shown); this is because the external surface of a DOTAP/DNA complex is likely to be uncharged lipid tails (in a micellar structure) and thus will not bind to negatively charged proteins present in serum.

In order to decrease the effect of serum macromolecules on oligolysine/DNA GDVs, one approach would be to create particles with overall near neutral charge capable of condensing DNA but which do not coagulate. However, formulation of polyplexes at near neutral zeta potential results in rapid aggregation of particles due to van der Waals interactions, therefore polyplexes are formulated at high positive charge ratios (zeta potential) for charge-mediated uptake to overcome the problem of coagulation. Another approach investigated by researchers is to graft uncharged hydrophilic polymers like PEG or HPMA to cationic polymers prior to complexing with DNA (see section 1.4). This approach, whilst successful in reducing protein adsorption to complexes, has been met with the problem of reduced DNA-binding affinity of the cationic polymer and reduced transfection efficiency[141]. To overcome the problem of reduced affinity and transfection efficiency resulting from modification of cationic polymers with hydrophilic polymers (pre-polyplex modification), some researchers have demonstrated improved salt and serum stabilization by modifying pre-formed polyplexes with hydrophilic polymers like PEG or HPMA[144,145] (post-polyplex modification). PEGlylation of preformed DNA/Tf-PEI complexes resulted in significantly increased blood circulation time and tumour-site gene expression after systemic injection in mice[86].

Unfortunately, the success of post-polyplex modification in decreasing protein adsorption cannot be adopted in a bifunctional peptide/DNA complex system to achieve a similar beneficial effect. In theory, post-complex modification of K_{25}AOA1/DNA complexes with hydrophilic polymers would have the advantage of increasing solubility of complexes and reduce adsorption of serum proteins to complexes. The disadvantage with such a modification, however, is that the fusogenic moiety of the bifunctional peptide will not be able to interact with membrane surfaces and the endosomal escape property of the bifunctional peptide will be lost. However, these approaches of using hydrophilic polymers to decrease protein adsorption of polyplexes stem from the fact that the cationic polymers used in these polyplexes were not custom-made for gene delivery. Work in this project has shown that K_{25}AOA1/DNA complexes have a higher solubility in the presence of salts than K_{25}/DNA (section 3.3.2.4), possibly due to the limited degree of steric stabilisation provided by the fusogenic moiety of the bifunctional peptide. It may thus be possible to design and construct a single molecule with a dimeric fusogenic component or another peptide sequence with mainly negatively charged amino acid residues, which would have the advantage of decreasing serum protein adsorption. The fact that DOTAP/DNA complexes could transfect cells *in vitro* in the presence of serum, suggests that modifying the structure of a multifunctional peptide with a relatively short hydrocarbon chain (compared to PEG with molecular weight >1 kDa) could reduce protein binding, albeit with the associated risk of reduced solubility in aqueous solutions. To improve salt and serum stability, a second bifunctional peptide consisting of oligolysine (DNA-binding moiety) and a combination of serine and aspartic/glutamic acid residues (hydrophilic moiety) could be synthesized and mixed with K_{25}AOA1 before mixing with DNA. This approach, although simple to formulate, is a retrograde step in design of formulations for gene delivery vehicles, as it will result in complexes of less defined structure, similar to ternary and quaternary complexes involving polylysine/polylysine-transferrin/DNA/fusogenic peptide. A preferred approach to increasing the salt stability and decreasing the surface positive charge of a peptide/DNA particle (and hence decrease serum protein adsorption) will be to include a number of serine and aspartic or glutamic acid residues as an extension to the fusogenic moiety of K_{25}AOA1, or attach it to the ε-amino of the lysine residue next to the fusogenic moiety.

3.3.17 Result and discussion: Effect of omission of asparagine in fusogenic sequence of in bifunctional peptide

Omission of a single amino acid (asparagine, Asn) to form $DK_{25}AOA1(N)$ resulted in substantial decrease in transfection activity. $DK_{25}AOA1(N)$ was over 100-fold less active than corresponding peptide ($DK_{25}AOA1$) without the asparagine omission (Figure 3.16 and Figure 3.17).

The omission of one amino acid within the fusogenic sequence of the bifunctional peptide caused a disruption in the pH mediated alpha helical structure resulting in diminution of disruptive membrane activity and corresponding decrease in transfection activity[188,189]. In agreement with observations by Gottschalk and colleagues[76] and Plank and colleagues[167], these results show that whilst individual residues to the original HA-2 sequence may be replaced to produce enhancement of transfection activity, complete omission of an amino acid residue was counter productive.

3.3.18 Influence of oleoyl-fusogenic peptide on DOTAP transfection activity

The inclusion of oleoyl-AOA1 peptide to DOTAP/DNA complex at a DOTAP to peptide molar ratio of 34:1 resulted in a modest increase (2-fold) in the transfection activity of DOTAP in B16 cells. Further increases in the proportion of peptide resulted in a decrease in activity (Figure 3.28). See section 3.3.19 for further discussion.

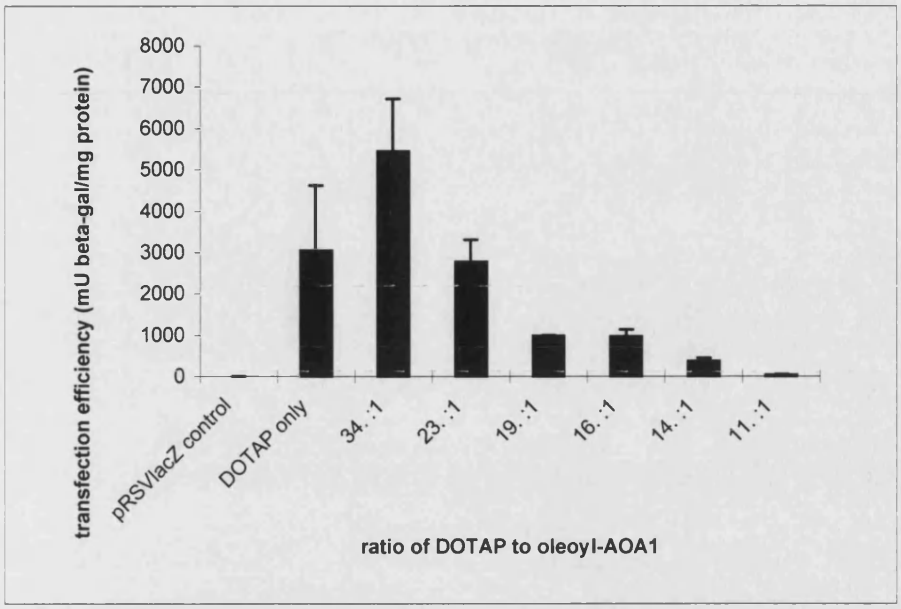

Figure 3.28 Investigating the effect of inclusion of oleoyl-fusogenic peptide on the transfection efficiency of DOTAP in B16 cells. Molar ratios of DOTAP:oleoyl-AOA1 of 34, 23, 19, 16, 14 and 11:1 were preformed by a modified reverse phase method by adding various quantities of oleoyl-AOA1 to a fixed quantity of DOTAP (11.52 μg). The DOTAP/oleoyl-AOA1 mixtures were then resuspended in 800 μl HBS. Complexes formed between pRSV*lacZ* (6.4 μg in 800 μl) and DOTAP/oleoyl-AOA1 (in 800 μl HBS) were incubated for 30 minutes before adding a 500 μl aliquot (containing 2 μg per 6-well plate) to cells. Cells were incubated with complexes for 4 hours at 37°C and harvested 48 hours post initiation of transfection for analysis. Data represent the mean of triplicate samples ± SEM.

3.3.19 The influence of an oleoyl-fusogenic peptide on DOTAP transfection activity

The rational behind this part of the project was to investigate if providing the cationic lipid DOTAP with an extra endosomal escape capability by adding a fusogenic peptide to the complex. In an attempt to facilitate the inclusion of the fusogenic peptide in the DOTAP/DNA complex through hydrophobic interaction, an oleoyl chain was attached to the fusogenic peptide via the side chain ε amino of a lysine residue through an amide bond. A schematic view of the aimed structure of the DOTAP/Oleoyl-AOA1/DNA complexed structure is shown in Figure 3.29. The achievement of this structure depended on the order in which the three components were mixed. However, difficulties in getting the oleoyl-AOA1 component, to mix with DOTAP, coupled with an attempt not to expose plasmid DNA to potentially damaging conditions, meant that the DOTAP

and oleoyl-AOA1 had to be assembled first and then DNA added. Under these conditions, ionic interactions would ensure that the charge head group of DOTAP would be associated with the negatively charged residues of the fusogenic component of the peptide. The introduction of negatively charged DNA in solution would cause a dynamic restructuring by attracting the positive head groups of DOTAP and repelling the negatively charged fusogenic peptides towards the surface of the complex.

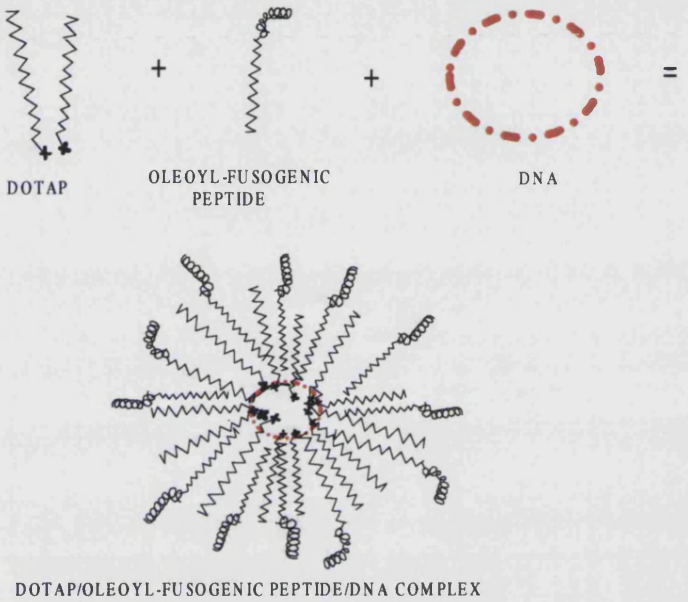

Figure 3.29 Schematic representation of structure of DOTAP/OLEOYL-PEPTIDE/DNA complex

Preliminary transfection results of the effect oleoyl-AOA1 on the transfection activity of DOTAP suggested that an inclusion of a fusogenic element to a DOTAP/DNA complex, could improve the transfection efficiency of DOTAP. The formulation of this three-component complex has yet to be optimised. Studies on the mechanism by which cationic liposomes deliver DNA have shown that endocytosis was the main process of internalisation for lipid/DNA complexes[107]. Therefore, the inclusion of an endosomal membrane destabilization component to a lipidic gene delivery vector must be beneficial as it has the potential to increase the release of complexes or free DNA release into the cytoplasm. The inclusion of fusogenic peptides in lipid/DNA complexes have been reported by Simões *et al.* who demonstrated a modest enhancement in the transfection activity of DOTAP/DOPE complexes by GALA or an HA-2 derived peptide in HeLa cells[210]. The formation of ternary complexes involving Lipofectin and a bifunctional integrin-targeting peptide with an oligolysine tail has been shown by

Jenkins *et al.* to be better than Lipofectin/DNA and comparable to adenovirus-mediated gene transfer in pulmonary gene transfer in mice[172]. These reports demonstrate that the gene transfer activity of cationic lipids can be improved by the inclusion of peptide sequences that target different aspects (e.g. integrin-targeting or endosomal escape) of the gene transfer process. The pursuance of this approach of using a lipidic fusogenic peptide in combination with a cationic lipid could be rewarding if the compound can be successfully synthesized and purified.

3.3.20 Effect of attempted inclusion of oligohistidyl residues in a bifunctional peptide sequence

Attempts were made to synthesize two oligohistidyl analogues of K_{25}AOA1, $K_{25}H_{10}$AOA1 and $K_{25}H_{20}$AOA1. The idea behind these constructs was to incorporate a "proton sponge" element to the construct. The histidyl molecules, which are partially protonated at physiological pH would become protonated at the lower pH environment of the endosome triggering osmotic swelling and destabilisation of the endosomal/lysosomal vesicle. However the target compounds $K_{25}H_{10}$AOA1 and $K_{25}H_{20}$AOA1, showed no *in vitro* transfection ability (data not shown). MALDI-TOF mass spectrometry of target compounds $K_{25}H_{10}$AOA1 and $K_{25}H_{20}$AOA1 (Chapter 2) indicated that the fractions of peptide collected during purification did not have the target peptide. Attempts at using electrospray mass spectrometry (at the University of Bath) to confirm the mass of collected purified fractions containing oligolysine was unsuccessful due to multiple protonation of the species, which made interpretation of the mass spectra impossible. The lack of access to a MALDI-TOF mass spectrometer at the time of the peptides was being synthesized and purified meant that as with all the other peptides synthesized, *in vitro* experiments had to proceed on the assumption that the sharpest and largest peak was that of the target peptide. MALDI-TOF mass spectrometer analysis on $K_{25}H_{20}$AOA1 revealed that the peak collected during purification by HPLC had a mass of 6443 whereas the calculated mass was 8477. The lack of transfection activity of the target compound is likely to be due to the unsuccessful synthesis of $K_{25}H_{20}$AOA1. It seems that in this case the largest peak did not correspond to the target peptide, the strongest evidence being its lack of haemolytic activity.

3.3.21 Discussion: Effect of attempted inclusion of oligohistidyl residues in a bifunctional peptide sequence

Histidine has a protonable nitrogen with a pKa of 6.0. At a physiological pH of 7.4, it is predominantly unionised but at an endosomal pH of 5, it will be predominantly ionised (about 86%) and should provide some buffering capacity to protect DNA from lysosomal degradation and trigger an osmotic swelling effect. Partial histidylation (38 ± 5%) of the ε-amino groups of polylysine has been recently shown to mediate the transfection of various mammalian cell lines *in vitro* without the aid of endosmolytic agents such as chloroquine or fusogenic peptides[284]. Even more significantly, the transfection activity of the histidylated polylysine was shown to be unaffected by the presence of up to 20% (v/v) serum. Although researchers found that histidylated polylysine was up to 20-fold less active than PEI, this finding is encouraging and provides support for the idea of including oligohistidine in the structure of a synthetic multifunctional peptide.

As mentioned in Chapter 2, all the compounds synthesized in this project were tested for their ability to mediate transfection before a MALDI-TOF mass spectrometer became available to identify compounds being used. The complete abolition of transfection activity of K_{25}AOA1 after the inclusion of 10 and 20 histidine residues in the sequence, to produce what was thought to be $K_{25}H_{10}$AOA1 and $K_{25}H_{20}$AOA1 respectively, was therefore initially postulated to be due to the histidyl component interfering with the either the DNA binding function of K_{25} or the membrane disruptive activity of the fusogenic moiety. Retrospective analysis of $K_{25}H_{10}$AOA1 and $K_{25}H_{20}$AOA1 by MALDI-TOF mass spectrometery revealed that either the synthesis had been unsuccessful or the fractions collected during purification did not contain the target peptides (Figure 2.30). As it was shown in section 3.3.2 the resulting compound could bind to DNA and exclude ethidium bromide, but lacked fusogenic activity, which indicated that the target compound was not isolated.

3.4 *IN VIVO* TESTING OF BIFUNCTIONAL PEPTIDE

3.4.1 INTRODUCTION

The *in vivo* models used to test the transfection activity of the bifunctional peptide K_{25}AOA1 were murine intramuscular and intratumour injection. The easy accessibility of the muscle was one reason for the choice of this model, but there are practical reasons why muscle expression is of interest. Firstly there are several publications in the literature on gene expression following injection of naked DNA into muscle, which could be used as a control. In addition the muscle is a site for expression of antigens for vaccine applications, or for correction of the single gene defects Duchenne muscular dystrophy. The latter clinical indication will require a huge improvement in efficiency, but remains a possibility. Given that reporter genes are expressed with sufficient sensitivity in muscle to allow easy detection, even after injection of DNA in solution, the muscle represented the most obvious test bed to compare condensed DNA with naked DNA. Injection into tumour was carried out because the group at Bath were interested in the concept of expressing immune-stimulatory genes in tumours. Naked DNA gives rise to low gene expression in tumours, so an improvement against naked DNA would be encouraging.

3.4.2 RESULTS OF *IN VIVO* TESTING OF BIFUNCTIONAL PEPTIDE

Attempts to formulate K_{25}AOA1/DNA complexes containing greater than 0.5 μg/μl DNA at a charge ratio of 3.2 resulted in a thick white gelatinous precipitate. A formulation containing approximately 0.3 μg/μl DNA complexed with K_{25}AOA1 at a charge ratio of 3.2 (6.25 μg pCMV luc DNA plus 16.7 μg K_{25}AOA1 in a total volume of 20 μl 0f 5% (w/v) glucose) resulted in a white suspension (with fine white precipitate) which could be drawn through a 30 gauge syringe needle. Figure 3.30 shows the results of expression of luciferase following injection of the above formulation 7 days before harvesting into the right hind leg muscle tissues, and a second dosing into the left hind leg muscle 5 days before harvesting.

The tumours growing on the back of the mice were injected with the same dose of complexes 2 days before excising the tissues. Clearly, the DNA complexes with either D or $LK_{25}AOA1$ did not result in luciferase expression in either muscle or tumours, whereas naked DNA resulted in expression (Figure 3.30) both in muscle and tumour. Also, it appeared that expression in the leg hind leg muscle, dosed 5 days before harvesting was greater than the right hind leg muscle dosed 7 days before harvesting.

The lack of *in vivo* transfection activity in the previous experiment using $K_{25}AOA1$/DNA complexes at a DNA concentration of 6.25 μg/ 20 μl of 5% (w/v) glucose solution (charge ratio of 3.2) was thought to be due to fact that the particles of the complex were
too large thereby prohibiting internalisation via the endocytotic pathway. Formulation of condensed DNA is a challenging problem, which at this stage was not resolved satisfactorily. Published literature indicated that the dose of DNA should be in excess of 10 μg. Typically 50-100 μg DNA is injected to allow detection of gene expression. Given that the volume of solution that can be injected into mice thigh in practice should be kept to a reasonable volume, which we considered to be less than 20 μl, a serious formulation problem is evident. Due to the cost and availability of materials it was not possible to study in detail the size of complexes versus concentration of DNA in the mixture. From earlier work it was known that DNA could be used at 50-100 μg/ml, but ideally the concentration required for *in vivo* work was ten times as high. It was necessary to strike a balance between the need for a high dose and the threat that the DNA may not be available from aggregated complexes.

In later experiments complexes were formed using 6.25 μg DNA (in 20 μl 5% (w/v) glucose solution) at lower charge ratios of 1.6 and 0.8 and also at a lower quantity of 3.125 μg DNA (in 20 μl of 5% (w/v) glucose solution) at charge ratios of 3.2, 1.6 and 0.8. The muscle injections were performed only in the right hind leg muscle at 7 days prior to harvesting and the tumour injections at 2 days prior to harvesting. The results of gene expression following muscle and tumour injections are shown in Figure 3.31 and Figure 3.32. Injection of 3.125 μg DNA produced no significant gene expression with the exception of one unrepresentatively high expression from one muscle tissue injected with naked DNA (Figure 3.31). Injection of 6.25 μg of DNA produced expression in

both tumour and muscle (Figure 3.31). Gene expression mediated by K_{25}AOA1/DNA (in 20 μl, 5% w/v glucose) at charge ratio of 0.8 was about 2-fold and 3-fold greater that expression mediated by naked DNA muscle in tumour and muscle respectively (Figure 3.32), but these increases were not statistically significant. A two-sample Student t-test (performed at a confidence interval of 95% using Minitab™ statistic program) between "DNA only" and K_{25}AOA1/DNA complex at a charge ratio of 0.8 in muscle and tumour returned p-values of 0.21 and 0.37 respectively. There was near total loss of transfection activity at a charge ratio of 1.6 in both tumour and muscle tissues. The formulation of K_{25}AOA1/DNA complex containing 6.25 μg DNA at a charge ratio of 1.6 was a hazy suspension (not a clear solution) unlike the other formulation at a charge ratio of 0.8, suggesting that the particles that had been formed were not in the colloidal size range.

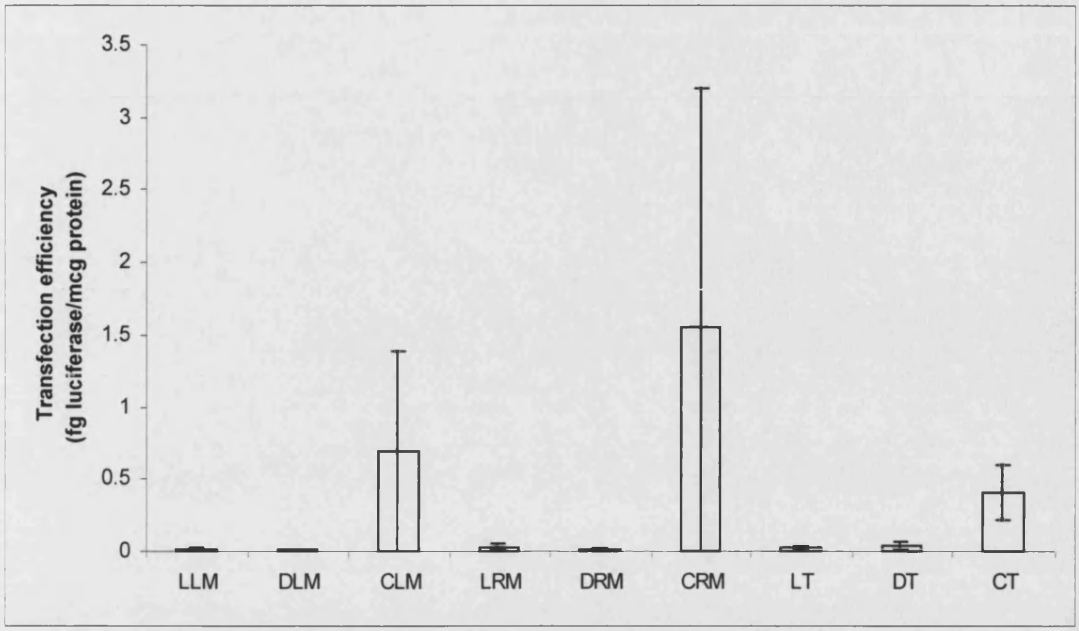

Legend:

LLM	**L**K_{25}AOA1/DNA complex injected in **L**eft hind leg **M**uscle
DLM	**D**K_{25}AOA1/DNA complex in **L**eft hind leg **M**uscle
CLM	**C**ontrol DNA only injected in **L**eft hind leg **M**uscle
LRM	**L**K_{25}AOA1/DNA complex injected in **R**ight hind leg **M**uscle
DRM	**D**K_{25}AOA1/DNA complex injected in **R**ight hind leg **M**uscle
CRM	**C**ontrol DNA only injected in **R**ight hind leg **M**uscle
LT	**L**K_{25}AOA1/DNA complex injected in **T**umour
DT	**D**K_{25}AOA1/DNA complex injected in **T**umour
CT	**C**ontrol DNA only injected in **T**umour

Figure 3.30 Effect of LK_{25}AOA1/DNA complex mediated transfection on luciferase expression in mice muscle and tumour compared to naked DNA (Control). 6.25 μg pCMVluc complexed with 16.7 μg LK_{25}AOA1 or DK_{25}AOA1 (+/- charge ratio of 3.2) in a total volume of 20 μl of 5% (w/v) glucose was injected directly into muscle or tumour tissue. Control: 6.25 μg DNA in 20 μl of 5% (w/v) glucose solution. The left and right hind leg muscle of each mouse was injected with the preparations 5 and 7 days respectively, before sacrificing the mice (and excising the tissues) whilst the tumours were injected 2 days before. n=5

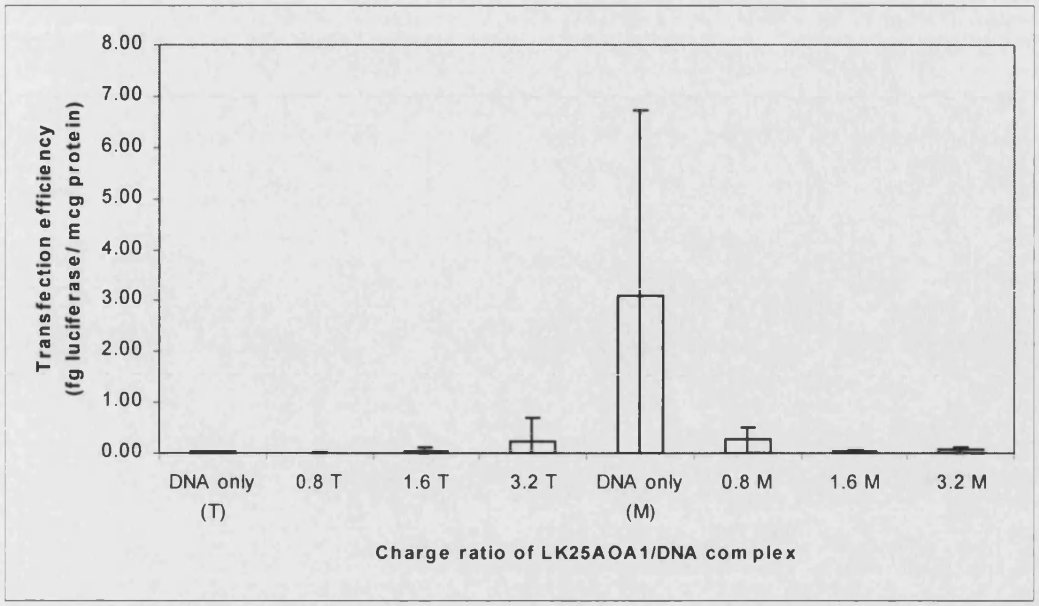

Figure 3.31 Effect of LK_{25}AOA1/DNA complex mediated transfection on luciferase expression in mice muscle (M) and tumour (T) compared to naked DNA (Control). 3.13 μg pCMVluc complexed with 8.35, 4.18 or 2.09 μg of LK_{25}AOA1 (corresponding to +/- charge ratio of 3.2, 1.6 or 0.8 respectively) in a total volume of 20 μl (5% (w/v) glucose) was injected directly into muscle or tumour tissue. Control: 3.13 μg DNA in 20 μl of 5% (w/v) glucose solution. The tumour and right hind leg muscle tissue of each mouse was injected 2 and 7 days respectively, before sacrificing the mice (and excising the tissues). n=4

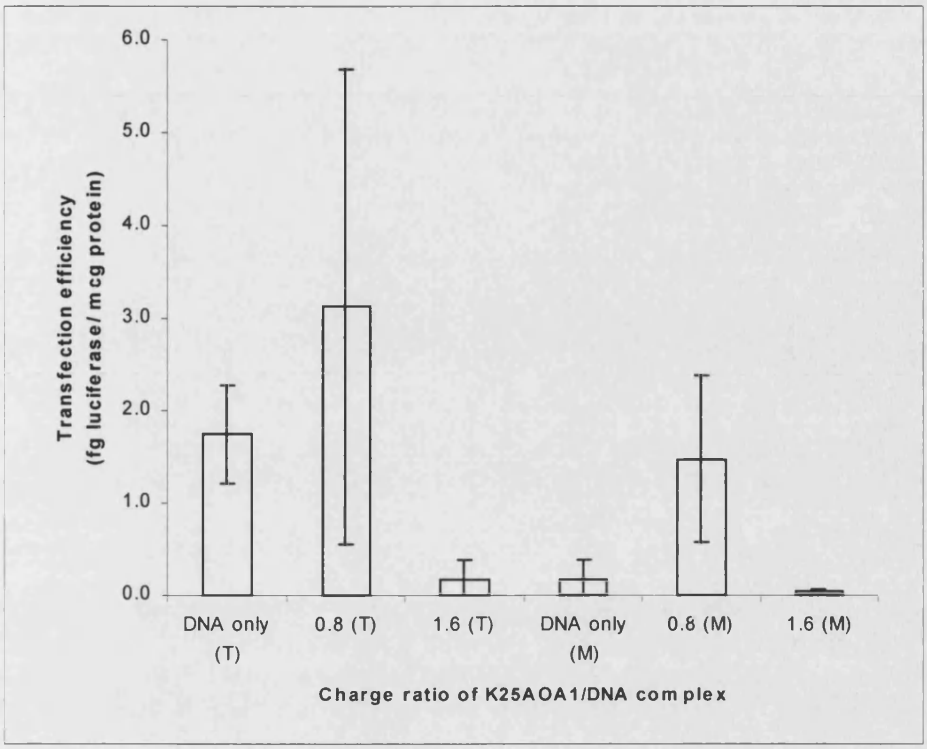

Figure 3.32 Effect of $LK_{25}AOA1$/DNA complex mediated transfection on luciferase expression in mice muscle (M) and tumour (T) compared to naked DNA (Control). 6.25 μg pCMVluc complexed with 8.35 μg or 4.18 μg $LK_{25}AOA1$ (corresponding to +/- charge ratio of 1.6 or 0.8 respectively) in a total volume of 20 μl (5% (w/v) glucose) was injected directly into muscle or tumour tissue. Control: 6.25 μg DNA in 20 μl of 5% (w/v) glucose solution. The tumour and right hind leg muscle tissue of each mouse was injected 2 and 7 days respectively, before sacrificing the mice (and excising the tissues). n=4

3.4.3 Discussion

The lack of transfection activity of $K_{25}AOA1$/DNA complexes at a charge ratio of 3.2 at a DNA concentration of 6.25 μg/ 20 μl was probably the result of aggregation of the complex resulting in large particles, which could not be taken up by cells by through the process of endocytosis. $K_{25}AOA1$/DNA formulation at a charge ratio of 1.6 was less turbid (as visualised by the naked eye). Though a charge ratio of 1.6 is sub-optimal for *in vitro* transfection, this resulted in greater gene expression compared to naked DNA. At this stage it is not clear whether this is explained by the ability of these complexes better to diffuse within the tissue, or whether the intrinsic activity of these complexes is higher *in vivo*. It is also possible that the activity of complexes formed at low charge

ratio could have been explained by some naked DNA in the formulation. Naked DNA was certainly active following injection into muscle *in vivo*. This is in agreement with observations by other workers[47,285,286], but the mechanism by which myocytes take up plasmids *in vivo,* or how the DNA escapes lysosomal degradation is not yet known[94]. Even though there appeared to be an increase in transfection efficiency in muscle and tumour as a result of formulation with K_{25}AOA1, this improvement was not statistically significant. This was because of one exceptionally large luciferase expression in the sample group transfected with K_{25}AOA1/DNA complex, both in muscle and tumour. A larger sample size (n=8) would have been preferable during *in vivo* experiments which are prone to wider variations in transfection efficiency. However, an improvement of 2 or 3-fold in transfection efficiency is too modest given the cost of producing K_{25}AOA1. The inability to formulate K_{25}AOA1/DNA complexes at higher concentration in small volumes (20 µl), means that these modest improvements would be offset by injecting larger quantities of naked DNA. The poor activity of condensed DNA *in vivo* has also been reported after intratumour or intramuscular injection of lipoplexes. Quite why condensed DNA has low activity is not clear. Uptake into cells could be limited by movement of the particles through the interstitial fluids, and aggregation would have added to the problem of mobility. Thus in the future it will be important to use methods which prevent aggregation of primary particles. One method by which the concentration of bifunctional peptide/DNA formulation could be increased and reduce the risk of precipitation is to formulate the complex in a large volume and concentrate it to a smaller volume by ultrafiltration[138]. Some researchers have got around the volume constraints imposed by injection into solid tissue, by using a micropump delivering 20 µl/min which permitted injection of a volume of 100 µl into solid tumour[43]. Lack of time and resources did not permit this method to be tried. In the medium term, solubility of complexes could be increase by inclusion of hydrophilic groups (-OH) e.g. the amino acid serine, into the structure of a multifunctional peptide.

Other future work *in vivo* should include testing of K_{25}AOA1/DNA complexes in the lungs by bronchial instillation as much higher volumes can be instilled, thereby avoiding the volume constraints encountered in this study.

4 CONCLUDING REMARKS

The main objective of this project was to develop a single multifunctional peptide, which would complex plasmid DNA in order to mimic the attributes of capsid viruses such as adenoviruses. The viral genome is condensed and packaged by capsid proteins to facilitate entry into target cells through receptor-mediated endocytosis. After internalisation of the virus, the acidic pH of the endosome triggers activation of viral proteins that disrupt the endosome and release the viral capsid into the cytosol before there is fusion of endosome with primary lysosomes. Plank *et al.* formed virus-free, synthetic systems by ionically binding fusogenic peptides (analogues of the 23 N-terminal amino acids of HA-2 protein) unto the surface of DNA/polylysine complex to create a self-assembled ternary complex and these authors demonstrated that transfection was improved several fold by the presence of the fusogenic peptides[167]. The addition of fusogenic peptides to DNA-polylysine complexes provided endosome escape activity in the absence of a viral capsid, but was not able to fully reproduce the efficiency of the whole viral particle[1].

Such 'three-component' self-assembly systems rely on ionic interactions between positively charged polylysines and phosphate groups in DNA as well as negatively charged residues on fusogenic peptides. Although the formation of complexes of some description is not in doubt, a question remains whether the whole (three-dimensional structure) of the fusogenic sequence is available for interaction with membranes after complexation within the self-assembled system. We aimed to stabilise the localisation of the fusogenic peptide at the surface of the particle and allow the full sequence to be available for interaction with the target lipid bilayers. The working hypothesis was that a fusogenic peptide which is not partially engaged in binding to polylysine should be better at transfection in cells.

One reported method of binding fusogenic peptides to polylysine involves the use of a streptavidin-biotin bridge [167]. Plank *et al.* reported that monomeric influenza peptide INF3 sequence did not significantly enhance gene transfer through self-assembly by ionic interactions, whereas a 100-fold increase in gene expression was observed when INF3-biotin was incorporated into a transfection complex using a complex with

streptavidin-polylysine and transferrin polylysine. It is very likely that transferrin-mediated uptake was the main contributory factor to this improvement in transfection efficiency but as there was no control group without transferrin, it is not possible to determine the effect of the streptavidin-biotin bridge in their report. Streptavidin is a large polypeptide (127 residues). When used in conjunction with long polylysine chains e.g. polylysine$_{290}$, the large size of streptavidin is not inhibitory[167]. But with short chain oligolysine, it was thought that the size of streptavidin would sterically inhibit the binding of the lysine chain to plasmid DNA and interfere with the interaction between the fusogenic peptide and cell/endosomal membrane. The reliance on ionic interaction and/or a streptavidin-biotin bridge in self-assembled systems by previous workers has been explored because commercially available polylysine is cheap, but this approach has the drawback of heterogeneity and inability subsequently to covalently link active peptides in a controlled manner due to unprotected amino groups present.

An alternative method of coupling fusogenic peptides to polylysine was the hitherto unreported method of synthesizing a single linear peptide with DNA-binding oligolysine chain covalently linked to a fusogenic peptide by means of solid-phase synthesis. It was suspected that the presence of a 23-residue fusogenic moiety covalently linked to the oligolysine would interfere with the ability of the oligolysine to bind to DNA. The initial aim of this project was to determine the optimum length of lysine residues required for effective binding to DNA whilst retaining the functionality of the fusogenic moiety. It was planned to synthesis K_5, K_{10}, K_{15}, K_{20}, K_{25} analogues of the fusogenic peptide INF7 and a single amino acid mutant of INF7 called AOA1. Due to the difficulties encountered during the peptide synthesis and purification, and the lack of resources to contract outside help with synthesis, only K_{10} and K_{25} analogues of INF7 and the K_{25} analogue of AOA1 were synthesized. This at least allowed the project to establish that K_{10} was too short, but it is possible that it is not necessary to use a chain as long as K_{25}. The future determination of the minimum number of lysine residues required in this construct would be beneficial in terms of reducing the cost and also reduce the degree of heterogeneity of the construct due to unnecessary lengthening of the oligolysyl chain.

The project was able to establish that a single bifunctional peptide K_{25}AOA1 was a much superior GDV to the ternary self-assembly complex of K_{25}/AOA1 or K8/JTS1 in transfection *in vitro*. This work provided proof in principle that a single linear peptide consisting of DNA-binding K_{25} and an endosomal escape mediating fusogenic peptide is able to retain the functions of its constituent parts.

Only a limited amount of physical characterisation work could be carried out in this project due to the limited amount of peptide available. Particle sizing and zeta potential measurements showed that K_{25}AOA1/DNA complexes were more stable than K_{25}/DNA complexes. This finding is important because it signals that the close proximity of non-charged peptide sequences has a stabilizing effect on the resulting peptide/DNA complex. If $K_{25}H_{10}$AOA1 and/or $K_{25}H_{20}$AOA1 had been successfully synthesized and isolated by HPLC it would have been interesting to see the effect these compounds would have on particle stability of the DNA/peptide complex.

FUTURE WORK

The attributes that a virus-like particle must possess to be an efficient GDV in non-dividing cells *in vitro* can be speculated to include DNA-condensing, receptor mediated-uptake, endosomal escape, movement along microtubules to the nucleus and uptake into the nucleus. In addition to these attributes, the *in vivo* environment provides an extra set of challenges that required the GDV to possess tissue targeting and ionic solution stability and serum stability. The ability for gene delivery researchers to include many of these attributes in a single gene delivery particle requires an accurate knowledge and control over where ligands are positioned on a gene delivery particle and the effect of altering these positions. One of the advantages of a relatively successful non-viral gene delivery reagent, PEI, is that it is inexpensive. However, the presence of multiple reactive sites on PEI means that researchers have, to date, been unable to incorporate more than one potentially beneficial attribute to a PEI/DNA particle in addition to PEI's inherent DNA condensing and endosomal escape properties. The post-polyplex formation PEGylated Tf-PEI/DNA complex is probably the most advanced polymer-based particle that has been designed[86,145]. These particles were shown to be more stable in serum and ionic solutions and able to increase tumour-site gene expression, but the

scope for improving on the gene delivery attributes of such a particle is limited because of the lack of further reactive sites to attach ligands post PEGylation.
In order to be able to create gene delivery particles with a predetermined molecular structure, there may need to be a departure from the use of polymers with multiple reactive sites to designing proteins with the aid of solid phase peptide synthesis. The advantage of using solid phase synthesis to produce proteins is that by using a combination of different permanent protecting groups and synthetic conditions, different ligands can be attached to a synthetic protein in a specific position and the effect of that modulation can be determined with a greater certainty.

In this project, HPLC and mass spectra analysis showed that peptides with the size of 48 amino acid residues had a low yield of the target peptide in the crude product. The transfection experimental data suggest that the difference between a whole peak and the corresponding peak splicing batch is a 20% decrease in transfection activity. In addition to the fact that the estimated percentage of the target compound was probably less than 10% in the peak splicing batch of K_{25}AOA1 (#2) according to HPLC, an important inference from this project is that the use of HPLC purification method and analysis of peptides of this size and composition by HPLC and mass spectra was perhaps more stringent than was required for gene therapy purposes. In other words, crude products of solid phase peptide synthesis are much less heterogeneous than products that could be generated by for instance reacting polymers; for example, three molar equivalents of PEI with one molar equivalent of activated MeOPEG2000 (PEG2000 monomethyl ether).

The advantages of using solid-phase synthesis method to create bifunctional peptides capable of promoting the transfection of dividing mammalian cells have been demonstrated in this project. Bifunctional peptides with two fusogenic sequences per molecule could increase the fusogenic property and further improve the ionic salt stability of the construct by reducing the zeta potential on the surface of the DNA/bifunctional peptide particle. A successful synthesis and purification of a peptide containing oligolysine, oligohistidine and a fusogenic component, perhaps with the oligohistidyl sequence furthest from the fusogenic sequence, could potentially have two advantages: firstly the ability of the imidazole side chain to be ionised at lower pH

within the endosome could produce a proton sponge effect similar to that attributed to the activity of PEI and increase the endosomolytic potency of such a compound; secondly the bulkier imidazole ring which will be only partially ionised at a pH of 7 could increase the ionic solution and serum stability of the DNA/peptide formulation against precipitation. Ligands could also be attached to K_{25}AOA1 to improve uptake in non-dividing cells.

This project shows that the ability to design and create a single more defined multifunctional gene delivery vehicle using solid-phase peptide synthesis method will be advantageous but will come at a considerable financial cost.

REFERENCES

1 **Wagner, E., Zatloukal, K, Cotten, M., Kirlappos, H., Mechtler, K, Curiel, D.T. and Birnstiel, M.L** (1992) Coupling of adenovirus to transferrin-polylysine/DNA complexes greatly enhances receptor-mediated gene delivery and expression of transfected genes. *Proceedings of the National Academy of Sciences of the United States of America,* **89**, 6099-6103.

2 **Ledley, F.D.** (1995) Non-viral gene therapy: The promise of genes as pharmaceutical products. *Human Gene Therapy*, **6**, 1129-1144.

3 **Behr, J-P.** (1994) Gene transfer with synthetic cationic amphiphiles: prospects for gene therapy. *Bioconjugate Chemistry,* **5**, 382-389.

4 **Felgner, J.H., Kumar, R., Sridhar, C.N., Wheeler, C.J., Tsai, Y.J., Border, R., Ramsey, P., Martin, M. and Felgner, P.L.** (1994) Enhanced gene delivery and mechanism studies with a novel series of cationic lipid formulations. *Journal of Biological Chemistry,* **269**, 2550-2561.

5 **Boussif, O., Lezoualc'h, F., Zanta, M. A., Mergny, M., Scherman, D., Demeneix, B. and Behr, J. P.** (1995) A versatile vector for gene and oligonucleotide transfer into cells in culture and *in vivo*: polyethyleneimine. *Proceedings of the National Academy of Sciences of the United States of America*, **92**, 7297-7301.

6 **Tang, M.X, Redemann, C.T. and Szoka, F.C.** (1996) *In vitro* gene delivery by degraded polyamidoamine dendrimers. *Bioconjugate Chemistry,* **7**, 703-714.

7 **Alton, E. W. F. W. and Geddes, D. M.** Gene therapy for cystic fibrosis: a clinical perspective (1995) *Gene Therapy,* **2**, 88-95.

8 **Berkner, K. L.** (1988). Development of adenovirus vectors for the expression of heterologous genes *BioTechniques* **6**, 616-629.

9 **Zsengeller, Z. K.,Wert, S. E., Hull, W. M., Hu, X., Yei, S., Trapnell, B. C. and Whitsett, J. A.** (1995) Persistence of replication deficient adenovirus-mediated gene transfer in lungs of immune-deficient (nu/nu) mice. *Human Gene Therapy,* **6**, 457-467.

10 **Miller, A. D.** (1990) Retrovirus packaging cells. *Human Gene Therapy,* **1**, 5-14.

11 **Temin, H.M.** (1990) Safety considerations in somatic gene therapy of human disease with retrovirus vectors. *Human Gene Therapy* **1**, 111-123.

12 **Miller, A.D., Miller, D.G., Garcia, J.V. and Lynch, C.M.** (1993) The use of retroviral vectors for gene-transfer and expression. *Methods in Enzymology*, **217**, 581-599.

13 **Culver, K.W., Ram, Z., Wallbridge, S., Ishii, H., Oldfield, E.H. and Blaese, R.M.** (1992) *In vivo* gene-transfer with retroviral vector producer cells for treatment of experimental brain-tumours. *Science*, **256**, 1550-1552.

14 **Sajjadi, N., Kamantingue, E., Edwards, W., Howard, T., Jolly, D. Mento, S. and Chada, S.** (1994) Recombinant retroviral vectors delivered intramuscularly localise to the site of injection in mice. *Human Gene Therapy*, **5**, 693-699.

15 **Cornetta, K., Morgan, R., A., Gillio, A., Sturm, S., Baltrucki, L., O'Reilly, R. and Anderson, W.F.** (1990) No retroviraemia or pathology in long-term follow-up of monkeys exposed to a murine amphotropic retrovirus. *Human Gene Therapy*, **2**, 215-219.

16 **Rigg, R.J., Chen, J.Y., Dando, J.S., Forestell, S.P., Plavec, I. and Bohnlein, E.** (1996) A novel human amphotropic packaging cell line, high-titre, complement resistant and improved safety. *Virology*, **218**, 290-295.

17 **Donahue, R.E., Kessler, S.W., Bodine, D., McDonagh, K., Dunbar, C., Goodman, S., Agricola, B., Byrne, E., Raffeld, M., Moen, R., Bacher, J., Zsebo, K.M. and Nienhuis, A.W.** (1992) Helper virus induced T-cell lymphoma in non-human primates after retroviral mediated gene transfer. *Journal of Experimental Medicine*, **176**, 1125-1135.

18 **Trapnell, B.C.** (1993) Adenoviral vectors for gene transfer. *Advanced Drug Delivery Reviews*, **12**, 185-199.

19 **Wivel, N.A., Gao, G.-P. and Wilson, J.M.** (1999) Adenovirus vectors. In: *The Development of Human Gene Therapy.* Cold Spring Harbor Laboratory Press. Edited by Friedmann, T. Chapter 5 (87-110)

20 **Dai, Y., Schwartz, E.M., Gu, D., Zhang, W.-W., Sarvetnick, N. and Verma, I.M.** (1995) Cellular and humoral immune responses to adenoviral vectors containing factor IX gene:tolerization of factor IX and vector antigens allows for long-term expression. *Proceedings of the National Academy of Sciences of the United States of America,* **92**, 1401 - 1405.

21 **Wilson, J.M.** (1996) Adenoviruses as gene delivery vehicles. *New England Journal of Medicine,* **334,** 1185-1187.

22 **Yei, S., Mittereder, N., Tang, K., O'Sullivan, C., Trapnell, B.C.** (1994) Adenovirus-mediated gene transfer for cystic fibrosis: Quantitative evaluation of repeated *in vivo* vector administration to the lungs. *Gene Therapy*, **1**, 192-200.

23 **Gao, G.-P., Yang, Y. and Wilson, J.M.** (1996) Biology of adenovirus vectors with E1 and E4 deletions for liver-directed gene therapy. *Journal of Virology,* **70,** 8934-8943.

24 **Jooss, K., Yang, Y. and Wilson, J.M.** (1996) Cyclophosphamide diminishes inflammation and prolongs transgene expression following delivery of adenoviral vectors to mouse lung and liver. *Human Gene Therapy,* **7,** 1555-1566.

25 **Knowles, M.R., Hohneker, KW., Zhou, Z., Olsen, J.C., Noah, T.L., Hu, P.-C., Leigh, M.W., Engelhardt, J.F., Edwards, LJ., Jones, KR., Grossman, M., Wilson, J.M., Johnson, L.G. and Boucher, R.C.** (1995) A controlled study of adenoviral-vector-mediated gene transfer in the nasal epithelium of patients with cystic fibrosis. *New England Journal of Medicine,* **333,** 823-831.

26 **Kotin, RM.** (1994) Prospects for the use of adeno-associate virus as a vector for human gene therapy. *Human Gene Therapy,* **5,** 793-801.

27 **Flotte, T.R., Carter, B.J.** (1995) Adeno-associated virus vectors for gene therapy. *Gene Therapy*, **2,** 357-362.

28 **Anderson, W.F.** (1998) Human gene therapy. *Nature,* **392,**6679 supplement, 25-30.

29 **Rolling, F. and Samulski, R.J.** (1995) AAV as a viral vector for human gene therapy, generation of recombinant virus. *Molecular Biotechnology,* **3,** 9-15.

30 **Flotte, T.R., Afione, S.A., Conrad, C., McGrath, S.A., Solow, R., Oka, H., Zeitlin, P.L., Guggino, W.B. and Carter, B.J.** (1993) Stable *in vivo* expression of the cystic fibrosis transmembrane conductance regulator with an adeno-associated virus vector. *Proceedings of the National Academy of Science*, **90**, 10613-10617.

31 **Li, J., Dressman, D., Tsao, Y.P., Sakamoto, A., Hoffman, E.P. and Xiao, X.** (1999) rAAV vector-mediated sarcoglycan gene transfer in a hamster model for limb muscular dystrophy. *Gene Therapy,* **6,** 74-82.

32 **Wang, D., Fisher, H., Zhang, L., Fan, P., Ding, R.X. and Dong, J** (1999) Efficient CFTR expression from AAV vectors packaged with promoters – the second generation. *Gene Therapy* **6**, 667-675.

33 **Wolff, J.A., Malone, R.W., Williams, P., Chong, W., Acsadi, G., Jani, A. and Felgner, P.L.** (1990) Direct gene transfer into mouse muscle *in vivo. Science,* **247**, 1465- 1468.

34 **Perales, J.C., Ferkol, T., Molas, M. and Hanson, R.W.** (1994) An evaluation of receptor-mediated gene transfer using synthetic DNA-ligand complexes. *European Journal of Biochemistry* **226**, 255-266.

35 **Cotten, M. and Wagner, E.** (1993) Non-viral approaches to gene therapy. *Current Opinion in Biotechnology* **4**, 705-710.

36 **Baker, A. and Cotten, M.** (1997) Useful delivery of Bacterial Artificial Chromosomes into mammalian cells using psoralen-inactivated adenovirus carrier. *Nucleic Acids Research,* **25**, 1950-1956.

37 **Hengge, U.R., Walker, P.S. and Vogel, J.C.** (1996) Expression of naked DNA in human, pig, and mouse skin. *Journal of Clinical Investigations.* **97**, 2911-2916.

38 **Hickman, M.A., Malone, R.W., Lehmann-Bruinsma, K., Sih, T.R., Knoell, D., Szoka, F.C., Walzem, R., Carlson, D.M. and Powell, J.S.** (1994) Gene expression following direct injection of DNA into liver. *Human Gene Therapy,* **5**, 1477-1483.

39 **Budker, V., Zhang, G., Knechtle, S. and Wolff, J.A.** (1996) Naked DNA delivered intraportally expresses efficiently in hepatocytes. *Gene Therapy,* **3**, 593-598.

40 **Buttrick, P.M., Kass, A., Kitsis, R.N., Kaplan, M.L. and Leinwand, L,A.** (1992) Behaviour of genes directly injected into the rat heart *in vivo. Circulation Research,* **70**, 193-198.

41 **Meyer, K.B., Thompson, M.M., Levy, M.Y., Barron, L.G. and Szoka, F.C.** (1995) Intratracheal gene delivery to the mouse airway: characterization of plasmid DNA expression and pharmacokinetics. *Gene Therapy,* **2**, 450-460.

42 **Vile, R.G. and Hart, I.R.** (1993) *In vitro* and *in vivo* targeting of gene expression to melanoma cells. *Cancer Research* **53**, 962-967.

43 **Coll, J-C., Chollet, P., Brambilla, E., Desplanques, D., Behr, J.-P. and Favrot, M.** (1999) *In vivo* delivery to tumours of DNA complexed with linear polyethylenimine. *Human Gene Therapy,* **10**, 1659-1666.

44 **Ascadi, G.,Dickson, G., Love, D.R., Jani, A., Walsh, F.S., Gurusinghe, A., Wolff, J.A. and Davies, K.E.** (1991) Human dystrophin expression in mdx mice after intramuscular injection of DNA constructs. *Nature* **352**, 815-818.

45 **Danko, I., Fritz, J.D., Latendresse, J.S., Herweijer, H., Schultz, E. and Wolff, J.A.** (1993) Dystrophin expression improves myofibre survival in mdx muscle following intramuscular plasmid DNA injection. *Human Molecular Genetics*, **2**, 2055-20612.

46 **Mumper, R.J., Duguid, J.G., Anwer, K., Barron, M.K., Nitta, H. and Roiland, A.P.** (1996) Polyvinyl derivatives as novel interactive polymers for controlled gene delivery to muscle. *Pharmaceutical Research* **13**, 701-709.

47 **Mumper, R.J. and Rolland, A.** (1998) Plasmid delivery to muscle: Recent advances in polymer delivery systems. *Advanced Drug Delivery Reviews* 30, 151-172.

48 **Furth, P.A., Shamay, A., Wall, R.J. and Hennighausen, L.** (1992) Gene transfer into somatic tissues by jet injection. *Analytical Biochemistry,* **20**, 365-368.

49 **Yang, N.-S., Burkholder, J., Roberts, B., Martinell, B. and McCabe, D.** (1990) *In vivo* and *in vitro* gene transfer to mammalian somatic cells by particle bombardment. *Proceedings of the National Academy of Sciences of the United States of America,* **87**, 9568-9572.

50 **Lodmell, D.L., Ray, N.B., Parnell, M.J., Ewalt, LC., Hanlon, C.A., Shaddock, J.H., Sanderlin, D.S. and Rupprecht, C.E.** (1998) DNA immunization protects nonhuman primates against rabies virus. *Nature Medicine* **4**, 949-952.

51 **Vahlsing, HL., Yankauckas, M.A., Sawdey, M., Gromkowski, S.H. and Manthorpe, M.** (1994) Immunization with plasmid DNA using a pneumatic gun. *Journal of Immunological Methods* **175**, 11-22.

52 **Heller, R., Jaroszeski, M., Atkin, A., Moradpour, D., Gilbert, R., Wands, J. and Nicolau, C.** (1996) *In vivo* gene electroporation and expression in rat liver. *FEBS Letter,* **389**, 225-228.

53 Ulmer, J.B., Donnelly, J.J., Parker, S.E., Rhodes, G.H., Felgner, P.L., Dwarki, V.J., Gromkowski, S.H., Deck, R.R., DeWitt, C.M., Friedman, A., Hawe, L.A., Leander, K.R., Martinez, D., Perry, H.C., Shiver, J.W., Montgomery, D.L. and Liu, M.A. (1993) Heterologous protection against influenza by injection of DNA encoding a viral protein. *Science,* **259**, 1745-1749.

54 **Tang, D.C., Devit, M. and Johnston, S.A.** (1992) Genetic immunization is a simple method for eliciting an immune response. *Nature*, **356**, 152-154.

55 **Felgner, P.L., Gadek, T.R., Holm, M., Roman, R., Chan, H.W., Wenz, M., Northrop, J.P., Ringold, G,M. and Danielsen, M.** (1987) Lipofection: a highly efficient, lipid-midiated DNA-transfection procedure. *Proceedings of the National Academy of Sciences of the United States of America,* **84**, 7413-7417.

56 **Lee, E.R., Marshall, J., Siegel, C.S., Jiang, C., Yew, N.S., Nichols, M.R., Nietupski, J.B., Ziegler, R.J., Lane, M.B., Wang, K.X., Wan, N.C., Scheule, R.K., Harris, D.L., Smith, A.E. and Cheng, S.H.** (1996) Detailed analysis of structures and formulations of cationic lipids for efficient gene transfer to the lung. *Human Gene Therapy* 7,1701-1717.

57 **Li, S. and Huang, L.** (2000) Non-viral gene delivery: promises and challenges. *Gene Therapy,* **7**, 31-34.

58 **Gao, X and Huang, L.** (1995) Cationic liposome-mediated gene transfer. *Gene Therapy,* **2**, 710-722.

59 **Behr, J-P., Demeneix, B., Loeffler, J-P. and Perez-Mutul, J.** (1989) Efficient gene transfer into mammalian primary endocrine cells with lipopolyamine-coated DNA. *Proceedings of the National Academy of Science*, **86**, 6982-6986.

60 **Hawley-Nelson, P., Ciccarone, V., Gebeyehu, G. and Jessee, J.** (1993) LipofectAimne reagent: A new, high efficiency polycationic liposome transfection reagent. *Focus*, **15**, 73-79.

61 **Barthel, F., Remy, J-S., Loeffler, J-P. and Behr, J-P.** (1993) Gene transfer optimisation with Lipospermine-coated DNA. *DNA and Cell Biology*, **12** (6), 553-560.

62 **Walker, S., Sofia, M.J., Kakarla, R., Kogan, N.A., Wierichs, L, Longley, C.B., Bruker, K., Axelrod, H.R., Midha,S., Babu, S. and Khane, D.** (1996) Cationic facial amphiphiles: A promising class of transfection agents. *Proceedings of the National Academy of Science*, **93** (4), 1585-1590.

63 **Zhou, X., Klibanov, A. L. and Huang, L.** (1991) Lipophilic polylysine mediate efficient DNA transfection in mammalian cells. *Biochimica et Biophysica Acta*, **1065**, 8-14.

64 **Kato, T., Iwamoto, K., Ando, H., Asakawa, N., Tanaka, I., Kikuchi, J. and Murakami, Y.** (1996) Synthetic cationic amphiphile for liposome-mediated DNA transfection with less toxicity. *Biological and Pharmaceutical Bulletin*, **19**, 860-863.

65 **Legendre, J. Y. and Szoka, F. C.** (1992) Delivery of plasmid DNA into mammalian cell lines using pH-sensitive liposomes: comparison with cationic liposomes. *Pharmaceutical Research* **9**, 1235-1242.

66 **Budker, V., Gurevich, V., Hagstrom, J.E., Bortzov, F. and Wolff, J.A.** (1996) pH sensitive, cationic liposomes: A new synthetic virus-like vector. *Nature Biotechnology,* **14**, 760-764.

67 **Bond, V.C., Wold, B.** (1987) Poly-L-ornithine-mediated transformation of mammalian cell. *Molecular and Cellular Biology*, 7 (6), 2286-2293.

68 **Dong, Y., Skoultchi, A. I. and Pollard, J. W.** (1993) Efficient DNA transfection of quiescent mammalian cells using poly-L-ornithine. *Nucleic Acids Research,* **21**, 771772.

69 **Lemnaouar, M., Cajero-Juarez, M. and Houdebine, L.-M.** (1995) High efficiency of animal cell DNA transfection using poly-L-ornithine in optimized conditions. *Transgenics,* **1**, 671-677

70 **Fritz, J. D., Herweijer, H., Zhang, G. and Wolff J. A.** (1996) Gene transfer into mammalian cells using histone-condensed plasmid DNA. *Human Gene Therapy,* **7**, 1395-1404.

71 **Cherng, J.-Y., van de Wetering, P., Talsma, H., Crommelin, D. J. A. and Hennink, W. E.** (1996) Effect of size and serum proteins on transfection efficiency of poly ((2-dimethylamino)ethyl methacrylate)-plasmid nanoparticles. *Pharmaceutical Research,* **13**,1038-1042.

72 **Bottger, I., Vogel, F., Platzer, M., Kiessling, U., Grade, K. and Strauss, M.** (1988) Condensation of vector DNA by the chromosomal protein HMG1 results in efficient transfection. *Biochimica et Biophysica Acta,* **950**, 221-228.

73 **Haensler, J. and Szoka, F. C.** (1993) Polyamidoamine cascade polymers mediate efficient transfection of cells in culture. *Bioconjugate Chemistry,* **4**, 372-379.

74 **Kukowska-Latallo, J. F., Bielinska, A. U., Johnson, J., Spindler, R., Tomalia, D. A. and Baker J. R.** (1996) Efficient transfer of genetic material into mammalian cells using Starburst polyamidoamine dendrimers. *Proceedings of the National Academy of Sciences of the United States of America* **93**, 4897-4902.

75 **Tang, M X. and Szoka, F.C.** (1997) The influence of polymer structure on the interactions of cationic polymers with DNA and morphology of the resulting complexes. *Gene Therapy,* **4**, 823-832.

76 **Gottschalk, S., Sparrow, J.T., Hauer, J., Mims, M.P., Leland, F.E., Woo, S.L.C. and Smith, L.C.** (1996) A novel DNA-peptide complex for efficient gene transfer and expression in mammalian cells. *Gene Therapy,* **3**, 448-457.

77 **Plank, C., Tang, M.X., Wolfe, A.R. and Szoka, F.C.** (1999) Branched cationic peptides for gene delivery: Role of type and number of cationic residue formation and *in vitro* activity of DNA polyplexes. *Human Gene Therapy,* **18,** 319-332.

78 **Wadhwa M.S., Collard, W.T., Adami, R.C., McKenzie, D.L. and Rice, K.G.** (1997) Peptide-mediated gene delivery: Influence of peptide structure on gene expression. *Bioconjugugate Chemistry,* **8,** 81-88.

79 **Wolfert M.A., Dash, P.R., Nazarova, O., Oupicky, D., Seymour, L.W., Smart, S., Strohalm, J. and Ulbrich. K.** (1999) Polyelectrolyte vectors for gene delivery: Influence of cationic polymer on biophysical properties of complexes formed with DNA. *Bioconjugugate Chemistry,* **10,** 993-1004.

80 **Cotten, M., Wagner, E. and Birnstiel, M.L.** (1993) Receptor-mediated transport of DNA into eukaryotic cells. *Methods in Enzymology,* **217,** 635-644.

81 **Wagner E, Zauner W. and Ogris M.** (1998) Polylysine-based transfection systems utilizing receptor-mediated delivery. *Advanced Drug Delivery Reviews,* **30,** 97-113.

82 **Katayose, S. and Kataoka, K.** (1997) Water-soluble polyion complex associates of DNA and poly(ethylene glycol)-poly(L-lysine) block copolymer. *Bioconjugate Chemistry,* **8,** 702-707.

83 **Kwoh, D.Y., Coffin, C.C., Lollo, C.P., Jovenal, J., Banaszczyk, M.G., Mulien, P., Phillips, A., Amini, A., Fabrycki, J., Bartholomew, R., Brostoff, S.W. and Carlo, D.J.** (1999) Stabilization of poly-L-lysine/DNA polyplexes for in *vivo* gene delivery to the liver. *Biochimica et Biophysica Acta* **1444,** 171-190.

84 **Kwok, D.Y., McKenzie, D.L., Evers, D.L. and Rice, K.G.** (1999) Formulation of highly soluble poly(ethylene glycol)-peptide DNA condensates. *Journal of Pharmaceutical Science,* **88,** 996-1003.

85 **Toncheva, V., Wolfert, M.A., Dash, P.R., Oupicky, D., Ulbrich, K., Seymour, L.W. and Schacht, E.H.** (1998) Novel vectors for gene delivery formed by self-assembly of DNA with poly(L-lysine) grafted with hydrophilic polymers. *Biochimica et Biophysica Acta* **1380,** 354-468.

86 **Ogris, M., Brunner, S., Schuller, S., Kircheis, R. and Wagner, E.** (1999) PEGylated DNA/transferrinPEI complexes: reduced interaction with blood components, extended circulation in blood and potential for systemic gene delivery. *Gene Therapy* **6,** 595-605.

87 **Maruyama, A., Katoh M., Ishihara, T. and Akaike, T.** (1997) Comb-type polycations effectively stabilize DNA triplex. *Bioconjugate Chemistry,* **8,** 3-6.

88 **Wagner, E., Zauner, W. and Ogris, M** (1998) Polylysine-based transfection systems utilizing receptor-mediated delivery. *Advanced Drug Delivery Reviews*, **30**, 97-113.

89 **Yovandich, J., O'Malley, B.W. Jr., Sikes, M. and Ledley, F.D.** (1995) Gene transfer to synovial cells by intra-articular administration of plasmid DNA. *Human Gene Therapy* **6**, 603-610.

90 **Wolff, J.A., Dowty, M.E., Jiao, S., Repetto, G., Berg, R.K., Ludtke, J., Williams, P. and Slautterback, D.B.** (1992) Expression of naked plasmids by cultured myotubes and entry of plasmids into T tubules and caveolae of mammalian skeletal muscle. *Journal of Cell Science* **103**, 1249- 1259.

91 **Wolff, J.A., Ludtke, J.J., Ascadi, G., Williams, P., and Jani, A.** (1992) Long-term persistence of plasmid DNA and foreign gene expression in mouse muscle. *Human Molecular Genetics* **1**, 363-369.

92 **Dowty, M.E., Williams, P., Zhang, G., Hagstrom, J.E. and Wolff, J.A.** (1995) Plasmid DNA entry into postmitotic nuclei of primary rat myotubes. *Proceedings of the National Academy of Sciences of the United States of America,* **92**, 4572-4576.

93 **Yang, J.-P. and Huang, L** (1996) Direct gene transfer to mouse melanoma by intratumour injection of free DNA. *Gene Therapy,* **3**, 542-548.

94 **Pouton, C.W. and Seymour, L.W.** (1998) Key issues in non-viral gene delivery. *Advanced Drug Delivery Reviews,* **34**, 3-19.

95 **Uduehi, A.N., Moss, S.H., Nuttall, J. and Pouton, C.W. (1999)** Cationic lipid-mediated transfection of differentiated Caco-2 cells: a filter culture model of gene delivery to a polarized epithelium. *Pharmaceutical Research*, **16**, 1805-1811.

96 **Mortimer, I., Tam, P., MacLachlan, I., Graham, R.W., Saravolac, E.G. and Joshi, P.B.** (1999) Cationic lipid-mediated transfection of cells in culture requires mitotic activity. *Gene Therapy,* **6**, 403-411.

97 **Hazinski, T.A., Ladd, P.A. and Dematteo, C.A.** (1991) Localisation and induced expression of fusion genes in the rat lung, *American journal of Respiratory Cell and Molecular Biology,* **4**, 206-209.

98 **Stribling, R., Brunette, E., Liggitt, D., Gaensler, K. and Debs, R.** (1992) Aerosol gene delivery *in vivo.* P*roceedings of the National Academy of Science and the United States of America.* **89**, 11277-11281.

99 **McLachlan, G., Davidson, D.J., Stevenson, B.J., Dickinson, P., Davidson-Smith, H., Dorin, J.R. and Porteous, D.J.** (1995) Evaluation *in vitro* and *in vivo* of cationic liposome-expression construct complexes for cystic fibrosis gene therapy. *Gene Therapy*, **2**, 614-622.

100 **Canonico, A.E., Conary, J.T., Meyrick, B.O. and Brigham, K.L.** (1994) Aerosol and intravenous transfection of human α1-antitrypsin gene to lungs of rabbits. *American Journal of Respiratory Cell and Molecular Biology*, **10**, 24-29.

101 **Logan, J.J., Bebok, Z., Walker, L.C., Peng, S., Felgner, P.L., Siegal, G.P., Frizzell, R.A., Dong, J., Howard, M., Matalon, S., Lindsey, J.R., DuVall, M. and Sorscher, E.J.** (1995) Cationic lipids for reporter gene and CFTR transfer to rat pulmonary epithelium. *Gene Therapy*, 2, 38-49.

102 **Yoshimura, K., Rosenfeld, M.A., Nakamura, H., Scherer, E.M., Pavirani, A., Lecocq, J.P. and Crystal, R.G.** (1992) Expression of the human cystic fibrosis transmembrane conductance regulator in the mouse lung after *in vivo* intratracheal plasmid-mediated gene transfer *Nucleic Acid Research,* **20**, 3233-3240.

103 **Alton, E.W.F.W., Middleton, P.G., Hart, S.L., Williamson, R., Fasold, K.I. and Miller, A.D.** (1993) Non-invasive liposome-mediated gene delivery can correct the ion-transport defect in cystic fibrosis mice. *Nature Genetics*, **5** (2), 135-142.

104 **Hyde, S.C., Gill, D.R., Higgins, C.F., Trezise, A.E.O., MacVinish, L.J. and Cuthbert, A.W.** (1993) Correction of the ion-transport defect in cystic fibrosis transgenic mice by gene therapy. *Science*, **362**, 250-255.

105 **Rosefeld, M.A., Yoshimura, K, Trapnell, B., Yoneyama, K, Rosenthal, E., Dalemans, W., Fukayama, M., Stier, J., Stratford-Perricaudet, L.D., Perricaudet, M., Guggino, W., Pavirani, A., Leeoeq, P.-P. and Crystal, R.G.** (1992) *In vivo* transfer of the human cystic fibrosis transmembrane conductance regulator gene to the airway epithelium. *Cell,* **68**, 143- 155.

106 **Caplen, N.J., Alton, E.W.F.W., Middleton, P.G., Dorin, J.R, Stevenson, B.J., Durham, S.R., Gao, X., Jeffery, P.K, Hodson, M.E., Coutelle, C., Huang, L, Porteous D. J, Williamson, R. and Geddes, D.M.** 1995) Liposome-mediated CFTR gene transfer to the nasal epithelium of patients with cystic fibrosis. *Nature Medicines* **1**, 39-46.

107 **Zabner, J., Fasbender, A.J., Moninger, T., Poellinger, K.A. and Welsh, M.J.** (1995) Cellular and molecular barriers to gene transfer by a cationic lipid. *Journal of Biological Chemistry.* **270**, 18997-19007

108 **Gao, L., Wagner, E., Cotten, M., Agarwal, S., Harris, C., Romer, M., Miller, L., Hu, P.-C. and Curiel, D.** (1993) Direct *in vivo* gene transfer to the airway epithelium employing adenovirus-polylysine-DNA complexes. *Human Gene Therapy* **4**, 17-24.

109 **Nguyen, D.M., Wiehle, S.A., Roth, J.A. and Cristiano, R.J.** (1997) Gene delivery into malignant cells *in vivo* by a conjugated adenovirus/DNA complex. *Cancer Gene Therapy,* **4**, 183-190.

110 **Patel, H.M.** (1992) Serum opsonins and liposomes: their interaction and opsonophagocytosis. *Critical Reviews in Therapeutic Drug Carrier Systems* **9**, 39-90.

111 **Miller, N. and Vile, R.** (1995) Targeted vectors for gene therapy. *FASEB Journal*, **9**, 190-199

112 **Allen, T.M.** (1994) Long-circulating (sterically stabilised) liposomes for targeted drug delivery. *TIPS* **15**, 215-220

113 **Stavridis, J.C., Deliconstantinos, G. Psallidopoulos, M. C., Armenakas, N. A., Hadjiminas, D. J. and Hadliminas, J.** (1986) Construction of transferrin-coated liposomes for *in vivo* transport of exogenous DNA to bone marrow erythroblasts in rabbits. *Experimental Cell Research,* **164**, 568-572.

114 **Walther, F.J., David-Cu, R., Supnct, M. C., Longo, M. L., Fan, B. R. and Bruni, R.** (1993) Uptake of antioxidants in surfactant liposomes is enhanced by SP-A. *American Journal of Physiology* **265**, L330-L339

115 **Mizano, M., Yoshida, J., Susita, K., Inoue, 1., Seo, H., Hayashi, Y., Koshizaka, T. and Yagi, K.** (1990) Growth inhibition of glioma cells transfected with the human ,B-interferon gene by liposomes coupled with a monoclonal antibody. *Canner Research,* **50**, 7826-7829.

116 **Morishita, R., Gibbons, G. H., Kaneda, Y., Ogihara, T. and Dzau, V. J.** (1993) Novel *in vitro* gene transfer method for study of local modulators m vascular smooth muscle cells. *Hypertension* **21**, 889-899.

117 **Bagai, S. and Sarkar, D.P.** (1993) Targeted delivery of hygromycin B using reconstituted Sendai viral envelopes lacking haemagglutinin-neuraminidase. *FEBs letters* **326**, 183-188

118 **Schreier, H. Gonzalez-Rothi, R.J. and Stecenko, A.A.** (1993) Pulmonary delivery of liposomes. *Journal of Controlled Release* **24**, 209-223.

119 **Zhu, N., Liggitt, D., Liu, Y. and Debs, R.** (1993) Systemic gene expression after intravenous DNA delivery into adult mice. *Science,* **261**, 209-211.

120 **Liu, Y., Mounkes, L.C., Liggitt, H.D., Brown, C.S., Solodin, I., Heath, T.D. and Debs, R.J.** (1997) Factors influencing the efficiency of cationic liposome-mediated intravenous gene delivery. *Nature Biotechnology*, **15**, 167-173.

121 **Hong, K.L, Zheng, W.W., Baker, A and Papahadjopoulos, D.** (1997) Stabilization of cationic liposome-plasmid DNA complexes by polyamines and poly(ethylene glycol)-phospholipid conjugates for efficient *in viva* gene delivery. *FEBS Letters,* **400**, 233-237.

122 **Li, S. and Huang, L.** (1997) *In vivo* gene transfer via intravenous administration of cationic lipid-protamine-DNA (LPD) complexes. *Gene Therapy,* **4**, 891-900.

123 **Barron, L.G., Meyer, K.B. and Szoka, F.C.** (1998) Effects of complement depletion on the pharmacokinetics and gene delivery mediated by cationic lipid-DNA complexes. *Human Gene Therapy* **9**, 315-323.

124 **Templeton, N.S., Lasic, D.D., Frederik, P.M., Strey, H.H., Roberts, D.D. and Pavlakis, G.N.** (1997) Improved DNA:liposome complexes for increased systemic delivery and gene expression. *Nature Biotechnology*, **15**, 647-652.

125 **Li, S., Tseng, W.-C., Beer Stolz, D., Wu, S.-P., Watkins, S.C. and Huang, L.** (1999) Dynamic changes in the characteristics of cationic lipidic vectors after exposure to mouse serum: implications for intravenous lipofection. *Gene Therapy,* **6**, 585-594.

126 **Liu, Y., Liggitt, D., Zhong, W., Tu, G., Gaensler, K. and Debs, R.** (1995) Cationic liposome-mediated intravenous gene delivery. *Journal of Biological Chemistry,* **270**, 24864-24870.

127 **Wu, G.Y. and Wu, C.H.** (1988) Receptor-mediated gene delivery and expression *in vivo*. *Journal of Biological Chemistry,* **263**, 14621- 14624.

128 **Wu, G.Y. and Wu, C.H.** (1987) Receptor-mediated *in vitro* gene transformation by a soluble DNA carrier system. *Journal of Biological Chemistry,* **262**, 4429-4432.

129 **Wagner, E., Zenke, M., Cotten, M., Beug, H. and Birnstiel, M.L.** (1990). Transferrin-polycation conjugates as carriers for DNA uptake into cells. *Proceedings of the National Academy of Sciences of the United States of America* **87**, 3410-3414.

130 **Huckett, B., Ariatti, M. and Hawtrey, A.O.** (1990) Evidence for targeted gene transfer by receptor-mediated endocytosis: Stable expression following insulin-directed entry of neo into HepG2 cells. *Biochemical Pharmacology,* **40**, 253-263.

131 **Ferkol, T., Perales, J.C., Eckman, E., Kaetzel, C.S., Hanson, R.W. and Davis, P.B.** (1995) Gene transfer into the airway epithelium of animals by targeting the polymeric immunoglobulin receptor. *Journal of Clinical Investigation,* **95**, 493-502.

132 **Buschle, M., Cotten, M., Mechtler, K., Birnstiel, M.L. and Wagner, E.** (1995) Receptor-mediated gene transfer into T-lymphocytes via binding of DNA/CD3 antibody particles to the CD3 T cell receptor complex. *Human Gene Therapy,* **6**, 753-761.

133 **Lee, R.J. and Huang, L.** (1996) Folate-targeted, anionic liposome-entrapped polylysine-condensed DNA for tumour cell-specific gene transfer. *Journal of Biological Chemistry,* **271**, 8481 –8487

134 **Williams, R.S.** (1995) Human gene therapy - of tortoises and hares. *Nature Medicine* **1**, 1137- 1138.

135 **Chowdhury, N.R., Wu, C.H., Wu, G.Y., Yernen, P.C., Bommineni, V.R. and Chowdhury, J.R** (1993) Fate of DNA targeted to the liver by asialoglycoprotein receptor-mediated endocytosis *in vivo*, prolonged persistence in cytoplasmic vesicles after partial hepatectomy. *Journal of Biological Chemistry* **268**, 11265-11271.

136 **Perales, J.C., Ferkol, T., Beegen, H., Ratnoff, O.D. and Hanson, R.W.** (1994) Gene transfer *in vivo*: Sustained expression and regulation of genes introduced into the liver by receptor-targeted uptake. *Proceedings of the Naiional Academy of Sciences of the United States of America,* **91**, 4086-4090.

137 **Wu, G.Y. and Wu, C.H.** (1993) Liver-directed gene delivery *Advanced Drug Delivery Reviews,* **12**, 159-167.

138 **Kircheis, R., Schuller, S., Brunner, S., Ogris, M., Heider, K.-H., Zauner, W. and Wagner, E.** (1999) Polycation-based DNA complexes for tumor-targeted gene delivery *in vivo. Journal of Gene Medicine* **1**, 111-120.

139 **Dash, P.R., Read, M.L., Barrett, L.B, Wolfert, M.A. and Seymour, L.W.** (1999) Factors affecting blood clearance and in *vivo* distribution of polyelectrolyte complexes for gene delivery. *Gene Therapy,* **6**, 643-650.

140 **Erbacher, P., Bettinger, T., Belquise-Valladier, P., Zou, S., Coll, J.-L., Behr, J.-P. and Remy, J.-S.** (1999) Transfection and physical properties of various saccharide, poly(ethylene glycol), and antibody-derivatized polyethylenimines (PEI). *Journal of Gene Medicine,* **1**, 210-222.

141 **Nguyen, H.-K., Lemieux, P., Vinogradov, S.V., Gebhart, C.L., Guerin, N., Paradis, G., Bronich, T.K., Alakhov, W. and Kabanov, A.V.** (2000) Evaluation of polyether-polyethyleneimine graft copolymers as gene transfer agents. *Gene Therapy*, 7, 129-138.

142 **Garrett, S.W., Davies, O.R., Milroy, D.A., Wood, P.J., Pouton, C.W. and Threadgill, M.D.** (2000) Synthesis and characterisation of polyamine-poly(ethylene glycol) constructs for DNA binding and gene delivery. *Bioorganic Medicinal Chemistry,* **8,** 1779-1797.

143 **Vinogradov, S.V., Bronich, T.K. and Kabanov, A.V.** (1998) Self-assembly of polyamine-poly(ethylene glycol) copolymers with phosphorothioate oligonucleotides. *Bioconjugate Chemistry,* **8,** 805-812.

144 **Gref, R., Lück, M., Quellec, P., Marchand. M., Dellacherie, E., Harnisch, S., Blunk, T. and Müller, R.H.** (2000) 'Stealth' corona-core nanoparticles surface modified by polyethylene glycol (PEG): Influences of the corona (PEG chain length and surface density) and of the core composition on phagocytic uptake and plasma protein adsorption. *Colloids and Surfaces B: Biointerfaces,* **18,** 301-313.

145 **Finsinger, D., Remy, J.-S., Erbacher, P. Koch, C. and Plank, C.** (2000) Protective copolymers for non-viral gene vectors: Synthesis, vector characterisation and application in gene delivery. *Gene Therapy,* **7,** 1183-1192.

146 **Oupicky, D., Howard, K.A., Konák, C., Dash, P.R., Ulbrich, K. and Seymour, L.W.** (2000) Steric stabilisation of poly-L-Lysine/DNA complexes by the covalent attachment of semitelechelic poly[*N*-(2-hydroxypropyl)methacrylamide]. *Bioconjugate Chemistry,* **11,** 492-501

147 **Dash, P.R., Read, M.L., Fisher, K.D., Howard, K.A., Wolfert, M., Oupicky, D., Subr, V., Strohalm, J., Ulbrich, K. and Seymour, L.W.** (2000) Decreased binding to proteins and cells of polymeric gene delivery vectors surface modified with a multivalent hydrophilic polymer and retargeting through attachment of transferrin. *Journal of Biological Chemistry,* **275,** 3793-3802.

148 **Adami, R.C. and Rice, K.G.** (1999) Metabolic stability of glutaraldehyde cross-linked peptide DNA condensates. *Journal of Pharmaceutical Science,* **88,** 739-746.

149 **Trubetskoy, V.S., Loomis, A., Slattum, P.M., Hagstrom, J.E., Budker, V.G. and Wolff, J.A.** (1999) Caged DNA does not aggregate in high ionic strength solutions. *Bioconjugate Chemistry,* **10,** 624-628.

150 **Plank, C., Mechtler, K., Szoka, F.C. and Wagner, E.** (1996) Activation of the complement system by synthetic DNA complexes: A potential barrier for intravenous gene delivery. *Human Gene Therapy,* **7,** 1437-1446.

151 **Plank, C. Tang, M.X., Wolfe, A.R. and Szoka, F.C.** (1999) Branched cationic peptides for gene delivery: Role of type and number of cationic residues in formation and *in vitro* activity of DNA polyplexes. *Human Gene Therapy,* **10,** 319-332.

152 **Shinoda, T., Maeda, A., Kagatani, S., Konno, Y., Goto. M., Sonobe, T. and Akaike, T.** (1999): Specific interaction with hepatocytes and acute toxicity of new carrier molecule galactosyl-polylysine. *Drug Delivery,* **6,** 127-133.

153 **Goula, D., Remy, J.-S., Erbacher, P., Wasowicz, M., Levi, G., Abdallah, B. and Demeneix, B.A.** (1998): Size, diffusibility and transfection performance of linear PEI/DNA complexes in the mouse central nervous system. *Gene Therapy,* **5,** 712-717.

154 **Fischer D, Bieber T. Li Y. Elsasser H-P, Kissel T.** (1999), A novel non-viral vector for DNA delivery based on low molecular weight, branched polyethylenimine: Effect of molecular weight on transfection efficiency and cytotoxicity. *Pharmaceutical Research,* **16,** 1273-1279.

155 **Wolfert, M.A. and Seymour, L.W.** (1996): Atomic force microscopic analysis of the influence of the molecular weight of poly(L)lysine on the size of polyelectrolyte complexes formed wtih DNA. Gene *Therapy,* **3,** 269-273.

156 **Richardson, S.C., Kolbe, H.V. and Duncan, R.** (1999): Potential of low molecular mass chitosan as a DNA delivery system: biocompatibility, body distribution and ability to complex and protect DNA. *IntJ Pharm* **178,** 231-243.

157 **Wolfert, M.A., Dash, P.R., Nazarova, O. Oupicky, D., Seymour, L.W., Smart, S., Strohalm, J. and Ulbrich, K.** (1999) Polyelectrolyte vectors for gene delivery: Influence of cationic polymer on biophysical properties of complexes formed with DNA. *Bioconjugate Chemistry,* **10,** 993-1004.

158 **Lynn, D.M. and Langer, R.** (2000) Degradable poly(-amino esters): Synthesis, characterization, and self-assembly with plasmid DNA. *Journal of American Chemical Society,* **122,** 10761 -10768.

159 **Choi, Y.H., Liu, F., Kim, J.-S., Choi, Y.K., Park, J.S. and Kim, S.W.** (1998) Polyethylene glycol~graRed poly-L-lysine as polymeric gene carrier. *Journal of Control Release,* **54,** 39-48.

160 **Pouton, C.W.** (1998) Biological barriers to gene transfer. *Advanced Gene Deliver: from concepts to pharmaceutical products.* 65-102. Edited by Rowland, A. Harwood Press.

161 **Gruenberg, J. and Maxfield, F.R.** (1995) Membrane transport in the endocytic pathway. *Current Opinion in Cell Biology, 7,* 552-563.

162 **Robinson, M.S., Watts, C., and Zerial, M.** (1996) Membrane dynamics in endocytosis. *Cell,* **84,** 13-21.

163 **Watanabe, Y., Nomoto, H., Takezawa, R., Miyoshi, N. and Akaike, T** (1994) Highly efficient transfection into primary cultured mouse hepatocytes by use of cation-liposomes: an application for immunization. *Journal of Biochemistry,* **116,** 1220-1226.

164 **Owen, D.J. and Luzio, J.P.** (2000) Structural insights into clathrin-mediated endocytosis. *Current Opinion in Cell Biology,* **12,** 467-474.

165 **Schintzer, J.E.** (1993) Update on the cellular and molecular basis of capillary permeability. *Cardiovascular Medicine,* **3,** 124-130.

166 **Lamaze, C. and Schmid, S.L.** (1995) The emergence of clathrin-independent pathways. *Current Opinion in Cell Biology,* 7, 573-580.

167 **Plank, C., Oberhauser, B., Mechtler, K., Koch, C. and Wagner, E.** (1994) The influence of endosome-disruptive peptides on gene transfer using synthetic virus-like gene transfer systems. *Journal of Biological Chemistry,* **269,** 12918-12924.

168 **Wagner, E., Cotten, M., Foisner, R. and Birnstiel, M.L.** (1991) Transferrin-polycation-DNA complexes: The effect of polycations on the structure of the complex and DNA delivery to cells. *Proceedings of the National Academy of Sciences of the United States of America,* **88,** 4255-4259.

169 **Zenke, M., Steinlein, P., Wagner, E., Cotten, M., Beug, H. and Birnstiel, M.L.** (1990) Receptor mediated endocytosis of transferrin-polycation conjugates: An efficient way to introduce DNA into hematopoietic cells. *Proceedings of the National Academy of Sciences of the United States of America,* **87,** 3655-3659.

170 **Hart, S.L, Harbottle, R P., Cooper, M J., Miller, A., Williamson, R. and Coutelle, C.** (1995) Gene delivery and expression mediated by an integrin-binding peptide. *Gene Therapy,* **2,** 552-554.

171 **Hart, S.L., Arancibia-Cárcamo, C.V., Wolfert, M.A., Mailhos, C., O'Reilly, N.J., Ali, R.R., Coutelle, C., George, A.J.T., Harbottle, R.P., Knight, A.M., Larkin, D.F.P., Levinsky, R.L., Seymour, L.W., Thrasher, A.J. and Kinnon, C.** (1998) Lipid-mediated enhancement of transfection by a non-viral integrin-targeting vector. *Human Gene Therapy,* **9**, 575-585.

172 **Jenkins, R.G., Herrick, S.E., Meng,Q.-H., Kinnon, C., Laurent, G.J., McAnulty, R.J. and Hart, S.L.** (2000) An integrin-targeted non-viral vector for pulmonary gene therapy. *Gene Therapy,* **7**, 393-400.

173 **Wilke, M., Fortunati, E., Broek, M.V.d., Hoogeveen, A.T. and Holte, B.J.** (1996) Efficacy of a peptide-based gene delivery system depends on mitotic activity. *Gene Therapy,* **3**, 1133-1142.

174 **Benachir, T. and Lafleur, M.** (1995) Study of vesicle leakage induced by melittin. *Biochimica et Biophysica Acta,* **1235**, 452-60.

175 **Epand, R.M., Cheetham, J.J., Epand, R.F., Yeagle, P.L., Richardson, C.D., Rockwell, A. and DeGrado, W.F.** (1992) Peptide models for the membrane destabilizing action of viral fusion proteins. *Biopolymers,* **32**, 309-314.

176 **Epand, R.M., Shai, Y., Segrest, J.P. and Anantharamaiah, G.M.** (1995) Mechanisms for the modulation of membrane bilayer properties by amphipathic helical peptides, *Biopolymers,* **17**, 319-338.

177 **Fujii, G., Selsted, M.E. and Eisenberg, D.** (1993) Defensins promote fusion and lysis of negatively charged membranes, *Protein Sciences,* **2**, 1301-1312.

178 **Gazit, E., Boman, A., Boman, H.G. and Shai, Y.** (1995) Interaction of the mammalian antibacterial peptide cecropin P1 with phospholipid vesicles. *Biochemistry,* **34**, 11479-11488.

179 **Wagner, E., Plank, C., Zatloukal, K., Cotten, M. and Birnstiel, M.L.** (1992) Influenza virus hemagglutinin HA-2 N-terminal fusogenic peptides augment gene transfer by transferrin-polylysine/DNA complexes: Towards a synthetic virus-like gene transfer vehicle. *Proceedings of the National Academy of Sciences of the United States of America,* **89**, 7934-7938.

180 **Midoux, P., Mendes, C., Legrand, A., Raimond, J., Mayer, R., Monsigny, M. and Roche, A.C.** (1993) Specific gene transfer mediated by lactosylated poly-Liysine into hepatoma cells. *Nucleic Acids Research,* **21**, 871-878.

181 **Plank, C., Zatloukal, K., Cotten, M., Mechtler, K. and Wagner, E.** (1992) Gene transfer into hepatocytes using asialoglycoprotein receptor mediated endocytosis of DNA complexed with an artificial tetra-antennary galactose ligand. *Bioconjugate Chemistry,* **3**, 533-539.

182 **Cotten, M., Wagner, E., Zatloukal, K., Phillips, S., Curiel, D.T. and Birnstiel, M.L.** (1992). High-efficiency receptor-mediated delivery of small and large (48kb) gene constructs using the endosome disruption activity of defective or chemically inactivated adenovirus particles. *Proceedings of the National Academy of Sciences of the United States of America,* **89**, 6094-6098.

183 **Mechtler, K. and Wagner, E.** (1997) Influenza peptide enhanced gene transfer: The role of peptide sequences. *New Journal of Chemistry,* **21**, 105-111.

184 **Parente, R. A., Nir, S. and Szoka, F. C.** (1990) Mechanism of leakage of phospholipid vesicle contents induced by the peptide GALA, *Biochemistry,* **29**, 8720-8728.

185 **Murata, M., Sugahara, Y., Takahashi, S. and Ohnishi, S.** (1987), pH-dependent membrane fusion activity of a synthetic 20 amino acid peptide with the same sequence as that of hydrophobic segment of influenza virus haemagglutinin. *Journal of Biochemistry,* **102,** 957-962.

186 **Lear, J. D. and DeGrado, W. F.** (1987) Membrane binding and conformational properties of peptides representing the NH2 terminus of influenza HA-2 *Journal of Biological Chemistry,* **262,** 6500-6505.

187 **Gething, M-J., Doms, R. W., York, D. and White, J.M.** (1986) Studies on the mechanism of membrane fusion: Site-specific mutagenesis of the hemagglutinin of influenza virus. *Journal of Cell Biology,* **102,** 11-23.

188 **White, J.M.** (1992), Membrane Fusion. *Science,* **258,** 917-924.

189 **Wharton, S. A., Martin, S. R., Ruigrok, R. W. H., Skehel, J. J. and Wiley, D. C.** (1988), Membrane fusion by peptide analogues of Influenza virus haemagglutinin. *Journal of General Virolorogy,* **69,** 1847-1857.

190 **Felgner, P.L.** (1999) Prospects for synthetic self-assembling systems in gene delivery. *Journal of Gene Medicine,* **1,** 290-292.

191 **Gao, X. and Huang, L.** (1996) Potentiation of cationic liposome-mediated gene delivery by polycations. *Biochemistry,* **35,** 1027-1036.

192 **Sternberg, B., Sorgi, F. L. and Huang, L.** (1994) New structures in complex formation between DNA and cationic liposomes visualized by freeze-fracture electron microscopy. *FEBS Letters,* **356,** 361-366.

193 **Zhou, X. and Huang, L.** (1994) DNA transfection mediated by cationic liposomes containing lipopolylysine: characterisation and mechanism of action. *Biochimica et Biophysica Acta,* **1189**, 195-203.

194 **Wrobel, I. and Collins, D.** (1995) Fusion of cationic liposomes with mammalian cells occurs after endocytosis. *Biochimica et Biophysica Acta,* **1235**, 296-304.

195 **Leventis, R. and Silvius, J. R.** (1990) Interactions of mammalian cells with lipid dispersions containing novel metabolizable cationic amphiphiles. *Biochimica et Biophysica Acta,* **1023**,124-132.

196 **Xu, Y. and Szoka, F. C.** (1996) Mechanism of DNA release from cationic liposome/DNA complexes used in cell transfection. *Biochemistry,* **35**, 5616-5623.

197 **Schwartz, B., Benoist, C., Abdallah, B., Scherman, D., Behr, J-P. and Demeneix, B. A.,** (1995) Lipospermine-based gene transfer into new born mouse brain is optimized by a low lipospermine/DNA charge ratio. *Human Gene Therapy,* **6**, 1515-1524.

198 **Allen, T. M., Hong, K. and Papahadjopoulos, D.** (1990) Membrane contact, fusion, and hexagonal (HII) transitions in phosphatidylethanolamine liposomes. *Biochemistry,* **29**, 2976-2985.

199 **Farhood, H., Serbina, N. and Huang, L.** (1995) The role of dioleoyl phosphatitylethanolamine in cationic liposome-mediated gene transfer. *Biochimica et Biophysica Acta,* **1235**, 289-295.

200 **Kaneda, Y., Iwai, K. and Uchida, T.** (1989) Increased expression of DNA co-introduced with nuclear protein in adult rat liver. *Science,* **243**, 375-78.

201 **von der Leyen, H.E., Gibbons, G.H., Morishita, R., Lewis, N.P., Zhang, L., Nakajima, M., Kaneda, Y., Cooke, J.P. and Dzau, V.J.** (1995) Gene therapy inhibiting neointimal vascular lesion: *in vivo* transfer of endothelial cell nitric oxide synthase gene. *Proceedings of the National Academy of Sciences of the United States of America,* **92**, 1137-41.

202 **Mizuguchi, H., Nakagawa, T., Nakanishi, M., Imazu, S., Nakagawa, S. and Mayumi, T.** (1996) Efficient gene transfer into mammalian cells using fusogenic liposomes. *Biochemical and Biophysical Research Communications,* **218**, 402-407.

203 **Schoen, P., Chonn, A., Cullis, P.R., Wilschut, J. and Scherrer, P.** (1999) Gene transfer mediated by haemagglutinin reconstituted in cationic lipid vesicles. *Gene Therapy,* **6**, 823-832.

204 **Tikchonenko, T.I., Glushakova, S.E., Kislina, O.S., Grodnitskaya, N.A., Manykin, A.A. and Naroditsky, B.S.** (1988) Transfer of condensed viral DNA into eukaryotic cells using proteoliposomes. *Gene,* **63**, 321-330.

205 **Legendre, J. Y. and Szoka, F. C.** (1993) Cyclic amphipathic peptide-DNA complexes mediate high-efficiency transfection of adherent cells, *Proceedings of the National Academy of Sciences of the United States of America,* **90**, 893-897.

206 **Legendre, J.Y. and Supersaxo, A.** (1995) Short-chain phospholipids enhance amphipathic peptide-mediated gene transfer. *Biochimical and Biophysical Research Communications*, **217**, 179-85.

207 **Hara, T., Kuwasawa, H., Aramaki, Y., Takada, S., Koike, K., Ishidate, K., Kato, H. and Tsuchiya, S.** (1996) Effects of fusogenic and DNA-binding amphiphilic compounds on the receptor-mediated gene transfer into hepatic cells by asialofetuin-labeled liposomes. *Biochimica et Biophysica Acta,* **1278**, 51-58.

208 **Kichler, A., Mechtler, K., Behr, J.-P. and Wagner, E.** (1997) The influence of membrane-active peptides and helper lipids on lipospermine/DNA complex mediated gene transfer. *Bioconjugate Chemistry,* **8**, 213-221.

209 **Kamata, H., Yagisawa, H., Takahashi, S. and Hirata, H.** (1994) Amphiphilic peptides enhance the efficiency of liposome-mediated DNA transfection. *Nucl. Acids Research,* **22**, 536-537.

210 **Simões, S., Sleushkin, V., Gaspar, R., Pedroso de Lima, M.C. and Düzgüneş** (1998) Gene delivery by negatively charged tenary complexes of DNA, cationic liposomes and transferrin or fusogenic peptides. *Gene Therapy,* **5**, 955-964.

211 **Mortimer, I, Tam, P., MacLachlan, I., Graham, R.W., Saravolac, E.G. and Joshi, P.B.** (1999) Cationic lipid-mediated transfection of cells in culture requires mitotic activity. *Gene Therapy,* **6**, 403-411.

212 **Fasbender, A., Zaboer, J., Zeiher, B.G. and Welsh, M.J.** (1997) A low rate of cell proliferation and reduced DNA uptake limit cationic lipid-mediated gene transfer to primary cultures of ciliated human airway epithelia. *Gene Therapy,* **4**, 1173-1180.

213 **Michael, S. I. and Curiel, D. T.** (1994) Strategies to achieve targeted gene delivery via the receptor-mediated endocytosis pathway. *Gene Therapy,* **1**, 223-232.

214 **Perales, J.C., Ferkol, T., Molas, M. and Hanson, R.W.** (1994) An evaluation of receptor-mediated gene transfer using synthetic DNA-ligand complexes. *European Journal of Biochemistry,* **226**, 255-266.

215 **Wu, G.Y., Zhan, P., Sze, L.L., Rosenberg, A.R. and Wu, C.H.** (1994) Incorporation of adenovirus into a ligand-based DNA carrier system results in retention of original receptor specificity and enhances targeted gene expression. *The Journal of Biological Chemistry,* **269**, 11542-11546.

216 **Cotten, M., Laengle-Rouault, F., Kirlappos, H., Wagner, E., Mechtler, K., Zenke, M., Beug, H. and Birnstiel, M.L.** (1990) Transferrin-polycation-mediated introduction of DNA into human leukemic cells: stimulation by agents that affect the survival of transfected DNA or modulate transferrin receptor levels. *Proceedings of the National Academy of Sciences of the United States of America,* **87**, 4033-4037.

217 **Zauner, W., Kichler, A., Schmidt, W., Sinski, A. and Wagner, E.** (1996) Glycerol enhancement of ligand-polylysine/DNA transfection. *Biotechniques,* **20**, 905-913.

218 **Curiel, D.T., Agarwal, S., Wagner, E. and Cotten,** M. (1991) Adenovirus enhancement of transferrinpolylysine-mediated gene delivery. *Proceedings of the National Academy of Sciences of the United States of America,* **88**, 8850-8854.

219 **Wu, G.Y., Zhan, P., Sze, L.L., Rosenberg, A.R. and Wu, C.H.** (1994) Incorporation of adenovirus into a ligand-based DNA carrier system results in retention of original receptor specificity and enhances targeted gene expression. *The Journal of Biological Chemistry,* **269**, 11542-11546.

220 **Zauner, W., Blaas, D., Kuchler, E. and Wagner, E.** (1995) Rhinovirus mediated endosomal release of transfection complexes. *Journal of Virology,* **69**, 1085-1092.

221 **Curiel, D.T., Wagner, E., Cotten, M., Birnstiel, M.L., Agarwal, S., Li, C.-M., Loechel, S. and Hu, P.-C.** (1992) High-efficiency gene transfer by adenovirus coupled to DNA-polylysine complexes. *Human Gene Therapy,* **3**, 147-154.

222 **Wu, G.Y., Zhan, P., Sze, L.L., Rosenberg,A.R. and Wu, C.H.** (1994) Incorporation of adenovirus into a ligand-based DNA carrier system results in retention of original receptor specificity and enhances targeted gene expression. *Journal of Biological Chemistry,* **269**, 11542-46.

223 **Cotten, M., Saltik, M., Kursa, M., Wagner, E., Masss, G. and Birnstiel, M.L.** (1994) Psoralen treatment of adenovirus particles eliminates virus replication and transcription while maintaining the endosomolytic activity of the virus capsid. *Virology,* **205**, 254-261.

224 **Wyman, T.B., Nicol, F., Zelphati, O., Scaria, P.V., Plank, C. and Szoka, F.C.** (1997) Design, synthesis and characterization of a cationic peptide that binds to nucleic acids and permeabilizes bilayers. *Biochemistry,* **36**, 3008-3017.

225 **Kircheis, R., Kichler, A., Wallner, G., Kursa, M., Ogris, M., Feizmann, T., Buchberger, M. and Wagner, E.** (1997) Coupling of cell-binding ligands to polyethylenimine for targeted delivery. *Gene Therapy,* **4**, 409-418.

226 **Fominaya, J. and Wels, W.** (1996), Target cell-specific DNA transfer mediated by chimeric multidomain protein. *Journal of Biological Chemistry.* **271**, 10560-10568.

227 **Luby-Phelps, K, Castle, P.E., Taylor, D.L, and Lanni, F.** (1987) Hindered diffusion of inert tracer particles in the cytoplasm of mouse NIH3T3 cells. *Proceedings of the National Academy of Sciences of the United States of America,* **84**, 4910-4913.

228 **Meyer, KB., Uyochi, LS. and Szoka, F.C.** (1997) Manipulating the intracellular trafficking of nucleic acids. In: *Gene Therapy for Diseases of the Lung,* 135-180. Edited by Brigham, K.L., New York, Marcel Dekker.

229 **Seksek, O., Biwersi, J. and Verkman, A.S.** (1997) Translational diffusion of marcromolecule-sized solutes in cytoplasm and nucleus. *Journal of Cell Biology,* **138**, 131-142.

230 **Walker, R.A. and Sheetz, M.P.** (1993) Cytoplasmic microtubule-associated motors. *Annual Review of Biochemistry,* **62**, 429-451.

231 **Cole, N.B. and Lippincott-Schwartz, J.** (1995) Organisation of organelles and membranetraffic by microtubules. *Current Opinion in Cell Biology,* 7, 55-64.

232 **Hamm-Alvarez, S.R.** (1998) Molecular motors and their role in membrane traffic. *Advanced Drug Delivery Reviews,* **29**, 229-242.

233 **Karki, S. and Holzbaur, E.LF.** (1999) Cytoplasmic dynein and dynactin in cell division and intracellular transport. *Current Opinion in Cell Biology,* **11**, 45-53.

234 **Mandelkow, E. and Hoenger, A.** (1999) Structures of kinesin and kinesin-microtubule interactions. *Current Opinion in Cell Biology,* **11**, 34-44.

235 **Pollard, H., Remy, J.-S., Loussouarn, G., Demolombe, S., Behr, J.-P. and Escande, D.** (1998) Polyethylenimine but not cationic lipids promotes transgene delivery to the nucleus in mammalian cells *Journal of Biological Chemistry,* **273,** 7507-7511.

236 **Wolfert, M.A. and Seymour, L.W.** (1998) Chloroquine and amphipathic peptide helices show synergistic transfection *in vitro. Gene Therapy,* **5,** 409-414.

237 **Coonrod, A., Li, F.-Q. and Horwitz, M.** (1997) On the mechanism of DNA transfection: efficient gene transfer without viruses. *Gene Therapy,* **4,** 1313- 1321.

238 **Pouton, C.W.** (1998) Nuclear import of polypeptides, polynucleotides and supramoleeular complexes. *Advanced Drug Delivery Reviews* **34,** 51-64.

239 **Sebestyén, M.G., Ludtke, J.J., Bassik, M.C., Zhang, G., Buder, V., Lukhtanov, E.A., Hagstrom, J.E. and Wolff, J.A.** (1998) DNA vector chemistry: The covalent attachment of signal peptides to plasmid DNA. *Nature Biotechnology,* **16,** 80-85.

240 **Ciolina, C., Byk, G., Blanche, F., Thuillier, V., Scherman, D. and Wils, P.** (1999) Coupling of nuclear localisation signals to plasmid and specific interaction of the conjugates with importin α. *Bioconjugate Chemistry,* **10,** 49-55.

241 **Gorlich, D. and Mattaj, I.W.** (1996) Nucleocytoplasmic transport. *Science,* **271,** 1513- 1518.

242 **Jans, D.A. and Hubner,** S. (1996) Regulation of protein transport to the nucleus: Central role of phosphorylation. *Physiological Reviews,* **76,** 651 -685.

243 **Pante, N. and Aebi, U.** (1996) Toward the molecular dissection of protein import into nuclei. *Current Opinion in Cell Biology* **8,** 397-406.

244 **Feldherr, C.M. and Akin, D.** (1990) The permeability of the nuclear envelope in dividing and nondividing cell cultures. *Journal of Cell Biology,* **111,** 1-8.

245 **Clever, J., Yamada, M. and Kasamatsu, H.** (1991) Import of simian virus 40 thorugh nuclear pore complexes. *Proceedings of the National Academy of Sciences of the United States of America,* **88,** 7333-7337.

246 **Yamada, M and Kasamaysu, H.** (1993) Role of nuclear pore complex in simian virus 40 nuclear targeting. *Journal of Virology.* **67,** 119-130.

247 **Whittaker, G., Bui, M. and Helenius, A.** (1996) The role of nuclear import and export in influenza virus infection. *Trends in Cell Biology.* **6**, 67-71.

248 **Greber, U.F and Kasamatsu, H.** (1996) Nuclear targeting of SV40 and adenovirus. *Trends in Cell Biology.* **6**, 189-195.

249 **Dean, D.A.** (1997) Import of plasmid DNA into the nucleus is sequence specific. *Experimental Cell Research,* **230**, 293-302.

250 **Vacik, J., Dean, B.S., Zimmer, W.E. and Dean, D.A.** (1999) Cell-specific nuclear import of plasmid DNA. *Gene Therapy,* **6**, 1006-1014.

251 **Barany, G., Alberico, F., Solé, N.A., Griffin, G.W., Kates, S.A. and Hudson, D.** (1993) Polyethylene glycol-polystyrene (PEG-PS) graft supports for solid-phase peptide synthesis. In: *Peptides 1992: Proceedings of the twenty-second European Peptide Symposium*, **267**; Edited by Schneider, C.H. and Eberle, A.N.).

252 **Carpino, L.A., El-Faham, A and Albericio, F.** (1994). Advantageous applications to azabenzotriazole-based couplings to solid-phase peptide synthesis. *Journal of the Chemistry Society, Chemical Communications.* 201

253 **Atherton, E. and Sheppard, R. C.** Solid-phase peptide synthesis, A practical approach (1989) Rickwood, D. and Hames, B. D series) IRL Press, Oxford.

254 **Sambrook, J., Fritsch, E.F. and Maniatis, T.** (Eds). (1989) Molecular cloning - A laboratory manual. Second edition. New York: Cold Spring Harbour Laboratory Press.

255 **Birnboim, H.C. and Doly, J.** (1979) A rapid alkaline extraction procedure for screening recombinant plasmid DNA. *Nucleic Acids Research,* **7**, 1513-1522.

256 **Uduehi, A.** (1997) Transfection of Mammalian Cell Lines with Polycationic/DNA Complexes. Ph.D. thesis, Department of Pharmacy and Pharmacology, University of Bath.

257 **Szoka, F. and Papahadjopoulous, D.** (1978) Procedure for preparation of liposomes with large internal aqueous space and high capture by reverse-phase evaporation. *Proceedings of the National Academy of Science,* **75**, 4194-4198.

258 **Twentyman, P.R, Brown, J.M., Gray, J.W., Franko, A.J., Scoles, M.A. and Kallman, R.F.** (1980) A new mouse tumor model system (RIF-I) for comparison of end-point studies. *Journal of National Cancer Institute,* **64**, 595-604.

259 **Skehel, J.J, Bayley, P.M., Brown, E.B., Martin, S.R., Waterfield, M.D., White, J.M., Wilson, I.A. and Wiley, D.C.** (1982) Changes in the conformation of influenza virus haemagglutinin at the pH optimum of virus-mediated membranefusion. *Proceedings of the National Academy of Sciences of the United States of America,* **79**, 968-972.

260 **Doms, R.W., Helenius, A. and White. J.** (1985) Membrane fusion activity of the influenza virus hemagglutinin. The low pH-induced conformational change. *Journal of Biological Chemistry,* **260**, 2973-2981.

261 **Ruigrok, R.W., Aitken. A., Calder. L.J., Martin. S.R., Skehel. J.J., Wharton, S.A., Weis. W. and Wiley, D.C.** (1988). Studies on the structure of the influenza virus haemagglutinin at the pH of membrane fusion. *Journal of Virology.* **69**, 2785-2795.

262 **Harter C, Bachi T, Semenza G and Brunner J.** (1988). Hydrophobic photolabeling identifies BHA-2 as the subunit mediating the interaction of bromelain-solubilized influenza virus hemagglutinin with liposomes at low pH. *Biochemistry.* **27**, 1856-1864.

263 **Junankar, P.R. and Cherry, R.J.** (1986) Temperature and pH dependence of the haemolytic activity of influenza virus and of the rotational mobility of the spike glycoproteins. *Biochimica et Biophysica Acta,* **854**, 198-206.

264 **Fasbender, A.J., Zabner, J. and Welsh, M.J.** (1995) Optimisation of cationic lipid-mediated gene transfer to airway epithelia. *American Journal of Physiology - Lung Cellular and Molecular Physiology,* **269**, L45-L51.

265 **Wilson, I.A., Skehel, J.J. and Wiley, D.C.** (1981) Structure of the haemagglutinin membrane glycoprotein of influenza virus at 3 A resolution. *Nature,* **289**, 366-373.

266 **Takahashi, S.** (1990) Conformation of membrane fusion-active 20-residue peptides with or without lipid bilayers. Implication of alpha-helix formation for membrane fusion. *Biochemistry,* **29**, 6257-6264.

267 **Lear, J.D. and Degrado, W.F.** (1987) Membrane binding and conformational properties of peptides representing the NH-2 terminus of influenza HA-2. *Journal of Biological Chemistry,* **262**, 6500-6505.

268 **Thomas, B.J** (1997) Gene Therapy of Melanoma: Therapeutic and pharmaceutical investigations. Ph.D. Thesis, University of Bath.

269 **Bowman, E. J., Siebers, A. and Altendorf, K.** (1988) Bafilomycins: a class of inhibitors of membrane ATPases from microorganisms, animal cells, and plant cells. *Proceedings of the National Academy of Sciences of the United States of America,* **85**, 7972-7976.

270 **Trubetskoy, V.S., Loomis, A., Hagstrom, J.E., Budker, V.G. and Wolff, J.A.** (1999) Layer-by layer deposition of oppositely charged polyelectrolytes on the surface of condensed DNA particles. *Nucleic Acid Research,* **27**, 3090-3095.

271 **Midoux, P., Mendes, C., Legrand, A., Raimond, J., Mayer, R., Monsigny, M. and Roche, A-C.** (1993) Specific gene transfer mediated by lactosylated polylysine into hepatoma cells. *Nucleic Acids Research,* **21**, 871-878.

272 **Erbacher, P., Roche, A.C, Monsigny, M. and Midoux, P.** (1996) Putative role of chloroquine in gene transfer into a human hepatoma cell Ine by DNA lactosylated polylysine complexes. *Experimental Cell Research* **225**, 186- 194.

273 **MacGregor, G.R., Nolan, G.P., Fiering, S., Roederer, M. and Herzenberg, L.A.** (1991) Use of E. coli lacZ (β-galactosidase) as a reporter gene. *Methods in Molecular Biology*, **7**, 217-235.

274 **Hidalgo, I.J., Raub, T.J. and Borchardt, R.T.** (1989). Characterisation of the human colon carcinoma cell line (Caco-2) as a model for intestinal permeability. *Gastroenterology*, **96**, 736-749.

275 **Artusson, P. and Magnusson, C.** (1990) Epithelial transport of drugs in cell culture. II: Effect of extracellular calcium concentration on the paracellular transport of drugs of different lipophilicities across monolayers of intestinal epithelial (Caco-2) cells. *Journal of Pharmaceutical Sciences*, **79**, 595-600.

276 **Hilgers, A.R., Conradi, R.A. and Burton, P.S.** (1990) Caco-2 cell monolayer as a model for drug transport across the intestinal mucosa. *Pharmaceutical Research*, 1990, 7 (9), 902-910.

277 **Boulenc, X., Bourrie, M., Fabre, I., Roque, C., Joyeux, H., Berger, Y and Faber, G.** (1989) Regulation of cytochrome P4501A1 gene expression in a human intestinal cell line, Caco-2 cells. *Journal of Pharmacological and Experimental Therapy*, **263**, 1471-1478.

278 **Quaroni, A. and Hochman, J.** (1996) Development of intestinal cell culture models for drug transport and metabolism studies. *Advanced Drug Delivery Reviews*, **22**, 3-52.

279 **Rubas, W., Villagran, J., Cromwell, M., McLeod, A., Wassenberg, J. and Mrsny, R. (1995)** Correlation of solute flux across Caco-2 monolayers and colonic tissue *in vitro*. *STP Pharma Sciences*, **5**, 93-97.

280 **Artursson, P., Palm, K. and Luthman, K.** (1996) Caco-2 monolayers in experimental and theoretical predictions of drug transport. *Advanced Drug Delivery Reviews*, **22**, 67-84.

281 **Bailey, C.A., Bryla, P. and Malick, A.W.** (1996) The use of the intestinal epithelial cell culture model, Caco-2, in pharmaceutical development. *Advanced Drug Delivery Reviews*, **22**, 85-103.

282 **Voet, D. and Voet, J.** (1990) Biochemistry, pages 1114-1118, published by J. Wiley and Sons Inc. New York, USA.

283 **Legendre, J-Y. and Szoka, F.C.** (1992) Delivery of plasmid DNA into mammalian cell lines using pH sensitive liposomes: Comparison with cationic liposomes. *Pharmaceutical Research*, **9**, 1235-1424.

284 **Midoux, P. and Monsigny, M.** (1999) Efficient gene transfer by histidylated polylysine/pDNA complexes. *Bioconjugate Chemistry* **10**, 406-411.

285 **Jiao, S., Williams, P., Berg, R.K., Hodgeman, B.A., Liu, L., Repetto, G. and Wolff, J.A.** (1992) Direct gene transfer into nonhuman primate myofibers *in vivo*. *Human Gene Therapy* **3**, 21-33.

286 **Davis, H.L, Demeneix, B.A., Quantin, B., Coulombe, J. and Whalen, R.G.** (1993) Plasmid DNA is superior to viral vectors for direct gene transfer into adult mouse skeletal muscle. *Human Gene Therapy* **4**, 733-740.